NASA Tech Briefs

National
Aeronautics and
Space
Administration

A worker maneuvers an
irrigation pipe that was fabricated
using automated arc-welding guidance equipment
originally developed for NASA's Marshall Space Flight
Center. Employing the latest techniques in optical tracking
and microprocessor control, the system can improve
welding speed and accuracy in a broad range of
nonaerospace applications. [See
the bottom of page A1.]

About the NASA
Technology Utilization Program

The National Aeronautics and Space Act of 1958, which established NASA and the United States civilian space program, requires that "The Administration shall provide for the widest practicable and appropriate dissemination of information concerning its activities and the results thereof."

To help carry out this objective, NASA's Technology Utilization (TU) Program was established in 1962. Now, as an element of NASA's Technology Utilization and Industry Affairs Division, this program offers a variety of valuable services to help transfer aerospace technology to nonaerospace applications, thus assuring American taxpayers maximum return on their investment in space research; thousands of spinoffs of NASA research have already occurred in virtually every area of our economy.

The TU program has worked for engineers, scientists, technicians, and businessmen; and it can work for you.

NASA Tech Briefs

Tech Briefs is published quarterly and is free to engineers in U.S. industry and to other domestic technology transfer agents. It is both a current-awareness medium and a problem-solving tool. Potential products . . . industrial processes . . . basic and applied research . . . shop and lab techniques . . . computer software . . . new sources of technical data . . . concepts . . . can be found here. The short section on New Product Ideas highlights a few of the potential new products contained in this issue. The remainder of the volume is organized by technical category to help you quickly review new developments in your areas of interest. Finally, a subject index makes each issue a convenient reference file.

Further Information on Innovations

Although some new technology announcements are complete in themselves, most are backed up by Technical Support Packages (TSP's). TSP's are available without charge and may be ordered by simply completing a TSP Request Card found at the back of this volume. Further information on some innovations is available for a nominal fee from other sources, as indicated. In addition, Technology Utilization Officers at NASA Field Centers will often be able to lend necessary guidance and assistance.

Patent Licenses

Patents have been issued to NASA on some of the inventions described, and patent applications have been submitted on others. Each announcement indicates patent status and availability of patent licenses if applicable.

Other Technology Utilization Services

To assist engineers, industrial researchers, business executives, Government officials, and other potential users in applying space technology to their problems, NASA sponsors Industrial Applications Centers. Their services are described on page A7. In addition, an extensive library of computer programs is available through COSMIC, the Technology Utilization Program's outlet for NASA-developed software.

Applications Program

NASA conducts applications engineering projects to help solve public-sector problems in such areas as safety, health, transportation, and environmental protection. Two applications teams, staffed by professionals from a variety of disciplines, assist in this effort by working with Federal agencies and health organizations to identify critical problems amenable to solution by the application of existing NASA technology.

Reader Feedback

We hope you find the information in *NASA Tech Briefs* useful. A reader-feedback card has been included because we want your comments and suggestions on how we can further help you apply NASA innovations and technology to your needs. Please use it; or if you need more space, write to the Manager, Technology Transfer Division, P.O. Box 8757, Baltimore/Washington International Airport, Maryland 21240.

NASA Tech Briefs

National
Aeronautics and
Space
Administration

The photographs on the front and back covers illustrate developments by NASA and its contractors that have resulted in commercial and nonaerospace spinoffs. You can use the TSP Request Card at the back of this issue to learn more about the Automated Arc-Welding Guidance System [Circle 86] and Flame-Resistant Polyimide Foam [Circle 87].

About This NASA Publication

Change of Address

If you wish to have NASA Tech Briefs forwarded to your new address, use the Subscription Card enclosed at the back of this volume of NASA Tech Briefs. Be sure to check the appropriate box indicating change of address, and also fill in your identification number (T number) in the space indicated.

Communications Concerning Editorial Matter

For editorial comments or general communications about NASA Tech Briefs, you may use the Feedback card in the back of NASA Tech Briefs, or write to: The Publications Manager, Technology Utilization Office (LGT-1), NASA Headquarters, Washington, DC 20546. Technical questions concerning specific articles should be directed to the Technology Utilization Officer of the sponsoring NASA Center (addresses listed on page A4).

Acknowledgements

NASA
TU SERVICES

NASA TECHNOLOGY UTILIZATION NETWORK

★ TECHNOLOGY UTILIZATION OFFICERS

Stanley A. Miller
Ames Research Center
Code 240-10
Moffett Field, CA 94035
(415) 965-6471

Stanley A. Miller
Hugh L. Dryden Flight Research Center
Code 240-10
Moffett Field, CA 94035
(415) 965-6471

Donald S. Friedman
Goddard Space Flight Center
Code 702.1
Greenbelt, MD 20771
(301) 344-6242

John T. Wheeler
Lyndon B. Johnson Space Center
Code AT-3
Houston, TX 77058
(713) 483-3809

U. Reed Barnett
John F. Kennedy Space Center
Code PT-SPD
Kennedy Space Center, FL 32899
(305) 867-3017

John Samos
Langley Research Center
Mail Stop 139A
Hampton, VA 23665
(804) 827-3281

Harrison Allen, Jr.
Lewis Research Center
Mail Code 7-3
21000 Brookpark Road
Cleveland, OH 44135
(216) 433-4000, Ext. 6422

Ismail Akbay
George C. Marshall Space Flight Center
Code AT01
Marshall Space Flight Center, AL 35812
(205) 453-2224

Leonard A. Ault
NASA Headquarters
Code ETD-6
Washington, DC 20546
(202) 755-2244

Aubrey Smith
NASA Resident Office-JPL
4800 Oak Grove Drive
Pasadena, CA 91103
(213) 354-4849

Gilmore H. Trafford
Wallops Flight Center
Code OD
Wallops Island, VA 23337
(804) 824-3411, Ext. 201

● INDUSTRIAL APPLICATIONS CENTERS

Aerospace Research Applications Center
1201 East 38th Street
Post Office Box 647
Indianapolis, IN 46223
John M. Ulrich, director
(317) 264-4644

**Computer Software Management
and Information Center (COSMIC)**
Suite 112, Barrow Hall
University of Georgia
Athens, GA 30602
John A. Gibson, director
(404) 542-3265

Kerr Industrial Applications Center
Southeastern Oklahoma State University
Durant, OK 74701
James Harmon, director
(405) 924-0121, Ext. 413

NASA Industrial Applications Center
710 LIS Building
University of Pittsburgh
Pittsburgh, PA 15260
Paul A. McWilliams, executive director
(412) 624-5211

**New England Research Applications
Center**
Mansfield Professional Park
Storrs, CT 06268
Daniel Wilde, director
(203) 486-4533

**North Carolina Science and
Technology Research Center**
Post Office Box 12235
Research Triangle Park, NC 27709
James E. Vann, director
(919) 549-0671

Technology Applications Center
University of New Mexico
Albuquerque, NM 87131
Stanley Morain, director
(505) 277-3622

NASA Industrial Applications Center
University of Southern California
Denny Research Building
University Park
Los Angeles, CA 90007
Robert Mixer, acting director
(213) 743-6132

■ STATE TECHNOLOGY APPLICATIONS CENTERS

**NASA/University of Florida
State Technology Applications Center**
500 Weil Hall
University of Florida
Gainesville, FL 32611
J. Ronald Thornton, director
Gainesville: (904) 392-6760
Boca Raton: (305) 395-5100, Ext. 2292
Fort Lauderdale: (305) 776-6645
Jacksonville: (904) 646-2478
Orlando: (305) 275-2706
Pensacola: (904) 476-9500, Ext. 426
Tampa: (813) 974-2499

**NASA/University of Kentucky
State Technology Applications Program**
109 Kinkead Hall
University of Kentucky
Lexington, KY 40508
William R. Strong, manager
(606) 258-4632

◆ PATENT COUNSELS

Robert F. Kempf
Asst. Gen. Counsel for patent matters
NASA Headquarters
Code GP-4
400 Maryland Avenue, SW.
Washington, DC 20546
(202) 755-3954

Darrell G. Brekke
Ames Research Center
Mail Code: 200-11A
Moffett Field, CA 94035
(415) 965-5104

Paul F. McCaul
Hugh L. Dryden Flight Research Center
Code OD/TU Office - Room 2015
Post Office Box 273
Edwards, CA 93523
(213) 354-2734

John O. Tresansky
Goddard Space Flight Center
Mail Code: 204
Greenbelt, MD 20771
(301) 344-7351

Marvin F. Matthews
Lyndon B. Johnson Space Center
Mail Code: AL-3
Houston, TX 77058
(713) 483-4871

James O. Harrell
John F. Kennedy Space Center
Mail Code: SA-PAT
Kennedy Space Center, FL 32899
(305) 867-2544

Howard J. Osborn
Langley Research Center
Mail Code: 279
Hampton, VA 23665
(804) 827-3725

Norman T. Musial
Lewis Research Center
Mail Code: 500-311
21000 Brookpark Road
Cleveland, OH 44135
(216) 433-4000, Ext. 346

Leon D. Wofford, Jr.
George C. Marshall Space Flight Center
Mail Code: CC01
Marshall Space Flight Center, AL 35812
(205) 453-0020

Paul F. McCaul
NASA Resident Office-JPL
Mail Code: 180-601
4800 Oak Grove Drive
Pasadena, CA 91103
(213) 354-2700

▲ APPLICATION TEAMS

Doris Rouse, *director*
Research Triangle Institute
Post Office Box 12194
Research Triangle Park, NC 27709
(919) 541-6980

James P. Wilhelm, *director*
SRI International
333 Ravenswood Avenue
Menlo Park, CA 94026
(415) 326-6200, Ext. 3520

TECHNOLOGY UTILIZATION OFFICERS

Technology transfer experts can help you
apply the innovations in NASA Tech Briefs.

The Technology Utilization Officer
at each NASA Field Center is an
applications engineer who can help
you make use of new technology
developed at his center. He brings you
NASA Tech Briefs and other special
publications, sponsors conferences,
and arranges for expert assistance in
solving technical problems.

Technical assistance,
in the form of further information about
NASA innovations and technology, is
one of the services available from the
TUO. Together with NASA scientists
and engineers, he can often help you
find and implement NASA technology
to meet your specific needs.

Technical Support Packages (TSP's)
are prepared by the center TUO's.
They provide further technical details
for articles in NASA Tech Briefs. This
additional material can help you
evaluate and use NASA technology.
You may receive most TSP's free of
charge by using the TSP Request Card
found at the back of this issue.

Technical questions about articles
*in NASA Tech Briefs are answered in
the TSP's. When no TSP is available,
or you have further questions, contact
the Technology Utilization Officer at
the center that sponsored the re-
search [see page A4].*

NASA INVENTIONS AVAILABLE FOR LICENSING

Over 3,500 NASA inventions are available for licensing
in the United States — both exclusive and nonexclusive.

Nonexclusive licenses
for commercial use of NASA inventions
are encouraged to promote competition
and to achieve the widest use of inven-
tions. They must be used by a netotiated
target date.

Exclusive licenses
may be granted to encourage early
commercial development of NASA
inventions, especially when consider-
able private investment is required.
These are generally for 5 to 10 years
and usually require royalties based on
sales or use.

Additional licenses available
include those of NASA-owned foreign
patents. In addition to inventions
described in NASA Tech Briefs,
"NASA Patent Abstract Bibliography"
(PAB), containing abstracts of all
NASA inventions, can be purchased
from National Technical Information
Service, Springfield, VA 22161. The
PAB is updated semiannually.

Patent licenses for Tech Briefs
*are frequently available. Many of the
inventions reported in NASA Tech
Briefs are patented or are under
consideration for a patent at the time
they are published. The current patent
status is described at the end of the
article; otherwise, there is no state-
ment about patents. If you want to
know more about the patent program
or are interested in licensing a
particular invention, contact the
Patent Counsel at the NASA Field
Center that sponsored the research
[see page A5]. Be sure to refer to the
NASA reference number at the end of
the Tech Brief.*
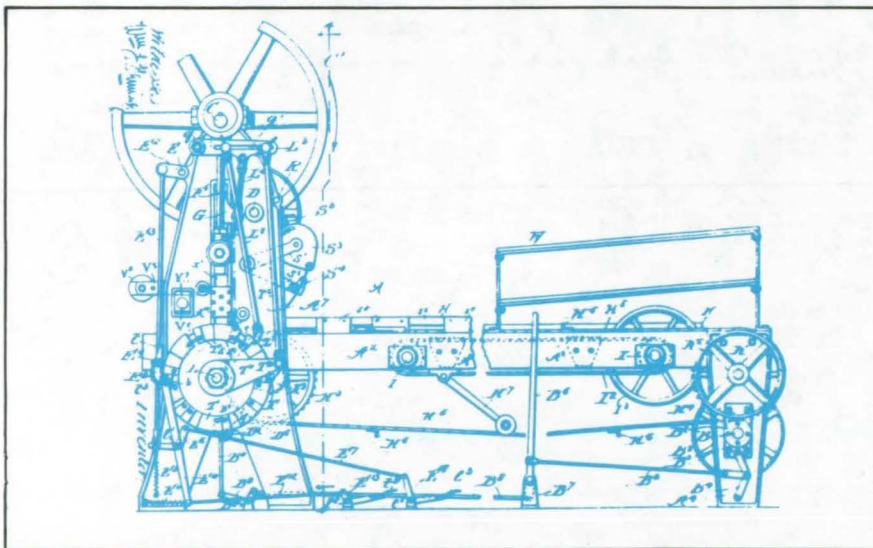
APPLICATION TEAMS
Technology-matching and problem-solving
assistance to public-sector organizations

Application engineering projects
are conducted by NASA to help solve
public-sector problems in such areas
as safety, health, transportation, and
environmental protection. Some appli-
cation teams specialize in biomedical
disciplines; others, in engineering and
scientific problems. Staffed by profes-
sionals from various disciplines, these
teams work with other Federal agen-
cies and health organizations to

identify critical problems amenable to
solution by the application of existing
NASA technology.

Public-sector organization
*representatives can learn more about
application teams by contacting a
nearby NASA Field Center Technology
Utilization Office [see page A4].*

INDUSTRIAL APPLICATIONS CENTERS
Computerized access to over
10 million documents worldwide

Computerized information retrieval
from one of the world's largest banks of
technical data is available from NASA's
network of industrial Applications Cen-
ters (IAC's). The IAC's give you access to
1,800,000 technical reports in the NASA
data base and to more than 10 times that
many reports and articles found in near-
ly 200 other computerized data bases.

The major sources include:
- *750,000 NASA Technical Reports*
- *Selected Water Resources Abstracts*
- *NASA Scientific and Technical
  Aerospace Reports*
- *Air Pollution Technical Information
  Center*
- *NASA International Aerospace
  Abstracts*
- *Chem Abstracts Condensates*
- *Engineering Index*
- *Energy Research Abstracts*
- *NASA Tech Briefs*
- *Government Reports
  Announcements*

and many other specialized files on
food technology, textile technology,
metallurgy, medicine, business, eco-
nomics, social sciences, and physical
science.

The IAC services
range from tailored literature searches
through expert technical assistance:

- *Retrospective Searches:* Published
or unpublished literature is screened,
and documents are identified accord-
ing to your interest profile. IAC engi-
neers tailor results to your specific
needs and furnish abstracts consid-
ered the most pertinent. Complete
reports are available upon request.
- *Current-Awareness Searches:* IAC
engineers will help design a program
to suit your needs. You will receive
selected monthly or quarterly ab-
stracts on new developments in your
area of interest.

- *Technical Assistance:* IAC engineers
will help you evaluate the results of
your literature searches. They can
help find answers to your technical
problems and put you in touch with
scientists and engineers at appropri-
ate NASA Field Centers.

Prospective clients
*can obtain more information about
these services by contacting the
nearest IAC [see page A4]. User fees
are charged for IAC information ser-
vices.*

STATE TECHNOLOGY APPLICATIONS CENTERS

Technical information services for industry
and state and local government agencies

Government and private industry
in Florida and Kentucky can utilize the services of NASA's State Technology Applications Centers (STAC's). The STAC's differ from the Industrial Applications Centers described on page A7, primarily in that they are integrated into existing state technical assistance programs and serve only

the host state, whereas the IAC's serve multistate regions.

Many data bases,
including the NASA base and several commercial bases, are available for automatic data retrieval through the STAC's. Other services such as document retrieval and special

searches are also provided. (Like the IAC's, the STAC's normally charge a fee for their services.)

To obtain information
about the services offered, write or call the STAC in your state [see page A4].

COSMIC®

An economical source of computer programs
developed by NASA and other government agencies

A vast software library
is maintained by COSMIC — the Computer Software Management and Information Center. COSMIC gives you access to approximately 1,600 computer programs developed for NASA and the Department of Defense and selected programs for other government agencies. Programs and documentation are available at reasonable cost.

Available programs
range from management (PERT scheduling) to information science (retrieval systems) and computer operations (hardware and software). Hundreds of engineering programs perform such tasks as structural analysis, electronic circuit design, chemical analysis, and the design of fluid systems. Others determine building energy requirements and optimize mineral exploration.

COSMIC services
go beyond the collection and storage of software packages. Programs are checked for completeness; special announcements and an indexed software catalog are prepared; and programs are reproduced for distribution. Customers are helped to

identify their software needs; and COSMIC follows up to determine the successes and problems and to provide updates and error corrections. In some cases, NASA engineers can offer guidance to users in installing or running a program.

Information about programs
described in NASA Tech Briefs articles can be obtained by completing the COSMIC Request Card at the back of this issue. Just circle the letters that correspond to the programs in which you are interested.

NEW PRODUCT
IDEAS
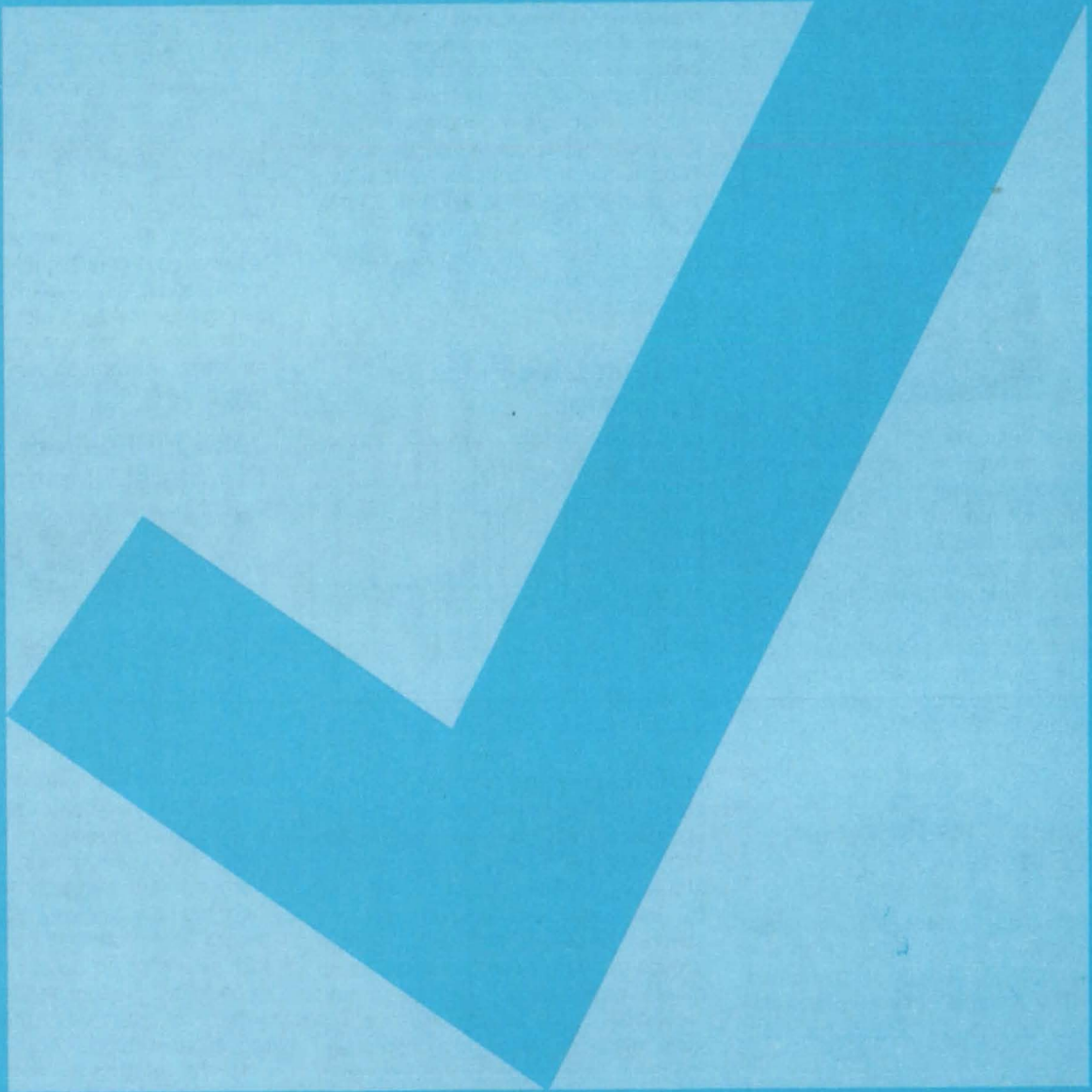
NEW PRODUCT IDEAS are just a few of the many innovations described in this issue of NASA Tech Briefs and having promising commercial applications. Each is discussed further on the referenced page in the appropriate section in this issue. If you are interested in developing a product from these or other NASA innovations, you can receive further technical information by requesting the TSP referenced at the end of the full-length article or by writing the Technology Utilization Office of the sponsoring NASA center (see page A4). NASA's patent-licensing program to encourage commercial development is described on page A6.

Cryogenic Heat Pipe

A new heat pipe with axial grooves performs better with cryogenic working fluids than do heat pipes with more-conventional rectangular grooves. The novelly-configured aluminum heat pipe reduces cryogenic charge and increases wicking height for better efficiency. The pipe is extruded, which makes its fabrication in large numbers possible. In performance tests, the heat pipe demonstrated good startup from a completely frozen condition.
(See page 422.)

Long-Life/Low-Power Ion Gun Cathode

Substantially longer life and less heater power are qualities of an improved cathode for ion-implantation guns. The cathode lifetime is approxi-

mately 1,000 hours, and it requires 30 watts of heater power; previous cathodes were useful for only about 20 hours and required 300 watts of heater power. The new cathode is generally made of tungsten that is coated to produce a copious electron emission at low temperature and hence low power. It emits electrons that bombard the gas in an ion source; the ions are then accelerated out of the source.
(See page 372.)
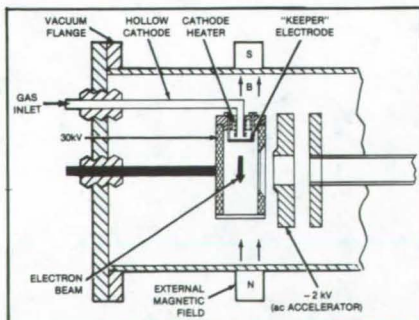
Programable Pulse Generator
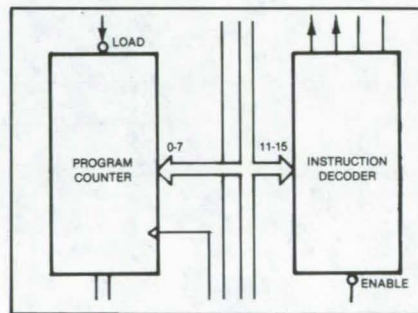
A new pulse generator can be programed to produce pulses from several ports at different pulse lengths and intervals and in virtually any combination and sequence. The generator operates at intervals between pulses as short as 0.5 μs. High-speed logic circuits and special instructions that can be read in groups of two or more between output pulses give the unit its speed and resolution. Once loaded with instructions, either manually or by computer, the pulse generator operates independently of the computer.
(See page 379.)

Two-Speed Valve

A two-speed valve permits fine control of flow as it is first opened yet opens rapidly as it approaches full flow. The valve should be useful for flow control of gases and liquids in such equipment as home appliances and laboratory instruments. To open the valve, the
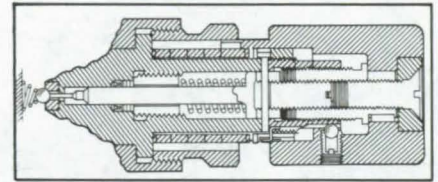
user rotates the valve handle counterclockwise; the first several turns of the valve open it only slightly, and the last turn opens it fully. The valve is similarly two speeded when it is closed: It is fast acting for the first turn and slow acting for the last several turns.
(See page 448.)

## Joint for Folding Structural Elements

Structural elements are locked in place quickly and easily by a new center joint. The joint alines the column elements automatically and fastens them together securely. Consisting of a pair of spring-loaded hinged hubs, the joint allows the hollow column elements to be folded in pairs and to be stacked within each other. When the column elements are to be joined, they are unfolded, causing the mating faces of the joint to contact and latch. If liquid or gas seals are added to the center joints, they could be used in a deployable pipeline.
(See page 440.)

Glass for Solid-State Devices

Two glass formulations are suitable as isolation layers in solid-state devices that incorporate magnetic films. The
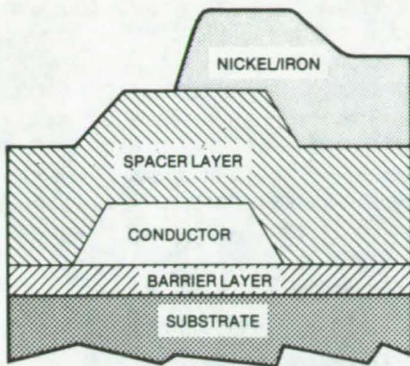
glasses have the low intrinsic compressive stress required for such layers so that stress in the conductor layer, or other layers, is isolated from the magnetic layer. One of the formulations may be used on a substrate as a barrier layer, and the other formulation may be deposited to separate the conductor from the other layers. Typical thickness of the glass used as a barrier layer over a substrate is from 1,000 to 4,000 Å. (See page 407.)

Fluid-Injection Tool for Inaccessible Areas
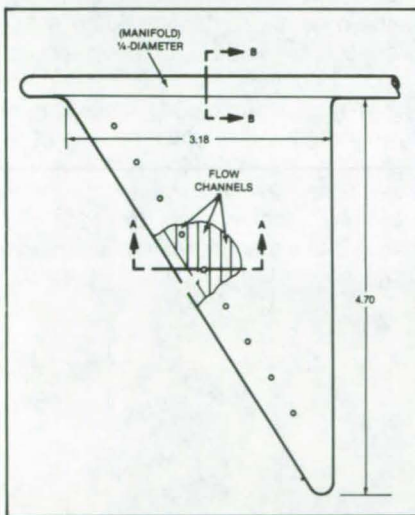
Liquids or gases are injected into narrow crevices by a new tool that can be used to apply caulking and waterproofing compounds, adhesives, and oil and to aerate hard-to-reach places. The tool consists of a thin, flat, triangular nozzle, containing many channels, attached to a distribution manifold. The nozzle can reach into an opening 1/32 inch wide to a depth of more than 4 inches. Gas or liquid flowing through the manifold and channels exits through holes on the flat face of the nozzle. (See page 438.)

Compression Ratio Adjuster

Higher fuel efficiency in internal-combustion engines is possible with a new mechanism that alters the compression ratio of the engine according to the load.
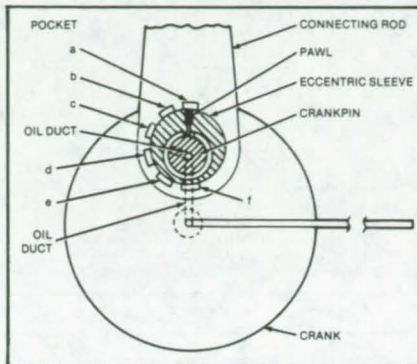
The mechanism ensures that the engine operates as efficiently under partial load and at low-speed full load conditions as it does at high load and high speed. The mechanism alters the compression ratio by altering the length of the connecting rod to increase or decrease the cylinder volume at the moment fuel combustion starts. It does this automatically under the control of a pressure sensor in the engine intake manifold. (See page 435.)

Cable-Twisting Machine
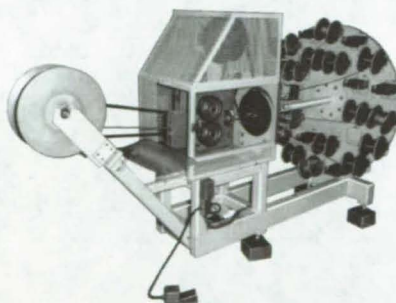
Uniformly twisted cable composed of up to 26 wires is made by a new machine that is ideal for short production runs. Using it, one operator produces finished cable in about one-fourth the time it previously took three people working by hand. This fast operation is made possible by using smaller spools of wire. The speed of rotation of the machine is varied to generate different twists, and a meter registers the cable length as it passes through tension rollers. (See page 448.)

Moving-Surface Follower Aids Microsurgery
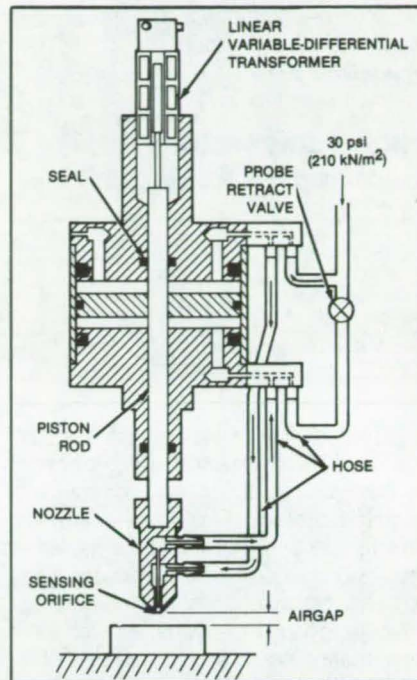
The movements of arteries and muscles are followed by a novel manipulator that enables precise placement of microsurgical tools. A "microprobe" mounted on the output of the pneumatic servo of a commercial noncontacting thickness gage senses arterial, muscular, or other bodily motion. The probe moves to maintain a constant position relative to the moving tissue. (See page 416.)

Improved Thermoplastics

High-temperature solvent-resistant adhesives, laminating resins, protective coatings, membranes, and films are some of the potential uses of polyphenylquinoxaline (PPQ) thermoplastics that have been improved by adding cross-linking groups. Preparing the PPQ's with relatively low levels of cross-linking pendent ethynyl groups and pendent phenylethynyl groups creates thermoplastics with higher use temperature
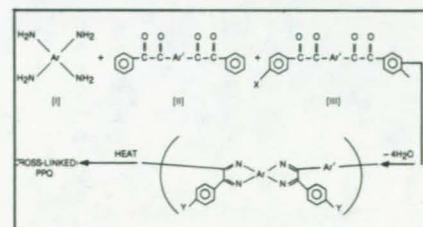
and solvent resistance — without compromising their toughness and thermoformability. In general, the phenylethynyl groups have shown better properties when cross-linked with the PPQ's than have the ethynyl groups.
(See page 396.)

High-Temperature Captive-Nut Assembly
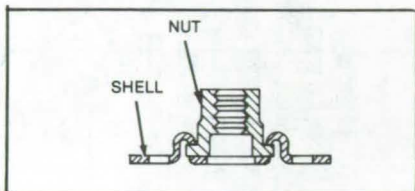
Functional at service temperatures of up to 1,600° F, an improved captive nut is both easy to install and remove with simple handtools. Designed for working environments where high-temperature corrosion is a problem, the nut assembly should be useful in fastening heat shields to vacuum ovens, as well as in assembling home appliances and other machinery. Made of corrosion- and heat-resistant nickel alloy, the captive nut floats in a shell to accommodate misalinement of a mating bolt.
(See page 440.)

Robot End Effector To Place and Solder Solar Cells

A robot end effector or "hand" heats a solar cell to soldering temperature while the robot transports the cell from a preparation station to a solar panel where the cell is simultaneously placed in position and soldered. The end effector is used in conjunction with a work
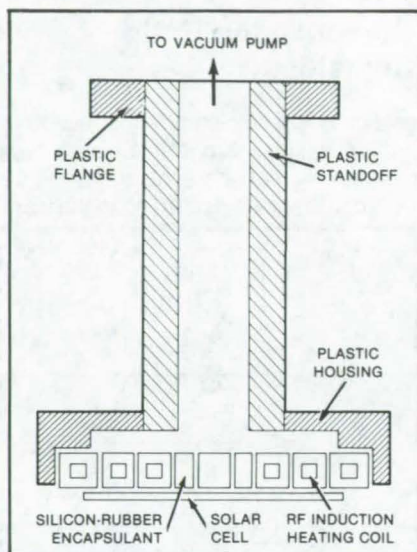

station that prepares the cells for soldering. An encapsulated RF induction-heating coil heats the solar cell while it is in transit. The cell is held by vacuum transferred through holes in the encapsulant.
(See page 458.)

Nonslip Wristlet

A new wristlet protects from flame, heat, corrosive or caustic substances, and sharp objects. Worn under a glove,
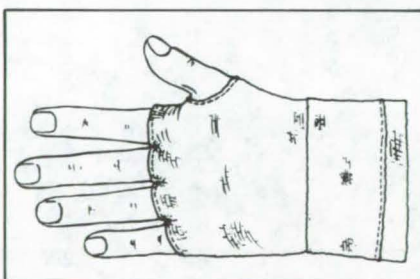
the wristlet provides an additional layer of protective material over the palm and the back of the hand and over the web of the thumb. The arm opening of the wristlet may be permanently attached to a coat sleeve by stitches, or it may be temporarily attached by snaps or a zipper. Possible applications of the wristlet are in forge and foundry work and fire-fighting.
(see page 466.)

Portable Radiometer Identifies Minerals in the Field
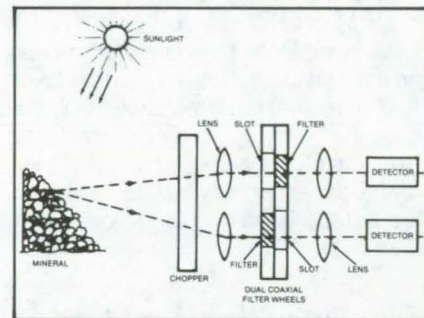
A portable radiometer that can be used either on foot or from an aircraft aids in identifying minerals in the field. It is especially suitable for identifying clay and carbonates. The radiometer measures the reflectances of a mineral at two wavelengths, computes the ratio of the reflectances, and displays the ratio to the user. The reflectance ratios for common minerals are provided in a table that accompanies the instrument.
(See page 419.)

Electronic Components and Circuits
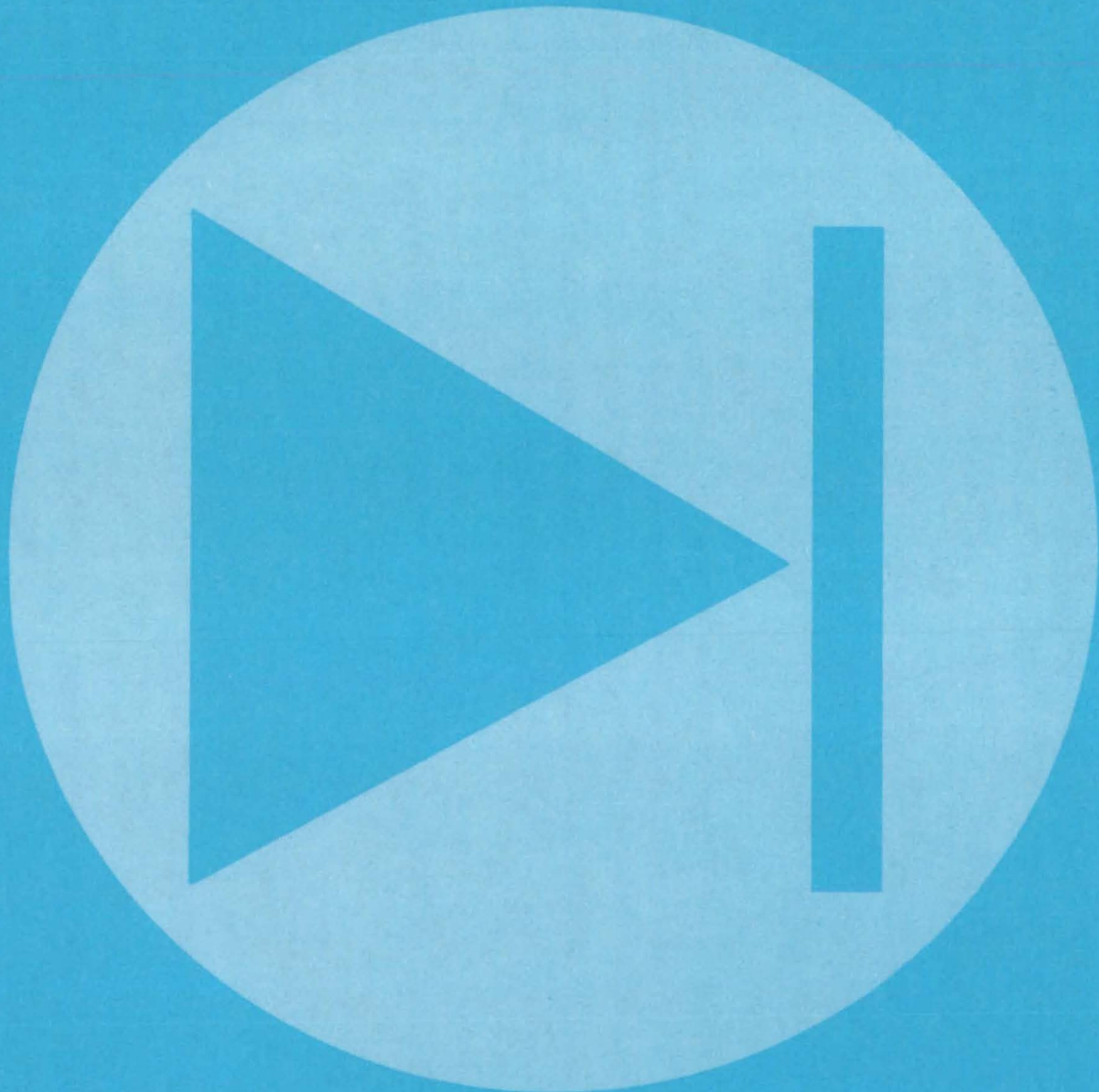
Hardware, Techniques, and Processes

Simple Temperature Regulator for a Cold Chamber

Circuit generates an overtemperature warning
independent of the regulation function.

Lyndon B. Johnson Space Center, Houston, Texas
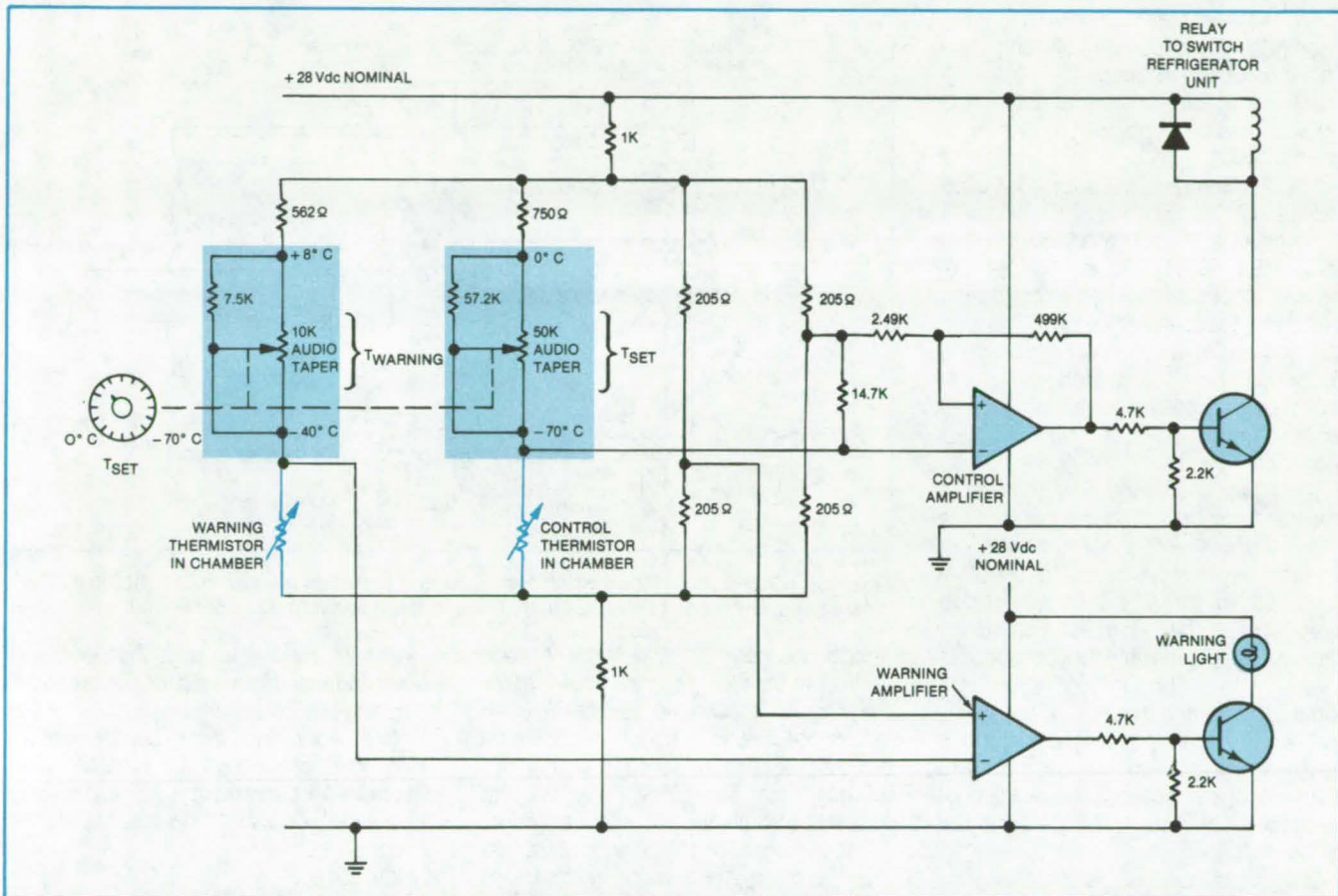
The **Temperature Regulator Circuit and Warning-Light Circuit** are independent of one another, but their reference-level potentiometers are ganged. The temperature control circuit includes some feedback to prevent the refrigeration unit from cycling on and off too frequently.

An electronic control circuit holds a cold chamber at a selectable temperature and lights a warning light if the temperature exceeds a predetermined level above the control temperature. The circuit uses only two standard operational amplifiers.

The regulator and alarm are shown schematically in the diagram. If the temperature in the cold chamber is greater than T_{SET}, the resistance of the control thermistor is less than that of the shunted T_{SET} potentiometer plus 750 ohms. Therefore the voltage applied to the inverting input of the control op-amp is low, and the output from the op-amp is high. The high voltage turns on the transistor, energizing the relay that turns on the refrigeration unit.

When the refrigeration unit reduces the temperature in the chamber, the re-

sistance of the control thermistor increases, and the voltage applied to the inverting input of the control op-amp goes low. This low voltage turns off the transistor, the relay, and the refrigeration unit.

To avoid cycling the refrigeration unit on and off too frequently, $3°$ C of hysteresis are included in the control circuit. The positive feedback introduced through the 499K and 2.49K resistors makes it necessary to decrease the thermistor temperature by $3°$ C below T_{SET} before the control op-amp shuts off the transistor.

The warning portion of the controller works in much the same way: If the warning thermistor temperature is above T_{WARN}, then the thermistor resistance is low; the voltage fed to the inverting input of the warning op-amp is

low; the op-amp output is high; and the transistor and the warning light are turned on. No hysteresis is built into the warning circuit.

The T_{SET} and T_{WARN} potentiometers are ganged so that for every control temperature selected (T_{SET}), a corresponding warning temperature is selected, a predetermined amount above the control temperature. At $T_{SET} = 0°$ C, T_{WARN} is $+8°$ C; at $T_{SET} = -70°$ C, T_{WARN} is $-40°$ C.

This work was done by William G. Redmond of Vought Corp. for **Johnson Space Center.** *For further information, including the selection of a potentiometer taper for linear dial control, Circle 1 on the TSP Request Card.*
MSC-18927

Long-Life/Low-Power Ion-Gun Cathode

Hollow tungsten cathode, tipped with barium oxide,
gives copious electron emission at low temperature.

NASA's Jet Propulsion Laboratory, Pasadena, California

An improved cathode for ion-implantation guns has a substantially longer life than those used in the past — approximately 1,000 hours instead of 20 — and requires less heater power (30 watts instead of 300).

A typical ion gun, used for controlled doping of semiconductors, has a cathode as a source of electrons that bombard a gas to produce ions. Beam-forming electrodes and an accelerating grid then direct the ions to the target. The cathode is a tungsten rod running through a gas-filled chamber, but the geometry of that design is inefficient in terms of ion output per unit of input heater power.

The figure shows the new cathode. It has the form of a hollow tube through which the gas enters a region of high electron density, produced by an electric discharge with an auxiliary electrode referred to as the "keeper." The hollow cathode tip is generally tungsten that is coated with a barium- or strontium-enriched material having a low-work-function surface, to produce a copious electron emission at low temperature and hence low power. Two additional electrodes collimate and accelerate the ion beam.

One other advantage of this new structure is that there is room within the
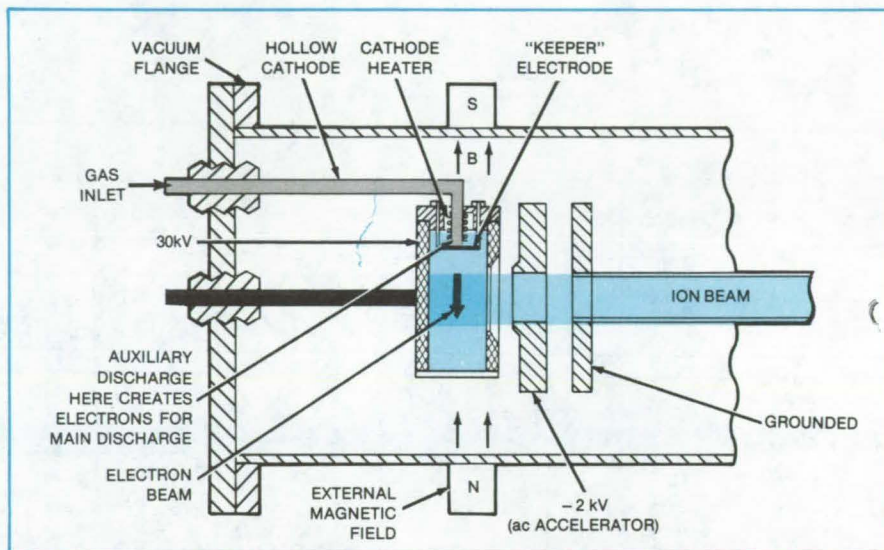
The **Hollow Ion-Gun Cathode** emits electrons that bombard the gas in the chamber. The ions accelerated out of the source are used to dope semiconductor material.

anode chamber for a second cathode and an ionizable gas inlet. This feature may make it possible to obtain even longer lifetime for the ion-implantation device, because in the case of a failure of the first assembly, the second assembly could be put into operation. Disadvantages of this new design are that the geometry is more complicated (both the hollow cathode itself and the

"keeper" electrode) and that another power supply is required for operation of the "keeper" discharge.

This work was done by Dennis J. Fitzgerald of Caltech for **NASA's Jet Propulsion Laboratory.** *For further information, Circle 2 on the TSP Request Card.*
NPO-15328

# Electrical Connector for Graphite Heating Elements

Heat loss and contact resistance are minimized,
and thermal stresses are accommodated.

NASA's Jet Propulsion Laboratory, Pasadena, California

A new connection method solves some difficult problems posed by the interface between an electrical heating element at incandescent temperature and a metal current carrier at essentially room temperature. The heat carried from the heating element and out of the heated zone through the metal conductor should be kept to a minimum. At the same time, the electrical contact resistance between the heating element and

the metal conductor should be as low as possible and should remain essentially constant over the temperature range of the heated zone — despite different rates of thermal expansion of the heating element and the metal conductor. Moreover, the electrical connection should allow for the weak, brittle character of the heating element — usually graphite.

The new connection method (see figure) applies force to two interfaces: that between the heating element proper and heating-element support members and that between the heating-element support members and the metal conductor. The latter connection is compliant so that the forces do not change appreciably when the parts undergo thermal expansion or contraction at different rates.

Compliance is provided by a compression spring (for example, a Belleville spring) that keeps the inner rod in tension. The electrical terminals are liquid-cooled to prevent the spring from overheating.

In assembly, a heating element is set on support outer members, and a support inner member is inserted in an outer member at each support location. A nut is screwed on each inner member until the spring starts to become compressed. The nut is then tightened a given number of turns to provide the proper contact force.

This work was done by Brian H. Mackintosh of Mobil Tyco Solar Energy Corp. for **NASA's Jet Propulsion Laboratory.** *For further information, Circle 3 on the TSP Request Card.* NPO-15056
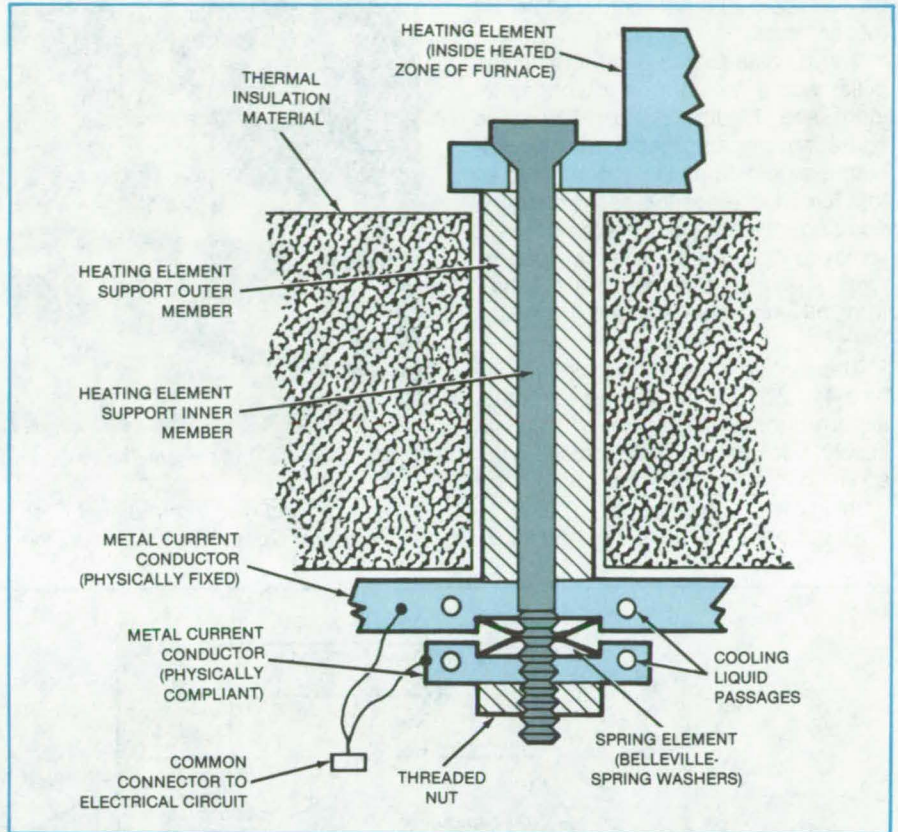
The **Inner Rod** of the new connector system is maintained in tension by means of a spring (for example, Belleville washers). The connection is sufficiently compliant so that the tension remains within the desired range, regardless of thermal expansion and contraction of the various elements.

Low-Speed Control for Automatic Welding

A simple module extends the speed range to lower-than-normal values.

Lyndon B. Johnson Space Center, Houston, Texas

An amplifier module allows the rotating positioner of an automatic welding machine to operate at speeds below its normal range. The low speeds are precisely regulated by a servomechanism just as are the normal-range speeds. The addition of the module to a standard welding machine makes it unnecessary to purchase new equipment for low-speed welding.

Figure 1 shows the rotating positioner and the welding fixture. The control console and the electronics drawer containing the modified circuitry are seen in Figure 2. Although originally developed for the Sciaky model 1-25-40 rotational positioner, the technology should also
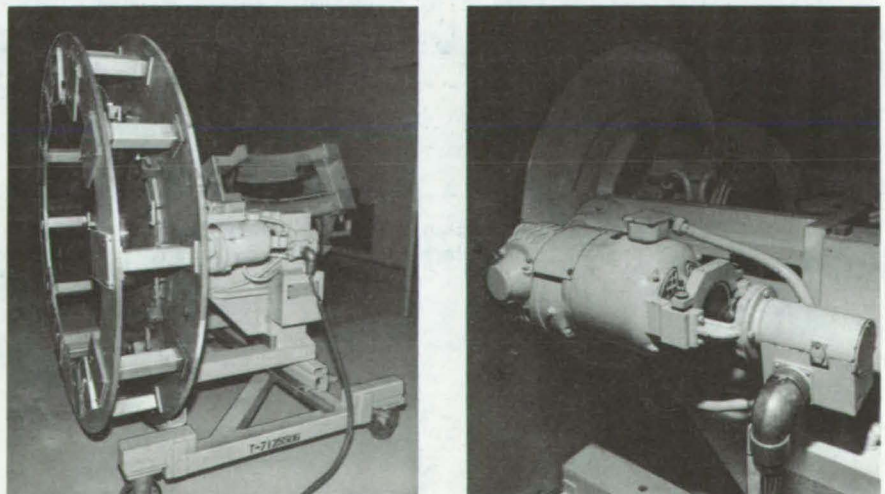
Figure 1. The **Rotating Positioner** is shown at the left. On the right are the drive motor and tachometer.

be adaptable to other motorized servo-mechanisms.

The module places a differential amplifier with a gain of 3 in a tachometer loop (see Figure 3). For low-speed operation, the amplifier boosts the low output signal from the tachometer so that it can operate the servo circuitry. For normal operation, the amplifier is removed from the tachometer loop by relay K_1 when the machine operator turns off single-pole, single-throw switch SW_1.

The system is isolated above ground by a 440-V/115-V transformer to protect it from damage by the welding power supply. Back-to-back Zener diodes in the speed control prevent the servo from running away at high-speed settings.

This work was done by William E.
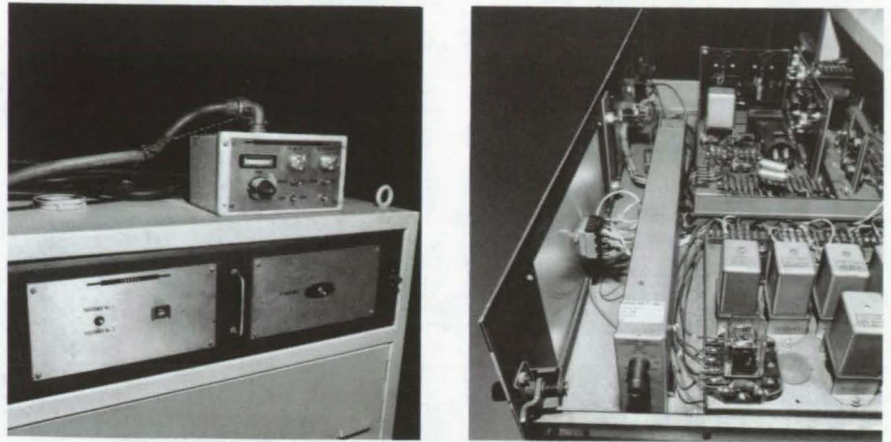
Figure 2. The **Control Console** and modified electronics drawer are shown in these views.

*Iceland of Rockwell International Corp. for **Johnson Space Center.** No further* documentation is available.
MSC-20114
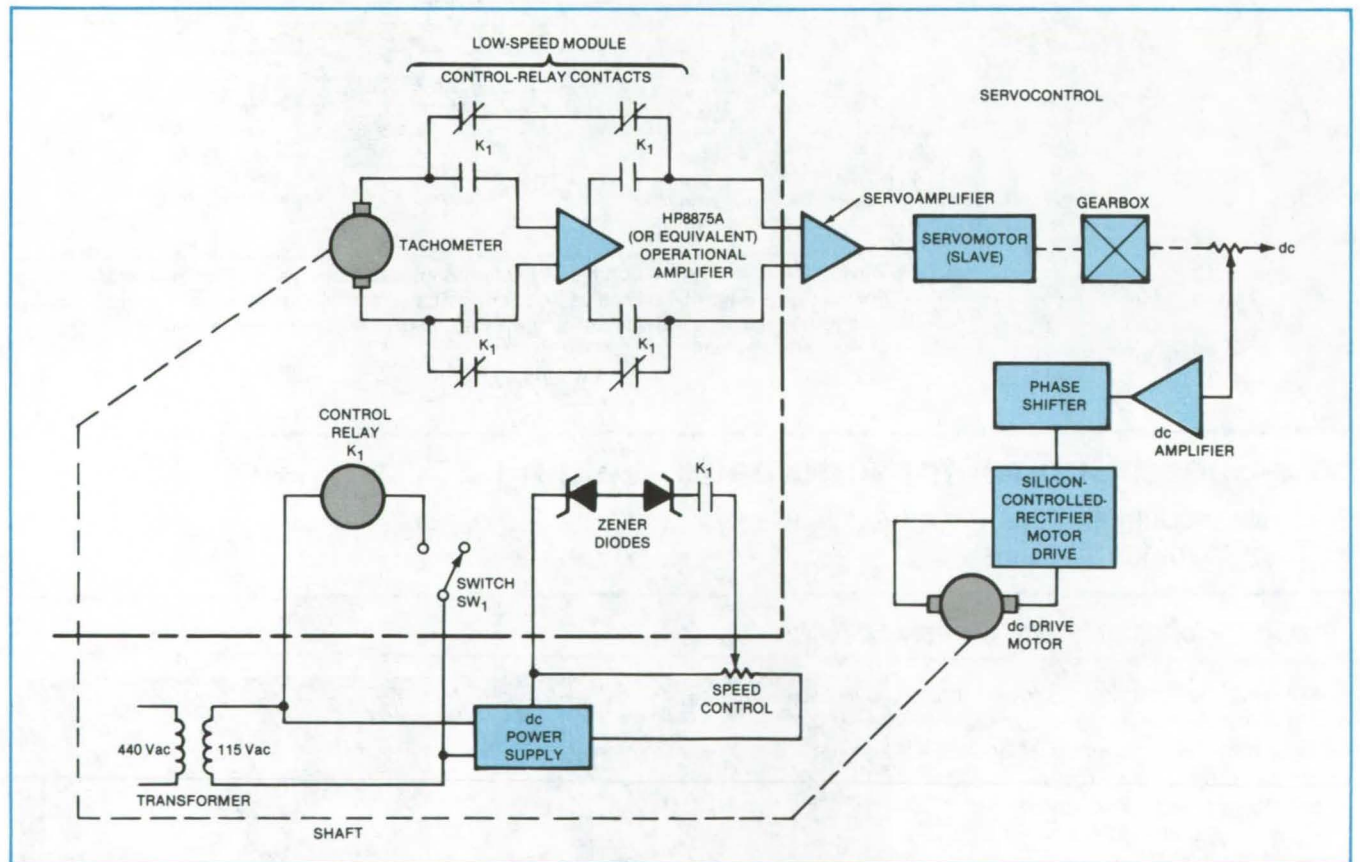
Figure 3. A **Module Amplifies a Low-Level Signal** from a tachometer at low speeds so that it can operate the servocontrol. The relay switches K_1 remove the amplifier from the tachometer loop for operation at normal speeds.

Parallel Connections Would Improve Array Reliability

Extra tabs along equipotentials would salvage
functioning cells in a fractured string.

*NASA's Jet Propulsion Laboratory, Pasadena, California*

A pattern of interconnecting tabs proposed for arrays of photovoltaic cells would be superior to simple end connections of strings. By placing tabs along equipotentials of adjacent strings, "good" portions of a string would not be lost even if one or more of the string elements fracture.

As shown in the figure, the hexagonally-packed solar cells are connected as vertical series strings. In the new scheme, additional tabs are placed between adjacent strings. These parallel connections are attached between equipotential surfaces and carry no current if all cells are matched and are functioning normally. If a cell fails though, these tabs carry current to bypass the inoperative cell.

Before assembly, each cell is pretabbed and pretinned. There are two types of cells. A type I cell is prepared with one series-interconnecting tab, plus a solder pad to receive the series tab from the next type I cell in the string, and two pads to receive the parallel-interconnection tabs from the adjacent equipotential type III cells. A type III cell is prepared with the series tab, two parallel tabs, and a solder pad to receive the series tab from the next type III cell in its string.

Type I cells are deposited face down in the series direction in alternating columns, so that the series tab connected to each cell contacts the solder pad of the next cell in the column. Then the type III cells are deposited face down in the columns between the type I cells, oriented so that the parallel tabs of the type III cells contact the parallel solder pads of the type I cells. The cells are held in place by vacuum. The assembly is then radiantly heated to reflow all solder joints, forming a completely interconnected array.

The two-dimensional connection pattern provides strength and structural
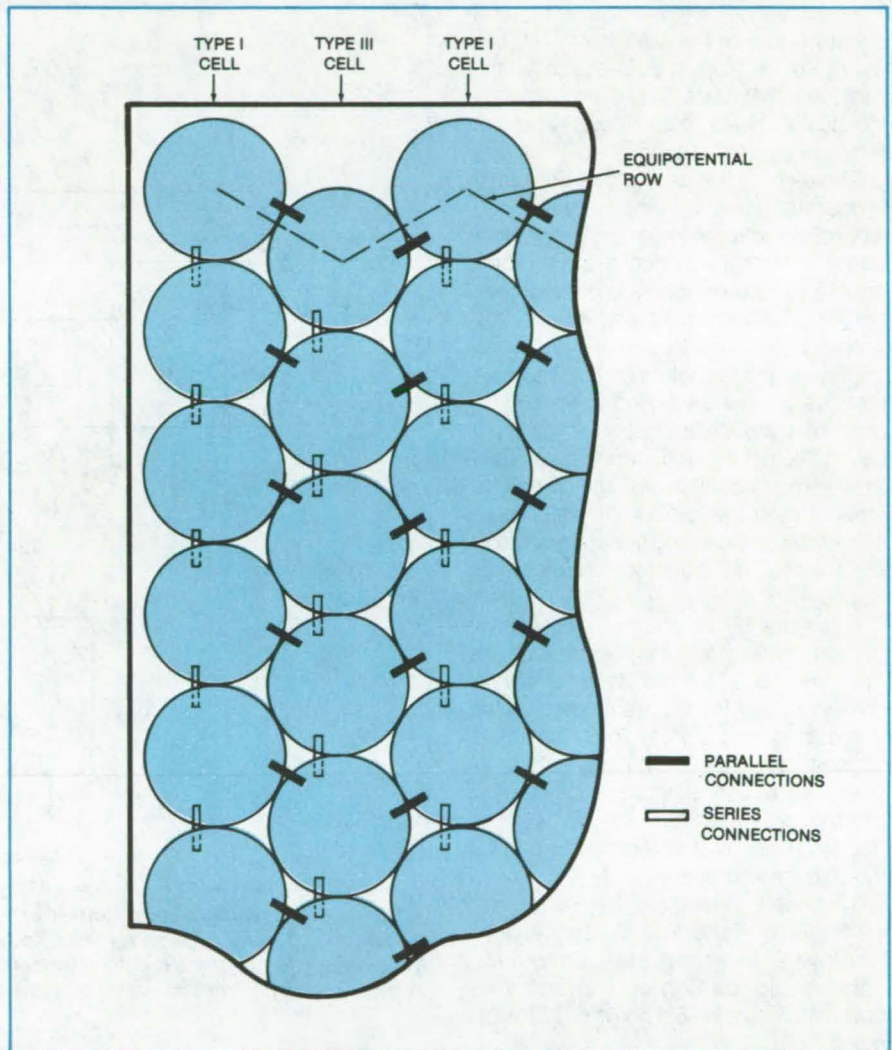
Hexagonally-Close-Packed Round Solar Cells are interconnected in series strings (vertical axis on this page). Parallel contacts between cells at equipotential in adjacent series strings insure redundant current paths to relieve the adverse effects of cell failures and mismatches.

integrity. The completed array can be moved as a unit and should withstand the lateral forces that tend to displace cells during the double-glass lamination process.

Inexpensive Logic-Level Converter

Transformer circuit allows two-way communication between a
high-level data bus and low-level TTL integrated circuits.

Lyndon B. Johnson Space Center, Houston, Texas

A relatively-simple transformer circuit
boosts 0-to-5-volt pulses from TTL cir-
cuitry to ± 10-volt pulses for trans-
mission over a data bus. It also reduces
the bus voltages to the lower voltages
required by TTL circuitry.

The new circuit consists of the trans-
former (the three windings of which are
wound in the turns ratio 3:1:1), two volt-
age-reference networks, a quad differ-
ential line receiver, and a line driver (see
figure). The common lead of the 1:1
windings is connected to + 5 volts. As
the remaining two leads on the 1:1 wind-
ings are alternately pulled to ground by
ones and zeros during transmission, a
bipolar ± 10-volt signal appears across
the 3 winding. The voltage range is
smaller than the ± 15 volts that would
otherwise be expected because of resis-
tive loading, and transformer and driver
losses.

Resistors R_2 and R_3 in the receive
branch provide a 4.5-volt reference so
that only bus signals with a swing
greater than 1.5 volts are passed on for
processing and conversion. The large
capacitor on the 1:1 winding acts as a
filter and a charge-storage device for
transmission. Resistors R_4 and R_1 in the
transmission branch provide a TTL
threshold reference.

*This work was done by Steven W.
Wilcox and Salvadore J. Zuccaro of
Rockwell International Corp. for*
Johnson Space Center. *For further in-
formation, Circle 5 on the TSP Re-
quest Card.*
MSC-18965
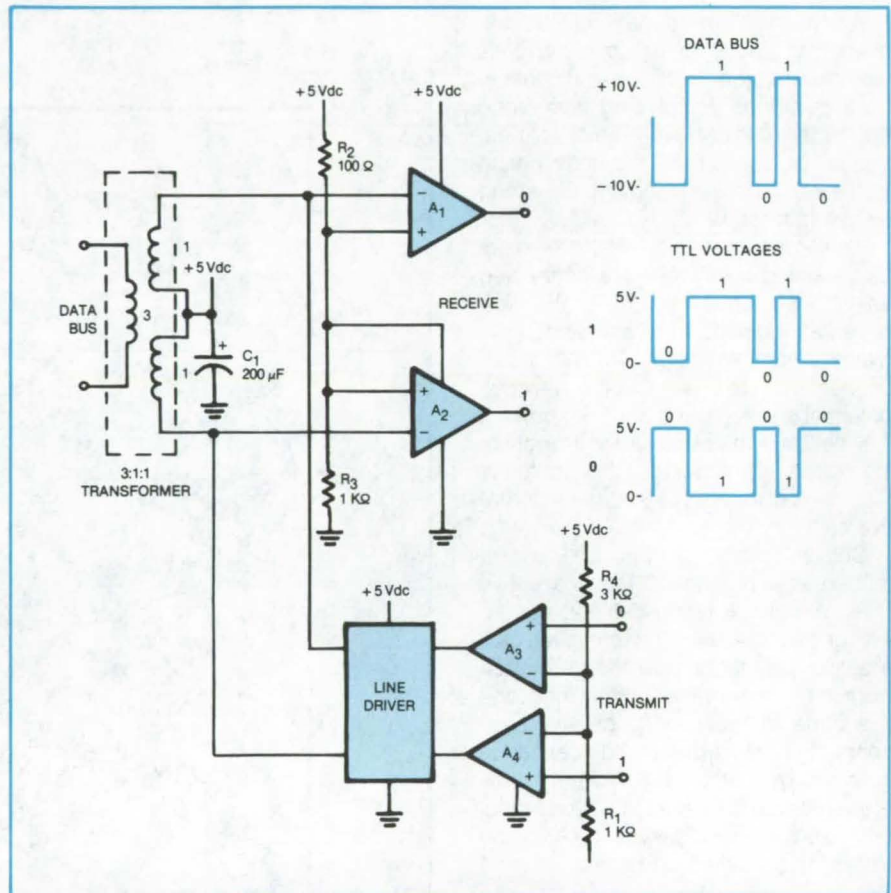
A **Bidirectional Voltage-Level Converter** links a data bus and TTL circuitry via a 3:1:1
transformer. A_1, A_2, A_3, and A_4 are differential amplifiers housed in the same package.
The waveforms show the relationship between the data bus voltage and ones and zeros
in the transmitting and receiving branches.

Electronic Systems
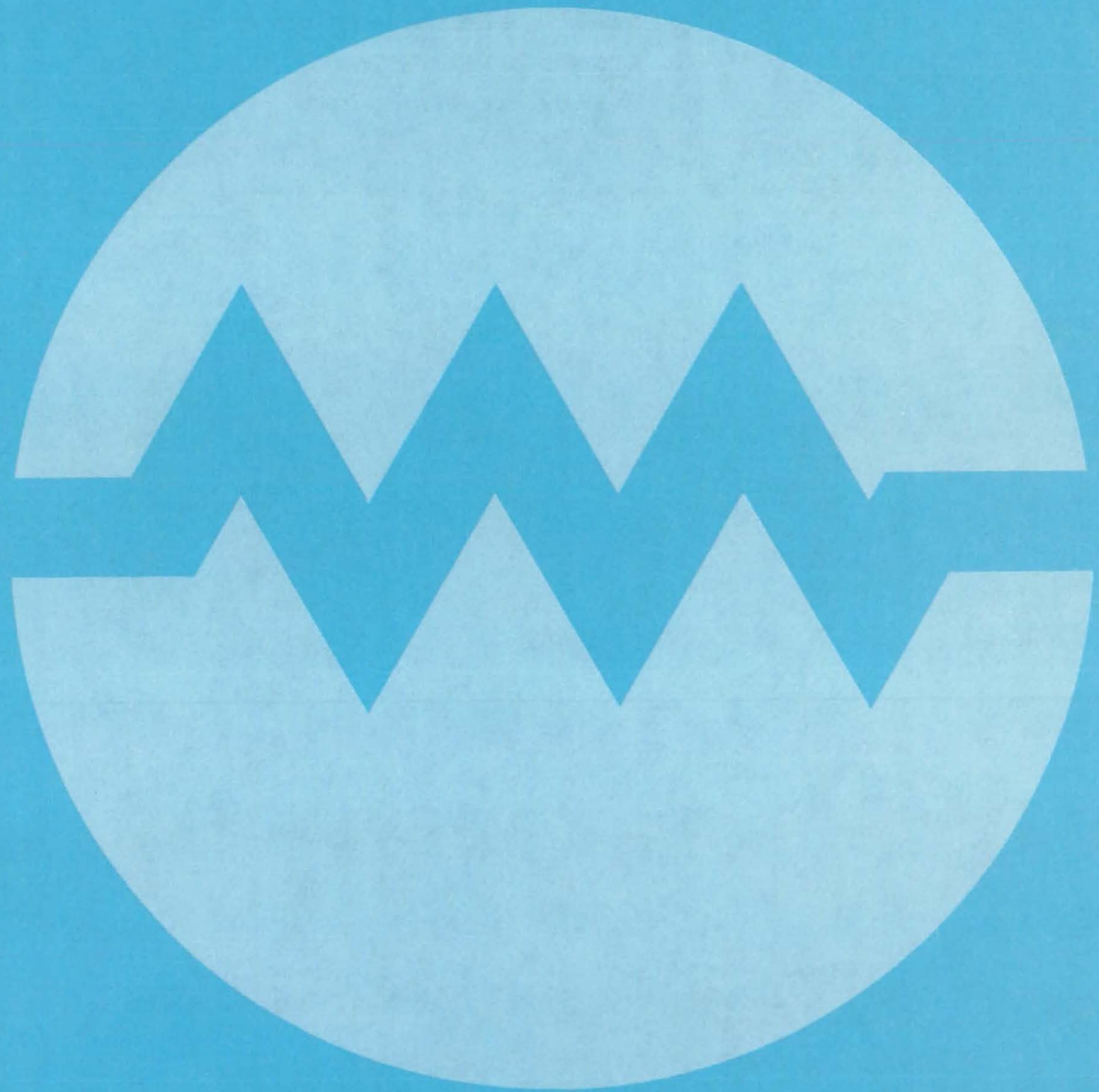
Hardware, Techniques, and Processes

Programable Pulse Generator

Pulse lengths and sequence from many
outputs are readily altered.

NASA's Jet Propulsion Laboratory, Pasadena, California
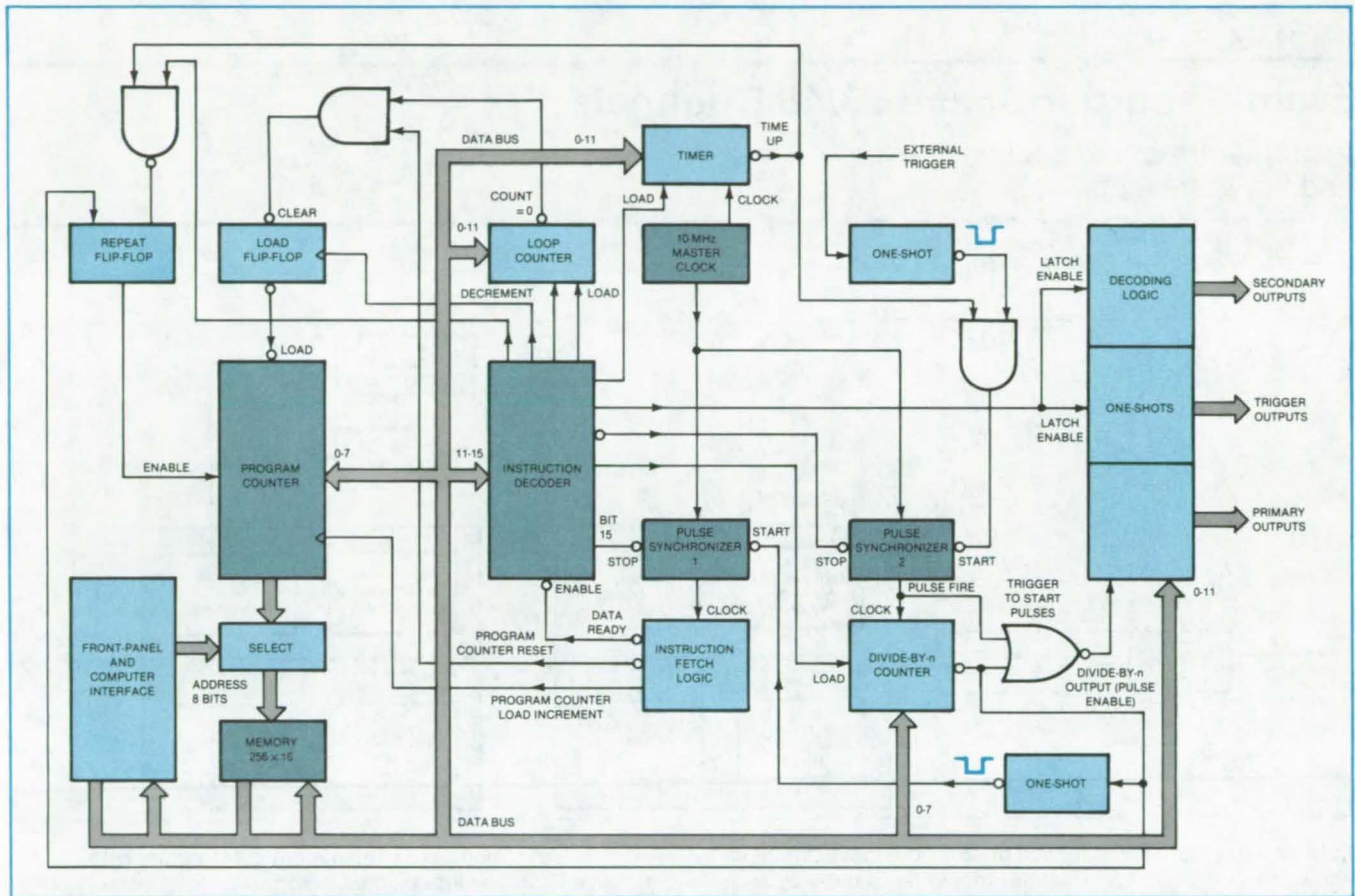
Fast Instruction Fetching is a feature of the programable pulse generator. It reads and executes instructions, under the control of pulse synchronizer 1, while pulse synchronizer 2 controls the timing of output pulses.

A new pulse generator can be programed to produce pulses from several ports at different pulse lengths and intervals and in virtually any combination and sequence. The generator operates at intervals between pulses as short as 0.5 μs. Its timing resolution is within 0.1 μs. High-speed logic circuits and specially designed instructions that can be read in groups of two or more between output pulses give the unit its speed and resolution.

The unit contains a 256-word-by-16-bit memory that is loaded with instructions either manually or by a computer. Once loaded, the unit operates independently of the computer.

The generator produces a total of 18 pulsed outputs under program control:
- Five primary outputs (X_1, Y_1, $-X_1$, $-Y_1$, and Z_1);
- Five secondary outputs (X_2, Y_2, $-X_2$, $-Y_2$, and Z_2); and
- Eight trigger outputs (A through H).

The primary and secondary outputs are pulses with lengths that are controlled either by the program or by manual adjustment of knobs on the unit front panel. The secondary pulses occur simultaneously with selected primary pulses, as directed by the program. The trigger outputs are 1-μs pulses used to initiate external events. One primary output, one secondary output, and any number of

trigger outputs may be turned on or off simultaneously.

The pulse sequence for a nuclear-spectroscopy application is as follows: When started by an external trigger, the programer first outputs a Y_1 pulse and an A-trigger pulse and turns X_2 on. It turns X_1 on 2 μs later. While X_1 remains on, X_2 is kept on for periods of 3 ms, followed by 5-ms periods during which 200 Z_1 pulses are sent out to trigger data collection. After 10 such cycles, during which 2,000 data points are gathered, X_1 is turned off.

Timing for the programer is derived from a 10-MHz master clock (see figure). The fetching and execution of instruc-

tions are controlled by a pulse synchronizer. A similar pulse synchronizer operates a divide-by-n counter, which controls the timing of the output pulses. While the programer is reading and executing instructions, the divide-by-n counter is being decremented every 0.1 μs. When the counter reaches zero, it generates a "pulse enable" signal, and the pulses selected by the programer are sent out on the next falling edge of the output from pulse synchronizer 2. The end of the pulse enable signal restarts pulse synchronizer 1 after each pulse is sent out, and instruction fetching and execution then resume.

Event Recorder Scans 2,048 Channels

Instrument records sequence
and time of events.

Marshall Space Flight Center, Alabama
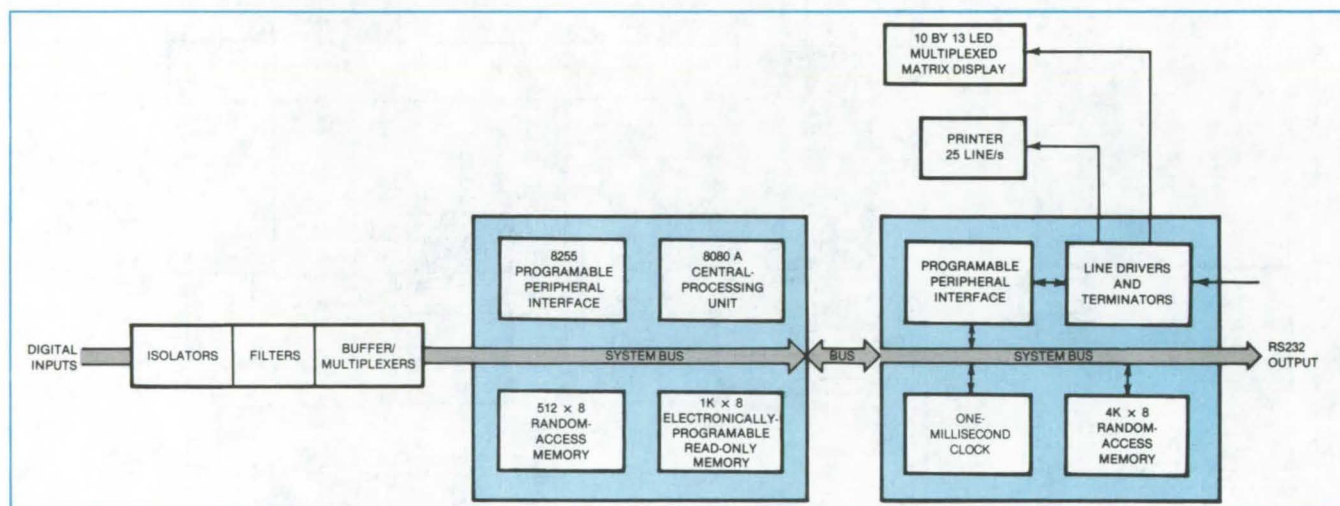
Up to 16 Input Signals Feed Each of up to 128 Input Circuit Cards. A single input circuit card contains optical isolators with input-diode clamping, RC filters, Schmitt-trigger input buffers, and a 16-to-1 multiplexer. The input circuit cards feed logic, memory, and input/output circuits, all of which are standard, off-the-shelf devices.

The nature and time of occurrence of each event in a complex sequence of events (for example, valves opening and closing or switches turning on and off) is recorded by a microcomputer-based instrument. After they have been recorded, the events could be analyzed to determine whether they occurred at the right time and in the proper sequence. The instrument could be useful in monitoring the operation of manufacturing machinery and in furnishing information useful in the diagnosis of machinery malfunctions.

The data-input section of the digital event recorder consists of 16-channel printed-circuit cards. The channels are multiplexed to a single output line. As many as 128 cards can be bused together for a total of 2,048 event channels.

The microcomputer consists of standard components: an 8080 microprocessor, read-only memory for program storage, random-access memory for data storage, and input/output ports for communication with external devices including a larger computer for data reduction.

A small 20-column strip printer prints channel number, time, and value of each event after all the data have been recorded. A light-emitting diode display, containing a diode for each of the input channels, is used to troubleshoot the inputs. The display scans the inputs at a rate of 100 channels per second. When assembled, the instrument measures less than 18 inches (45.7 cm) in height and fits into a standard equipment rack.

Scanning Seismic Intrusion Detector

An array of sensors is scanned
to locate a signal source.

*Ames Research Center, Moffett Field, California*

An intrusion detector developed by NASA may find uses in industrial-security systems. The new unit adds multiplexing and scanning electronics to conventional detector circuitry, so that a single operator can monitor an area served by a large number of seismic sensors. In a typical example, an array of 20 sensors spaced 23 feet (7 meters) apart can monitor a rectangular strip 23 feet wide and 460 feet (140 meters) long.

Typical sensors used with the new system are moving-coil seismic pickups. To sense vibrations caused by surface movements, they would be buried near the surface. To detect tunneling, they would be buried mounted on rigid metal rods, which serve as waveguides for tunneling noises originating farther below the surface. Each sensor is connected to the monitor by a pair of wires running in a buried cable.

The leads from each sensor are connected to a gate, as shown in the figure. When the system is operating in the summing mode, all the gates are turned on, so that the outputs of all the sensors are summed in the receiver. The receiver output is fed to the audio detector, where it is compared with a threshold or trigger signal level. If the received signal exceeds the threshold, the detector output activates an oscillator to produce an audible alarm.

In the scanning mode, an up/down counter run by a clock sequentially switches on the individual gates so that individual sensors are scanned rapidly. If the output of a sensor exceeds the threshold, the output of the audio detector triggers the alarm as before, and it also stops the scanning action at that sensor. A light-emitting-diode display indicates which sensor is being monitored. The operator can then manually increment or decrement the up/down counter to scan the sensors in the vicinity of the one that triggered the alarm, to locate the signal source more precisely. The operator restarts the scan by pressing the "start" button.

The monitor circuit includes manual- and automatic-gain-control options. The automatic-gain-control circuit reduces the receiver sensitivity in response to an increase in average input-signal amplitude, so as to prevent background noise from triggering the alarm.

*This work was done by Robert D. Lee of **Ames Research Center**. For further information, Circle 8 on the TSP Request Card.*

Inquiries concerning rights for the commercial use of this invention should be addressed to the Patent Counsel, Ames Research Center [see page A5]. Refer to ARC-11317.

The **Scanning Seismic Intrusion Detector** employs an array of automatically or manually scanned sensors to determine the approximate location of an intruder. The automatic-scanning feature enables one operator to tend a system of many sensors.

Measuring the Electrical Properties of Epoxies

Resistances of precisely molded specimens
are tested with a four-point probe.

Marshall Space Flight Center, Alabama

Two new techniques rapidly determine the low-frequency resistivity of conductive epoxies and the high-frequency dielectric properties of insulating epoxies.

Electrical resistivity of conductive epoxy resins can be determined conveniently and accurately with the aid of a mold that holds epoxy specimens while they cure and during property testing. Conductive epoxies are widely used as replacements for solder in semiconductor packages, and a wide variety of epoxy formulations is available.

The mold consists of a block of plastic in which a pattern of channels has been machined (see figure). Rexolite plastic was chosen as the mold material, in part because it is a high-quality dielectric. It can easily be machined to a high degree of precision and tolerance with standard shop equipment. Its dimensions are stable over a wide temperature range: Therefore curing and temperature-storage tests do not affect the dimensions of the epoxy sample. The channels can be machined to any required depth to simulate realistically the thickness of epoxy in a given application.

The channels are filled with the epoxy sample, which is then cured according to the manufacturer's specifications. Subsequent testing is done with the epoxy in the mold.

SIDE VIEW
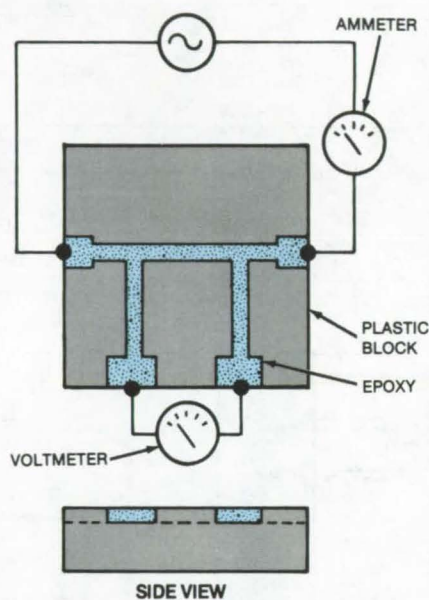
Conductive Epoxy Is Molded in channels in a plastic block. A four-point ohmmeter is used to apply current and sense the voltage; it reads out the resistance. Because the mold has precise and stable dimensions, it produces accurate and consistent measurements.

The resistivity of an epoxy is determined by a four-point ohmmeter, commercially available from several instrument manufacturers. As shown in the figure, the ohmmeter applies a known current through the long channel and measures the voltage drop along a portion of the channel. The resistivity is equal to the product of the measured resistance and channel cross-sectional area divided by the channel length between voltmeter contacts.

For an insulating epoxy, the dielectric constant and loss tangent (a measure of high-frequency resistivity) are determined from measurements of capacitance and Q of a capacitor in which a disk of the epoxy serves as the dielectric element. It is not necessary to metalize the epoxy. One merely places the disk between the electrodes (not touching the upper electrode), then performs the measurements at two different known upper-electrode positions. The relative dielectric permeability and loss tangent are easily calculated in terms of the measured quantities.

This work was done by Jerry E. Sergent of the University of South Florida for **Marshall Space Flight Center.** *For further information, Circle 9 on the TSP Request Card.*
MFS-25656

Automatic Calibration Systems

Several automated systems are available
for calibration of research instruments.

Langley Research Center, Hampton, Virginia

Over 25,000 research test instruments and instrumentation systems are in use at the multitude of test facilities at Langley Research Center. A continuous requirement exists for calibration and environmental testing of these instruments, in conjunction with their maintenance, development, and improvement.

Key calculator-based automatic-calibration and data-acquisition systems and programs for their implementation are summarized below:
• *Six-Component Balance:* Force balances having up to six components are calibrated using an automatic data-acquisition system with an uncertainty

of ±0.005 mV or approximately ±0.1 percent full-scale output. There are seven identical systems with interchangeable, commercially available components. The controller is a Tektronix 4051 calculator that acquires, displays, prints, and stores the data on internal magnetic tape. The

tape is transmitted to a centralized computer complex for data reduction.

• *Multimeter:* This system, using an HP 9830B calculator and a Fluke 5100A calibrator, automatically calibrates a variety of multimeters from various vendors, including Simpson, Data Technology, Triplett, Fluke, HP, Data Precision, United Systems, Newport, and Keithley. All multimeter functions and ranges are tested for accuracy and linearity, with the 5100A automatically flagging out-of-tolerance conditions.

• *Amplifier:* This system, using an HP 9830B calculator, a Fluke 5100A calibrator, and control panels, developed "in-house," is used to test Neff, Datametrics, and Kistler instruments. System tests include gain, linearity, and frequency response. As in the other calibration systems, a final data sheet is produced by the data system showing all tabulated results.

• *Pyrometer:* This system is comprised of an HP 9830B calculator, a Fluke 5100A calibrator, and a Joseph Kaye 140-4 ICE point reference. It tests Fluke, Ircon, and Thermo-Electric pyrometers and has a temperature calibration range of −212° to +1,760° C. Among the items tested are upper and lower range accuracies and linearity.

• *Decade Box:* This system uses an HP 3455A Digital Voltmeter, an HP 9830B calculator, and an HP 9866B thermal printer to test Shallcross, General Radio, Vishay, Rubicon, and ESI decade resistors. After all decades are tested, a final data sheet showing all data points, corrections, tolerances, and out-of-specification readings is supplied by the calculator system.

• *Voltage-Controlled Oscillator:* Among VCO's tested are those available from Conic and Space Age. The system is comprised of all commercially available equipment, including an HP 9830 calculator. It features calibration ranges of 0 to 5 volts, ±2.5 volts, and ±0.01 volt. Calibration uncertainty is <0.1 percent of linearity. Over 400 incremental voltage steps are applied to the VCO to characterize the voltage-to-frequency transfer function.

• *Pressure Transducer:* This system uses commercially available components to test pressure transducers with an analog voltage output. Calibration ranges are 0 to 50 psia, 0 to 10 psid (68×10^3 N/m^2) and 0 to 100 psid (680×10^3 N/m^2) and can be performed over a temperature range of −54° to +180° C. A maximum of 20 transducers can be calibrated at one time with a maximum of 21 data points each. Fewer transducers can be calibrated at correspondingly more data points. The system is interfaced to a programable pressure standard (Ruska DDR-6000) and provides completely-automatic control, acquisition, processing, and data-sheet preparation.

• *Accelerometer:* This system uses commercially available components to test accelerometers from a variety of manufacturers. It is used to determine the linearity, hysteresis, sensitivity, bias, misalinement, stability, and temperature coefficients of accelerometers. Calibration uncertainty is <100 micro-g's.

Radiometer Noise-Injection Control

A digital counter is used in a closed-loop noise-injection feedback microwave radiometer.

Langley Research Center, Hampton, Virginia

A new technique for controlling noise injection in a Dicke feedback noise-injection microwave radiometer utilizes a digital counter in which the noise injection is kept on during a countdown interval. The digital portion of the loop replaces analog filters used in previous systems.

Although the closed-loop noise-injection feedback concept is the most recent advance in microwave radiometers, the noise-injection scheme that has been used suffers from certain limitations. This process uses short pulses that turn off and on a PIN diode, which acts as a gate for a controlled precise noise source. The injection noise is balanced against the input electromagnetic signal, allowing a measurement of the
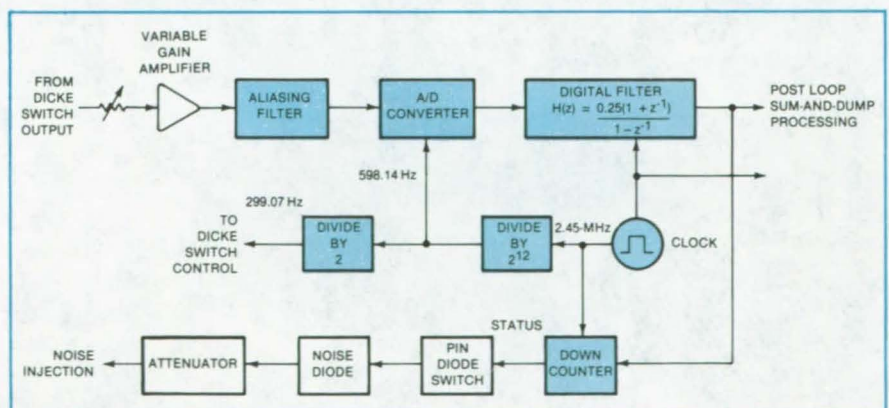
Loop Estimation and Feedback System is used in noise-injection control for a Dicke radiometer.

noise required to achieve the balance. The noise injection is controlled by varying the number of pulses per unit time, with the injected temperature a direct function of the number of pulses. Thus, a count of the number of pulses in a given time provides a means for determining the injected noise.

Limitations of the technique are related to the necessity to provide adequate bandwidth to process short pulses and the transient response resulting from the continual switching requirements. Since bandwidth is inversely proportional to pulse width, and since the resolution of the measurement is inversely proportional to the number of injected pulses, a large bandwidth is required for adequate pulse reproducibility. An inadequate bandwidth will result in serious pulse distortion and degraded resolution.

The new technique uses digitally-controlled continuous feedback (see figure) over a significant portion of a duty cycle rather than the short off/on pulses. The typical feedback interval would be of the order of 1 to 3 milliseconds, compared to time intervals of the order of 70 microseconds for previous schemes. The countdown time is directly proportional to the value of a digital word appearing at the output of a digital processing filter.

The digital-counter injection process has several distinct advantages over the analog system previously used. The noise is injected over a much longer interval of time, eliminating the need for the wide bandwidth associated with the short pulses. Measurement is made by digitally measuring the width of the much longer pulse rather than the number of short pulses, thus improving accuracy. Resolution can be arbitrarily

established based on the number of bits in the digital words, and the digital circuitry in the estimation and counter control circuit is less sensitive to drift and temperature than previous systems.

Physical
Sciences
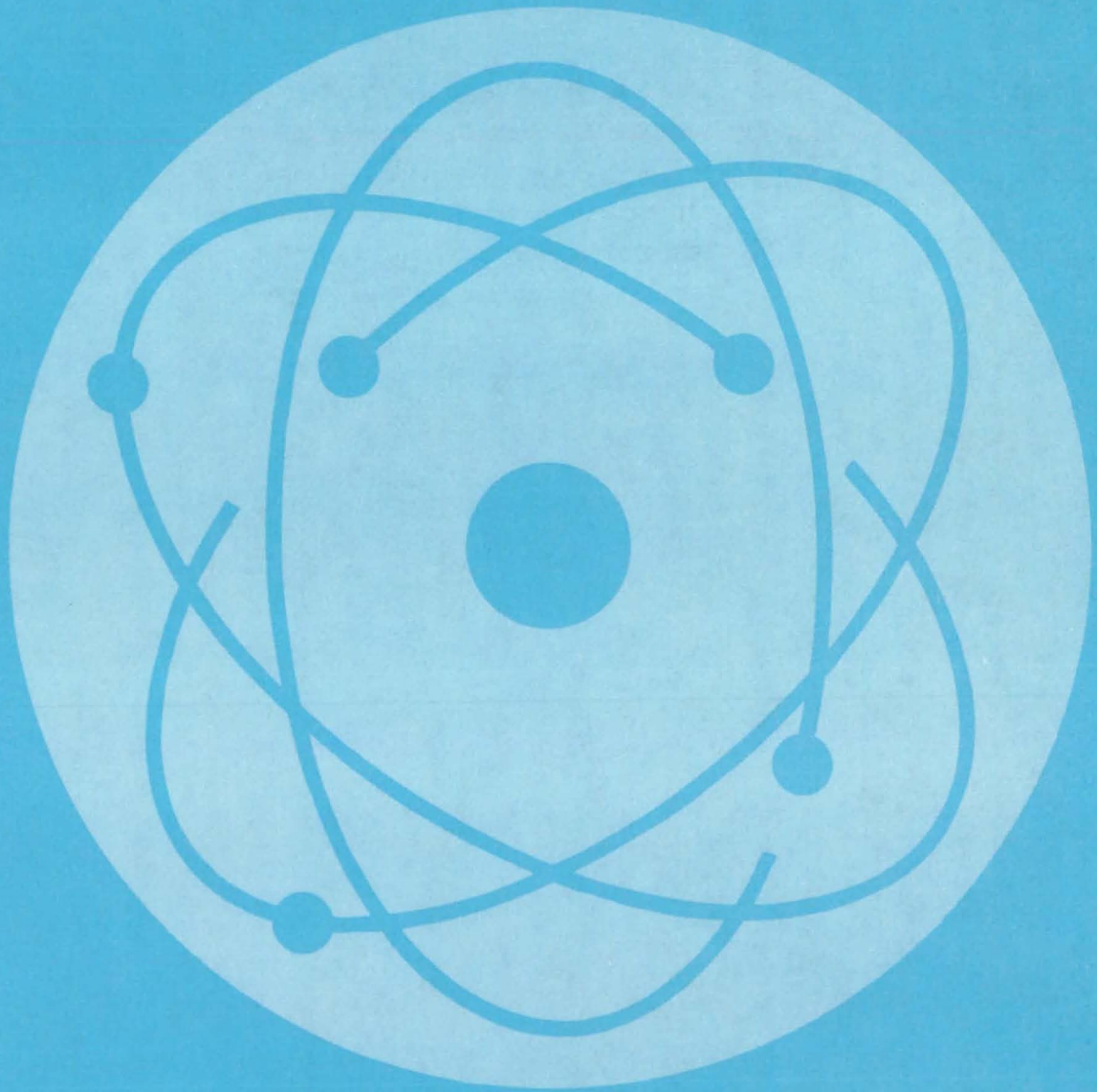
Hardware, Techniques, and Processes

Books and Reports

# Stable Stratification for Solar Ponds

A disodium phosphate brine forms density layers
spontaneously and reforms them after a disturbance.

NASA's Jet Propulsion Laboratory, Pasadena, California

Laboratory experiments have shown that a stable density gradient forms in a pond saturated with disodium phosphate (DSP). DSP increases in solubility with temperature, as does the density of the DSP solution. A volume of DSP-saturated water therefore tends to develop temperature and density layers. Since tests indicate that the thermal and density gradients remain in equilibrium at heat removal rates of 60 percent or more of the heat input rate, a pond containing DSP would be suitable for collecting solar energy and transferring it to a heat exchanger for practical use. Moreover, it appears that such a pond would restore its equilibrium gradient relatively quickly after its layers are mixed by wind action.

Experiments were conducted in a simulated pond in which hot water flowing through a coil provided the heat that would normally be furnished by the Sun. Water flowing through a second coil extracted heat from the pond (see figure). Temperature gradients were measured by copper-constantan thermocouples, and density gradients were measured by a Troemner balance. Measurements were made while the heat input was held constant and the heat output was varied (by varying the flow rate of cooling water). At low heat-extraction rates — about 60 percent — the temperature gradient in the pond remained unchanged, except near the bottom, where the heat was extracted.

DSP precipitation from the solution is expected to be a problem only when the temperature difference inside and outside the cooling coil is too large (more than 15° C). In the continuous heat-extraction test, the average water temperature in the cooling coil was 37° C, and the temperature of the pond brine was 49° C around the cooling coil.
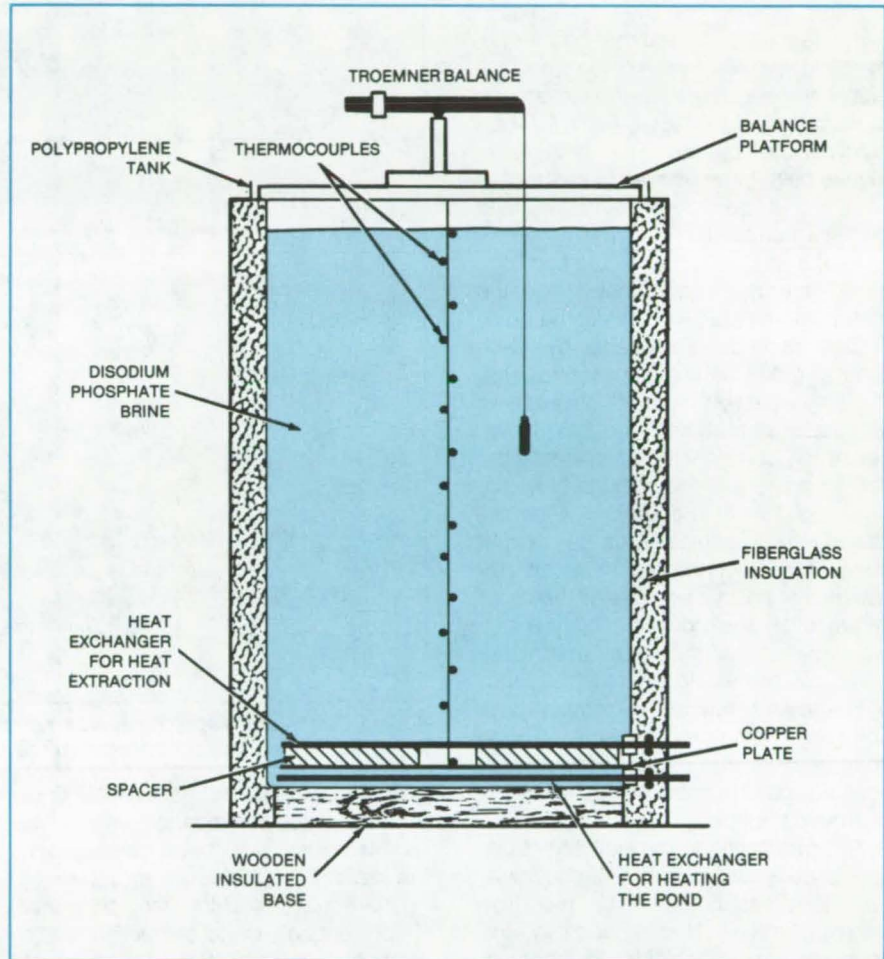
A **Simulated Solar Pond** contains provisions for heating the pond solution of disodium phosphate in water and removing heat from it, as well as for measuring the temperature and density of the solution at various depths.

As part of the experiments, the steady-state temperature and density profiles were disturbed by thorough mixing of the pond liquid. Within a few days, the profiles had begun to approximate their original states; and within 2 weeks, the original stratification was completely regenerated. This indicates that mixing caused by the wind or by the withdrawal of pond water has no lasting effect.

Improved Estimates of Thermodynamic Parameters

Techniques are refined for estimating heat of vaporization
and other parameters from molecular structure.

NASA's Jet Propulsion Laboratory, Pasadena, California

Improvements in the "group-additivity" technique for estimating thermodynamic parameters should make it easier for engineers to choose among candidate heat-exchange fluids for thermochemical cycles. The new techniques have been applied with success to several perfluorochemicals and hydrocarbon fluids.

In the group-additivity method, the molar energy of vaporization and the molar volume at 25° C are estimated by adding contributions made by each atom or group in the molecule structure.

Using a parabolic equation with three adjustable parameters, the heat of vaporization can be used to estimate the boiling point, and vice versa. New parameters for this equation were obtained from a least-squares best-fit curve for 19 perfluorochemicals for which the boiling points and heats of vaporization are known. Similarly, a simple equation using two parameters, α and β, can be used to estimate the vapor pressure as a function of temperature. The table compares measured boiling points and vapor pressures of some nonpolar liquids with those estimated by the improved method.

The miscibility or immiscibility of two liquids depends upon the negativity or positivity, respectively, of the free energy of mixing. This depends, in turn, on the square of the difference between the solubility parameters of the two liq-

Compound	Calculated ΔH_V (cal/mole)	Calculated Boiling Point (°C, at 760 Torr)	Measured Boiling Point (°C, at 760 Torr)	Calculated Vapor Pressure (Torr, 25° C)	Measured Vapor Pressure (Torr at/T° C)
$n - C_6F_{14}$	7,590	59	57	202	220/25
(F F ring structure)	10,608	141	142	11.1	6.6/25
$CF_3CHF[OCF_2CF(CF_3)]_3F$	11,110	152	152	7.4	10.0/37.5
$CF_3CHF[OCF_2CF(CF_3)]_5F$	15,766	244	224	0.4	0.4/37.5
$(CF_3CF_2CF_2CF_2)_3N$	12,524	183	174	2.6	2.5/37.5
(cyclohexanone structure)	11,870	179	155.8	1.6	2.7/25
$n - C_9H_{20}$	11,051	160	148.8	3.0	4.3/25
$n - C_8H_{18}$	9,860	130	123.0	14.0	7.7/25
(ring)$CH_2CH_2CH_2CH_2$	12,097	185	181.4	1.4	1.1/25
(ring)Br	10,839	154	152.3	3.5	4.2/25
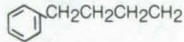
Boiling Points and Vapor Pressures for some nonpolar liquids were estimated by the improved method and compared with previously reported values.

uids. These parameters are obtained from the energy of vaporization and molecular volume, which are estimated on the basis of the molecular structure.

The equations of this method are all simple enough to be set up on a programable hand calculator. They are first-order approximations to be used as a guide in the rapid screening of candidate fluids for thermochemical systems.

This work was done by Daniel D. Lawson of Caltech for **NASA's Jet Propulsion Laboratory.** *For further information, Circle 13 on the TSP Request Card.*
NPO-14880

Equation for Combustion Noise

Mathematical expression relates noise to characteristics
of the combustion process.

NASA's Jet Propulsion Laboratory, Pasadena, California

A mathematical relationship has been derived for the interactions between a turbulent flame and combustion noise. The relationship is a rigorous theoretical correlation of combustion noise and the combustion process. As such, it establishes a foundation for acoustic measurements as a tool for investigating the structure of turbulent flames. The rela-

tionship was established by integrating previously-developed turbulent-flame models with the theories of combustion noise. Unsteady heat release is taken into account.

The mathematical relationship is expected to aid researchers in the field of noise generated by combustion. Such noise is a strong contributor to the total

noise radiated by turbine engines and heavy industrial burners. It is not only an annoyance to humans but also may cause the failure of liners and other components.

The derivation of the relationship starts with the wave equation describing pressure fluctuations in terms of the

speed of sound, specific heats of the gases, the heat of combustion, and reaction rate. The instantaneous reaction rate is idealized as a pulse train (see figure), the strength of which corresponds to the average amount of combustion product created per flame passage and the frequency of which varies across the reaction, eventually going to zero.

Whenever a flamelet passes through the turbulent reaction zone, it generates a pair of impulses separated by a time interval and thus causes pressure fluctuations. The frequency of the pulse train is related to the spacing of eddies. The final equation in the derivation describes
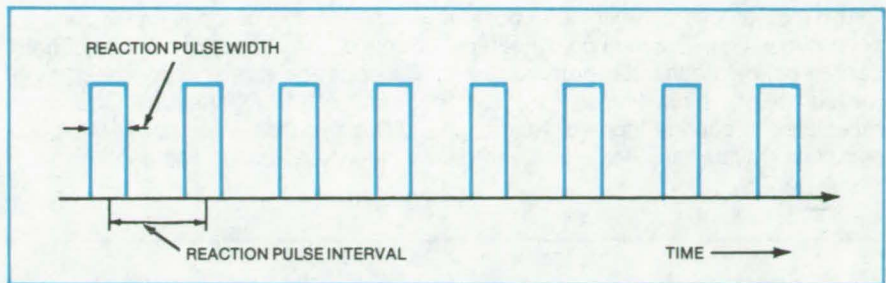
Reaction Rate Varies With Time as a pulsating waveform according to the simplified model used in the calculations. The reaction pulses generate the acoustic waves perceived as combustion noise.

the resultant sound pressure in terms of position, frequency, time, and a variety of physical parameters.

This work was done by Tsong-mou Liu *of Caltech for* **NASA's Jet Propulsion Laboratory.** *For further information, Circle 14 on the TSP Request Card.* NPO-15156

Finding the Focal Axes of Offset Antennas

A null technique reveals the direction of the true focal axis.

Goddard Space Flight Center, Greenbelt, Maryland

The focal axis of offset paraboloidal reflector antennas can now be determined by direct measurement instead of by trial and error. Knowledge of the focal axis is necessary for controlling squint, which occurs when the feed is located off the focal axis, or for controlling beamwidth by means of feed displacement along the focal axis away from the focal point.

With traditional symmetrical reflectors, determining the focal axis is not a problem; the axis can be established by passing a line through the vertex of the antenna perpendicular to the aperture plane defined by the physical rim. This is not the case, however, for such asymmetrical antennas as the offset versions now used in spacecraft and ground stations. In such antennas, the physical rim is not usually congruent with the aperture plane. The new method is a convenient and precise way of obtaining the required information.

Two transmitting feed horns, each having typically a half-wavelength aperture diameter, are placed side by side adjacent to the focal point of the reflector to be measured. The feed horns direct radio-frequency energy having a predetermined sum or difference radiation pattern (established by an amplitude and phase comparator) toward the reflector. The incident energy is reflected — again in a sum or difference pattern — to a far-field detector.
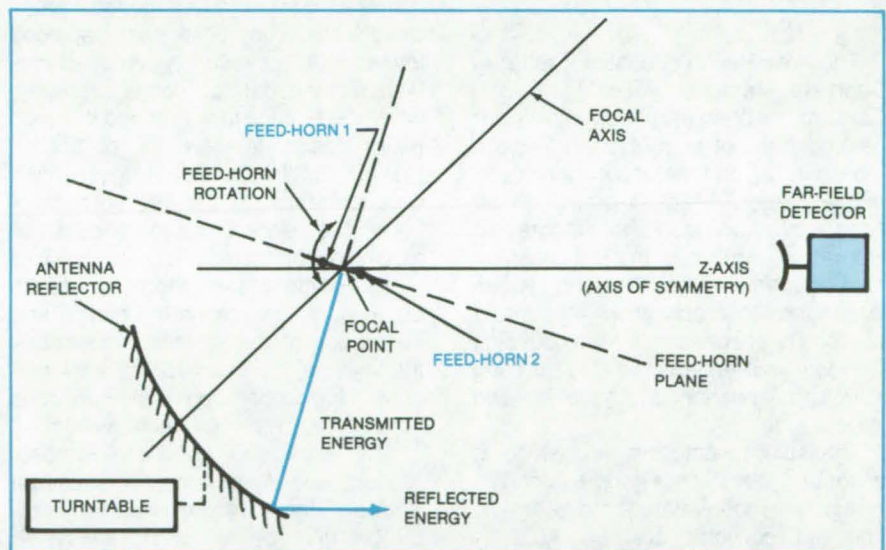
Two Feed Horns Transmit a sum or difference pattern to the antenna under test, which reflects the energy to a far-field detector. When the axis of the feed horns coincides with the focal axis of the antenna reflector, the far-field detector records a minimum in amplitude difference and a maximum in the absolute-magnitude phase difference between the sum and difference signals.

The feed horns are rotated in increments in a plane passing through the focal point while exciting the reflector (see figure). The reflector is also rotated on a turntable. The far-field detector records the far-field amplitude or phase pattern. The extreme minimum value of the amplitude difference signal occurs at that angular position of the feed horns when they are alined with the focal axis

of the reflector. When phase difference is measured instead of amplitude, a maximum of the absolute value of phase difference between the sum and difference signals indicates that the feed horns are alined with the focal axis. Four feed horns can be used instead of two. In that case, the focal axis can be resolved in not just one but two planes.

(continued on next page)

The method can be adapted to computer simulation. The method, whether carried out by a computer or by actual measurement, is not limited to offset reflectors; it can be applied to dual parabolic cylinder antennas, for example.

This work was done by Richard F. Schmidt of **Goddard Space Flight Center.** *For further information, Circle 15 on the TSP Request Card.*

This invention is owned by NASA, and a patent application has been filed. Inquiries concerning nonexclusive or exclusive license for its commercial development should be addressed to the Patent Counsel, Goddard Space Flight Center [see page A5]. Refer to GSC-12630.

Books and Reports

These reports, studies, and handbooks are available from NASA as Technical Support Packages (TSP's) when a Request Card number is cited; otherwise they are available from the National Technical Information Service.

Solar-Heated Health Education Center — North Carolina

Retrofit system supplies heat and hot water for a six-story building.

The Area Health Education Center at Charlotte Memorial Hospital in North Carolina has been retrofitted with a solar heating- and hot-water system. The six-story building contains a two-story multimedia center, 14 classrooms, 55 offices, a television studio, a photographic laboratory, and an outpatient-clinic reception area. The solar-heating system is designed to supply about 45 percent of the heat needs of the building with minimal effects on the existing structure, mechanical systems, and appearance.

The solar-heating system, which is described in a 55-page report, uses 171 collectors, roof-mounted in two arrays. The net collector area is 4,020 ft^2 (374 m^2). A water and ethylene glycol antifreeze solution is circulated through the collectors to a heat exchanger located in a lower-level equipment area. The heated water is supplied to a heating coil in the perimeter-zone air handler or to a 6,000-gal (23,000-l) storage tank, also in a lower level equipment area. Domestic hot water is provided through a secondary heat exchanger, augmented by 12-kW electrical-resistance heaters in each of three

manifolded 125-gal (473-l) hot-water tanks.

An electric heating coil is installed in the perimeter-zone air handler. The system controller first uses the heat available in the solar-energy heating coil, then makes up any deficit with the electric heating coil.

The report describes problems that arose during the first three years of operation of the system. For example, after one year of operation, most of the solar-collector panels were warped. Apparently, when the panels expand during the summer, they press against the ends and sides of their casings and become distorted. Several such panels developed leaks. They have been replaced and appear to be working. Another problem was that during summer operation, when the storage tank reached the maximum design temperature of 200° F (93° C), antifreeze heat-transfer fluid was lost through the pressure relief valve. The solution was to increase the expansion-tank size to 160 gal (606 l).

In addition, the report presents detailed information on the design and installation of the system. It describes the building, the design philosophy, and control logic operation. It also provides mechanical and electrical drawings.

This work was done by Ferebee, Walters and Associates for **Marshall Space Flight Center.** *Further information may be found in DOE/NASA CR-161731 [N81-23606/NSP], "Solar Heating and Hot Water System Installed at Charlotte Memorial Hospital, Charlotte, North Carolina" [$9]. A copy may be purchased [prepayment required] from the National Technical Information Service, Springfield, Virginia 22161. The report is also available on microfiche at no charge. To obtain a microfiche copy, Circle 16 on the TSP Request Card.*
MFS-25686

Solar Space and Water Heating for School — Dallas, Texas

Report gives overview of retrofitted circulating hot-water installation for 61-year-old high school.

The North Dallas High School, built in 1921, was retrofitted with a solar space-heating and hot-water system. A description, specifications, modifications, plan drawings — for the roof, three floors, and the basement, as well as correspondence and documents are part of a 90-page report that also gives an overview of the solar-energy project. The solar installation for the three-story brick/masonry/concrete frame school will preheat all the hot water and should supply approximately 47 percent of the annual heating. Because insufficient data were available, the actual percentage contribution of the system could not be determined. However, during the warmer months, the system will supply all of the hot water.

The solar-energy system, which circulates hot water, includes 4,800 ft^2 (44.6 m^2) of roof-mounted flat-plate liquid collectors and a 10,000-gallon (37,840-l) steel storage tank in the basement. It is designed to produce 690×10^8 Btu/year (2.3×10^7 watts). The system is interconnected with chilled-water central air-conditioning to convert to a two-pipe heating and cooling system. The existing steam boilers supply steam to hot-water generators for standby and to boost the hot-water temperature.

The existing air-handling units and water coils require only 95° F water for building heating. When the storage-tank temperature exceeds 95° F, the

steam valve is closed, and the steam boiler cycles off. Reverse-acting heating/cooling thermostats control interior conditions, and the air-unit control sequences were modified to meet heating needs. A switch controls the summer and winter modes of operation.

To prevent heat loss from the storage tank to the collectors, a comparator energizes the solar pump, and the collector drain valve closes whenever the temperature of the solar collectors is greater than the temperature in the storage tank. A timer keeps the solar pump energized for 3-minute intervals until the collector temperature falls below the storage-tank temperature, regardless of the temperature at the collectors. At the end of a 3-minute interval, if the collector temperature is less than the storage-tank temperature, a comparator deenergizes the solar pump. However, the timer allows an additional 3 minutes of "on" time before the solar pump is deactivated.

Safety features protect the system when temperatures are below 47° F or above 212° F. When the solar pump is deenergized and outdoor temperature is below 47° F, motorized vacuum breakers open and allow the collectors and their exposed piping to drain into the solar water-storage tank. The solar water-storage tank is at atmospheric pressure and will not support temperatures in excess of 212° F; the solar pump remains energized, and temperatures above 212° F are vented as steam at the water-storage tank.

This work was done by the Dallas Independent School District, Office of the General Superintendent, for **Marshall Space Flight Center.** *Further information may be found in DOE/NASA CR-161482 [N80-29847/NSP], "Solar Heating and Domestic Hot Water System Installed at North Dallas High School — Final Report" [$12]. A paper copy may be purchased [prepayment required] from the National Technical Information Service, Springfield, Virginia 22161. The report is also available on microfiche at no charge. To obtain a microfiche copy, Circle 17 on the TSP Request Card.*
MFS-25514

Solar-Heated Office Building — Dallas, Texas

Attractive building design incorporates solar-energy features.

A solar-heating system is designed to supply 87 percent of the space heating and 100 percent of the potable hot-water needs of a 10,200-ft^2 (950-m^2) office building in Dallas, Texas. A contractor report includes basic system drawings, test data, operating procedures, and maintenance instructions.

An array of 76 flat-plate solar collectors having a total area of 1,596 ft^2 (148 m^2) is mounted on a surface tilted 42° from the horizontal. A unique feature of the array is that it serves as the roofing over the office lobby and gives the building an attractive triangular appearance.

In the solar loop, an ethylene glycol/water mixture circulates through the collectors into a heat exchanger. The hot-water-storage subsystem includes two 2,300-gallon (8,700-liter) concrete storage tanks with built-in heat exchangers, and a backup electric boiler.

The building cold-water system supplies makeup water to the solar loop, the heating loop, and the concrete storage tanks. The potable hot-water system includes a water heater, a hot-water/cold-water mixing valve, a pressure-reducing valve, and expansion tanks.

This work was done by Travis-Braun & Associates, Inc., for **Marshall Space Flight Center.** *Further information may be found in DOE/NASA CR-161483 [N80-29846/NSP], "Solar Heating and Hot Water System Installed at Office Building, One Solar Place, Dallas, Texas — Final Report" [$12]. A paper copy may be purchased [prepayment required] from the National Technical Information Service, Springfield, Virginia 22161. The report is also available on microfiche at no charge. To obtain a microfiche copy, Circle 18 on the TSP Request Card.*
MFS-25515

Solar Hot-Air System — Memphis, Tennessee

System furnishes space heating for an office complex.

Solar collectors that use air as the collection medium provide space heating for a four-building office complex in Memphis. An array of flat-plate air collectors of 780 ft^2 (72 m^2) area on each building furnishes about two-thirds of the space-heating needs of the complex.

A special air-handling unit moves air through the collectors, into and out of a vessel containing heat-storage rocks [390 ft^3(11 m^3) per building], and into the heating-air ducts of the building. The air-handler motor has class B heat-resistant insulation so that it does not deteriorate as hot air flows over it.

A 98-page report furnishes details on the installation, including: A description of the system; System startup and acceptance-test results; Technical data on the collector; Installation manuals for collectors, air handler, and heat-storage unit; A system owner's manual for operation and maintenance; and as-built drawings.

If solar heat is insufficient to maintain space temperature, an electric heater in the air duct is automatically turned on. The electric heater operates in conjunction with the collectors and rock storage so that all available solar heat is utilized.

This work was done by Belz Investment Co. for **Marshall Space Flight Center.** *Further information may be found in DOE/NASA CR-161803 [N81-28521/NSP] "Solar Heating System Installed at Belz Investment Company, Memphis, Tennessee — Final Report" [$9.50]. A paper copy may be purchased [prepayment required] from the National Technical Information Service, Springfield, Virginia 22161. The report is also available on microfiche at no charge. To obtain a microfiche copy, Circle 19 on the TSP Request Card.*
MFS-25727

Modified Evacuated-Tube Collector Tested in Solar Simulator

Larger manifold improves efficiency.

According to a new report, a particular commercial evacuated-tube solar collector performs slightly more efficiently with a larger manifold. Tests were performed with the Marshall Space Flight Center solar simulator.

The solar collector uses water as the heat-transfer medium. It has a gross area of 17.17 ft^2 (1.6 m^2) and a net collection aperture of 14 ft^2 (1.3 m^2). Its thermal performance was measured while it was mounted on a table inclined 10° from the horizontal and irradiated with simulated Sunlight from tungsten-halogen lamps. Effluent water from the collector was stored in an insulated reservoir after being cooled in a heat exchanger. Measured quantities included ambient air temperature, fluid inlet and outlet temperatures, fluid-flow rate, and total solar flux.

The report describes test conditions and procedures. It provides an analysis of the results and presents tables and graphs of data, both measured and calculated.

This work was done by Wyle Laboratories for **Marshall Space Flight Center.** *Further information may be found in DOE/NASA CR-161845 [N81-32606/NSP], "Indoor Test for the Thermal Performance Evaluation of the DEC 8A Large Manifold Sunmaster Evacuated Tube (Liquid) Solar Collector" [$7.50]. A paper copy may be purchased [prepayment required] from the National Technical Information Service, Springfield, Virginia 22161. The report is also available on microfiche at no charge. To obtain a <u>microfiche</u> copy, Circle 20 on the TSP Request Card.*
MFS-25764

Onsite Measurement of All-Day Efficiency

Field Tests confirm the validity of a data base.

The all-day efficiency of selected flat-plate and evacuated-tube solar collectors has been computed from measurements taken at 36 sites in the United States. The measurements were performed month by month under actual solar and meteorological conditions. The results are documented in a 158-page report.

The purposes of the measurements were to evaluate "all-day-efficiency" calculation methods and to justify the use of available data bases in predicting solar-collector performance. All-day collector efficiency is computed from a variety of data, including hourly insolation in the plane of the collector, hourly ambient temperatures, collector fluid-inlet temperatures, collector site and orientation (latitude, tilt, and deviation from true south), and effective area of the collector.

It was found that predictions of system performance based on actual hourly data recorded by the National Oceanic and Atmospheric Agency (NOAA) are more useful for system evaluations than those based on data developed by the American Society of Heating, Refrigerating and Air-Conditioning Engineers (ASHRAE). The ASHRAE data characterize clear-day available insolation in the horizontal plane on the 21st day of each month for several latitudes within the contiguous United States. However, using the clear-day values overpredicts the monthly output of a solar-collector system, since clouds occur on many days during a month. Although ASHRAE clear-day values can be multiplied by a cloudiness factor, which has been determined for about 200 cities, the results are underpredictions of monthly outputs.

The ASHRAE clear-day solar radiation can be used to predict the highest-possible collector performance during any given month, but will not give a true measure of system performance. With the NOAA data, in contrast, the performance of evacuated-tube collectors can be accurately predicted. The performance of flat-plate collectors is overpredicted because of the higher heat loss of this type of collector; however, an accurate correction factor can be established for any given solar-collector model.

The test report provides background for the study, gives details of the all-day-efficiency calculation procedure, and discusses the ASHRAE and NOAA data bases. It presents details of the algorithm used to convert total horizontal radiation to the collector tilt plane at a given site. The report contains tables and graphs of the test results.

This work was done by Wyle Laboratories for **Marshall Space Flight Center.** *Further information may be found in DOE/NASA CR-161866 [N82-10504/NSP], "Evaluation of All-Day Efficiency for Selected Flat-Plate and Evacuated Tube Collectors" [$15]. A paper copy may be purchased [prepayment required] from the National Technical Information Service, Springfield, Virginia 22161. The report is also available on microfiche at no charge. To obtain a <u>microfiche</u> copy, Circle 21 on the TSP Request Card.*
MFS-25782

Materials

Ensuring the Consistency of Silicide Coatings

The optimum fusion time is
determined from a simple diagram.

Lyndon B. Johnson Space Center, Houston, Texas

A diagram specifies the optimum fusion time for given thicknesses of refractory metal-silicide coatings on columbium C-103 substrates. Adherence to the indicated fusion times ensures consistent coatings and avoids underdiffusion and overdiffusion.

The diagram was developed as a result of X-ray tests on chamber-nozzle assemblies for the Space Shuttle reaction-control-system thrustors. For oxidation protection, the columbium parts of the assemblies are coated with silicide. The coating is applied as a slurry of silicon, chromium, and titanium powders then vacuum-fused at 2,580° F (1,415° C). X-ray diffraction inspection revealed structural anomalies in the coatings on some of the parts. The anomalies were traced to a metal-trisilicide hexagonal phase on the coating surface. This phase rapidly oxidizes, then spalls when it is heated.

Excessive time at the fusion temperature causes a loss of silicon by vaporization and promotes formation of the hexagonal phase after the normal metal-disilicide phase is formed. Figure 1 shows the development of the hexagonal phase as the time increases, for one coating thickness.

The phase diagram that relates coating thickness to fusion time is seen in Figure 2. It shows the allowable combinations of coating thickness and fusion time that ensure that only the normal phase is present. The accuracy of the diagram has been confirmed by tests.

This work was done by Ven Ramani and Francis K. Lampson of The Marquardt Co. for **Johnson Space Center.** *No further documentation is available.*
MSC-18900
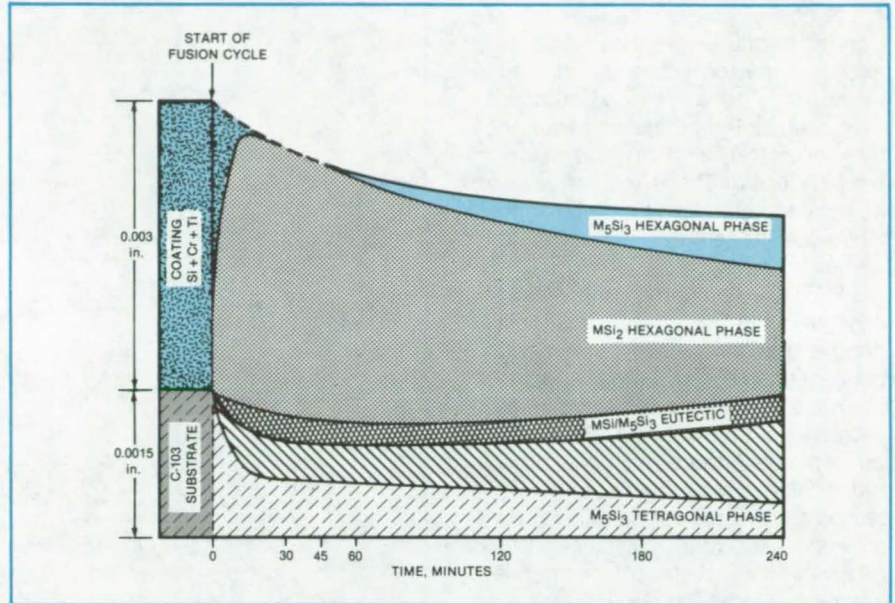
Figure 1. The **Development of the M_5Si_3 Hexagonal Phase** on silicide coatings is seen in this graph. For this coating thickness [0.003 in. (0.076 mm)], the optimum cycle time is between about 20 and 45 minutes.
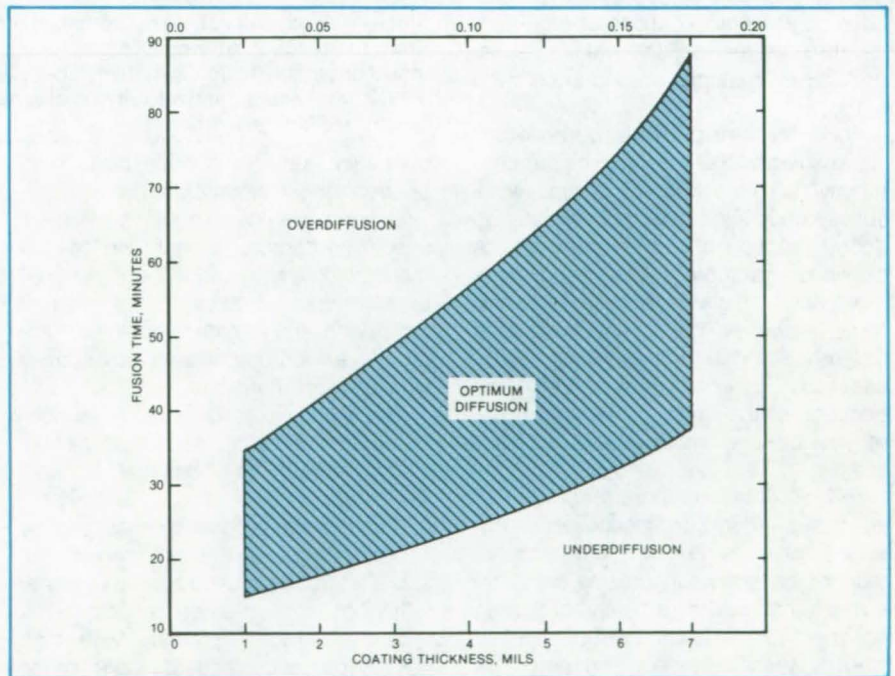
Figure 2. The **Time-vs.-Thickness Diagram** for refractory metal-silicide coatings shows an area of acceptable combinations of fusion time and coating thickness. Within the area, the normal metal-disilicide phase results. Outside the area, overdiffusion, with production of the trisilicide hexagonal phase, or underdiffusion results.

PPQ's Containing Pendent Ethynyl and Phenylethynyl Groups

Polyphenylquinoxalines containing cross-linking groups
have higher use temperature and solvent resistance.

Langley Research Center, Hampton, Virginia

Polyphenylquinoxalines (PPQ's) are high-temperature thermoplastics with excellent performance as structural resins (e.g., adhesives and composite matrices) at temperatures lower than their glass-transition or heat-distortion temperatures. These polymers also have good potential as protective coatings even though they are sensitive to certain solvents.

PPQ's were prepared containing various amounts of latent cross-linking groups: pendent ethynyl groups and pendent phenylethynyl groups. As these polymers are exposed to elevated temperatures, a thermally induced reaction of the pendent groups occurs to provide cross-linking, which raises the use temperature of the polymer and also improves its solvent resistance. When relatively low levels of the pendent groups are used, this is accomplished without severely compromising the attractive features of PPQ's, such as toughness and thermoformability. The polymers prepared in this synthesis have potential applications as high-temperature adhesives, laminating resins, protective coatings, membranes, and films.

Relatively-high-molecular-weight linear soluble PPQ's containing pendent ethynyl or phenylethynyl groups were successfully synthesized. Thermally induced reaction of the pendent groups provides insoluble cross-linked polymers with high glass-transition temperatures. However, the ethynyl-containing polymers exhibit fair-to-poor processability by compression molding because of the thermal reaction of the ethynyl groups, which inhibits polymer flow.

PPQ's containing more than 10 mole percent of ethynyl groups are not amenable to processing in the conventional manner as laminating resins or adhesives. The cured ethynyl-containing polymers exhibit lower thermo-oxidative stability than corresponding polymers with no ethynyl groups. These drawbacks are somewhat alleviated using pendent phenylethynyl groups. For instance, processability is good for PPQ's
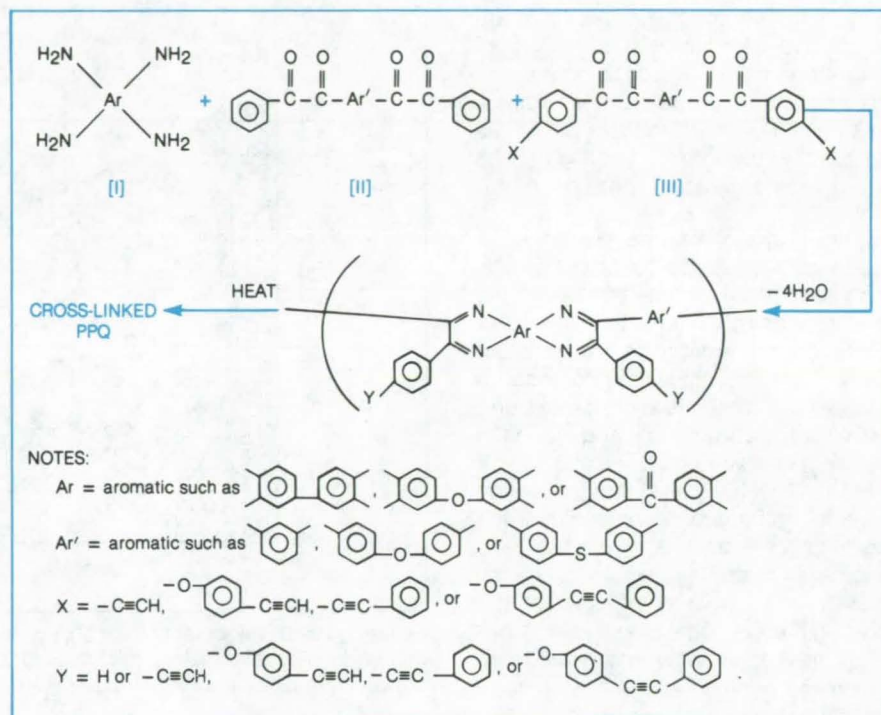
Phenylquinoxaline Polymers Containing Pendent Phenylethynyl Groups are synthesized from the reaction of aromatic bis(o-diamines) [I] with aromatic bis(α-diketones) [II] and novel aromatic bis(phenylethynylphenyl-α-diketones) [III]. The scheme is similar for PPQ's containing pendent ethynyl groups, except for the use of aromatic bis(ethynylphenyl-α-diketones) [III].

containing up to 30 mole percent of pendent phenylethynyl groups.

Several previous routes have been used in attempts to improve the dimensional stability of PPQ's at elevated temperatures. However, the current work with the pendent phenylethynyl groups exhibits significant advantages over previous methods:

1. The cross-linked density of the polymer can be readily controlled, permitting the tailoring of polymers for specific applications.

2. The uncured polymers containing the pendent groups are still readily soluble and can be used for the preparation of films, membranes, coatings, and prepregs. Polymers with high T_g's from prior methods have limited or no solubility.

3. PPQ's containing low levels (less than 30 mole percent) of pendent phenylethynyl groups exhibit good processa-

bility; polymers from previous methods exhibit difficult processability.

4. The temperatures required to induce cross-linking in these materials are lower than those from previous methods.

5. This synthesis consistently provides a cured material with higher use temperature and solvent resistance. Materials of previous methods are not always solvent-resistant.

*This work was done by Paul M. Hergenrother of **Langley Research Center**. For further information, Circle 22 on the TSP Request Card.*

This invention is owned by NASA, and a patent application has been filed. Inquiries concerning nonexclusive or exclusive license for its commercial development should be addressed to the Patent Counsel, Langley Research Center [see page A5]. Refer to LAR-12838.

Low-Waste Purification of Silicon

A continuous-flow process converts metallurgical-grade silicon to semiconductor-grade silicon.

NASA's Jet Propulsion Laboratory, Pasadena, California
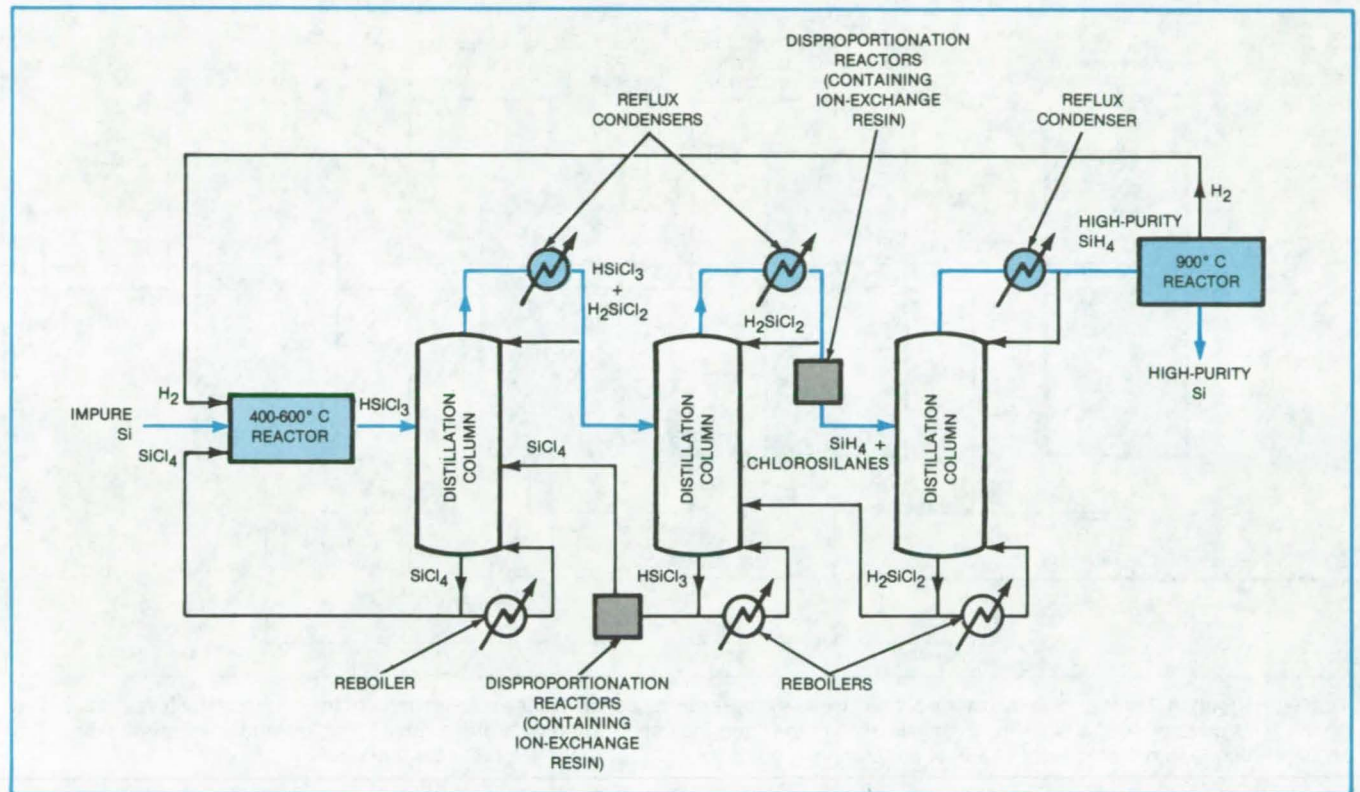
This **Purification Process** starts with impure (metallurgical-grade) silicon and produces high-purity silicon suitable for semiconductor applications. The input silicon is reacted with hydrogen and silicon tetrachloride to produce chlorosilanes; by a combination of distillation and disproportionation in resins, the silicon is converted to silane that is pyrolyzed to pure silicon. The H_2 and $SiCl_4$ are recycled in the continuous-flow process.

The ultra-high-purity silicon required for solar cells, transistors, and integrated circuits can be produced from metallurgical-grade silicon by the formation and pyrolysis of silane gas (SiH_4) in a continuous-flow process that maximizes product purity with a minimum amount of equipment. The integrated process recycles unreacted and byproduct materials, thus minimizing material losses and simplifying waste disposal. It also ensures the effective removal of impurities, including boron.

The metallurgical-grade silicon is reacted with H_2 and $SiCl_4$ in the system shown in the figure to produce chlorosilanes (H_xSiCl_{4-x}). By a combination of

distillation and redistribution, the lighter (hydrogen-rich) chlorosilanes progress through the system, and the heavier (chlorine-rich) ones are fed back to distillation columns and to disproportionation or hydrochlorination reactors. The overall process consumes the silicon and produces high-purity SiH_4 that is pyrolyzed to high-purity submicron particles of silicon. The H_2 produced in the pyrolysis is fed back to the hydrochlorination reactor.

Metallic impurities are fluxed out of the system by periodic draining of small amounts of contaminated $SiCl_4$. Boron is specially removed by the disproportionation resins and controlled distillation.

The principal merit of this system is the specific sequence in which the different steps are integrated. As the figure shows, the first distillation column recycles $SiCl_4$, the third column separates out ultra-high-purity SiH_4, and the intermediate second column separates fractions that pass to resin disproportionation-reaction zones.

This work was done by William C. Breneman and Larry M. Coleman of Union Carbide Corp. for **NASA's Jet Propulsion Laboratory.** *For further information, Circle 23 on the TSP Request Card.*
NPO-15033

Eliminating Impurity Traps in the Silane Process

The extraction of a small slipstream from separators
prevents impurities from building up.

NASA's Jet Propulsion Laboratory, Pasadena, California
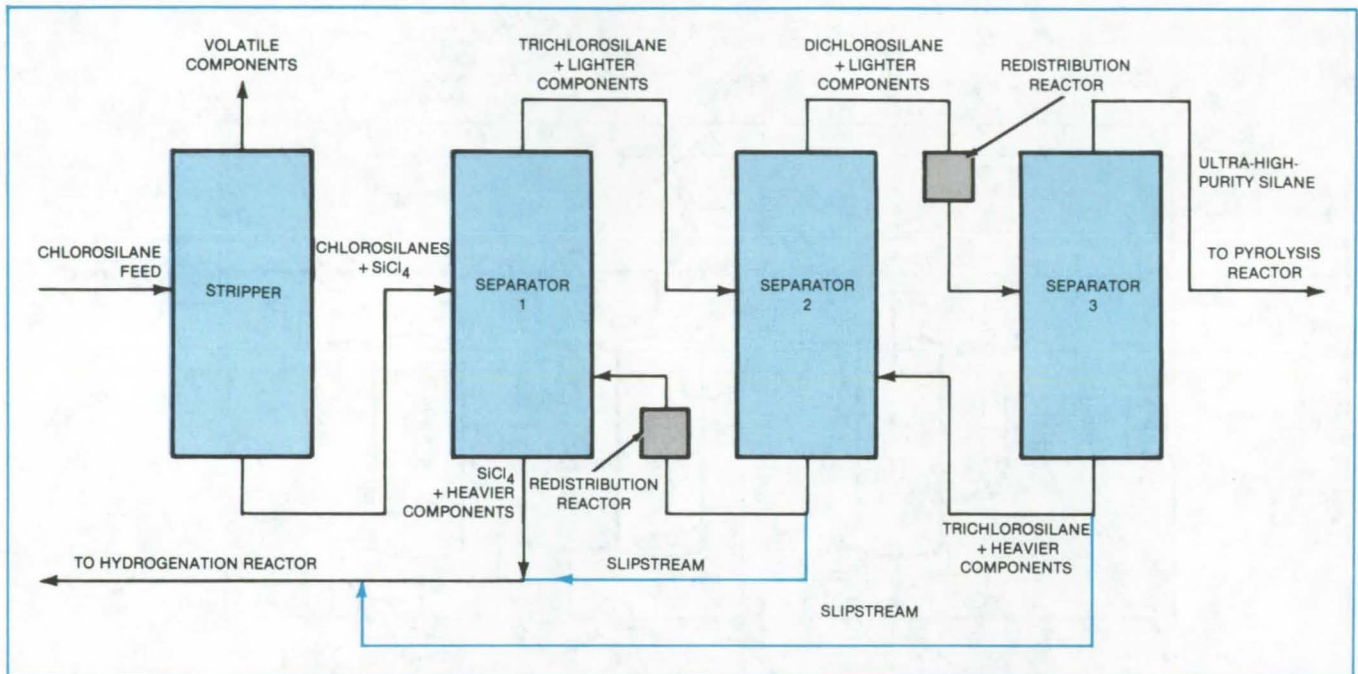
The **Redistribution Reaction Section** of the silane process progressively separates the heavier parts of the chlorosilane feedstock until a light silane product is available for pyrolysis. The color lines indicate additions to the process that prevent impurity buildup. The redistribution reactors catalytically adjust the composition of the feed for more favorable separations.

A modification has been proposed to reduce impurity trapping in the silane process for producing semiconductor-grade silicon. A small amount of liquid containing impurities is withdrawn from the processing stages in which trapping occurs and is passed to an earlier processing stage in which such impurities tend to be removed via chemical reactions.

The silane process is one of the most promising methods for producing silicon for low-cost solar cells by converting inexpensive metallurgical-grade silicon to semiconductor-grade silicon. In the silane process, the metallurgical-grade material is first hydrogenated to produce a feed stream composed primarily of trichlorosilane and silicon tetrachloride but also containing other chlorosilanes. The feedstock is passed through a series of separator columns that produce ultra-high-purity silane (SiH_4). A pyrolysis reactor breaks down the silane into hydrogen, which is recycled to the hydrogenator, and semiconductor-grade silicon.

A problem with the silane process has been that certain impurities of intermediate volatility can become trapped in the separator loops. Eventually the impurities build up to the point where they overload the separator columns and contaminate the silane product.

In the modified process (see figure) a small stream of liquid is withdrawn from the last two separator columns and returned with recycled silicon tetrachloride to the hydrogenator. There, some impurities are converted to insoluble metal complexes that settle and are removed with the heavy-waste stream. Other impurities continue to the stripper column, where they pass off with other volatile components. (The stripper column removes such gases as nitrogen and methane dissolved in the feed stream from the hydrogenator — all components having volatility equal to or greater than that of hydrogen sulfide.)

The effluent from the stripper — primarily trichlorosilane and silicon tetrachloride essentially free of high-volatility contaminants — enters separator column 1. There, trichlorosilane and lighter components are extracted and sent as the feed to separator column 2. Silicon tetrachloride and heavier components are removed and returned to the hydrogenator.

In separator 2, dichlorosilane and lighter components are extracted and sent to separator column 3. Heavier chlorosilanes are returned to separator 1, except that in the new process a small slipstream is diverted to the recycling silicon tetrachloride. The slipstream prevents impurities with volatility greater than that of tricholorosilane but less than that of dichlorosilane from becoming trapped and accumulating in the loop between separators 1 and 2. Such impurities include boron trichloride, phosphorus chloride, and arsenic chloride.

In separator 3, silane is extracted as the product. Diborane and other impurities are returned to separator 2, and a slipstream is added to the silicon tetrachloride return. The slipstream prevents such impurities as boron hydride, phosphorus hydride, and arsenic hydride

from building up in the loop between separators 2 and 3.

Very small slipstreams are sufficient. A continuous bleed of only 0.01 to 0.1 percent of the column-bottom recycle stream is enough to maintain any of the impurities in the separator loops at less than 1 part per million.

This work was done by Larry M. Coleman of Union Carbide Corp. for

---

Removing Chlorides From Metallurgical-Grade Silicon

Process for making low-cost silicon for
solar cells is further improved.

NASA's Jet Propulsion Laboratory, Pasadena, California
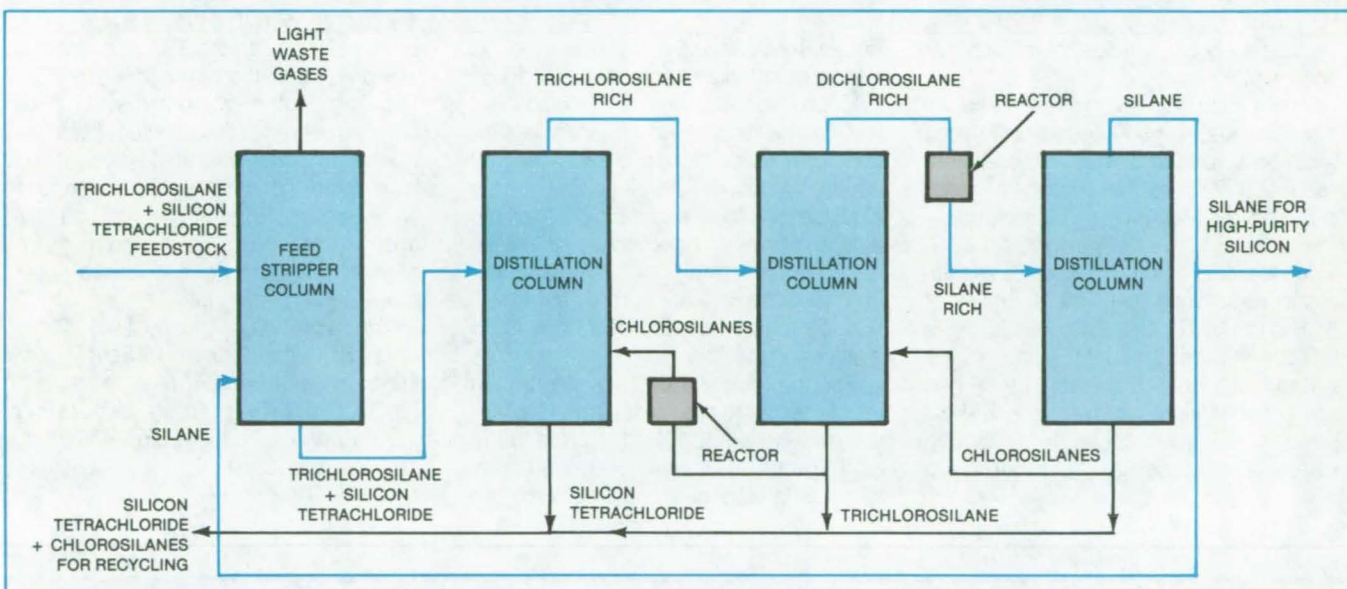
Silane Product Recycled To Feed Stripper Column converts some of the heavy impurities to volatile ones that pass off at the top of the column with light wastes. The impurities — chlorides of arsenic, phosphorus, and boron — would otherwise be carried to subsequent distillations where they would be difficult to remove. Since only a small amount of silane is recycled, silicon production efficiency remains high.

Upgrading metallurgical-grade silicon to high-purity semiconductor-grade silicon for low-cost solar cells requires a critical step in which chlorosilanes are separated from a silicon tetrachloride carrier for further processing. When the chlorosilanes are separated, such impurities as arsenic chloride, phosphorus chloride, and boron chloride tend to stay with them. The retention of these impurities in the feedstock imposes a heavier impurity load on downstream processing equipment and makes it more difficult to maintain high purity in the silicon product.

However, a small amount of silane added to the chlorosilane and silicon tetrachloride mixture eliminates the impurities. A small portion of the silane produced in a later reaction is simply diverted to the feed stripper column in which the chlorosilane and silicon tetrachloride are separated (see figure). The silane reacts with the chloride impurities to form hydrides, such as arsenic hydride, phosphorus hydride, and boron hydride. These volatile compounds are readily removed along with other light wastes in the column.

The silane enters at the bottom of the feed stripper column. Since silane is a volatile substance, it rises the entire length of the column. It thus has a longer time to react with impurities than if it were injected at a higher level in the column. Excess silane passes off at the top with the other light gases.

Of course, the impurity concentrations in the feedstock are already low — usually less than 1 ppm to about 10 ppm. To ensure complete reaction, the silane should be added in concentrations of 10 to 100 ppm (moles of silane per milion moles of feedstock). This concentration represents an insignificant loss of product silane for conversion to semiconductor-grade silicon.

Extracting Silicon From Sodium-Process Products

An acid solution dissolves unwanted byproducts of the
reaction between sodium and silicon fluoride.

NASA's Jet Propulsion Laboratory, Pasadena, California

A new acid leaching process purifies the silicon produced in the reaction between silicon fluoride and sodium. The concentration of sodium fluoride and other impurities and byproducts remaining in the silicon are within acceptable ranges for semiconductor devices. The leaching process makes the sodium reduction process more attractive for making large quantities of silicon for solar cells.

The process also removes sodium silicofluoride (Na_2SiF_6), which is formed with the silicon and NaF in the sodium reduction process. The amount of water required for leaching is determined by the amount of Na_2SiF_6 in the product, since Na_2SiF_6 is considerably less soluble in water than NaF (the solubility of NaF is about 1M, and that of Na_2SiF_6 is 0.042M in water and 0.072M in concentrated acid). The amount of Na_2SiF_6 in the product varies between 1 and 30 percent by weight; higher reaction temperatures tend to decompose Na_2SiF_6 and thus produce lower amounts.

An acid leaching solution is used to prevent the silicon from oxidizing, a reaction that occurs spontaneously in alkaline solution. The acid also neutralizes unreacted sodium, which would otherwise create an alkaline leaching solution.

Leaching should be performed as rapidly as possible because even in acid solutions some silicon is oxidized, and the yield is decreased accordingly. Oxidation in acid solution is promoted by fluoride ions in the leaching batch (fluoride ions form a complex with silicic acid and prevent a protective film of oxide from forming on the silicon). Therefore NaF — the primary source of fluoride ions — should be removed as quickly as possible.

For the leaching of 1 kg of reaction products, six to nine leaching steps are performed with 0.5N to 1.2N sulfuric acid. A total volume of 150 to 350 liters of solution is required to decrease the residual fluoride-ion concentration to 10^{-4}M. The final leaching is done with water. Between the leaching steps, the leachant is separated from the remaining solid by filters or a centrifuge. The entire procedure can be carried out in 3 to 4 hours.

Emission spectroscopy indicates that 4 ppm copper, 6 ppm magnesium, 7 ppm calcium, and 1,500 ppm sodium are present in the leached silicon. The large amount of sodium may be from Na_2SiF_6 or unreacted sodium dissolved in the silicon. Elements present but below the quantitative detection limit were nickel, iron, chromium, barium, aluminum, vanadium, zirconium, manganese, boron, phosphorous, silver, molybdenum, and titanium.

Producing Cryolite From Waste Sodium Fluoride

Use of waste NaF could improve the
economics of silicon production.

NASA's Jet Propulsion Laboratory, Pasadena, California

A simple chemical process makes synthetic cryolite (Na_3AlF_6) by utilizing the byproducts of one kind of silicon production process. The potential result of commercialization could be an economic benefit to the silicon industry or to the aluminum industry, in which cryolite is used as a flux.

Both NaF and HF are byproducts of the process involving the reaction between Na and SiF_4 to produce solar-grade silicon. In the melt-separation version, molten NaF is produced and solidi-fied. In the leach-separation version, NaF is dissolved in water or dilute acids. The NaF solution may be combined with waste HF liquors.

Alumina hydrate [$Al(OH)_3$] is combined with the waste liquor, and the following reactions take place:

$$6NaF + Al(OH)_3 \rightarrow Na_3AlF_6\downarrow + 3NaOH$$

$$4NaF + 2HF + Al(OH)_3 \rightarrow$$
$$Na_3AlF_6\downarrow + NaOH + 2H_2O$$
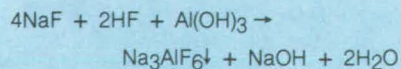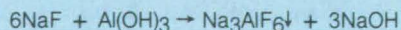
The cryolite, being relatively insoluble in water, readily precipitates out of solution. These reactions have been qualitatively demonstrated in beaker-scale laboratory experiments only.

Producing High-Purity Silicon With Sodium

Fed in solid form, the sodium
reduces silicon fluoride.

NASA's Jet Propulsion Laboratory, Pasadena, California

A simple technique for producing silicon for solar cells employs solid sodium to reduce silicon fluoride. Since solid rather than liquid sodium is used, careful temperature control is unnecessary, and simple feed equipment is used. The technique is energy-efficient, since the reaction produces enough heat to sustain itself.

Solid pieces of sodium at room temperature are dropped from a plastic-lined hopper into a vertical cylindrical reactor (see figure). The bottom of the reactor is heated to above 350° C. As the sodium (which melts at 97.5° C) reaches 150° C, it starts to react rapidly with SiF_4 flowing into the reactor. The heat liberated during the reaction is used to preheat subsequent sodium feedings.

In the laboratory, the process has produced kilogram-sized batches of reaction products consisting of silicon, sodium fluoride, and a small amount of sodium silicofluoride (Na_2SiF_6). The only impurity detectable by emission spectroscopy was calcium, which was present in concentrations ranging from 100 to 175 ppm. Possible impurities that were below the detection limit were titanium, vanadium, chromium, zirconium, iron, copper, aluminum, molybdenum, nickel, manganese, boron, and phosphorus.

The sodium pieces flow more smoothly if they are coated with sodium fluoride powder or a thin oxide. Such coatings minimize cold welding of the pieces to the reactor wall.

This work was done by Angel Sanjurjo of SRI International for **NASA's Jet Propulsion Laboratory.** For further information, Circle 28 on the TSP Request Card.
NPO-15381
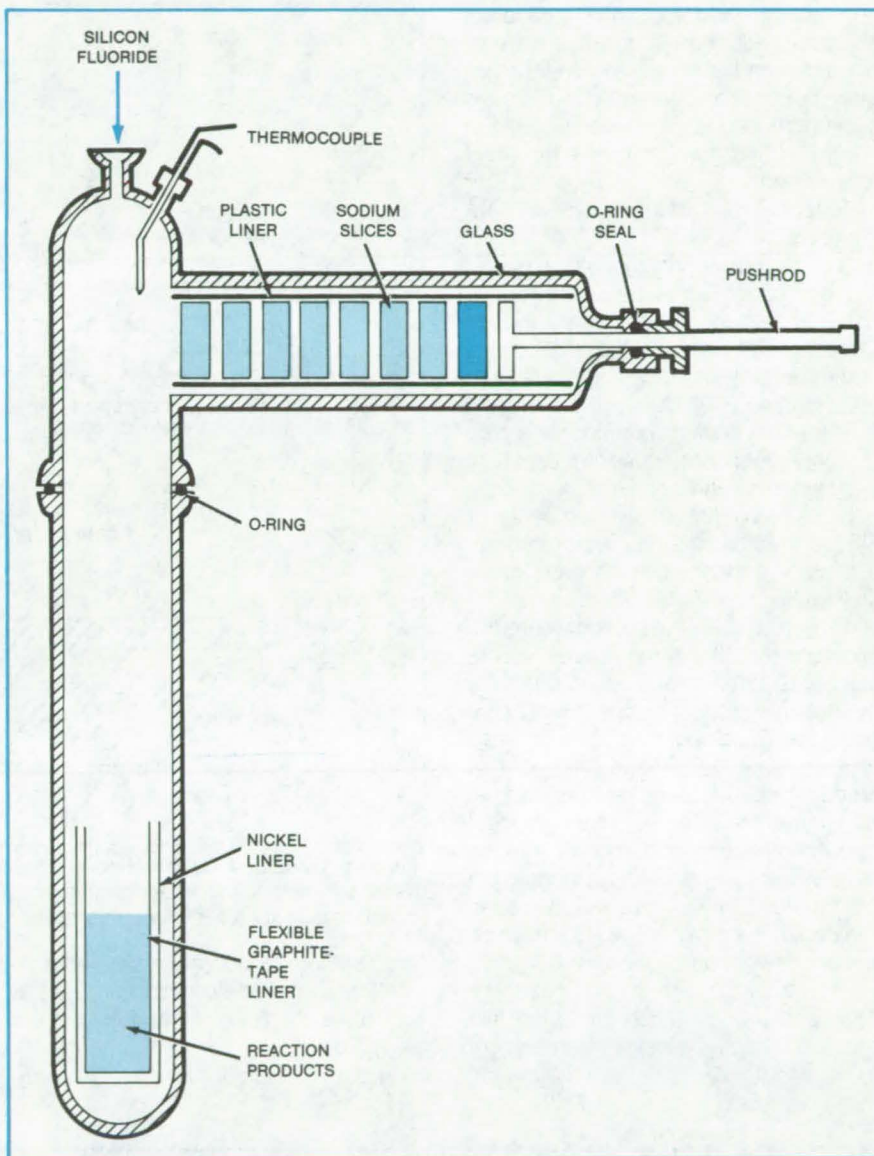
Slices of Sodium are pushed one by one into a reactor vessel. The slices react with silicon fluoride flowing into the vessel. The reaction products — silicon, sodium fluoride, and sodium silicofluoride — collect at the bottom.

Nonclogging Liquid-Sodium Nozzles

Reaction yielding high-purity silicon is
prevented from occurring at nozzle.

Reacting liquid sodium with gaseous
silicon tetrafluoride is an effective way
of producing high-purity silicon for solar
cells, but liquid sodium is such an active
substance that it can readily clog the
nozzle through which it is introduced
into a reactor.

Two new methods that prevent clog-
ging are:

1. Silicon tetrafluoride is passed over
   the nozzle to keep it below the 150° C
   reaction temperature, even though
   the heat of reaction at the bottom of
   the reactor produces temperatures
   as high as 900° C.
2. The liquid sodium is jetted at a rate
   high enough that it does not react until
   it is clear of the nozzle.

In the first method, room-temperature
SiF_4 is injected into the reactor through
a nozzle concentric with the liquid-
sodium nozzle (see figure). As the
sodium and SiF_4 react downstream,
depleting the SiF_4 in the reactor, a con-
stant-pressure valve feeds more SiF_4
through the nozzle. The gas flow not only
cools the liquid-sodium nozzle but also
creates a jet that keeps hot reaction
product particles away from the nozzle.

Batches of up to 1 kg of the product
mixture of silicon and sodium fluoride
have been produced without clogging of
the nozzle. Several nozzles have been
evaluated, the most successful of which
was a shower-head type.

In tests of the high-flow-rate method,
liquid sodium was jetted through a thin
nozzle having an inside diameter of
0.005 inch (0.127 mm). Even though the
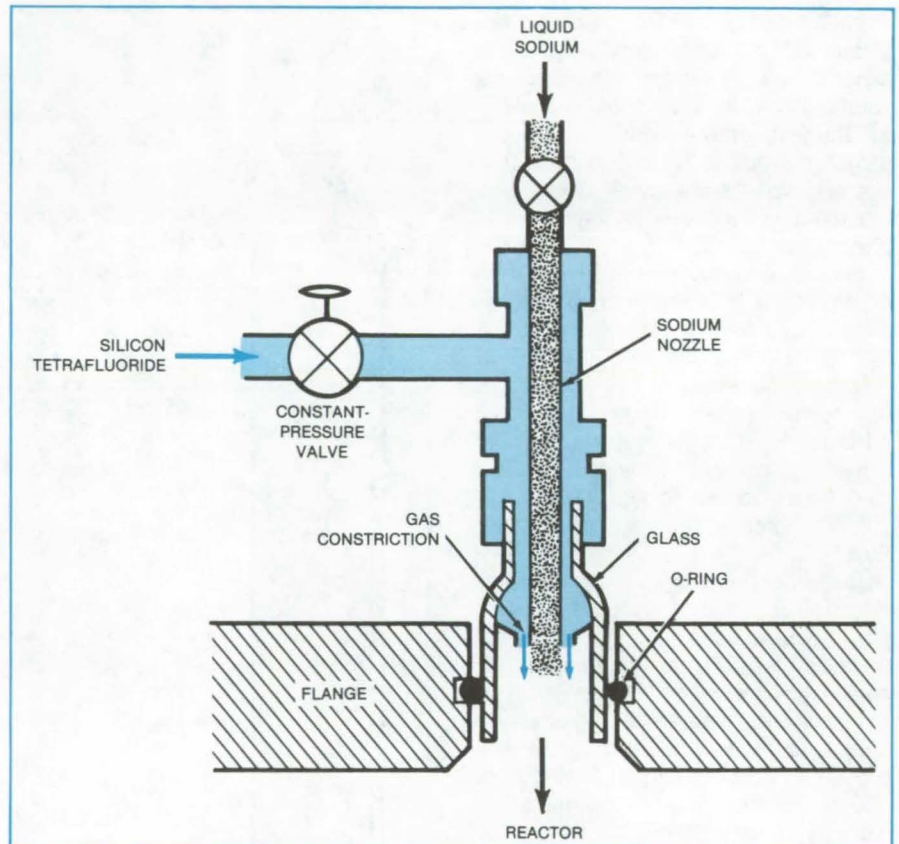
Flowing Through a Constriction around a sodium-delivery nozzle, silicon tetrafluoride
gas cools the liquid sodium emerging from the nozzle. The sodium-delivery nozzle
consists of a stainless-steel tube with a one-fourth inch (6.35 mm) outside diameter.

liquid-sodium temperature was as high
as 250° C, the sodium did not react at
the nozzle but, rather, a few centimeters
away from it.

This work was done by Angel Sanjurjo

of SRI International for **NASA's Jet Pro-
pulsion Laboratory.** *For further infor-
mation, Circle 29 on the TSP Request
Card.*
NPO-15259

Inexpensive Antireflection Coating for Solar Cells

Titanium oxide is applied in
a continuous spraying process.

A continuous method for applying an
antireflection coating to solar cells in-
creases the efficiency of these devices
by preventing energy from being re-
flected away, but adds little to manufac-

turing cost. The method consists of
spraying a solution on the cells or glass
collector plates, drying the sprayed
layer, and curing it. The solution is for-
mulated to spread evenly over the sur-
faces.

Previously, antireflection coatings
have been applied by vacuum deposition
or sputtering. These processes are ex-
pensive and awkward for mass produc-
tion. More recently, coatings have been
applied by dipping parts in solution or by

placing a drop of solution at the center of a part and spinning it so that the solution spreads out evenly. Although these methods are less costly than vacuum deposition or sputtering, the parts must still be handled in batches rather than as a continuous flow.

The sprayed coating has the required index of refraction (2.0 to 2.2). It has a uniform thickness of about 700 angstroms. It adheres strongly to the substrate and is unaffected by prolonged exposure to Sunlight.

The spraying solution consists of an organometallic titanium compound such as titanium isopropoxide, an inert ester diluent such as butyl acetate, 2-ethyl-1-hexanol and, optionally, a lower aliphatic alcohol. The last ingredient ensures that the solution wets the substrate, spreads evenly across it, and evaporates uniformly, leaving a continuous film of titanium compound. The proportions of the ingredients can be varied within limits, but the solution should contain at least 33 percent by volume of 2-ethyl-1-hexanol and no more than 33 percent of the lower aliphatic alcohol. The volume ratio of titanium compound to ester diluent should be about 1 to 3. The solution can be applied by commercial automatic spraying equipment.

The sprayed film is passed through an infrared furnace so that its solvents evaporate; the temperature at this stage should be about 70° C for at least 30 seconds. The film is then heated to about 200° C for 30 seconds and to about 350° to 400° C for another 30 seconds. The heat converts the titanium compound to a stable solid film of titanium oxide.

The antireflection coating has been applied successfully to glass plates and silicon solar cells. The spray orifice diameter was 0.31 mm, and the spray pressure was 172 kPa. The spray gun was 10 cm above the substrates and was moved at a speed of 36 cm/s.

*This work was done by Chester E. Tracy, Werner Kern, and Robert D. Vibronek of RCA Corp. for **NASA's Jet Propulsion Laboratory.** For further information, Circle 30 on the TSP Request Card.*
NPO-15025

Prepolymer Syrup for Encapsulating Solar Cells

N-butyl acrylate polymer/monomer syrup can be used for dipping and coating.

NASA's Jet Propulsion Laboratory, Pasadena, California
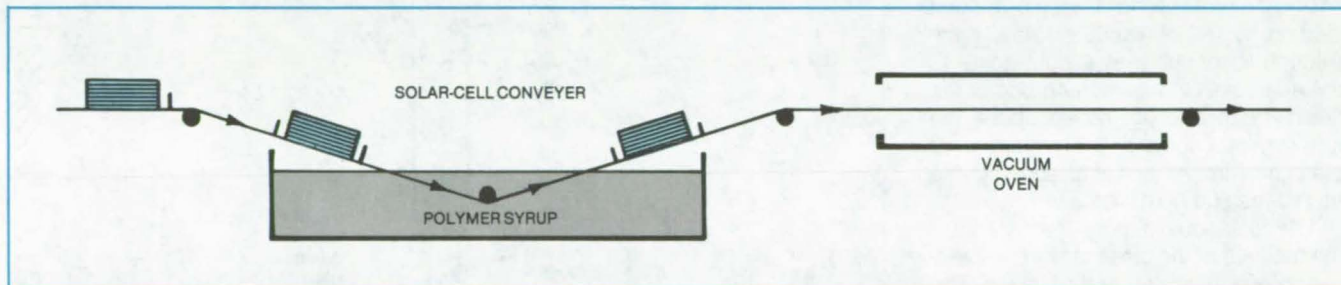
This **Continuous Encapsulation** process for solar-cell assemblies uses a polymer syrup containing prepolymer of high molecular weight.

A clear polymer syrup, made by dissolving n-butyl acrylate prepolymer in the monomer, can be used to encapsulate solar cells by any of three standard processes (dipping, multiple coating, or automated machine coating). [See also "Thermal Polymerization of N-Butyl Acrylate" (NPO-15010) on page 288 of *NASA Tech Briefs*, Vol. 6, No. 3.] The use of cyclohexane instead of a methanol/water solvent during the initial polymerization stage maintains high molecular weight and raises the yield of linear polymer to essentially 100 percent.

The n-butyl acrylate monomer is initially polymerized by mixing with an azoisobutyronitrile initiator in a cyclohexane solvent. The solvent is then removed, and the prepolymer is mixed with more of the monomer. More initiator and a stabilizer (to prevent yellowing of the polymer by ultraviolet rays) are added. The composition of the resulting encapsulant syrup is as follows:

- Poly (n-butyl) acrylate, with molecular weight of 200,000 to 600,000 — 40 to 70 weight percent
- N-butyl acrylate (monomer) — 30 to 60 weight percent
- Azoisobutyronitrile initiator — 0.05 to 1 weight percent
- Ultraviolet stabilizer — 0 to 3 weight percent

The figure shows the method of encapsulation with this polymer syrup by direct dipping or submerging of the solar-cell assembly into the polymer, followed by curing in a continuous process with a vacuum oven at about 80° C.

*This work was done by Amitava Gupta, John D. Ingham, and Andre H. Yavrouian of Caltech for **NASA's Jet Propulsion Laboratory.** For further information, Circle 31 on the TSP Request Card.*

Title to this invention has been waived under the provisions of the National Aeronautics and Space Act [42 U.S.C. 2457(f)], to Caltech.
NPO-15154

Precise Sealing of Fused-Quartz Ampoules

A new technique maintains wall
strength and pumping speed.

Langley Research Center, Hampton, Virginia

A new technique rapidly evacuates and seals a fused-quartz ampoule with precise clearance over its contents, without appreciably thinning the ampoule walls. Previous methods involved either heating the sides of the ampoule until the walls softened and collapsed or placing a plug of fused quartz in the ampoule before evacuation and then heat sealing the ampoule to the plug. The first method causes wall thinning and weakening and poor control of the clearance between the top of the charge and the top of the ampoule. A significant reduction in pumping speed occurs in the second method due to the constriction caused by the plug.

The new technique consists of mounting the ampoule vertically, as shown in the illustration. The ampoule is constructed so that the top section (approximately 15 cm) is wider than the working section by $\sqrt{2}$. A vacuum rotary feedthrough is mounted at a right angle to the ampoule. On the vacuum side of the feedthrough and positioned above the ampoule is a spool of 0.1-mm-diameter platinum wire. A hook is attached to the end of the platinum wire.

The fused-quartz plug that will form the top seal of the ampoule has a fused-quartz eye loop attached to its top. The hook on the platinum wire fits into the eye loop and supports the plug while the ampoule is connected to the vacuum system. The rotary feedthrough then positions the plug in the upper (larger diameter) section of the ampoule during pumpdown.

After evacuation, the plug is lowered into the working section of the ampoule. The vacuum-tight seal is made by fusing the ampoule to the plug. Ampoule wall strength is not significantly affected by this operation because the amount of wall collapse is kept to a minimum.

The hook on the platinum wire is released by lowering the hook until it releases from the eye on the plug. The sealed ampoule is then removed from the vacuum system, and the operation is repeated with a new ampoule.

This technique can be used to seal any cylindrical opening in any glasslike container, the interior of which is main-
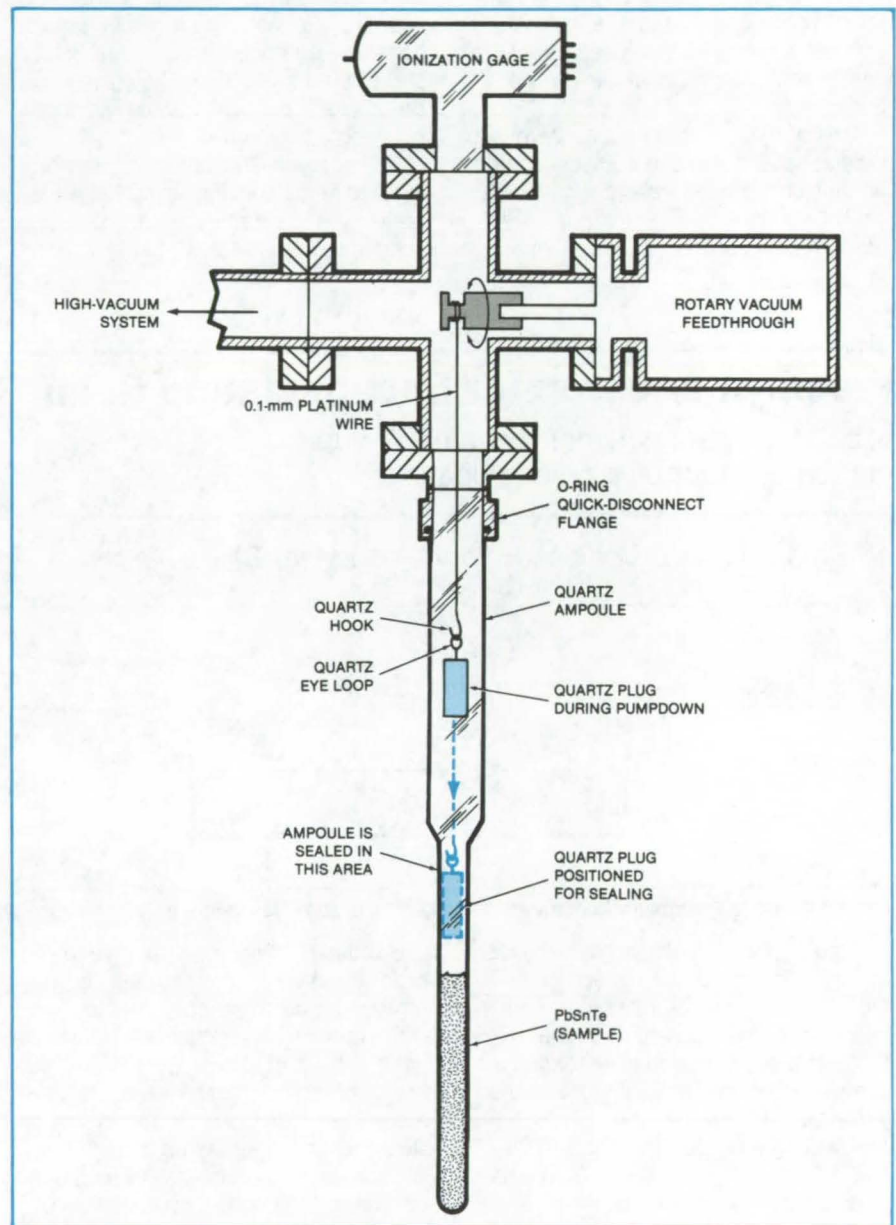
A **Quartz Plug Is Lowered** into the working section of the ampoule after the ampoule has been evacuated. The plug is then fused to the ampoule walls, forming a vacuum seal.

tained at lower than atmospheric pressure. The plug and ampoule must be of compatible materials to ensure proper sealing. Advantages of this technique over previous methods include precise positioning of the plug within the ampoule, the maintenance of ampoule shape and strength after sealing, the ease of sealing, and rapid pumpdown.

Oxidation-Strengthened High-Temperature Rivets

Shear strength of titanium-niobium
rivets improves with oxidation.

Lyndon B. Johnson Space Center, Houston, Texas

Titanium-niobium rivets are stronger when their surfaces are oxidized. Rivets composed of a 55-percent Ti/45-percent Nb alloy that had been oxidized at 1,700° F (927° C) for 10 hours were stronger — both at room temperature and at 1,700° C — than unoxidized rivets of the same composition.

Oxidized specimens showed a pronounced increase in hardness near the surface. This finding correlates with photomicrographs, which show an oxide crust and underlying diffused oxygen (see figure).

The Ti-Nb rivets were developed for fastening parts of Space Shuttle thrustors. They may be suitable also for other high-temperature applications in oxidizing environments — for example, in the burner cans of commercial jet engines and boilers and retorts for coal gasification systems.

This work was done by Robert L. McLemore of The Marquardt Co. for **Johnson Space Center.** *For further information, Circle 32 on the TSP Request Card.*
MSC-20095
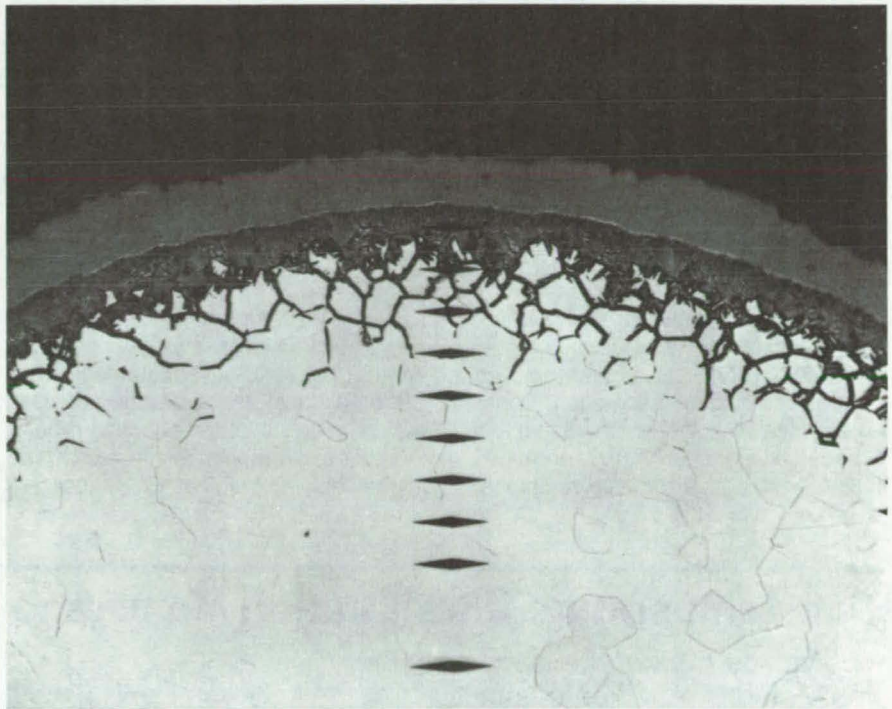
After Exposure to Air at 1,700° F for 2½ hours, the Ti-Nb rivet depicted in this cross-sectional photomicrograph has a hard outer crust of oxide.

Improved Supercritical-Solvent Extraction of Coal

Combining a catalyst with a conventional
aromatic solvent increases yields.

NASA's Jet Propulsion Laboratory, Pasadena, California

Raw coal is upgraded by a supercritical-solvent extraction system that uses two materials instead of one. [See also "Supercritical-Fluid Extraction of Oil From Tar Sands" (NPO-15476), *NASA Tech Briefs*, Vol. 6, No. 2, page 166.] The system achieved extraction yields of 29 to 49 weight percent. Single-solvent yields are about 25 weight percent.

Raw coal has varying amounts of mineral, sulfur, and nitrogen impurities. Therefore it cannot be used directly in many chemical conversion processes, such as coal liquefaction, because the impurities interfere with catalyst activity.

A number of single-solvent coal-extraction techniques recover and enable use of the soluble extract for one application and enable the use of residue or "char" for another application or for fuel. Yields of extract have not been sufficiently sizable for solvent extraction to be attractive commercially.

The supercritical extraction uses a coal-dissolution catalyst and a conventional aromatic solvent. Typically, phenanthrene and toluene are used together at 715° F (380° C) and 900 psig (6.2×10^6 N/m^2) for a 16-hour extraction. The process is carried out in any

conventional solid-extraction apparatus with provision for pressurized operation, controlled heating, and preferably some form of agitation. All the advantages of supercritical-fluid extraction are retained.

The more volatile solvent (toluene) volatilizes the somewhat nonvolatile coal-dissolution material at temperatures sufficiently low to avoid coal gasification and polymerization reactions that tend to reduce the yields of coal extract. The less volatile solvent (phenanthrene) is believed to catalyze the breakdown of raw coal structure in

Coal Type* (PSOC No.)	Ash (%)	Solvent (wt.%)	Solvent/ Coal Ratio (wt./wt.)	Temperature (°C)	Time (h)	Pressure (MN/m^2)	Gas Density (g/cm^3)	Coal Weight Loss (%)
174		Toluene 100	34.7	385	17	22	0.73	43.5
174	5.0	T/P** 62/38	29.5	379	16	6.2	0.69	49.3
086		Toluene 100	36.0	366	15.3	21	0.73	24.7
086		T/P 83/17	39.8	367	15.3	14	0.73	29.1

*PSOC #174 HVA Rank, Pittsburgh Seam, 84.1 Percent DMMF Carbon

PSOC #086 Lignite Rank, ZAP Seam, 73.2 Percent DMMF Carbon

**T/P = Toluene to Phenathrene Ratio

Supercritical-Fluid Extraction Yields are shown for experiments on two types of coal.

the gas phase and to volatilize the coal-fragment molecules into the super-critical fluid or mixture.

Phenanthrene, with a critical temperature of 1,112° F (600° C), is not sufficiently volatile at temperatures below about 797° F (425° C) to be employed separately in coal extraction under supercritical conditions. Coal is known to undergo some polymerization above 425° C. With concurrent use of toluene, which has a lower critical temperature, coal is volatilized at acceptably low temperatures at which no significant polymerization occurs. Conceivably, another solvent with a low critical temperature can be used instead of toluene, and another aromatic solvent that facilitates the breakdown and dissolution of coal can be used instead of phenanthrene.

Some experimental results are shown in the table. Extraction yields may be time-dependent. Observed decreases in the weight of coal agreed well with increases in the ash content of the residue.

This work was done by Leslie E. Compton of Caltech for **NASA's Jet Propulsion Laboratory.** *For further information, Circle 33 on the TSP Request Card.*
NPO-15210

High-Temperature Ultrafiltration Membrane

A polyimide membrane is made in a single step by solution casting.

NASA's Jet Propulsion Laboratory, Pasadena, California

Property Investigated	Polymer Concentration (%) in Dimethylacetamide								
	15			20			25		
Evaporation Time (min)	0	7	15	0	7	15	0	7	15
Water Content (%)	82	79	75	77	72	68	73	70	65
Overall Porosity	0.86	0.84	0.80	0.82	0.79	0.75	0.79	0.77	0.73
Hydraulic Permeability (cm/s-Dyne $\times$ 10^8)	5.2	0.69	0.29	1.5	0.36	0.16	0.44	0.21	0.1
Average Pore Size (Å)	400	340	200	320	250	130	230	175	95

Characteristic Properties for a high-temperature polyimide ultrafilter are tabulated here. The pore size decreases with increased concentration of the casting solution and/or a longer evaporation period.

An ultrafiltration membrane with high-temperature capability is prepared from a polyimide that is soluble in an organic solvent such as dimethylacetamide. It is made in a single step by solution-casting phase inversion.

Typical ultrafiltration membranes made of organic polymers are limited to operating temperatures below 50° or 60° C (120° or 140° F), and even at these moderate temperatures their lifetimes are often too short. Some applications demand higher operating temperatures — for example, the recycling of hot fluids in chemical processing.

In the new method, a fully-imidized aromatic polyimide is dissolved in dimethylacetamide. Then a film of polymer solution is cast on a glass plate by a casting blade inside a constant-temperature dry box. Dry air passes through the box to carry away the solvent vapor. After a

specific period of evaporation, the cast film is immersed in distilled water, and the polymer precipitates on the glass plate, forming a skin-type asymmetric membrane.

The porosity, hydraulic permeability, and pore size of the skin layer have been studied (see table). As casting-solution concentration and/or evaporation period increase, the average pore size decreases, and the skin thickness increases. At low casting-solution concentration, the membranes are highly porous, and the precipitated polymer phase has a granular structure. At high casting-solution concentrations, the precipitated polymer is less porous, and it has a spongy structure.

The polymer retains its useful physical properties at temperatures well above previous operating temperatures. Tensile strength is 2.9×10^7 Pa at 285° C, and the heat deflection temperature lies in the range 270° to 280° C. Compression creep per day (at a pressure of 1.87×10^9 Pa) is only 0.47 percent at 312° C.

This work was done by Mohammad N. Sarbolouki of Caltech for **NASA's Jet Propulsion Laboratory.** *For further information, Circle 34 on the TSP Request Card.*

This invention is owned by NASA, and a patent application has been filed. Inquiries concerning nonexclusive or exclusive license for its commercial development should be addressed to the Patent Counsel, NASA Resident Office-JPL [see page A5]. Refer to NPO-15431.

Glass for Solid-State Devices

Glass film has low intrinsic compressive stress for isolating active layers of magnetic-bubble and other solid-state devices.

Langley Research Center, Hampton, Virginia

Two glass formulations are suitable as isolation layers in solid-state devices that incorporate magnetic films. The glasses have the low intrinsic compressive stress required of such layers.

The illustration shows a cross section of a composite structure that might be used in a magnetic-bubble or other solid-state device. The substrate is a semiconductor or a magnetic-bubble-domain material. It may have a thin layer of material capable of supporting magnetic-bubble domains. The entire substrate together with the magnetic-bubble-domain layer may be any thickness, but a thickness of about 20 mils (0.51 mm) is preferred. Deposited over the surface of the thin layer on the substrate is a planar barrier layer of dielectric — in this case the low-stress glass film. The thickness of the glass is from 1,000 to 4,000 Å. It may be deposited on the substrate by sputtering or vacuum evaporation.

Over the barrier layer is a layer of a conductive material. This layer consists of discrete spaced-apart conductor elements or strips having a thickness of about 4,000 Å. The specific conductor chosen for this layer depends on the characteristics required by the microelectronic device. In a bubble-domain device, the conductor may be copper-doped aluminum. The conductor is deposited by the same technique as in the deposition of the barrier layer.

It is important that the barrier layer have specific mechanical properties so
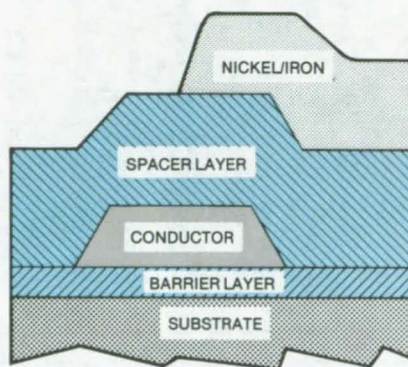
Solid-State Device Structure incorporates low-stress glasses as barrier and spacer layers. The glass layers mechanically isolate the substrate, conductor, and nickel/iron layers.

that stress in the conductor layer, or other layers, is isolated from the magnetic layer. This isolation is provided by a barrier material with low intrinsic compressive stress. A glass film with the following composition exhibits the low intrinsic compressive stress required:

Component	(Percent by Weight)
SiO$_2$	89 to 98.45
Al	0.5 to 5.0
Na	0.05 to 1.0
B	0.1 to 5.0

A spacer layer of paramagnetic material may be deposited to separate the conductor from the other active layers. Such a material may consist of the same type of glass used for the barrier layer. The spacer layer, with a thickness of from 2,000 to 6,000 Å, separates the barrier and conductor layers from other conductive or magnetically operative elements (such as nickel/iron). Typically 4,000 Å thick, this final layer may also be applied by sputtering or evaporation. Although glass with a composition in the range shown above is suitable, the preferred glass for this application has the following composition:

Component	(Percent by Weight)
SiO$_2$	93.3 to 97.7
Al	1.5 ± 0.5
Na	0.5 ± 0.2
B	2.5 ± 1.5

This work was done by Robert F. Bailey of Rockwell International Corp. for **Langley Research Center.** *No further documentation is available.*

Title to this invention has been waived under the provisions of the National Aeronautics and Space Act [42 U.S.C. 2457(f)], to the Rockwell International Corp., 3370 Miraloma Ave., Anaheim, CA 92803.
LAR-12781

Low-Cost Aqueous Coal Desulfurization

New chlorination process uses water
instead of an organic solvent.

NASA's Jet Propulsion Laboratory, Pasadena, California
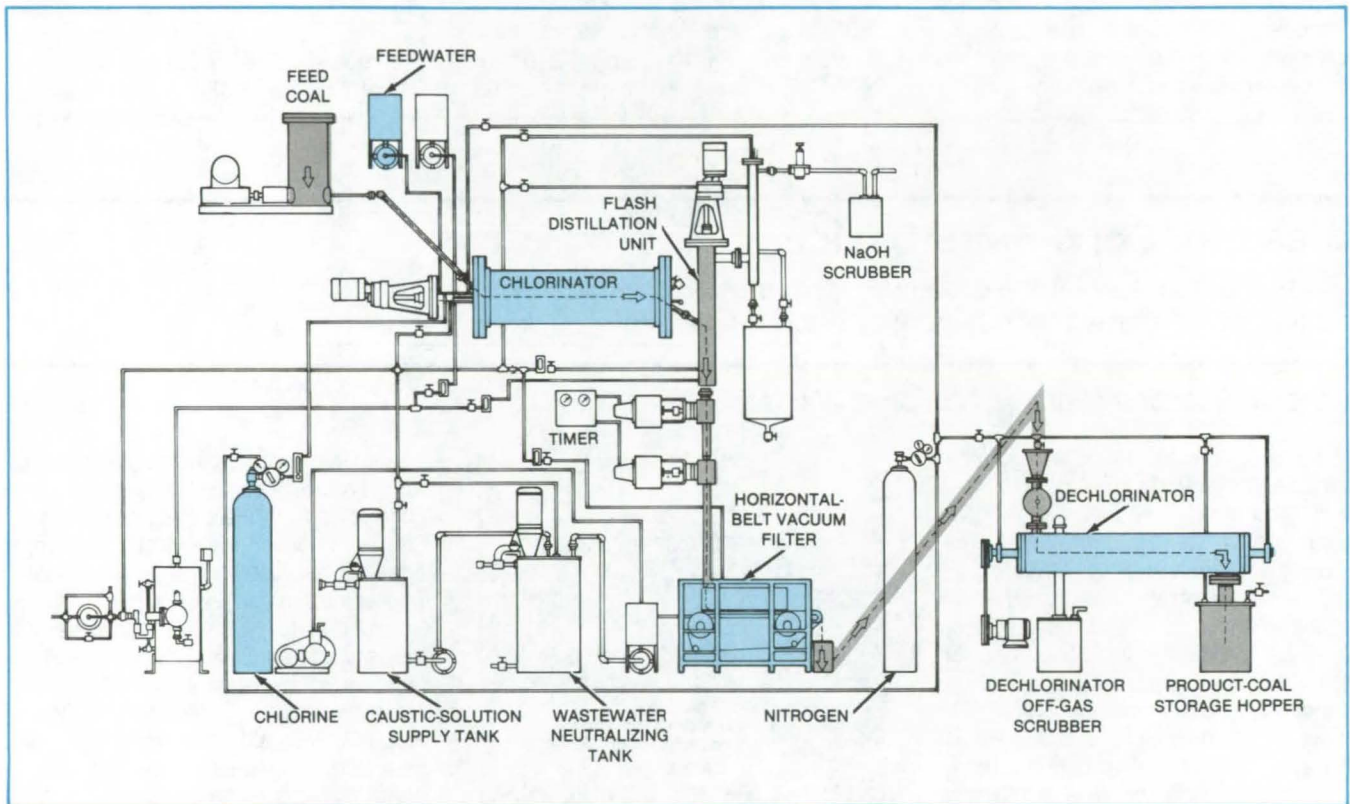
In a **Batch Coal-Desulfurization System,** the essential steps are the chlorination of sulfur in a waterborne coal slurry and the combined filtration, drying, and dechlorination of the powdered coal.

A water-based process for desulfurizing coal not only eliminates the need for a costly organic solvent but removes sulfur more effectively than does an earlier solvent-based process. The new process could provide a low-cost commercial method for converting high-sulfur coal into environmentally acceptable fuel.

A previous desulfurization process was based on methyl chloroform solvent. The three-stage process started with a room-temperature chlorine treatment of coal slurry suspended in the solvent and water. After the slurry was filtered, a batch hydrolysis and solvent-recovery step was carried out. Finally, the coal was dechlorinated, yielding desulfurized coal.

Methyl chloroform was selected as the solvent in the previous process because it is chlorine-resistant and was originally thought to aid sulfur removal.

However, sizable quantities of the solvent could be lost by absorption in tarry residues and solids or by hydrolysis, representing a substantial cost. Water was found to be an effective substitute for the solvent.

The new water-based process has been demonstrated in a continuous-flow minipilot plant (see figure). It includes a chlorinator, a horizontal-belt vacuum filter, and a dechlorinator that could be scaled up to a commercial-sized plant.

The concept for the new process emerged from theoretical studies of chlorine reactions with coal. The studies showed that the methyl chloroform solvent had no role in the chemical reactions of the chlorine other than serving as a carrier of the chlorine. An aqueous carrier in sufficient volume is at least as effective as a solvent carrier, because chlorine is the active reagent that penetrates and directly reacts with sulfur in the coal.

In the older process, the methyl chloroform helped to stabilize the reaction temperature, since evaporation at the 74° C boiling point of the solvent dissipates the heat generated in the exothermic chlorine-sulfur reaction. In the new process, this stabilization is provided by cooling of the reactor vessel.

Laboratory experiments have clearly demonstrated the superiority of the new process. In typical experiments, 2 kg of Illinois No. 6 coal were ground to −100 to 200 mesh. The total sulfur content was 1.59 percent, including both organic and inorganic sulfur. The ground coal was mixed with 4 kg of water. The mixture was chlorinated for 45 minutes in a stirred reactor equipped with a reflux condenser. Chlorine flow into the reactor was 12 stdft^3/h (3.4×10^{-2} m^3/h). The reactor temperature — in-

itially in the range of 60° to 90° C — rises sharply in the first 10 to 15 minutes unless cooling is imposed on the reaction system.

After chlorination, the coal was filtered, dried, and dechlorinated at 400° C for 1 hour with a nitrogen purge.

Analysis of the product showed that 51 percent of the sulfur had been removed. In contrast, the older solvent process removed 38 to 45 percent of the total sulfur content under similar operating conditions.

This work was done by John J. Kalvinskas, Nick Vasilakos, William H. Corcoran, Karel Grohmann, and Naresh K. Rohatgi of Caltech for NASA's Jet Propulsion Laboratory. For further information, Circle 35 on the TSP Request Card.
NPO-14902

Acid Solutions for Etching Corrosion-Resistant Metals

Etchants remove metal smears that
may mask surface defects.

Marshall Space Flight Center, Alabama

When a metal surface has been disturbed by machining, milling, or grinding, smeared metal can mask surface flaws from detection. To make the flaws visible, the smeared metal is often removed by a light etching of the surface prior to penetrant inspection.

A new study has characterized solutions for etching austenitic stainless steels, nickel-base alloys, and titanium alloys (annealed). The solutions recommended for use remove at least 0.4 mil (0.01 mm) of metal from a surface in less than an hour.

- For 6Al-4V Titanium: An HNO_3/HF solution is effective.
- For Inconel 718: Both $HCl/HNO_3/NiCl_2/FeCl_3/CrO_3$ and HCl/H_2O_2 solutions are effective.
- For A-286 and 21-6-9 Corrosion-Resistant Stainless Steels: $FeCl_3/HNO_3/H_3PO_4$, $HCl/HNO_3/NiCl_2/FeCl_3/CrO_3$, and HCl/H_2O_2 solutions are all effective.

None of these solutions causes intergranular attack on the metals for which they are effective, when used under the specified conditions.

This work was done by J. R. Simmons of Martin Marietta Corp. for Marshall Space Flight Center. For further information, Circle 36 on the TSP Request Card.
MFS-25467

Improved Ceramic for Heat Exchangers

Multicomponent formulation shows promise
for automotive gas-turbine engines.

Lewis Research Center, Cleveland, Ohio

Many problems remain to be solved in the expanded commercial use of gas-turbine engines in various applications. An important development area involves the selection of suitable materials for heat exchangers. Ideally, heat-exchanger components should be fabricated from dielectric refractory materials with good corrosion characteristics, excellent thermal-shock resistance, and moderate cost.

Potential heat-exchanger materials were evaluated at a contractor facility under NASA contract direction. In this program, numerous multiphase compositions were developed and evaluated. Screening tests of various chemistries included specimen fabrication and measurements of thermal expansion, thermal stability, dimensional stability, and corrosion resistance.

The most promising composition developed in this investigation consisted of mixed oxides of ZrO_2, MgO, Al_2O_3, and SiO_2 and is described generically as ZrMAS. It has been commercially designated as GE-7808. This material was obtained from a low-cost clay/talc mixture.

A major benefit of the multiphase nature of these materials was exhibited during the fabrication and firing of the heat-exchanger honeycomb structure. The rheological behavior and refractoriness of ZrMAS enabled an unfired honeycomb structure to hold its shape better than many single-phase (glass ceramic) materials considered for heat exchangers. Several full-size heat-exchanger honeycomb regenerator cores [4 in. (10.1 cm) in thickness by 22 in. (56 cm) in diameter] were fabricated and compared to a suitable reference material, Corning 9560 Aluminosilicate. The results indicated that ZrMAS is significantly more stable at 2,000° F (1,093° C), in the presence of sodium, and has similar thermal-expansion behavior to the reference material.

Overall assessment of this new material, ZrMAS, indicates that it is a viable candidate for heat-exchanger application in automotive gas-turbine engines and possibly other areas that require dielectric materials of moderate refractoriness, good corrosion resistance, and excellent thermal-shock resistance.

This work was done by T. P. Herbell of Lewis Research Center. and H. W. Rauch and L. R. McCreeght of General Electric Co. Further information may be found in NASA CR-159678 [N81-14082/NSP], "Improved Ceramic Heat Exchanger Materials" [$7.50]. A copy may be purchased [prepayment required] from the National Technical Information Service, Springfield, Virginia 22161.

Inquiries concerning rights for the commercial use of this invention should be addressed to the Patent Counsel, Lewis Research Center [see page A5]. Refer to LEW-13068.

Books and Reports

Resistance of Some Steels to Stress-Corrosion Cracking

Five high-strength low-alloy steels are highly resistant.

Evaluations of the stress-corrosion cracking resistance of five high-strength low-alloy steels are described in a report that is now available. Specimens of 4130, 4340, H-11, D6AC, and HY140 were stressed up to 100 percent of their yield strengths and were exposed to alternate immersion in saltwater, salt spray, and the environments of Alabama and the Florida seacoast.

The steels were heat-treated to various tensile strengths and were found to be highly resistant to stress-corrosion cracking (i.e., failures were not encountered at stress levels up to 75 percent of their ultimate tensile strengths) as follows:
- 4130 and 4340 — below 1,240 MPa (180 ksi);
- H-11 and D6AC — 1,450 MPa (210 ksi); and
- HY140 — 1,020 MPa (148 ksi).

Except for D6AC and HY140, which were tested only at the indicated strengths, the alloys were found to be susceptible to stress-corrosion cracking at stresses above these tensile strengths, and the susceptibility increased with increasing tensile strength.

The long and short transverse grain directions were more susceptible to stress-corrosion cracking than the longitudinal direction. Exposure to alternate immersion in saltwater or salt spray for longer than 1 month and exposure to the seacoast environment for longer than 3 months caused severe nonuniform corrosion and pitting that interfered with the interpretation of test results.

This work was done by T. S. Humphries and E. E. Nelson of **Marshall Space Flight Center.** *Further information may be found in NASA TM-78276 [N80-25413/NSP],"Evaluation of the Stress Corrosion Cracking Resistance of Several High Strength Low Alloy Steels" [$7.50]. A copy may be purchased [prepayment required] from the National Technical Information Service, Springfield, Virginia 22161.*
MFS-25470

Fatigue in Multidirectional Composites

Tests reveal how multidirectional graphite/epoxy composites behave under cyclical loads.

Data in a new report on fatigue properties of graphite/epoxy composites should prove valuable to the designers of aircraft, space vehicles, and automobiles. Graphite/epoxy composites are being used increasingly in lightweight load-bearing structures, and the fatigue of such structures is always a major concern of designers.

The data apply to multidirectional graphite/epoxy composite laminates, including $[0 \pm 30]_{6S}$, $[0/ \pm 45/90]_{4S}$, and $[0/ \pm 45/0]_{4S}$, in which the 0 ply represents the strongest direction when load is applied parallel to this direction. Such multidirectional composites are in contrast to unidirectional composites, in which all plies are oriented in the same direction. Both notched and unnotched specimens were tested under cyclically-varying tension loads, compression loads, and tension-to-compression loads.

For unnotched specimens, the fatigue limit is between 50 and 70 percent of the static ultimate strength, depending on the orientation of the laminate plies relative to the stress axis. Unidirectional graphite/epoxy composites, on the other hand, are insensitive to cyclical loads; they retain virtually all their static strength under fatigue conditions. However, unidirectional composites are prone to failure under off-axis loading, such as shear and torsional loading, since such loads cause failure of the weak fiber/matrix interface and hence the composite itself.

For some notched multidirectional composites, fatigue strength in tension cycling is higher than it is in the unnotched case: The stress concentration at the notch is relaxed over many tension-loading cycles. Under tension/compression cycling, fatigue damage in all the laminates propagates from the edge notches into the interior of the specimen; the specimen fails when a critical amount of damage builds up ahead of the notch root.

The fatigue tests were made on 150-mm-long specimens. The notched specimens were 25 and 50 mm wide, and the unnotched specimens were 9.5 mm wide. The fatigue limit was defined as the stress amplitude at 5 million cycles. The overall test results for the $[0 \pm 30]_{6S}$ laminate were expressed as a constant-life diagram showing the relationship between mean stress and stress amplitude.

Strain in the specimens was measured by an extensometer. Crack growth from edges was continuously monitored by a crack-opening displacement gage. A film of aluminum and a fine gold grid on the specimen surface revealed transverse cracks and surface damage. X-ray photographs were made after given numbers of cycles so that researchers could study damage propagation and identify failure modes and mechanisms.

This work was done by S. V. Ramani and D. P. Williams of **Ames Research Center.** *To obtain a copy of the report, Circle 37 on the TSP Request Card.*
ARC-11396.

Processing Materials in Space

Experiments with potential commercial paybacks are proposed.

A suggested program of material-processing experiments in space is described in an 81-page report. The goals of the program are:
- To learn more about terrestrial material processes by studying them in the absence of gravity and
- To determine whether material processes that benefit by a zero-gravity or ultra-high-vacuum environment can be carried out on a commercial basis in space.

Experiments in crystal growth cover growth from a melt, solution, vapor, or floating zone. Metallurgical solidification experiments cover casting, directional solidification, and undercooling. Containerless processing is the focus of experiments on nucleation and solidification, shaping and forming, and thermophysical measurements. The subjects of fluid- and chemical-process studies are bubble and drop dynamics, fluid dynamics, and thermophysical and physicochemical phenomena. The studies of biological separation processes include experiments on electrokinetic separation.

For each experiment, the report discusses the influence of such gravitational effects as convection, buoyancy, sedimentation, and hydrostatic pressure. The report contains estimates of the power and mission duration required for each experiment. It lists the necessary equipment and the appropriate spacecraft — whether Space Shuttle, Spacelab, or Materials Experiment Carrier.

Potential commercial applications are tabulated. For example, the crystal-growth studies may aid in manufacturing infrared detetors, nuclear detectors, and solar cells. The solidification-process experiments may contribute to the production of dispersed composites, directionally alined materials, metal foams, and superconductors. Experiments on biological separation processes may improve production methods for purified hormones, enzymes, and vaccines.

This work was done by Lowell K. Zoller of **Marshall Space Flight Center.** *To obtain a copy of the report, "Materials Processing in Space (MPS) Program Description," Circle 38 on the TSP Request Card.*
MFS-25667

Strength of Rewelded Inconel 718

Repeated repair welds do not affect joint strength.

Inconel 718, the nickel-based alloy used extensively for high-temperature structural service, can be welded repeatedly without detriment to its strength. According to a NASA report, tests show that 12 repairs on the same weld joint do not adversely affect ultimate tensile strength, yield strength, fatigue strength, metallurgical grain structures, or the ability of the weld joint to respond to postweld heat treatments.

However, at some point between the 6th and 12th welds, a loss of ductility appears. Elongation at break is reduced by about 50 percent — an effect that is attributable to a notch that develops on both sides of a weld joint after repeated repairs. The notches act as stress concentrators that produce a net loss in ductility.

For the tests, plates of Inconel 718 were butt-welded at intervals. Then selected sections of the butt welds were rewelded 2, 6, and 12 times. Coupons were cut from the welded plates to yield specimens containing longitudinal or transverse welds. The specimens were subjected to tensile stress tests or fatigue tests. For the tensile tests, the plates were ¼ inch (0.63 cm) thick; and for the fatigue tests, they were ½ inch (1.27 cm) thick. Tungsten/inert-gas welding with Inconel 718 filler wire and argon shielding gas was used to form the joints.

For the longitudinal specimens, the original welds were 2 inches (5 cm) long; and the repair welds were 1 inch (2.5 cm) long, centered in the original weld. For the transverse specimens, the original weld was 6 inches (15.2 cm) long, and three 1-inch welds were superimposed on the original. The plates were heat-treated and age-hardened, where necessary, before the original welds were made, so that they were all in the same metallurgical condition before the repair-welding experiments. A similar treatment was applied after each repair weld.

Regardless of the number of times specimens had been rewelded, they showed negligible change in strength compared with single-weld specimens. Fatigue strength was similarly unaffected; but elongation at break was markedly lower for the 12-times-rewelded specimens, dropping to 9.7 percent from the 17-percent value recorded for 6-times-rewelded specimens. In metallurgical examinations, no anomalies were found in either the fusion zone or the adjacent base material — no porosity, cracks, lack of weld penetration, or deleterious grain structures.

The tests indicate that rewelding of Inconel 718 is acceptable. Such rewelding is often necessary in complex structures, since Inconel 718 is a difficult material — it flows only sluggishly when molten, and such defects as inclusions and incomplete fusion frequently appear. Apparently, rewelding to correct the defects does not harm the material.

This work was done by E. O. Bayless, C. V. Lovoy, M. C. McIlwain, and P. Munafo of **Marshall Space Flight Center.** *To obtain a copy of the report, Circle 39 on the TSP Request Card.*
MFS-25649

Hydrazine-Compatible Elastomer

Hydrazine hardly reacts with ethylene propylene diene monomer, even at high temperatures.

Ethylene propylene diene monomer (EPDM), also known as material AFE-411, has been tested for compatibility with hydrazine at temperatures up to 400° F (204° C). According to a report on the tests, EPDM is the most hydrazine-compatible material among elastomers. It has strong potential as a valve-seat and O-ring seal with hydrazine (N_2H_4), especially at high temperatures.

The tests were performed to determine the thermal compatibility and basic mechanical-property changes of EPDM in extended exposure to hydrazine. Compatibility was determined in a liquid-phase exothermic test, in which heat generated by exothermic reactions was measured by evaluating the sensible heat changes in a chamber containing EPDM and hydrazine. An immersion test was used to determine changes in tensile strength, elongation, hardness, weight, and dimensions: EPDM samples were submerged in hydrazine at a given temperature for a predetermined period, and the preimmersion and postimmersion mechanical properties were measured.

In the liquid-phase exothermic test, a hydrazine-EPDM exothermic reaction produced about 0.43 Btu (450 joules) over a 16-minute period at an initial temperature of 314° F (157° C), and the reaction subsided after 16 minutes.

Raising the initial temperature to 404° F (207° C) produced an exothermic reaction that generated about 1 Btu (1 kilojoule) over a 30-minute period.

Immersion in hydrazine for 30 days at 150° and 300° F (66° and 149° C) produced no significant change in tensile strength. Increases in elongation of approximately 20 percent and 22 percent were measured for exposures at 150° and 300° F, respectively. Hardness decreased approximately 2 percent after the 150° F exposure and increased approximately 11 percent after the 300° F exposure. Only small increases — 2 percent or less — were measured in weight and thickness.

*This work was done by Orville F. Markles and Thomas G. Dye of Rockwell International Corp. for **Johnson Space Center**. To obtain a copy of the test report, Circle 40 on the TSP Request Card.*
MSC-20007

XPS Study of Oxide/GaAs and SiO₂/Si Interfaces

X-ray photoelectron spectroscopy shows complexity introduced by mixed oxides in the interface with GaAs.

Concepts developed in a study of the SiO_2/Si interface [see "XPS Study of SiO_2 and the Si/SiO_2 Interface" (NPO-14968) on page 281 of *NASA Tech Briefs*, Vol. 6, No. 3] have been applied to an analysis of the native oxide/GaAs interface. High-resolution X-ray photoelectron spectroscopy (XPS) has been combined with a precise chemical-profiling technique and resolution-enhancement methods to study the stoichiometry of the transitional layer. The results are presented in a report that is now available.

Metal-oxide-semiconductor (MOS) devices require a chemically stable interface between the oxide and the semiconductor. In silicon technology, the amorphous nature of the silicon dioxide (SiO_2) film allows the structure to accommodate lattice mismatches at the SiO_2/Si interface. For the compound semiconductor gallium arsenide (GaAs), however, the structure of the oxides is not as simple.

The key observation from the XPS study of the native oxide/GaAs interface is the complexity introduced by the large number of different oxide species. Not only the stable Ga_2O_3 and As_2O_3 observed but evidence for such mixed oxides as $GaAsO_2$, $GaAsO_3$, and $GaAsO_4$ is found. The presence of arsenic metal is also indicated from analysis of the As 3d spectra.

The profile data demonstrate that the native oxide is not vertically homogeneous. Towards the oxide surface, a mixture of As oxides and Ga oxides is found. As the oxide/GaAs substrate interface is approached, arsenic metal and primarily Ga oxides are found. This layer of Ga oxide is structurally and/or chemically distinct from the Ga oxides in the mixed region.

*This work was done by Frank J. Grunthaner, Paula J. Grunthaner, Richard P. Vasquez, Blair F. Lewis, Joseph Maserjian, and Anupam Madhukar of USC for **NASA's Jet Propulsion Laboratory**. To obtain a copy of the report, Circle 41 on the TSP Request Card.*
NPO-14969

Life
Sciences

Hardware, Techniques, and Processes

Low-Noise Implantable Electrode

A pocket configuration isolates the electrode/electrolyte interface from body tissue.

Ames Research Center, Moffett Field, California

A new implantable electrocardiogram electrode is much less sensitive than previous designs to spurious biological potentials. Designed in a novel "pocket" configuration, the new electrode is intended as a sensor for the radiotelemetry of biological parameters in experiments on unrestrained subjects.

The key element in the electrode, shown in the figure, is an electrically conductive pocket with a large mouth that permits the influx of conductive body fluid so that electrical current can reach the inner pocket surface. The pocket resembles a squashed cylinder that is open at one end and closed at the other. An electrical lead at the closed end carries the sensed biopotentials to radiotelemetry circuits.

The exterior and the mouth of the electrode are covered with silicone so that the only part of the electrode in electrical contact with the electrolyte is the interior of the electrode assembly. Thus the electrode/electrolyte interface is kept separate from body tissue. With previous electrodes, the rubbing of tissue against the active conductive surface generates artifacts on the baseline electrocardiogram.

Cloth strips, bonded to the pocket by its silicone coating, permit the electrode to be securely sutured to adjacent tissue. Additional cloth strips relieve stress on the telemetry lead.

In a comparison of the new unit with loop and disk electrodes usually used for implantation, pairs of electrodes were immersed in a saline bath, and one of each pair was rubbed between two fingers in a simulation of electrode/tissue motion in an active subject. The loop electrode generated more artifacts, by at least an order of magnitude, than the disk electrode. Neither baseline shifts nor oscillations were observed with the new pocket electrode.

NOTE: The two views are drawn to different scales.
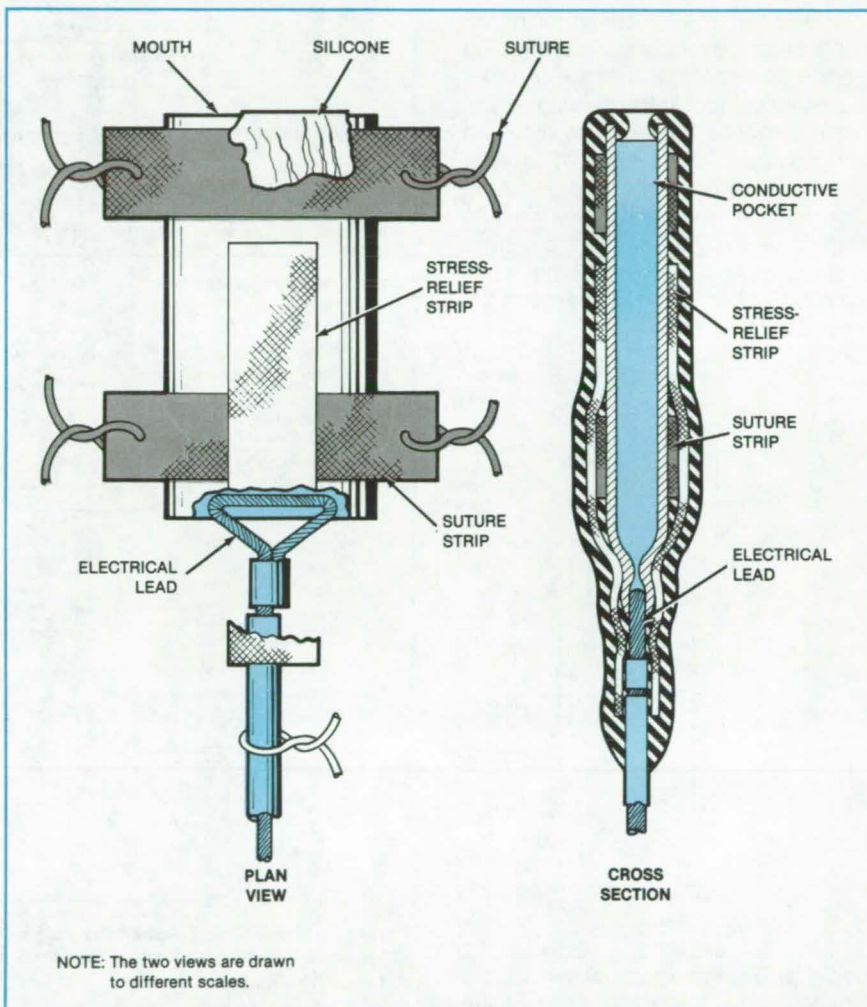
Implantable ECG Electrode, shown here in plan view and cross section, is essentially a squashed cylinder that admits body fluid into its interior. The cylinder and electrical lead are made of stainless steel. Spot welding and crimping are used for assembly, rather than soldering.

This work was done by Gorden F. Lund of **Ames Research Center.** For further information, Circle 42 on the TSP Request Card.

Inquiries concerning rights for the commercial use of this invention should be addressed to the Patent Counsel, Ames Research Center [see page A5]. Refer to ARC-11258.

Moving-Surface Follower Aids Microsurgery

Surgical implements are precisely positioned
in moving tissue.

NASA's Jet Propulsion Laboratory, Pasadena, California

A novel manipulator follows the move-
ments of arteries and muscles, enabling
precise placement of a probe or other
microsurgical tool in the moving tissue.
The microprobe assembly is mounted
on the output of the pneumatic servo of
a commercial noncontacting thickness
gage. Pulsations of the tissue surface to
be penetrated by the probe are sensed
by the gage and followed by the servo,
eliminating relative motion between the
tissue and the probe.
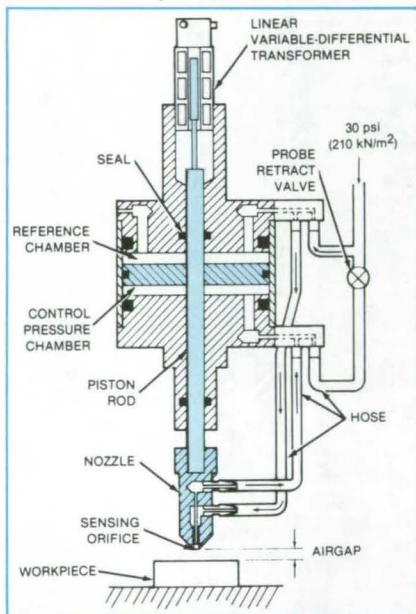
Figure 1. The **Pneumatic Servo** of the
noncontacting thickness gage main-
tains a nearly constant airgap between
the workpiece and the nozzle by re-
sponding to changes in back pressure in
the sensing orifice.

Figure 2. The **Sensing Assembly and Servo Probe Control** sense arterial, muscular, or
other bodily motion and move the probe so as to maintain a constant position relative to
the moving tissue.

A cross section of the pneumatic
servo is shown in Figure 1. Air at a regu-
lated pressure is fed to the reference
chamber and to the sensing orifice of
the nozzle. If the workpiece surface is
within the sensing range of the orifice,
the escaping air is impeded by the sur-
face, giving rise to a back pressure that
is transmitted up the tube and into the
control chamber. If the nozzle is too
close to the sensed surface, the back
pressure exceeds the reference pres-
sure, causing the nozzle to move up and
away from the workpiece. Similarly, the

back pressure will be lower, and the noz-
zle will move down if it is too far from the
workpiece. Thus, the pneumatic servo
maintains a constant gap between the
nozzle and the sensed surface.

The probe-retract valve is closed dur-
ing normal operation. When it is opened,
the control chamber is fully pressurized,
raising the nozzle away from the work-
piece. A linear variable-differential trans-
former attached to the piston rod is pro-
vided in case position measurements
are desired. For example, it could give
an indication of arterial motion during
use.

Figure 2 shows the servosystem cou-
pled with a follower assembly in a
system designed to sense arterial mo-
tion. The stirrup rests on the artery while

the guides and sensing cup transmit
arterial motion to the sensing nozzle.
The follower assembly is made from
thin-wall stainless-steel tubing and thin
sheet and has a mass of about 2 grams.
The probe mounts to the bracket
clamped to the sensing nozzle. For ac-
curacy, the probe penetrates the arterial
wall close to the stirrup.

Mechanics

Portable Radiometer Identifies Minerals in the Field

Field unit determines spectral reflectance ratios.

NASA's Jet Propulsion Laboratory, Pasadena, California

A hand-held optical instrument aids in identifying minerals in the field. It can be used in exploration for minerals on foot or by aircraft. The instrument — a radiometer — is especially suitable for identifying clay and carbonate minerals. It bases its identifications on the characteristic distributions of wavelengths in Sunlight reflected by minerals. For example, kaolinite absorbs and reflects Sunlight at micrometer wavelengths with a spectral pattern different from those of other layered silicates, such as montmorillonite or alunite (Figure 1).

Essentially, the radiometer measures the reflectances of a mineral at two wavelengths, computes the ratio of the reflectances, and displays the ratio to the user. The user then looks up that value in a table to find out to what mineral it corresponds. If there is any ambiguity — if the value is close to those for two or more minerals, the user can repeat the reflectance ratio measurement for two other wavelengths. The mineral that is common to both ratio values is thus identified.

By determining ratios rather than absolute values of reflectance, the radiometer eliminates the effects of variations in the intensity of the Sunlight that falls on the mineral. While the intensity of the
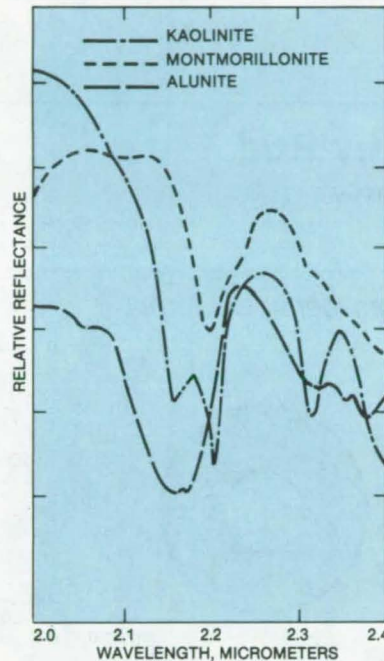
Figure 1. **Reflectance Spectra** of kaolinite, montmorillonite, and alunite are markedly different in the 2.0-to-2.4-μm range of wavelengths shown here. The vertical bars on the horizontal scale represent band-pass wavelengths of four filters commonly used in the mineral-identification radiometer.

reflected light at a given wavelength will depend on the brightness of the illumination, the ratio of the intensity at any two wavelengths will be essentially constant regardless of the brightness. Even when the Sun is partly obscured by high cirrus clouds, reflectance ratio differs from that when the sky is clear by no more than a few percent. Of course, the radiometer should be aimed at an area that is relatively free of shadows.

The radiometer contains two optical trains, each having two repeater lenses and a cooled lead sulfide detector (Figure 2). Each train is intersected by a filter wheel containing five interference filters. The filters pass light within a narrow wavelength band — some as narrow as 0.01 μm — at selected wavelengths between 0.4 and 2.5 μm. For compactness, the wheels are coaxial; slots in each allow light to pass unimpeded through a filter in the other. The detected signals are amplified in separate channels and applied to an analog divider circuit and digital display circuit.

The total time for a calibration and measurement is only a few seconds. The user connects the radiometer to a battery pack and turns each of the filter
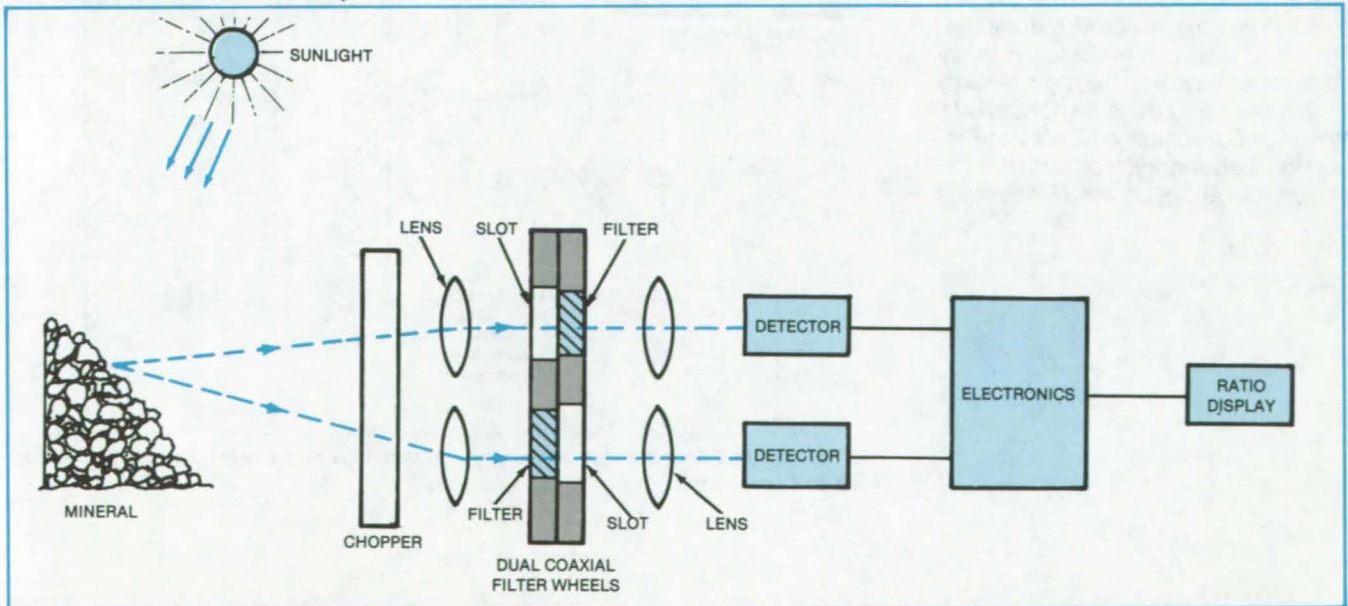
Figure 2. **Dual Optical Trains** provide electrical signals representing the reflectance of an unknown mineral at two different wavelengths. Electronic circuitry computes and displays the ratio of the two reflectances.

wheels (by knobs at the base of the instrument) to position filters at the desired wavelengths in the optical trains; for example, 2.17 μm in one train and 2.20 μm in the other. To calibrate the radiometer, the user aims it at a highly-reflective optical reference standard, such as Fiberfrax white ceramic wool, and adjusts channel gain so that the digital readout shows 1.00.

The user then aims the instrument at the mineral in question. For example, if the readout shows 1.20 for the 2.17- and 2.20-μm filters, montmorillonite would be suggested by a table of ratio values. If the user changes the filters to 2.20 and 2.22 μm and the readout shows 0.94, the table would confirm that montmorillonite is the mineral.

Anchor for Fiberglass Guy Rod
An aluminum fitting attaches securely to the rod end.

NASA's Jet Propulsion Laboratory, Pasadena, California

Fiberglass rods are excellent for guying antenna support structures, because the fiberglass is transparent to radio waves and therefore does not distort the radiation pattern. It is also strong, light, and weatherproof. However, anchoring the rods is difficult.

A solution to this problem is to install a nut with threads on the outer circumference, followed by an aluminum sleeve. As the figure shows, the sleeve has an opening that is oval at its upper end and round at the bottom end.

Next, the end of the rod is split so that a fiberglass wedge can be inserted to form a V-shaped end. The spread end of the rod fits into the tapered hole in the sleeve, and then a threaded aluminum coupling is put over the rod and sleeve. This coupling is screwed over the nut, thus holding the encased rod captive. The fitting then can be fastened to another structure to hold the rod in tension.

THREADED COUPLING

FIBERGLASS WEDGE (EPOXIED IN PLACE)

ALUMINUM SLEEVE

FIBERGLASS ROD

NUT (GALVANIZED STEEL OR ALUMINUM WITH ANTISEIZE COMPOUND)

ALUMINUM SLEEVE
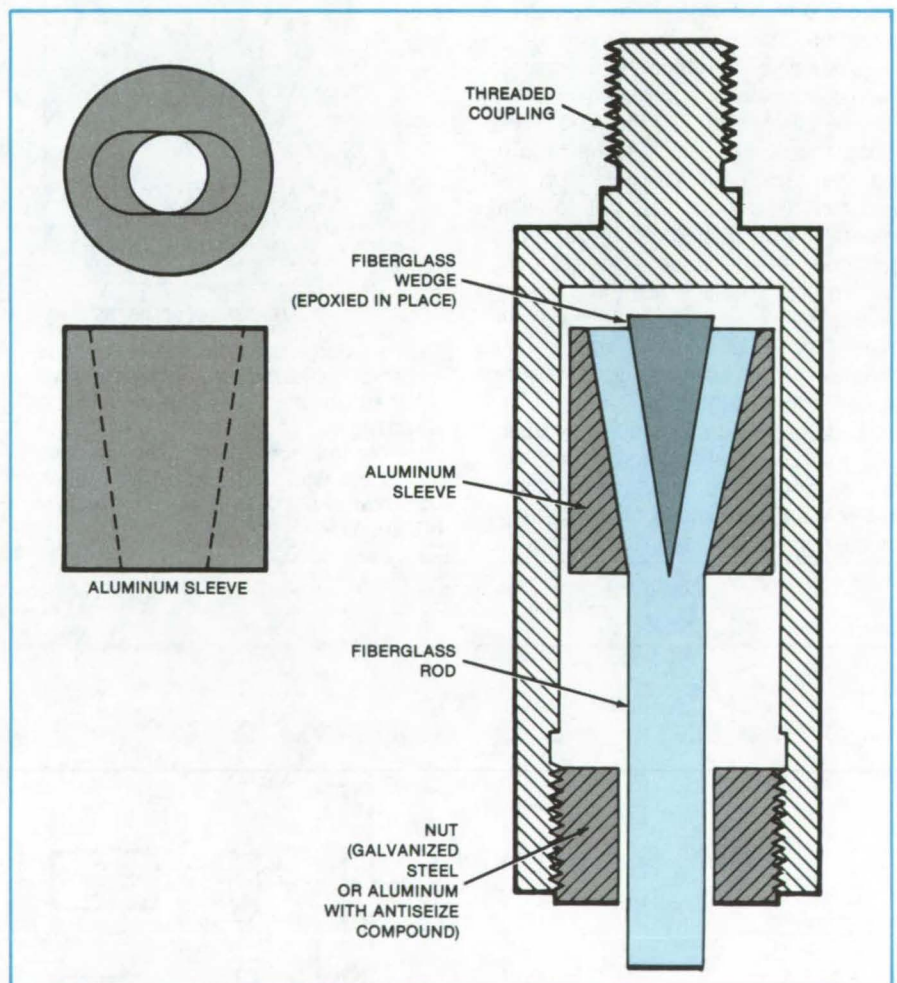
This **Tension Rod Anchor** holds a fiberglass guy rod firmly for use in supporting antenna feeds or structures.

Water-Vapor Sample Holder for Mass Spectrometers

A sample of ambient air is captured
for use as a calibration standard.

NASA's Jet Propulsion Laboratory, Pasadena, California

A metal sample holder introduces the reference standard sample of water vapor into a mass spectrometer. It contains a known volume that is sealed with a thin aluminum disk. The disk is punctured to inject the water vapor into the mass spectrometer.

The holder, shown in the figure, contains a sample of ambient air before the cap is attached. Thus, the sample captured when the cap is attached contains a sample of water vapor in the air. Because the relative humidity of the local atmosphere is measurable, the sample has a known composition that can be used in calibrating the peaks produced by mass spectroscopy.

The sample holder will be used in
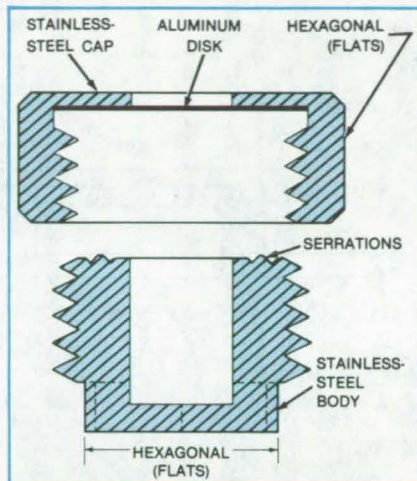
This **Water-Vapor Sample Holder** for a mass spectrometer contains water vapor for calibration. It is sealed by an aluminum disk. The calibration sample and the integrated circuit modules are tested sequentially in the same manner.

quality assurance testing and analytical testing of the water-vapor content of failed integrated-circuit modules. The modules and sample holders are heated for 24 hours in a high-vacuum chamber before they are punctured and the gas directed to the mass spectrometer for analysis. One of the gases of interest is water vapor, which is a significant contaminant of the modules. The water-vapor sample holder passed hermeticity testing in each of two trials.

This work was done by Ray F. Haack and William W. Reilly of Caltech for **NASA's Jet Propulsion Laboratory.** *For further information, Circle 46 on the TSP Request Card.*
NPO-15007

Measuring Hydrogen Properties in Aluminum

Real-time measurements of gas evolution
are correlated with porosity data.

Langley Research Center, Hampton, Virginia

A system in use at Langley Research Center measures the concentration and diffusion coefficient of hydrogen in pure aluminum. Its principal components are a high-temperature (0 to 1,500° C) ultra-high-vacuum furnace and a quadrupole mass spectrometer. The system operates at a base pressure of 1×10^{-11} torr. Quantities of hydrogen and other gases that evolve from the heated metal are measured in real time and correlated with data on aluminum porosity.

The technique permits the measurement of solubility, diffusion coefficients, and outgassing rates of gases in low vapor pressure materials either in solid or liquid phase. Measurements can be made with any material that does not contaminate the vacuum system. Further, the technique permits the separation of bulk gases from those desorbing

from the sample surface. Since it utilizes a mass spectrometer under ultra-high-vacuum conditions, it can detect any desorbing gas with a sensitivity approaching 1 ppb. The real-time measurement of evolving gases also allows the study of kinetic effects of both surface and bulk mechanisms occurring during the desorption interval.

Using the system, a statistical analysis of the porosity in 99.995-weight-percent pure commercially-available cast aluminum has been correlated with real-time hydrogen evolution data, to estimate the hydrogen partitioning in solid solution, in the porosity, and on the surface of the aluminum. The hydrogen evolves initially from the aluminum surface, along with carbon monoxide and water, followed by large hydrogen pres-

sure pulses (due to the rupture of gas-filled pores near the surface) superimposed on a smooth steady desorption from solid solution. The rupturing pores were observed visually and found to occur both in the solid state and after melting. After the train of gas pulses, the hydrogen signal dramatically decreases.

An analysis of pore- and pulse-size distributions indicates more than 99 percent of the bulk hydrogen is partitioned in pores greater than 25 μm. The total hydrogen content in the pores and in solid solution is 6.3×10^{17} atoms/cm^3 or 10.5 ppm (atomic).

This work was done by R. A. Outlaw of **Langley Research Center.** *For further information, Circle 47 on the TSP Request Card.*
LAR-12906

Three-Dimensional Air Curtains

Gas flow would partition a large
volume into separate spaces.

Lyndon B. Johnson Space Center, Houston, Texas

A proposed scheme for gas "curtains" would partition a large volume into several separate spaces. The containment concept was originally developed for possible use on the Space Shuttle main engines, where it would provide a dynamic barrier of nitrogen to prevent cold engine gases from reaching the aft fuselage skin, where they could cause tile freezing. The concept may also be useful in such terrestrial applications as unobtrusive isolation of smoking and nonsmoking sections in restaurants and offices. In general, the scheme is suitable for the isolation of objectionable or hazardous gases in a free space.

For the Space Shuttle, a circular manifold would be constructed around each main engine. Nitrogen would flow from holes 0.1 inch (2.54 mm) in diameter. The holes would point forward and be spaced at 3-inch (7.62-cm) intervals. The nitrogen jets issuing from the holes would coalesce, forming a nitrogen curtain that entrains the cold engine gas, carrying it forward.

To isolate a smoking area in a commercial building, air would flow from orifices in the floor (see figure). Rows of orifices 2 inches (5 cm) in diameter would delineate the smoking area. Exiting from the orifices at a maximum velocity of 4.8 ft/s (1.5 m/s), jets of air would form curtains that carry off the smoke-laden air and prevent it from mixing with air in the adjacent nonsmoking areas. The 4.8-ft/s velocity ensures that the cur-
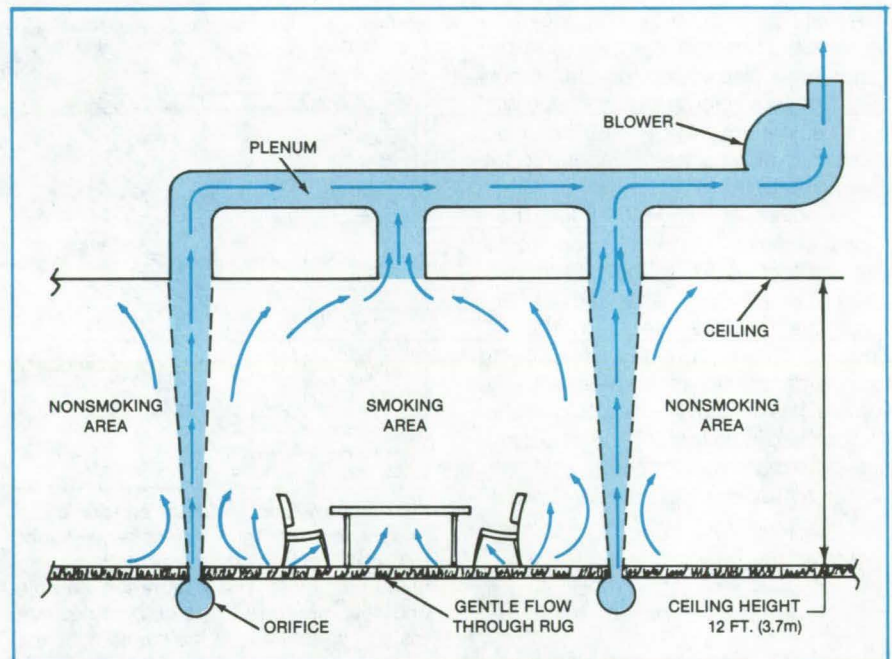
Smokers Are Separated From Nonsmokers by curtains of air issuing from orifices in the floor. An additional gentle flow of air through the rug aids the removal of air from the smokers' volume.

tains entrain air effectively without disturbing the occupants.

Channels in the ceiling would allow the curtain air and its entrained gases to be removed. The area of the plenum above the exhaust should be at least 100 times the total orifice area. An exhaust velocity of at least 30 ft/min (0.15 m/s) and a plenum suction of 4 inches of water (1 kN/m^2) below atmospheric pressure will ensure adequate air removal.

This work was done by James G. Stephenson and Charles E. Daniher, Jr., of Rockwell International Corp. for **Johnson Space Center.** *No further documentation is available.*
MSC-20058

Reentrant-Groove Hydrogen Heat Pipe

Novel configuration of extruded, axially grooved tubing
reduces cryogenic fluid charge and increases wicking height.

Ames Research Center, Moffett Field, California

Aluminum heat pipe can be extruded with reentrant axial grooves, which give better overall performance than conventional rectangular grooves. The reentrant grooves increase the wicking height of cryogenic fluids and also lower

the amount of fluid charge that is required.

The reentrant grooved tube is shown in the figure. The basic 6063-T6 aluminum extrusion has a 14.6-mm outside diameter, with a wall thickness of 1.66

mm, and contains 20 axial grooves that surround a central 9.3-mm-diameter vapor core. Each axial groove is 0.755 mm in diameter, with a 0.33-mm opening formed by pinched rounded fin tips.

The heat pipe was tested at room temperature with varying charges of ammonia working fluid. Once the proper charge had been determined, the heat pipe was filled with research-purity hydrogen and tested in a thermal vacuum chamber using a liquid-helium cooling system. The hydrogen test program was designed mainly to develop a performance map for the heat pipe, at the nominal 20 K operating temperature.

Transient effects in cooling down the hydrogen heat pipe were measured without an evaporator heat load. Heat-pipe action started about 2½ h into the cooldown, as evidenced by the convergence of evaporator, transport, and condenser temperatures within the expected 15 to 33 K operating range. The steady-state performance data, taken over a temperature range of 19 to 23 K, indicate a static wicking height of 1.42 cm and a maximum transport capacity of 5.4 W-m.

As a final test, the startup of heat-pipe operation from a completely frozen condition was also successfully demonstrated. The heat pipe was kept frozen for 3 h by holding the condenser at approximately 12 K with a 0.20-cm adverse tilt. Then a 1.8-W evaporator heat load was applied, and within 5 min the heat pipe was operational at 15 K.

This work was done by Joseph Alario and Robert Kosson of Grumman Aerospace Corp. for **Ames Research Center.** No further documentation is available.

Inquiries concerning rights for the commercial use of this invention should be addressed to the Patent Counsel, Ames Research Center [see page A5]. Refer to ARC-11381.

HEAT-PIPE
TUBE

MAGNIFIED SECTION
OF A SINGLE
REENTRANT GROOVE

The **Reentrant Grooves** in this aluminum heat pipe shown in cross section impart better performance than rectangular grooves, at a lower fluid inventory.

Reflective-Shield Radiative Cooler

Angled thin reflectors form cavity radiators
that reflect heat out into space.

NASA's Jet Propulsion Laboratory, Pasadena, California
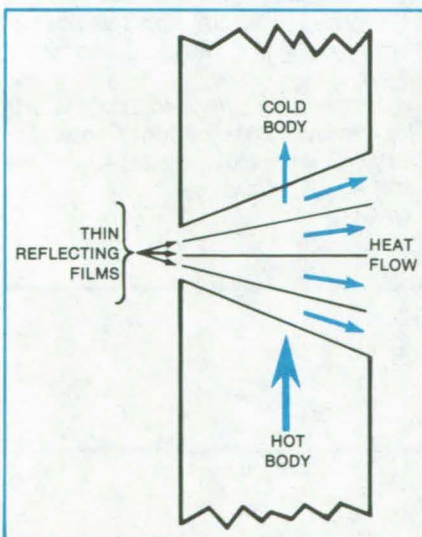
Thin Reflecting Films, set at angles to create triangular cavities, are effective in deflecting heat flow.

Recent tests show that a radiative cooler consisting of several thin reflective shields with a slight angle between them redirects the flow of heat very effectively. As shown in the figure, heat that flows toward the surfaces of the shields enters a triangular cavity and is radiated out to the side.

Experiments have confirmed the effectiveness of this heat-shielding technique. The shields were aluminized polyester, supported by polyester cords with an angle of about 1.5° between them. The experimental data provided calibration points for a theoretical model that can be used in the design of units for spaceborne radiative coolers and other applications.

The shield can be used for deflecting virtually any level of thermal radiation in vacuum. In air, only relatively high intensity thermal radiation can be deflected by this technique; but even so, it may be useful in constructing reflecting baffles in front of ovens or furnaces.

This work was done by Walt Petrick and Ramon D. Garcia of Caltech for **NASA's Jet Propulsion Laboratory.** *For further information, Circle 48 on the TSP Request Card.*
NPO-15465

Transducer System Traces Mine-Face Curve

Automated system measures angles
between track sections.

Marshall Space Flight Center, Alabama
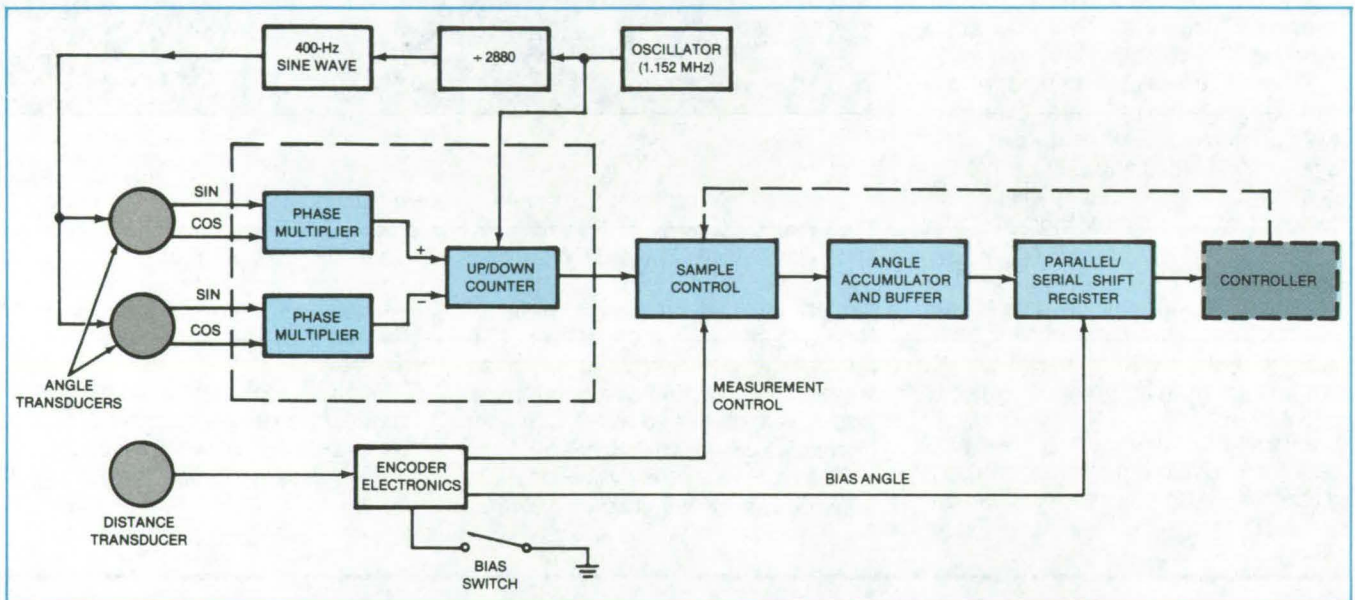
Angles Are Measured between adjacent track sections by means of the phase difference between the outputs of the two transducers. The distance transducer is an incremental optical encoder.

An electromechanical system is capable of obtaining contour information on a longwall coal face while a longwall shearer mines coal. Two heavy-duty angle transducers 2.5 feet apart are attached to a common reference surface and operate in conjunction with a distance encoder to measure the angle between adjacent track sections along the coal face.

As the machine travels, angle and distance measurements are transferred to the memory of a commercial automatic control unit (see figure). Uncertainties that arise because of surface irregularities are handled by taking many measurements over short track distances. To eliminate bias errors due to initial misalinement of the angle transducers, a large number of measurements are made along each track section, averaged, and subtracted from subsequent angle measurements. Upon completion of a run, the data are retrieved and processed by the controller to generate the coal-face curve.

Under simulated conditions, track position and angle parameters were measured and compared with actual values. The system calculated the curve for a 150-foot (46-m) coal face to within ± 8 inches (± 20 cm) of its true position while moving at a rate of 10 feet/minute (5 cm/s).

This work was done by Benton Corp. for **Marshall Space Flight Center.** *For further information, Circle 49 on the TSP Request Card.*
MFS-25289

X-Ray Measurement of Tank Liquid Level

The liquid surface can be observed through a metal container
wall, allowing direct determination of quantities and changes.

Lyndon B. Johnson Space Center, Houston, Texas

X-rays can show the liquid level inside a closed metal tank, thus offering a direct measurement to replace such indirect measurement methods as weighing, refilling, or offloading. The technique was first used for determining the levels in propellant tanks on the Space Shuttle, where it led to the explanation of pro-

pellant loss caused by stripping. Successful results were obtained on single-walled titanium tanks with wall thicknesses up to 0.125 in. (0.32 cm) and on stainless-steel tanks with walls 0.250 in. (0.64 cm) in thickness. The technique may work for other materials and dimensions, however each case

would have to be confirmed by tests.

As shown in the figure, a commercial portable X-ray source is used in the measurement. The liquid appears as a solid dark mass in the X-ray photograph, so the source should be approximately alined with the liquid level for accurate results. Reference indicators made of
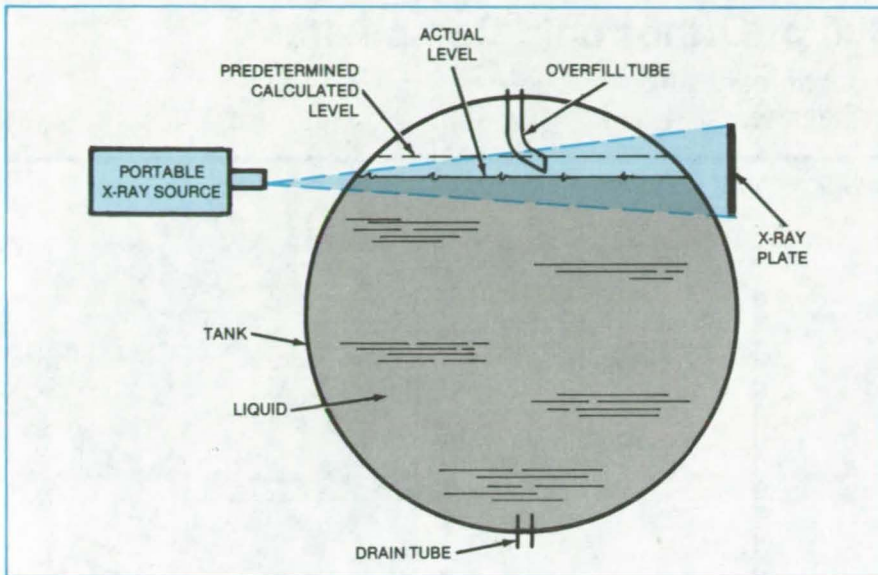
X-Ray Measurement of liquid level produces a photograph in which the liquid appears as a solid dark mass. A commercially-available portable X-ray machine is used.

lead may be taped on the tank at known heights to help in obtaining accurate results.

In the Space Shuttle tanks, pressurizing cycles are used to minimize the size of gas bubbles in the liquid. X-ray photographs taken after each cycle showed that they produced a stripping effect. Prior to the X-ray analysis, it had been expected that as soon as the top of the vent pipe opening was exposed, only gas would be vented. In fact, however, propellant was vented also because of the stripping effect. To avoid that loss, the loading technique was modified by slowing the vent rate to less than 5 psi per minute (0.6 kN/m^{2}s).

This work was done by R. Gilbert Macias of Rockwell International Corp. for **Johnson Space Center.** *No further documentation is available.*
MSC-18935

Heat and Pressure Seal for Doors

Refractory fibers provide resilience.

John F. Kennedy Space Center, Florida

A proposed tubular gasket for doors performs a dual function: It seals in pressure, and it seals out heat. Composed of a quartz fabric filled with alumina matting, the gasket is bonded with a room-temperature-vulcanizing material to the periphery of the door (see figure). When the door is closed, the gasket is compressed like an O-ring so that it fills the gap between the door and the frame and prevents leakage of air and heat.

The gasket is under consideration as a seal for a vent door on the Space Shuttle. It is 30 percent lighter than the seal previously used, withstands higher temperatures [up to 2,800° F (1,540° C)], and allows the door to be closed with less force. It may be suitable for other spacecraft and commercial aircraft. It may find automotive applications too, for example, as an exhaust manifold closure when a car is converted from a V-eight to a V-four engine.

This work was done by Charles A. Gillespie of Rockwell International Corp. for **Kennedy Space Center.** *No further documentation is available.*
KSC-11216
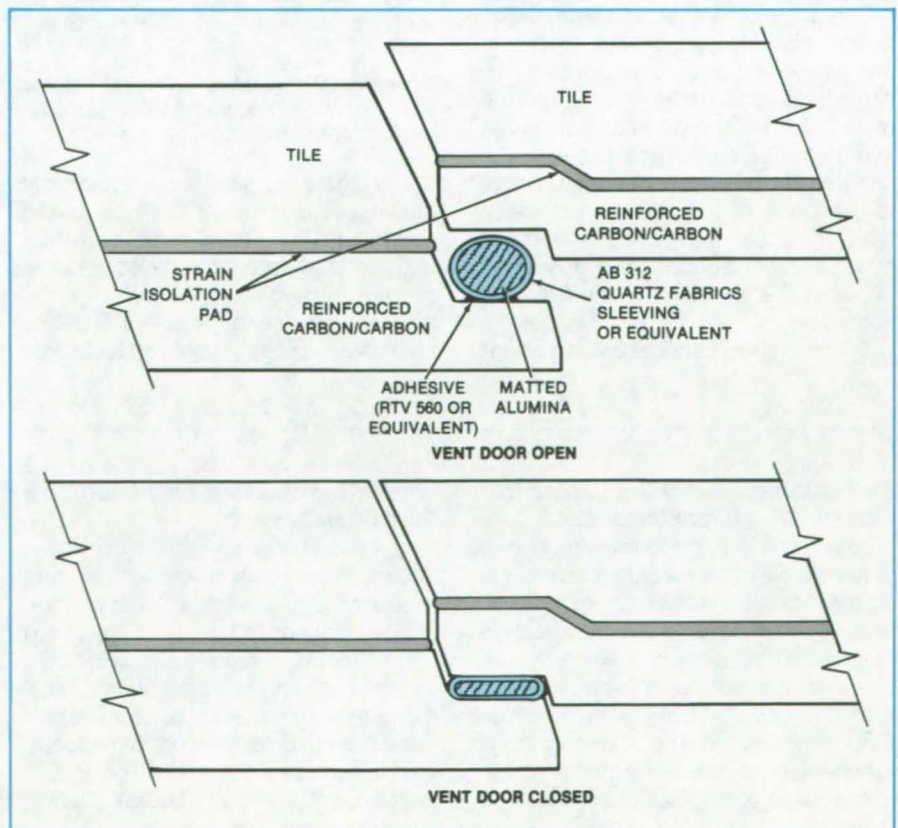
The **Quartz Fabric Gasket** serves as both a pressure seal and a thermal barrier.

Determining Shear Moduli of Orthotropic Composites

Tests show that composites differ substantially from
conventional materials under torsional shear.

Ames Research Center, Moffett Field, California

New torsion tests on specimens of the same orthotropic composite material having at least two different thicknesses enable the determination of the effective in-plane and out-of-plane shear moduli. The moduli are calculated from experimental data with elasticity-theory equations that relate the applied torque, torsional twist angle, specimen width/thickness ratio, and the ratio of the two shear moduli. The torsion tests were developed to yield information on the degradation of properties of a composite saturated by moisture.

The tests were made on 2-mm-thick commercially available specimens measuring 100 mm in length and 6.3, 9.6, 12.5, and 15.8 mm in width. The specimens were measured at a controlled angle of twist on an electrohydraulic servo test unit. A torsional force was applied at one end of a specimen, and the torque developed was measured by a strain-gage torque cell at the other end.

The angle of twist was determined by a potentiometer associated with the strain gage and by a noncontacting optical method. In the latter method, mirrors were glued to the specimens along the centerline. A low-power laser beam was directed at a mirror in a direction normal to the plane of the untorsioned specimen. The angle of twist was determined by measuring the tangent of the angle between the incident ray and the reflected beam.

The orthotropic model developed for
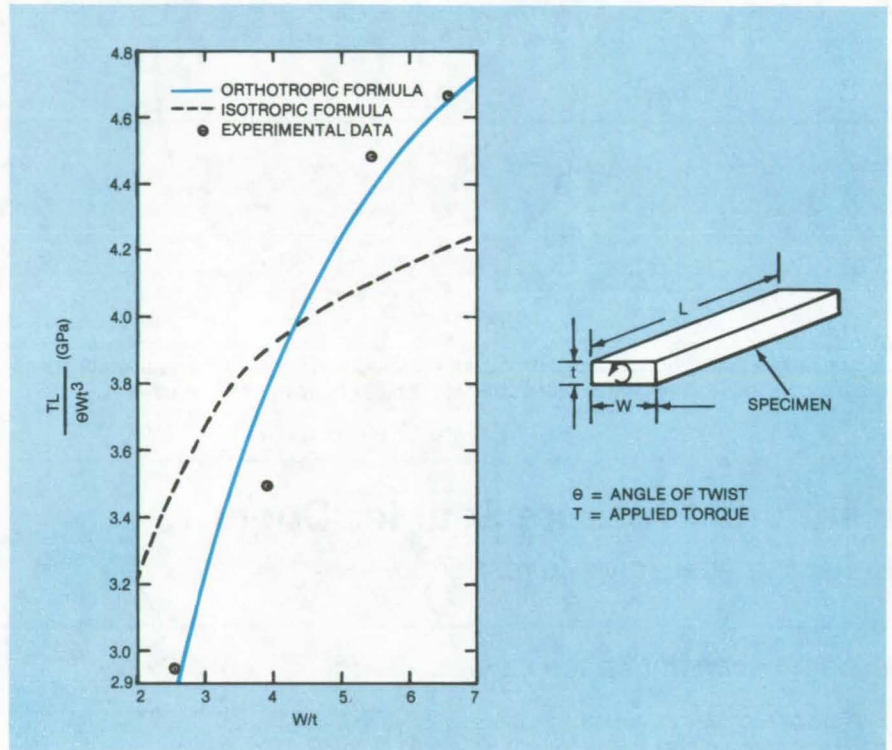
Specimen Dimensions, Torsional Twist Angles, and Applied Torque were measured and also calculated according to isotropic and orthotropic models, for specimens of a commercial graphite/epoxy composite.

the test data provided a much better fit than the conventional isotropic model (see figure). The tests made clear that both uniaxial and cross-ply composites are not transversely isotropic, and the difference between in-plane and out-of-plane shear moduli should be taken into account in structural design.

This work was done by H. Theodore Sumsion and Yapa D. S. Rajapakse of **Ames Research Center.** *For further information, Circle 50 on the TSP Request Card.*
ARC-11395

Self-Alining, Latching Joint for Folding Structural Elements

A new center joint, consisting of a pair of hinged hubs, alines column elements automatically and fastens them together securely. The paired hubs are attached to a folded pair of column elements. Until the columns are unfolded, spring-loaded rings on the hubs restrain latches that ultimately secure the assembly. When released, the locking rings rotate and engage teeth that latch the hubs together.
(See page 440.)

Simple Temperature Regulator for a Cold Chamber

Heat flow into a chamber is controlled and monitored by a simple temperature regulator. An electronic circuit operating in conjunction with a refrigeration unit holds the chamber at a selectable temperature and lights a warning light if the temperature exceeds a predetermined level above the control temperature. To avoid cycling the unit on and off too frequently, 3° C of hysteresis is built into the control circuit.
(See page 371.)

Two-Speed Valve

A two-speed valve, permits fine control of flow as it is first opened yet opens rapidly as it approaches full flow. For the first part of valve opening, a nut is turned on the screw, which advances the valve stem at a rate determined by the difference between the thread pitch on the inside of the nut and the pitch on the outside. For the fast, final part of valve opening, the nut contacts the valve shaft and drives it directly.
(See page 448.)

Books and Reports

Wrinkling of Stretched Films: Compressive Stress

Equations of motion are derived for small in-plane vibrations.

A recent report presents the derivation of equations of motion for wrinkles forming in planar films under compressive in-plane stress. This study was prompted by the wrinkling of thin-film solar-cell arrays with a consequent reduction in collection efficiency. The lack of an adequate theoretical understanding has made it difficult to design large film structures and to specify oscillation tests for large solar-array systems.

The basic physical model is a film sufficiently thin so that its stiffness may be ignored. The film buckles and wrinkles whenever one attempts to apply a compressive in-plane stress. The wrinkling process allows the film to deform further without any increase in applied stress; that is, the film behaves nonelastically.

Mathematically, this behavior is represented by requiring the terms for the principal tensile stresses, σ_{11} and σ_{22}, to be nonnegative under all conditions. The resulting inequalities are satisfied by transforming to a new representation of the stress tensor in which new principal stresses, σ_{11}^* and σ_{22}^*, vanish whenever σ_{11} or σ_{22}, respectively, becomes negative.

The new stress tensor σ^* is substituted into the equations of motion for a thin film. The equations are simplified and applied to the case of small in-plane vibrations transverse to the direction of stretching in a rectangular film stretched in one direction. The resulting equation of motion resembles a standard wave equation except for the presence of a nonlinear term that represents the zero-compressive-stress requirement.

The equation is approximately solved for both free and forced vibrations, using the technique of equivalent linearization. The solutions exhibit the effects of the nonlinear wrinkling term: The amplitudes of free vibrations increase and their frequencies decrease relative to vibrations in nonwrinkled films, while the center of vibration shifts from the equilibrium position toward the domain of film contraction. In the case of motions driven by external sources, the solution predicts that symmetrical applied forces produce nonsymmetrical vibrations. (Also see the following article.)

This work was done by Michail A. Zak of Caltech for **NASA's Jet Propulsion Laboratory.** *To obtain a copy of the report, Circle 51 on the TSP Request Card.*
NPO-15203

Wrinkling of Stretched Films: Shear Stress

Mathematical analysis aids understanding of wrinkle effects in blanket/boom solar arrays.

A new report presents a theoretical investigation of nonlinear shearing characteristics of wrinkling films under applied shear stress. In conjunction with the document described in the preceding article, the report helps explain the force/deflection characteristic of in-plane boom and solar-array blanket structural combinations. In addition, the investigation has made it possible to predict such nonlinear effects as the dependence of frequencies of vibrations on the vibration amplitude and the emergence of regions of parametric resonance between in-plane and out-of-plane resonance.

Large-area film structures are being deployed in the form of solar-cell arrays. Structural problems not previously known have arisen because of the nature of films. One such problem is the tendency of films to wrinkle under shear stress. The wrinkles behave oddly: Their force-vs.-deflection characteristic is nonlinear, and so is the relation between vibration frequency and amplitude.

The approach of the investigation was to formulate the stress state of the film as a function of the applied shear stress and to use the stress state to develop an equation of motion for the film wrinkling that develops. The equation, which is nonlinear, was then solved for particular vibrational states by the method of equivalent linearization.

This work was done by Michail A. Zak of Caltech for **NASA's Jet Propulsion Laboratory.** *To obtain a copy of the report, Circle 52 on the TSP Request Card.*
NPO-15204

A Closer Look at Track/Train Dynamics

A mathematical model is developed for derailment safety analysis.

A recent report describes an analytical approach to the question of operational safety for six-axle locomotives. The essential mathematical elements are a locomotive model with corresponding data on suspension characteristics, a method of track-defect characterization, and quantitative measures for characterizing operational safety.

The major derailment mechanisms are flange climbing (in which the wheel flange climbs up and over the top of the rail) and gage spreading (in which a track is pushed outward). (Vehicle rollover does not normally occur.) The causes involve excessive lateral wheel/track forces or vertical unloading: Clearly, an evaluation of the safety of a specific vehicle must therefore be concerned with the forces between wheels and rails.

The quantities related to dynamic wheel/rail interactions include:
- Locomotive parameters describing geometric properties, mass distribution, vibrational and rotational motions, and suspension characteristics including stiffness and damping;
- Operational parameters including speed, tractive effort, lateral coupler forces, and track parameters, especially curvature and superelevation; and

• Track-geometry parameters describing deviations from nominal track conditions with respect to cross-level, alinement, surface, or gage.

The nonlinear equations of motion containing these parameters are numerically solved to develop a time history for each dynamic variable of the particular locomotive and its specified track and operating conditions. Of particular interest are the time histories of the lateral/vertical (L/V) load ratios. These ratios are measures of safety and are monitored to determine whether they exceed certain critical values indicative of the risk of derailment:

• Single-wheel L/V ratio representing the tendency toward flange climbing;
• Net wheel-set L/V ratio representing

the tendency toward lateral track-panel shift; and
• Truck-side L/V ratio representing the tendency toward rail rollover and gage widening.

The computer program developed for this study automatically determines the peak L/V ratios that occur during a simulation. These values are printed out for each of the 12 wheels, each of the 6 wheel sets, and each of the 4 truck sides. Upon command, one can also obtain a printout of all important system variables at any instant or a plot of the time history of any system variable.

The method was applied to the comparison of three different locomotives operating at representative speeds and track conditions. Since the model has yet to be verified in tests, the absolute

values of measures of safety may be questionable, though the relative effects of parameter variations are considered valid by the authors. With respect to behavioral trends observed in previous experimental tests, the model was found to give a faithful representation of locomotive behavior. One indication of the value of the model is that it made possible the simulation of the little-understood large dynamic forces that are observed on the trailing axle of the trailing truck in real locomotives.

This work was done by P. P. Marcotte, K. J. R. Mathewson, and Robert L. Berry of Martin Marietta Corp. for **Marshall Space Flight Center.** *To obtain a copy of the report, Circle 53 on the TSP Request Card.*
MFS-25696

Computer Programs

Higher-Order Panel Method for Aerodynamic Flow Analysis

Linear potential-flow properties about arbitrary configurations are predicted for subsonic or supersonic flows.

PANAIR uses a higher-order panel method to predict inviscid subsonic or supersonic flows about an arbitrary configuration. In general, a panel method solves a linear partial differential equation numerically by approximating the configuration surface with panels on which unknown "singularity strengths" are defined. Boundary conditions are imposed at discrete points, and a system of linear equations is generated that relate the unknown singularity strengths. The equations are then solved for the singularity strengths, which provide information on the properties of the flow.

PANAIR differs from earlier panel methods by employing a "higher-order" panel method; that is, the singularity strengths are not constant on each panel. This is necessitated by the more stringent requirements of supersonic flow problems.

The potential for numerical error is greatly reduced in PANAIR by requiring the singularity strength to be continuous. It is also this "higher order" attribute that allows PANAIR to be used to analyze flow about arbitrary configurations. PANAIR can handle the simple configurations considered in the preliminary design phase and can later serve as the "analytical wind tunnel," which can analyze the flow about the final detailed complex configurations.

The PANAIR system includes the following capabilities:

1. The ability to handle, within the limitations of linear potential-flow theory, completely arbitrary configurations, using either exact or linearized boundary conditions;
2. The ability to handle asymmetric configurations as well as those with one or two planes of symmetry;
3. The ability to handle configurations in either symmetric or asymmetric flow;
4. The ability to superimpose an incremental velocity on the free stream, either locally or globally, to simulate such effects as a rotational motion, differing angles of attack for different portions of a configuration, or a propeller slipstream;

5. The ability to calculate pressures, forces, and moments using a variety of pressure formulas, such as isentropic or linear (forces and moments can be computed from pressure integrations over the configuration surface or from pressure and momentum integrated over permeable control-volume surfaces: the first approach gives the sum of wave and vortex drag, and the second approach allows the wave and vortex drag to be calculated individually);
6. The ability to calculate leading-edge and side-edge thrust forces and moments for thin configurations; and
7. The ability to design a configuration, a process in which a desired pressure or tangential velocity distribution at the surface is specified and PANAIR determines the "residual" normal flow through the surface (the normal flow is then used to revise the surface geometry).

Most problems are modeled by PANAIR with a minimum of user input. In general, the aircraft surface is partitioned into several networks of surface grid points, such as a forebody network or a wing network. The coordinates of the input grid points are computed and entered by the user (PANAIR does not generate grid-point coordinates). PANAIR connects the grid points in each network with piecewise flat panels. The user also supplies information concerning the free-stream onset flow mach

number, angle of attack, and angle of sideslip.

Numerous flow quantities are computed at points on the vehicle surface and at points in space. These include pressure coefficients, total and perturbation values of velocity and mass flux components, total and perturbation potentials, local mach number, and vacuum pressure coefficient. The pressure coefficients on individual panels are fitted with two-dimensional quadratic splines and integrated to obtain the three components of force and the three moments in coefficient form. These coefficients may be output for each panel, for columns of panels, for each network, or for any combination of networks. The user has extensive control over the type and quantity of data that are output during a PANAIR analysis.

PANAIR includes advanced software technology as well as advanced aerodynamic technology. It has been developed in accordance with an approach that emphasizes modular and structured software. The separate modules of PANAIR communicate with each other only through a data base of information on disk storage. A module-execution control and data-management system ensure that the PANAIR modules execute and communicate properly. This software design approach eases maintenance since changes in one module affect the other modules in a clearly identifiable manner.

PANAIR is written in FORTRAN IV and Assembler for batch execution on CDC systems. It has been successfully installed and executed in the following environments: CDC CYBER 175 under NOS 1.3 and NOS 1.4, CDC 7600 under SCOPE 2.1.3 and SCOPE 2.1.4, and CDC CYBER 750 and 760 under NOS/BE. The largest program module in the PANAIR system has a central memory requirement of approximately 145K (octal) of 60-bit words. The PANAIR system was developed in 1980.

This program was written by Larry Erickson, Ralph L. Carmichael, and Alan D. Levin of **Ames Research Center;** *Al Magnus, Mike Epton, Pranab Baruah, Bill Massena, John Bussoletti, Ken Sidwell, Forrester Johnson, Joe Zeppa, Glen Bates, Dick Clemens, Tom Derbyshire, Dave Purdon, Dave Chiang, Paul Rubbert, Frank Nelson, John Wai, and Kiyoharu Tsurusaki of Boeing Computer Services, Inc.; Neill Smith of the Naval Coastal Systems Center; James R. Snyder and William Sotomayer*

of Wright Patterson AFB; Jay DeJongh of the USAF Academy; and James L. Thomas and David S. Miller of Langley Research Center. For further information, Circle A on the COSMIC Request Card.
ARC-11398

Planar-Wing Flutter Analysis

Five programs compute flutter speeds and frequencies and generate V-g plots.

The Flutter Analysis System, FAST, is a group of five programs that perform a flutter analysis of a single planar wing. Each program performs certain portions of a flutter analysis and may be run sequentially or individually. This modular approach is very versatile and flexible. FAST uses natural vibration modes as input data and performs a conventional V-g solution. The unsteady aerodynamics programs in FAST are based on the subsonic kernel function lifting-surface theory although other aerodynamic programs may be used.

The first program, MPROC, processes the vibrational modes to give modal deflections, streamwise slopes, and certain integrals of the mode shapes used in calculating general aerodynamic forces. In addition, contour and oblique projection plots of the mode shapes may be generated. Input to MPROC consists of wing geometry and natural vibration mode data.

Program SUBCMAT generates the complex matrix elements used in solving the subsonic downwash equation. Input to SUBCMAT includes the mach number, reduced frequency specifications, and wing geometry data. Program LUCMAT performs an L-U decomposition of the complex matrices generated by SUBCMAT.

The fourth program, GENFLU, calculates the generalized aerodynamic forces using the modal output from MPROC and the L-U matrices output by LUCMAT. The last of the FAST programs is FLUTDET, the parametric flutter analysis program. Input to FLUTDET includes the generalized aerodynamic forces, generalized masses, modal frequencies, and air density information. Output includes tables of flutter speeds and frequencies and V-g plots.

FAST is written in FORTRAN IV and Assembler for batch execution and has been implemented on a CDC CYBER 170-series computer with the largest program having a central memory requirement of approximately 35K (octal) of 60-bit words. The FAST programs were developed in 1978.

This program was written by Robert N. Desmarais and Robert M. Bennett of **Langley Research Center.** *For further information, Circle B on the COSMIC Request Card.*
LAR-12610

Modeling of Large Latticed Surfaces

Lattices that approximate spherical and paraboloidal surfaces are analyzed.

The GEOMLLS program determines dimensions and coordinates of flat segmented triangular surfaces that approximate spherical and paraboloidal surfaces of revolution, where the vertexes of the triangles lie on the true surface. GEOMLLS calculates the complete geometry of the segmented surface and quantities that measure surface accuracy, such as maximum deviation and root-mean-square deviation from the true surface.

GEOMLLS was originally developed to assist in the design of large space structures for commercial and scientific purposes. For example, shallow shell structures have frequently been mentioned as candidates for building components in communication systems, orbiting antenna reflectors, and satellite solar-power systems.

GEOMLLS approximates a spherical or paraboloidal surface with a latticed surface by projecting a subdivided n-sided pyramid onto the true surface and then connecting grid points with straight lines. The user specifies the desired true surface geometry by inputting the aperture diameter and F/D, the ratio of the focal length to the aperture diameter. The lattice pattern is specified by inputting the number of shell circumferential sectors and the number of meridional subdivisions of the sectors desired. This lattice pattern defines a subdivided n-sided pyramid with its base at the aperture and its apex at the center

of the true surface. The final approximating surface is generated by projecting each grid point on the pyramid onto the true surface. The projection may be by a single center-of-projection method from a user-specified point or by a normal projection method.

Once the grid points have been projected onto the true surface, they are connected by straight-line segments to form the final approximating latticed surface. The program then calculates the maximum deviation and root-mean-square deviation of the latticed surface. The user might study several combinations of differing numbers of sectors and meridional subdivisions and both projection methods to obtain the latticed surface that best approximates the true surface for the intended application.

GEOMLLS is written in FORTRAN IV for batch execution and has been implemented on a CDC CYBER 70-series computer with a central memory requirement of approximately 52K (octal) of 60-bit words. GEOMLLS was developed in 1980.

This program was written by Melvin S. Anderson and Catherine L. Herstrom of Langley Research Center and Adnan H. Nayfeh and Mohamed S. Hefzy of the University of Cincinnati. For further information, Circle C on the COSMIC Request Card.
LAR-12888

Dynamic Analysis of Six-Axle Locomotives

Locomotive and track parameters are modeled by a program that can help improve rail safety.

The new generation of six-axle locomotives introduced in the last 15 years has been attractive from many points of view, such as tractive effort, horsepower, costs, and the ease of maintenance. However, under some operating conditions, in particular where the track routes are difficult or where the track strength is low, some railroads experience difficulties in locomotive ride, track damage, and occasionally derailment.

The Track Train Dynamic Analysis computer program models the dynamic behavior of six-axle locomotives. Dynamic behavior is determined by locomotive parameters (such as geometry, mass, and suspension characteris-

tics), operational parameters (including speed, tractive effort, lateral coupler forces, track curvature, and superelevation), and track-geometry parameters (such as deviations or defects from the nominal conditions with respect to cross level, alinement, surface, and gage). Since the model is nonlinear, the dynamic solution consists of time histories for each of the system variables.

The program models a locomotive supported by two three-axle tracks. The interface regions between the major functional parts of the locomotive suspension consist of the secondary suspension between the vehicle body and the track frame, the primary suspension between the track frame and the wheel sets, and the wheel/rail interface. Once the locomotive parameters have been specified, a set of operational parameters must be specified. Coupling forces may be considered both fore and aft, with coupling forces acting on the corresponding coupling pins.

The tractive effort of the locomotive is assumed to be contributed by equal amounts at each of the axles, with braking treated as a negative tractive effort. Within a single test run, the tractive effort is assumed to be constant in magnitude. The velocity of the locomotive is also assumed to be constant during any single test run. The track is assigned nominal and constant values for curvature, absolute superelevation, and kinematic gage. The user may also specify track-geometry irregularties in lateral alinement, vertical alinement, cross level, and track gage.

The program output consists of detailed time histories for each of the system variables. These data can readily be used to evaluate the operational safety of the locomotive being modeled. Sensitivity studies can be conducted by changing one or more parameters in a series of runs.

This analysis model and methodology could play an important role as a predictive technique, as well as a test support tool, in many areas of rail safety. Typical applications might include: assessment of the importance of specific suspension design details, comparison of different locomotive designs, determination of appropriate maintenance standards on locomotive suspension elements, determination of acceptable track-geometry defects and minimum track-strength, and investigation of specific derailment mechanisms.

The Track Train Dynamic Analysis program is written in FORTRAN IV for

interactive execution and has been implemented on a CDC CYBER 174/750 computer with a central memory requirement of approximately 66K (octal) of 60-bit words. The program was developed in 1981.

This program was written by the Denver Aerospace Division of Martin Marietta Corp. for Marshall Space Flight Center. For further information, Circle D on the COSMIC Request Card.
MFS-25710

Two-Dimensional Grids About Airfoils and Other Shapes

Program treats arbitrary boundaries through solutions of Poisson's equation.

The ability to treat arbitrary boundary shapes, including those about airfoils, is one of the most desirable characteristics of a method for generating grids. In a grid used for computing aerodynamic flow over an airfoil, or any other body shape, the surface of the body is usually treated as an inner boundary and often cannot be easily represented as an analytic function.

The GRAPE computer program generates two-dimensional finite-difference grids about airfoils and other shapes by the use of the Poisson differential equation. GRAPE can be used with any boundary shape, even one specified by tabulated points and including a limited number of sharp corners. Numerically stable and computationally fast, GRAPE provides the aerodynamic analyst with an efficient and consistent means of grid generation.

GRAPE generates a grid between an inner and an outer boundary by utilizing an iterative procedure to solve the Poisson differential equation subject to geometrical restraints. In this method, the inhomogeneous terms of the equation are automatically chosen such that two important effects are imposed on the grid: The first effect is control of the spacing between mesh points along mesh lines intersecting the boundaries. The second effect is control of the angles with which mesh lines intersect the boundaries. A technique of coarse/fine sequencing accelerates numerical convergence.

GRAPE program-control cards and input data are entered via the NAMELIST feature. Each variable has a default value such that user-supplied data are kept to a minimum. Basic input data consist of the boundary specification, mesh-point spacings on the boundaries, and mesh-line angles at the boundaries. Output consists of a data set containing the grid data and, if requested, a plot of the generated mesh.

GRAPE is written in FORTRAN IV for batch execution and has been implemented on a CDC 6000-series computer with a central memory requirement of approximately 135K (octal) of 60-bit words. For plotted output, the commercially-available DISSPLA graphics software package is required. GRAPE was developed in 1980.

This program was written by Reese Sorenson of **Ames Research Center.** *For further information, Circle E on the COSMIC Request Card.*
ARC-11379

Structural Analysis of Shells

Program includes stress, buckling, vibration, and transient analysis of multisegment shells.

The Structural Analysis of General Shells computer program STAGSC-1 analyzes thin shell structures that have separate shell branches or segments connected to one another along their boundaries. STAGSC-1 contains options for static stress analysis (including geometric and material nonlinearities), bifurcation buckling analysis (including nonlinear prestress), vibration analysis (including nonlinear prestress), and transient analysis (linear or with geometric and material nonlinearities). While intended primarily for analyzing shells, the STAGSC-1 capability is extended by the inclusion of axial and torsional springs, as well as general nonlinear beam elements.

STAGSC-1 models structural problems with a minimum of input preparation. Triangular and quadrilateral shell elements are available. The triangular element, developed by Clough and Felippa, is primarily used where quadrilateral elements are unsuitable. Quadrilateral elements may be selected from a

series based on the combination of two Clough-Felippa triangles. Presently, the "workhorse" element is a flat quadrilateral element, developed especially for STAGSC-1, which is very economical in most cases of nonlinear and stability analysis. A "transition element" with five nodes (three triangles) is included so that irregular grids may be defined more easily.

The definition of the structural configuration may include data from user-written subroutines, increasing the generality of the program and making the input more compact. Another feature that makes input preparation easier is that the user is allowed to define a number of substructures separately and indicate how these are to be connected.

The shell-wall properties are defined by a local stiffness matrix relating stress and moment resultants to reference surface strains and changes in curvature. The stiffness matrix is internally computed for a number of standard shell walls. Certain standard boundary conditions are readily modeled. Any linear displacement of 20 components or less may be entered via data cards. Initial shape imperfections and cutouts in the shell wall may also be defined on regular data cards. Thermal as well as mechanical loading may be considered. The latter includes the options of defining forces or displacements. The cases of constant direction as well as live pressure loads may also be considered.

The solution procedures in the STAGSC-1 code are accurate and efficient. The solution for linear systems is based on the "skyline method," taking full advantage of the zero terms following the last nonzero element in each equation. Bifurcation buckling and small vibration analyses lead to linear eigenvalue problems. These are solved by generating invariant subspaces by simultaneous inverse power iteration.

In contrast to many structural codes, STAGSC-1 solves the nonlinear algebraic equation rigorously — that is, the solution accuracy is independent of the load step size. The solution is based on the modified Newton Method with some automatic features for the control of step size and relaxation factors. The transient case is time-integrated by using the explicit central differences, the trapezoidal rule, or the stiffly stable methods.

This program was written by B. O. Almroth, F. A. Brogan, and G. M. Stanley of Lockheed Missiles & Space Co. for **NASA Headquarters.** *For further infor-*

mation, Circle F on the COSMIC Request Card.
HQN-10960

NASTRAN® : April 1982 Release

The most efficient and versatile release of NASTRAN® to date

Development of the NASA Structural Analysis computer program NASTRAN® was begun in the mid-1960's to provide NASA research centers with a powerful general-purpose finite-element computer program for structural analysis. Over the years, NASA has maintained and improved NASTRAN such that it remains a state-of-the-art finite-element program with a wide range of applications. The NASTRAN system has become widely accepted as a standard in the structural-analysis community. The latest public release of NASTRAN, April 1982, is the most efficient and versatile to date.

The intended range of applications of NASTRAN includes almost every kind of structure and construction. Structural modeling elements are provided for the specific representation of the more-common structural building blocks, including rods, beams, shear panels, plates, and shells of revolution. More-general building blocks can be treated as combinations of these simple elements or by the "general" element capability. The substructuring capability allows different sections of a structure to be modeled jointly after having already been modeled separately. NASTRAN incorporates the effects of control systems, aerodynamic transfer functions, and other nonstructural features.

The range of problems that NASTRAN automatically handles includes:
- Static response to concentrated loads, to distributed loads, to thermal expansion, and to enforced deformations;
- Dynamic response to transient loads, to steady-state sinusoidal loads, and to random excitation; and
- The determination of real and complex eigenvalues for use in vibration analysis, dynamic stability analysis, and elastic stability analysis.

NASTRAN also has a limited capability for the solution of nonlinear problems, including piecewise linear analysis of nonlinear static response and transient analysis of nonlinear dynamic response.

Users may develop their own analysis capabilities by using the Direct Matrix Abstraction Programming (DMAP) language to direct NASTRAN in the solution of general matrix problems.

NASTRAN treats large problems with many degrees of freedom. The only limitations on problem size are those imposed by the practical considerations of computer run time and by the ultimate capacity of auxiliary storage devices. Computational procedures were selected for maximum efficient utilization of computer resources. The NASTRAN system is programed in an overlaid structure to provide the user with a large selection of capabilities while requiring only a moderate amount of core resources.

The NASTRAN computer program is currently available for implementation on the following computer configurations: IBM 360/370 and IBM 303X series, CDC 6000 and CDC CYBER 70/170 series, UNIVAC 1100 series, and DEC VAX series.

This program was written by Robert L. Brugh of COSMIC for **NASA Headquarters.** *For further information, Circle G on the COSMIC Request Card.* HQN-10952

Steady, Oscillatory, and Unsteady Subsonic and Supersonic Aerodynamics

Modular program is compatible with most geometry preprocessors.

The computer program SOUSSA-P (Steady, Oscillatory, and Unsteady Subsonic and Supersonic Aerodynamics —

Production Version) accurately and efficiently evaluates steady and unsteady aerodynamic loads on aircraft having arbitrary shapes and motions, including structural deformations. These evaluations are essential for the accurate calculation of the aerodynamic and aeroelastic characteristics required for the design and analysis of high-performance aircraft. SOUSSA-P is based upon the theoretical formulation developed by Morino, in which the Green's function method is applied to the equation for the velocity potential.

The SOUSSA-P1.1 program is a pilot code for "production" applications. It is modular, allowing updating and incorporating improved or additional capabilities. SOUSSA-P1.1 is compatible with most of the currently-available geometry preprocessors. Furthermore, the program has been structured to facilitate the analysis of aerodynamic problems involving a wide range of flight speeds, multiple sets of vibration and deformation modes, and multiple sets of frequencies for flight vehicles having arbitrary geometry. The underlying method is applicable to both subsonic and supersonic flows. (The supersonic capability has not been incorporated into version 1.1 of the SOUSSA-P program.) The program can be used without extensive specialized training.

Applying Green's function method to the fully-unsteady (transient) potential equation yields an integro-differential delay equation. With spatial discretization by the finite-element method, this equation is approximated by a set of differential-delay equations in time. Determination of the time solution by Laplace transform yields a matrix equation relating the velocity potential to the normal wash. The simple frequency dependence of this matrix makes the

SOUSSA-P program very useful for multiple-frequency and repeated mode-shape evaluations. Premultiplying and postmultiplying by the matrices relating generalized forces to the potential and the normal wash to the generalized coordinates, one obtains the matrix of the generalized aerodynamic forces.

Basic input to the SOUSSA-P program consists of the geometrical definitions of the aircraft body, the prescribed wake, the generalized-force mode(s), the boundary-condition mode(s), the integration-scheme choice parameter, the free-stream mach number, and the set of complex reduced frequencies. It is assumed that the user will obtain this information via state-of-the-art geometry preprocessors and structural analysis processors. Output from the SOUSSA-P program generally includes the velocity potential distribution, the pressure distribution, and the matrix of generalized aerodynamic forces.

The SOUSSA-P program is written in FORTRAN IV and Assembler for batch execution and has been implemented on a CDC CYBER 70-series computer using the NOS 1.4 operating system with a central memory requirement of approximately 60K (octal) of 60-bit words. Version 1.1 of the SOUSSA-P program was developed in 1980.

This program was written by Robert N. Desmarais, Herbert J. Cunningham, and E. Carson Yates, Jr., of **Langley Research Center** *and Luigi Morino, Robert D. Preuss, Scott A. Smolka, Kadin Tseng, and Jeffrey Averick of Aerospace Systems, Inc. For further information, Circle S on the COSMIC Request Card.* LAR-12433

Machinery

Hardware, Techniques, and Processes

Compression Ratio Adjuster

Automatic adjustment conserves fuel at any power setting, from idle to full throttle.

Lyndon B. Johnson Space Center, Houston, Texas

A new mechanism alters the compression ratio of an internal-combustion engine according to the load so that the engine operates at top fuel efficiency. Ordinary gasoline, diesel, and gas engines with their fixed compression ratios are inefficient at partial load (that is, part throttle) and at low-speed full load (full throttle). The mechanism ensures that the engines operate as efficiently under these conditions as they do at high load and high speed.

The mechanism alters compression ratio — the ratio of cylinder volume with the piston at bottom dead center to that with the piston at top dead center — by altering the length of the connecting rod. It can thus increase or decrease the cylinder volume at the moment fuel combustion starts, to suit the load and speed conditions. The mechanism does this automatically under the control of a pressure sensor in the engine intake manifold.

The heart of the mechanism is an eccentric sleeve containing a projectable latch, or pawl (see figure). The pawl can be inserted by hydraulic pressure into any of several pockets in the connecting rod.

If the pawl latches the eccentric sleeve to the connecting rod at the bottom of the stroke — that is, in pocket f, the effective rod length is reduced. There will then be a large clearance volume when the piston is moved to top dead center. On the other hand, latching the sleeve to the rod at the top of the stroke (pocket a), as the pawl is positioned to do in the figure, increases the effective rod length. Clearance volume will then be smaller at top dead center.

The pawl engages the rod pocket only during the compression stroke. During the expansion stroke, the hydraulic fluid is vented, allowing the pawl to recede under the force of its springs into the eccentric sleeve. During the intake and exhaust strokes, the pawl is fully retracted so that a full fuel charge can be drawn in and virtually all of the combustion prod-
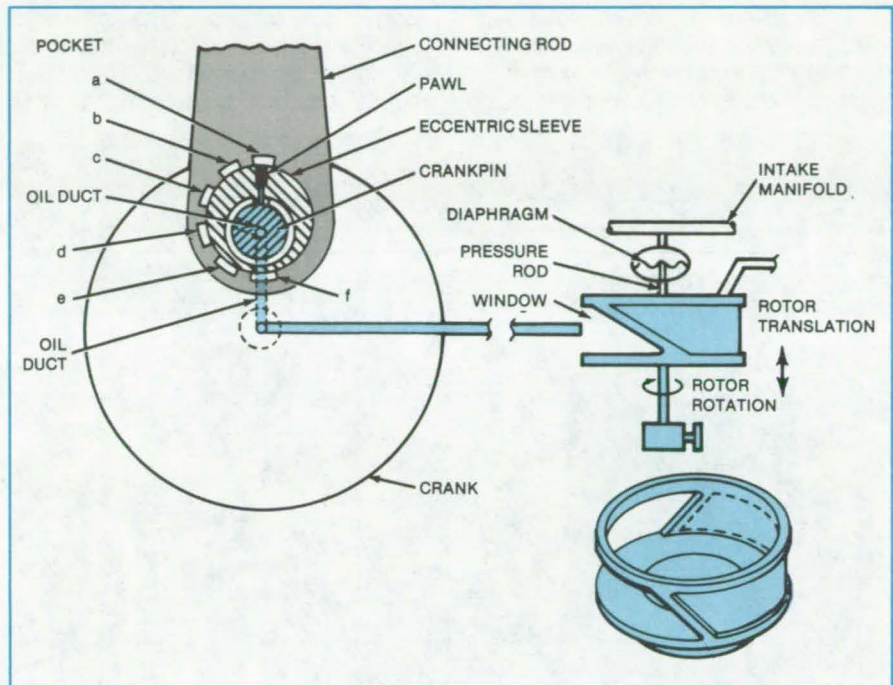
A **Pawl Adjusts Connecting-Rod Length** by engaging one of the pockets a through f. Which of the pockets is engaged is determined by the vertical position of the rotor in the control valve (right). The mechanism responds quickly to changes in the power setting, as reflected in the intake manifold pressure. Engine speed up to 4,000 revolutions per minute is feasible with the mechanism. The engine lubricating oil can be used as the hydraulic fluid that operates the pawl.

ucts can be forced out of the cylinder, even at high speeds.

The flow of oil to actuate the pawl is controlled by a rotor (shown at the right in the figure) in a control valve. Besides turning in synchronism with the crankshaft, the rotor also moves up and down in response to the pressure on a diaphragm vented to the intake manifold. When manifold pressure is high, the diaphragm pushes the rotor downward; when pressure is low, the diaphragm pulls the rotor upward.

The up-and-down motion regulates the time at which hydraulic fluid is sent from the rotor to actuate the pawl and thus determines which of the pockets the pawl engages. A window on the rotor admits the fluid to an oil tube leading to the eccentric sleeve. The window has a

parallelogram shape; when the rotor is in a low position, the leading edge of the window passes the oil tube port sooner than it would with the rotor in a high position. The pawl is therefore forced into pocket a, under the influence of high manifold pressure, a position that lengthens the rod and ensures efficient fuel combustion under the prevailing operating conditions.

*This work was done by James W. Akkerman of **Johnson Space Center.** For further information, Circle 54 on the TSP Request Card.*

This invention is owned by NASA, and a patent application has been filed. Inquiries concerning nonexclusive or exclusive license for its commercial development should be addressed to the Patent Counsel, Johnson Space Center [see page A5]. Refer to MSC-18807.

Reaching High Bookshelves From a Wheelchair

A simple mechanical device extends
a user's reach.

Goddard Space Flight Center, Greenbelt, Maryland

A "book retriever" developed at Goddard Space Flight Center allows people confined to wheelchairs to remove or replace books from the upper shelves of library stacks (Figure 1). The retriever is a mechanical device composed of an aluminum tube approximately 5 feet (1.5 meters) long with two jaws at the upper end. The jaws securely clamp a selected book (Figure 2); they are thin enough that they can be inserted between adjacent books.

The user actuates the jaws by rotating a crank near the lower end of the tube. A sprocket drive inside the aluminum tube transmits the rotary motion of the crank to a screw at the top of the tube that opens or closes the jaws. A simple slip clutch in the crank handle prevents the user from overtightening the jaws.

Figure 1. At the **Goddard Space Flight Center Library,** a patron uses the retriever to extract a book on a high shelf.
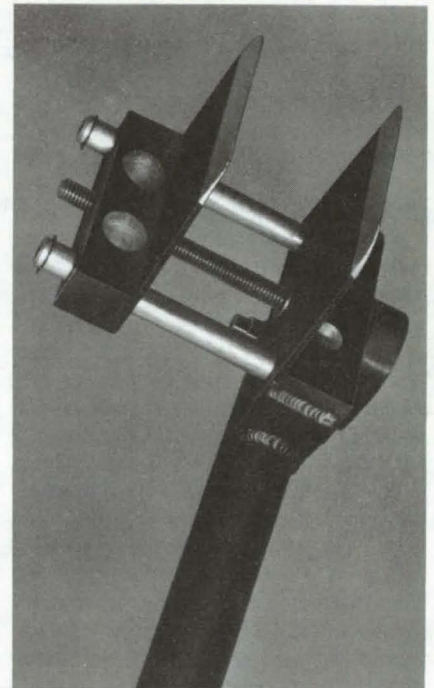
Figure 2. **Book-Clamping Jaws** are opened and closed by a screw.

A sleeve at the lower end of the tube can be slid up or down so that the bottom can rest on the seat of the wheelchair when the clamp jaws are at the correct height for extracting or replacing books on a given shelf. The user therefore does not have to support the full weight of a book. The sleeve is locked in position by an eccentric bore.

This work was done by Anthony Walch, Jr., of **Goddard Space Flight Center.** *For further information, Circle 55 on the TSP Request Card.*
GSC-12772

Lightweight Shield for Centrifuge

Laminated aluminum supplants
heavy metal construction.

Lyndon B. Johnson Space Center, Houston, Texas
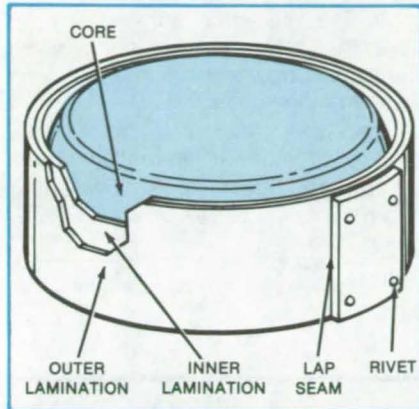
With **Wall Thickness Totaling Only Three-sixteenths Inch** (4.8 mm), a laminated aluminum centrifuge bowl can restrain large fragments from a broken rotor without breaking.

A centrifuge bowl composed of laminated aluminum offers the required combination of high strength at reduced weight. Around the outside wall of the bowl core of 1/16-inch-thick (1.6-mm-thick) spun aluminum are wrapped two layers of aluminum, each also one-sixteenth inch thick (see figure). The layered structure prevents cracks from propagating through the wall.

Because centrifuge rotors turn at very high speed, they are subjected to intense stress. In some cases they can disintegrate under the stress, causing serious accidents. For safety, therefore, the rotor is usually covered by a shield, or bowl, that prevents the pieces of broken rotor from leaving the apparatus.

For one commercial centrifuge developing a centrifugal force equivalent to 1,600 × gravity, the layer thickness of one-sixteenth inch (1.6 mm) was found to be adequate by laboratory tests. The layers of the laminate are held together by rivets spaced at 15° intervals around the upper and lower peripheries of the bowl. A riveted lap seam joins the ends of the wrapped aluminum layers.

This work was done by C. Luper of Beckman Instruments, Inc., for **Johnson Space Center.** *For further information, Circle 56 on the TSP Request Card.*
MSC-18995

High-Ratio Gear Train

Very high gear ratios would be obtained
from a small mechanism.

Lyndon B. Johnson Space Center, Houston, Texas

A proposed arrangement of two connected planetary differentials can result in a gear ratio many times that obtainable in a conventional series gear assembly of comparable size. Ratios of several thousand would present no special problems. A selection of many different ratios is available with substantially-similar gear diameters.

The configuration is shown in the figure: in cross section at the left and schematically at the right. The input shaft turns the two sun gears. The first and second planet gearsets are mounted on a common planet carrier, so that they revolve at the same velocity. The first ring gear is fixed to the frame. The output is taken from the second ring gear.

With the gears having the numbers of teeth designated algebraically in the
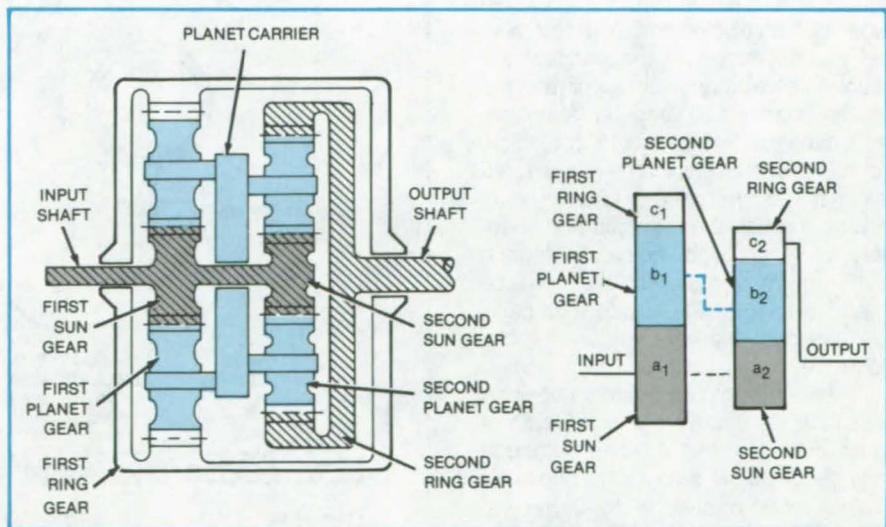
The **High-Ratio Gear Train** incorporates two planetary differential gearsets in an arrangement that can provide very high ratios with only a few similarly sized gears in a small space (a_1, b_1, a_2, and b_2 denote the numbers of teeth in the gears.)

schematic diagram, the overall gear ratio is given by

$$R = \frac{\text{input-shaft angular speed}}{\text{output-shaft angular speed}}$$

$$= \frac{\left(\dfrac{c_2}{a_2}\right)\left(\dfrac{c_1}{a_1} + 1\right)}{\dfrac{c_2}{a_2} - \dfrac{c_1}{a_1}} \qquad (1)$$

$$= \frac{(a_1 + b_1)\,(a_2 + 2b_2)}{a_1 b_2 - a_2 b_1} \qquad (2)$$

While these expressions enable the ratio of any given set to be easily calculated, it is somewhat more difficult to design a gearset to provide a specified ratio. A number of graphical and analytical techniques are available to accelerate the design process. In general, they involve the prior selection, from a table of different combinations, of a set having approximately the ratio desired. Changes are made in a_1, b_1, a_2, or b_2 according to methods developed to give small ratio changes, large ratio changes, or sign reversals. The ratio of the new combination is then calculated, and this new combination is used as the starting point for the next iteration. The process is repeated as many times as necessary to achieve the desired ratio.

Since the denominator in the equations contains a difference of two positive quantities, it is clear that very high ratios may be obtained by selecting gears to give the smallest possible denominator. For example, the most diameter-efficient configuration is one in which $b_1 = 1 + a_1$, $b_2 = 1 + a_2$, and $a_1 = b_2$. In this case, the denominator of equation (2) equals unity, which is the smallest possible nonzero value; and the two ring gears are similarly sized.

The tooth loading on the differentials will be nearly equal throughout the gear train. The efficiency will probably be lower than in a series gear train in which the loading decreases with each stage away from the output.

This work was done by Alan E. LeFever of Rockwell International Corp. for **Johnson Space Center.** *For further information, Circle 57 on the TSP Request Card.*
MSC-20054

Fluid-Injection Tool for Inaccessible Areas

Sandwich construction is both thin and strong.

John F. Kennedy Space Center, Florida

A new tool injects liquids or gases into narrow crevices. It can be used to apply caulking and waterproofing compounds, adhesives, detergent, undercoats, and oil and to aerate hard-to-reach places.

The tool consists of a thin, flat, triangular nozzle, containing many channels, attached to a distribution manifold (see figure). The manifold is a stainless-steel tube, ¼ inch (6.4 mm) in diameter, slotted to accommodate the ends of the stainless-steel strips that separate the nozzle channels. Triangular stainless-steel panels, 0.006 inch (0.15 mm) thick, contain the strips, which have the same thickness as the panels. Gas or liquid flowing through the manifold and channels exits through holes 3/64 inch (1.19 mm) in diameter on the flat face near the edge of the nozzle. The parts are bonded together by an epoxy adhesive.

The nozzle can reach into an opening 1/32 inch (0.79 mm) wide to a depth of more than 4 inches (10 cm). Although thin, the device is rigid and strong.

This work was done by James E. Myers of Rockwell International Corp. for **Kennedy Space Center.** *No further documentation, is available.*
KSC-11217
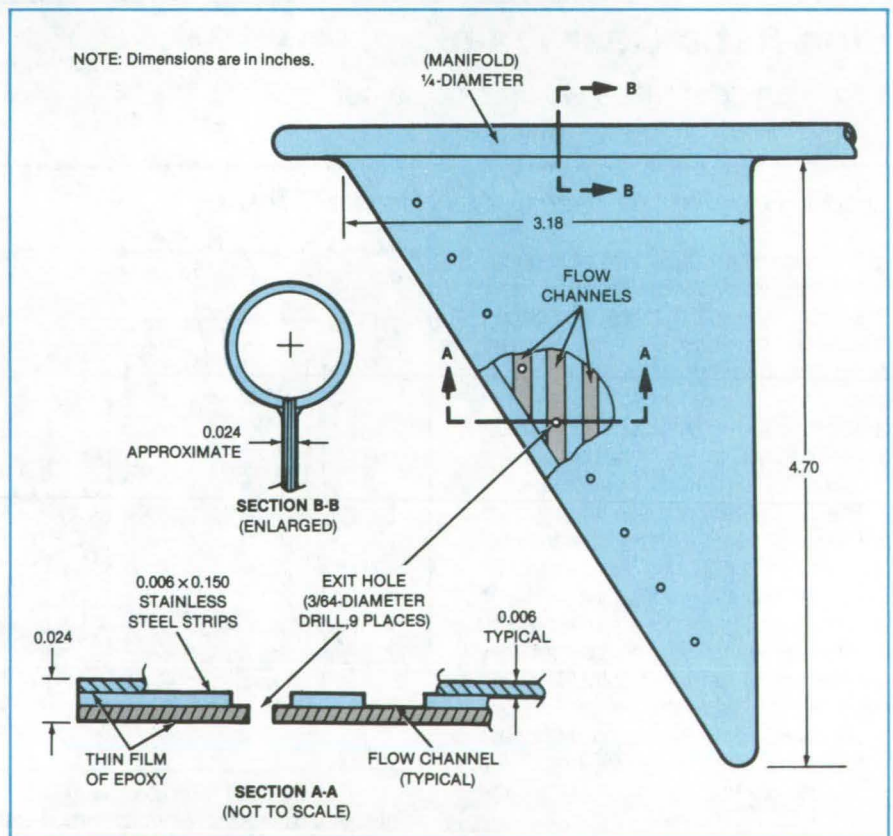
Channels Between Metal Strips carry liquids or gases to exit holes near the trailing edge of this injection tool. Developed for applying a waterproof coating to the Space Shuttle tiles, the tool ensures that the waterproofing compound reaches remote crevices.

Continuously-Variable Positive-Mesh Power Transmission

Speed ratio is controlled by coupling mechanical trigonometric-function generators.

Marshall Space Flight Center, Alabama

A proposed transmission with continuosly-variable speed ratio would couple two mechanical trigonometric-function generators. The transmission is expected to handle higher loads than conventional variable-pulley drives; and, unlike a variable pulley, there is positive traction through the entire drive train with no reliance on friction to transmit the power. It would be able to vary speed continuously through zero and into reverse. Possible applications are in instrumentation where drive-train slippage cannot be tolerated.

As shown in Figure 1, the input turning at angular speed ω_0 is split into two shafts, each connected to a function-generator input. The function generator consists of a disk with parallel grooves and a cylindrical reel gear in a yoke. The shaft of the yoke is parallel to the input shaft. The yoke shaft is free to rotate, but may be offset laterally. As the disk turns, the yoke rotates with the same angular velocity.

The combined sliding and rotating action of the reel gear gives enough degrees of freedom to the system to permit the output shaft to be fixed at any lateral offset or to be moved laterally without affecting the output rotation frequency, which is always equal to that of the input rotation. One plate gear can drive several reel-gear and yoke assemblies. Each shaft also connects to the function-generator output through cam-and-lever linkages. Thus, in addition to the rotation of each output shaft about its axis, the shafts also oscillate with an amplitude R_0. Movable pivots in the levers determine the magnitude of R_0.

The phase angle of one mechanical trigonometric-function generator is set so that its output shaft rotates at speed ω_1 where:

$$\omega_1 = \omega_0 - \frac{\omega_0 R_0}{r} \cos^2 \omega_0 t$$

The parameter r is the radius of the gear at the output of the function generator.
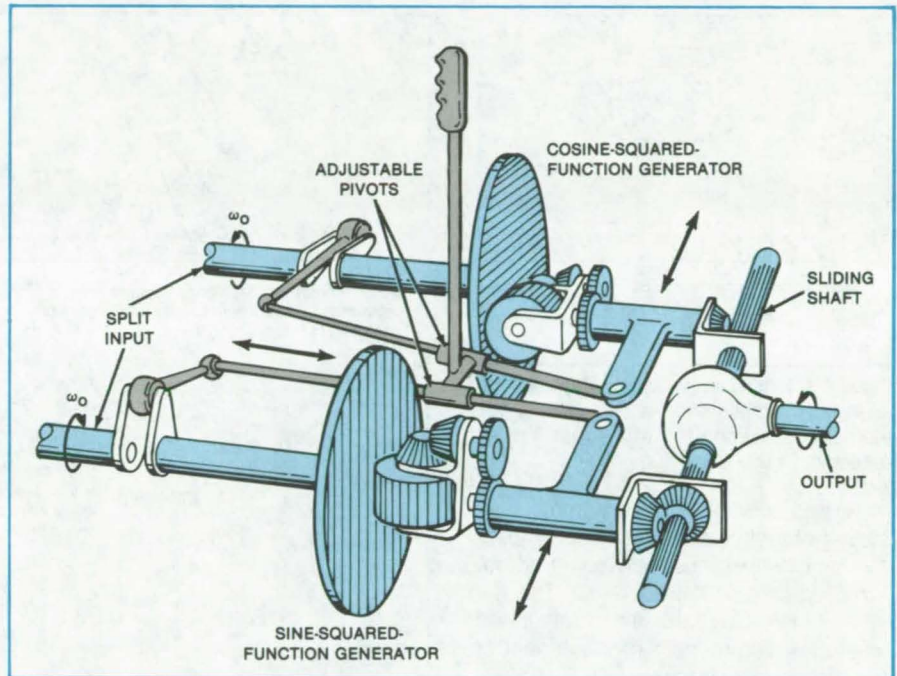
Figure 1. **Trigonometric-Function Generators** set to a phase difference of 90° produce output shaft speeds that vary with time. The two generator outputs are combined in a standard differential to produce a constant output speed. The speed is varied by moving the pivots of the lever arms.
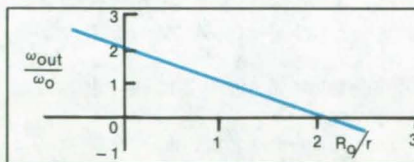
Figure 2. A **Typical Output Characteristic** of the variable-speed drive is shown here. Unlike a variable-pulley drive, there is positive gear-mesh action through the entire drive train, and the output speed can be continuously decreased to zero and then reversed.

For the other function generator, the phase angle is set so that:

$$\omega_2 = \omega_0 - \frac{\omega_0 R}{r} \sin^2 \omega_0 t$$

The two outputs are coupled into a standard differential by 90° gearsets and sliding shafts. The differential produces an output angular speed that is the sum of the two inputs:

$$\omega = \omega_1 + \omega_2 = 2\omega_0 \left(1 - \frac{R_0}{2r}\right)$$

Variation of the pivot points causes a continuous change in R_0 and, therefore, in ω. Steady-state operation occurs when $R_0 = 0$, in which case the function generators are centered and are subject to minimum stress. As R_0 is varied up to 2r, the direction of the output rotation reverses. Figure 2 shows a typical output characteristic for the drive.

High-Temperature Captive-Nut Assembly

In an improved design, nuts corroded by
high temperatures are replaceable.

Lyndon B. Johnson Space Center, Houston, Texas
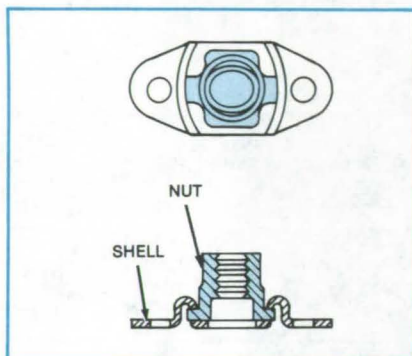
Figure 1. **High-Temperature Captive-Nut Assembly** consists of a removable nut element that snaps into loose-fitting recesses in the shell.

An improved plate-nut assembly, consisting of a shell and a self-locking captive nut, withstands service temperatures up to 1,600° F (870° C). The nut element is replaceable and floats in the shell to accommodate misalinement of the mating bolt or screw.

Captive-nut assemblies are widely used in home appliances and other machinery to expedite assembly when nuts must be held in inaccessible places. Nut replacement is usually not required unless threads are stripped or otherwise damaged. However, in other applications where the nuts encounter high temperatures, high-temperature corrosion can cause thermal wear of the threads, thus making replacement necessary. This is so even when the nut assembly is made from the best heat- and corrosion-resistant alloys.

An improved assembly and its parts are shown in Figure 1. The nut element

STEP 1
Insert removal tool, with downward pressure, between nut and shell, as shown. Lean against nut barrel to insure engagement.

STEP 2
Maintain downward pressure. Nut will snap out easily with a simple prying motion.

STEP 3
Install new nut by inserting one lug in shell and striking the opposite lug with a screwdriver.
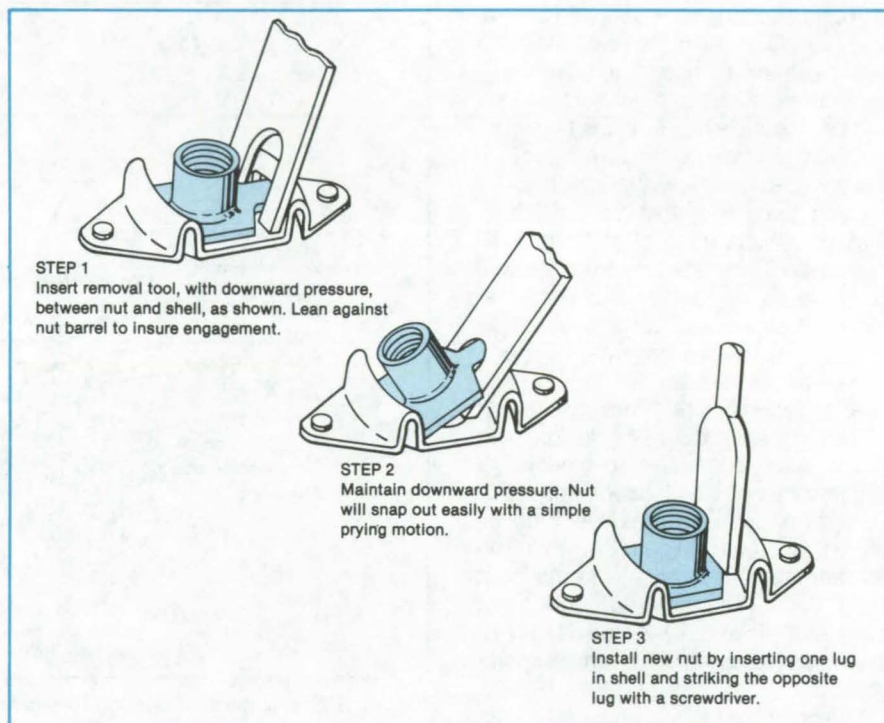
Figure 2. **Replacement of a Nut Element** is easily accomplished with simple handtools. The old nut is pried out and a new one pushed into position.

is made from a corrosion- and heat-resistant nickel-base alloy, U-500, and is silver plated. The shell is made from A-286 stainless steel, and its surface is passivated.

The nut element is held loosely in the shell by the two lugs. Removal is easily accomplished with the help of a U-shaped tool, as shown at the top and middle of Figure 2. A new nut is inserted simply by pushing it into place with a screwdriver, as shown at the bottom.

The improved high-temperature captive nut should prove useful in many industrial applications. A typical use would be in the heat shields of laboratory and vacuum ovens.

This work was done by Michael L. Marke and James F. Charles of Rockwell International Corp. for **Johnson Space Center.** *For further information, Circle 59 on the TSP Request Card.*
MSC-20010

Self-Alining, Latching Joint for Folding Structural Elements

Center joint requires no special skills
or equipment.

Langley Research Center, Hampton, Virginia

Structural column elements can be assembled quickly and easily with the aid of a new center joint. The joint alines the column elements automatically and

fastens them together securely. Tapered half columns are stacked like paper cups, unfolded, and connected to other similar elements to form truss

structures. Originally developed for space-erectable structures, the column elements and center joints can be assembled without special tools or by a
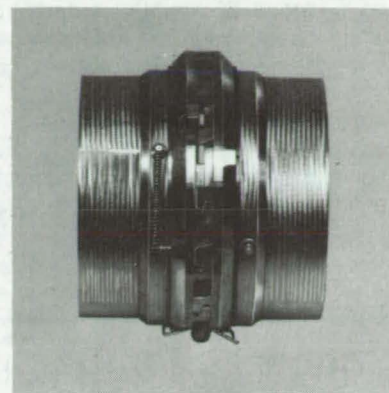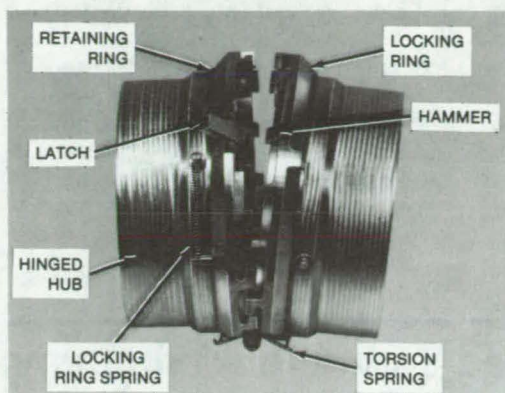
Three Stages in the Deployment of a Center Joint are shown here. At the left, the joint starts to close under torque supplied by the torsion spring. At center, the joint is almost closed; the hammer is ready to trigger the latch. At the right, the joint is fully closed, and teeth are engaged. Half-column elements, which would normally be attached to the hubs, are not shown in these photographs.

simple remotely-operated handling device.

The new center joint (see figure) consists of a pair of hinged hubs. Spring-loaded locking rings are fitted around the hubs. Each locking ring is secured by a retaining ring and is held in a cocked position (in the folded state) by a latch.

When a column is being unfolded, the hinged column halves are rotated by the energy stored in the torsion spring attached to the hinge, so that the mating faces of the hubs are brought into proximity. Just before the mating faces make contact, small hammers in the hubs trigger the latches, releasing the locking rings, which rotate under the torque furnished by the locking-ring springs. The rotation engages the locking-ring teeth and thus fastens the mating faces of the joint together.

Previous center joints for space structural elements were more susceptible to damage and required careful alinement of the mating elements. In addition, opposing forces had to be applied to the column halves, and special alining and joining tools were needed.

The new center joint has potential terrestrial applications as well. For example, the vertical members of radio-transmission towers could be made from several short tubular elements that incorporate the joints on each end, so that the tower elements can be folded and stacked for transportation and quickly unfolded and erected onsite. If liquid or gas seals were added to the center joints, they could be used in a deployable pipeline.

This work was done by Harold G. Bush of **Langley Research Center** and Richard E. Wallsom of Kentron International Inc. For further information, Circle 60 on the TSP Request Card.

Inquiries concerning rights for the commercial use of this invention should be addressed to the Patent Counsel, Langley Research Center [see page A5]. Refer to LAR-12864.

Automatic Flushing Unit With Cleanliness Monitor

Particle content of flushing solution
is measured continuously.

Lyndon B. Johnson Space Center, Houston, Texas

A liquid-level probe is kept clean — and therefore at peak accuracy — by a unit that flushes the probe with a solvent, monitors the effluent for contamination, and determines when the probe is particle-free. Originally developed for probes on propellant tanks in the Space Shuttle, the approach may also be adaptable to industrial cleaning. Possible applications are in flushing filters and pipes and ensuring that manufactured parts have been adequately cleaned.

The probe is removed from the tank and installed in the flushing fixture, shown in the Figure, which is equipped with a mounting flange that can accommodate different bolthole configurations
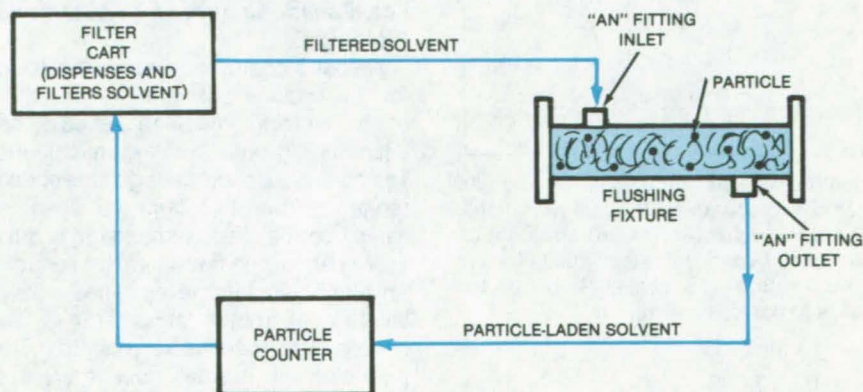
Continuously Circulated and Filtered, a solvent removes contaminating particles from a liquid-level probe inside the flushing fixture. When the automatic particle counter indicates that the probe is releasing no more contamination, flushing is stopped.

on the probe. Solvent is dispensed from a filter cart, through an "AN" fitting, and through the probe. The solvent exits through an "AN" fitting outlet into an automatic particle-density counter. The solvent returns to the filter cart for filtration and is recycled. Flushing continues until the particle count drops to an acceptable level.

Before the unit was developed, the practice was to hang a probe in a clean room or in a clean plastic bag, flush it, collect the effluent, and analyze the effluent for cleanliness. The flushing process consumed three working shifts and required the services of a mechanic and an engineer. Now, the process takes only 2 hours, including setup time, and

requires only one mechanic for about one-half hour to set up and monitor the unit periodically.

This work was done by Nick E. Hildebrandt of McDonnell Douglas Corp. for **Johnson Space Center.** *No further documentation is available.*
MSC-18971

Squeeze-Film-Damped Spring for Turbopumps

Axial turbopump vibrations would be damped by capillary action.

Marshall Space Flight Center, Alabama

SECTION A-A
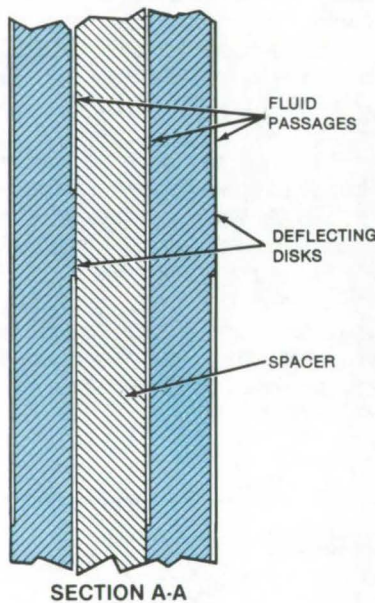
A new use for squeeze-film damping has been proposed for turbopump bearings. The damping of axial shaft vibrations may be improved with a properly-designed squeeze-film spring.

In a turbopump, axial shaft vibrations or rapid axial movements occur when the engine is started or stopped. In order to prevent these vibrations from damaging the bearings, the shaft is installed with a spring to apply a specified axial bearing preload.

The proposed squeeze-film spring is shown in the figure. It includes three disks, two of which can deflect to the left and right, thus displacing the fluid in the thin passages between them. The middle disk is a spacer to ease fabrication. The figure shows only the cross-section of the disks. The complete disk is oriented perpendicularly to the plane of the page.

The thicknesses of the passages between the disks, and the total amount of lateral movement, must be chosen so that the capillary effect takes place immediately and fills the space after deflection. Thus, the gap size depends upon the properties of the damping fluid. The thicknesses of the disks must be chosen on the basis of stress analysis to accommodate the anticipated loads.

The spring might be made out of one piece by cutting slots with wire electrical-discharge machining. Alternately, a single piece of shim or other spring material could be folded over itself so as to form the capillary spaces between the folds.

This work was done by K. Rothe of Rockwell International Corp. for **Marshall Space Flight Center.** *No further documentation is available.*
MFS-19690
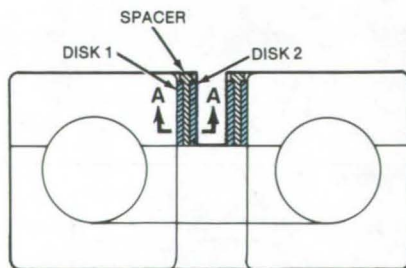
Capillary-Squeeze-Film Springs would damp turbopump-shaft axial vibrations. The disks deflect to the left and right as the pump bearing vibrates. Fluid fills and empties from the spaces between the disks to damp the vibration.

Low-Speed Control for Automatic Welding

A speed control originally developed for the rotating positioner of an automatic welding machine should be adaptable to other rotating machinery. The control extends the regulated speed range to lower-than-normal values. A servo controls the low-speed range, just as it does for the normal-range speeds. An electronic module amplifies a low-level signal from a tachometer at low speeds to operate the servocontrol. For operation at normal speeds, relays remove the amplifier from the tachometer loop.

Moving-Surface Follower Aids Microsurgery

A manipulator originally designed as an aid in microsurgery could assist in machine-tool operations. The manipulator utilizes the pneumatic servo of a commercial noncontacting thickness gage. The servo maintains a nearly constant gap between a workpiece and the manipulator by responding to changes in back pressure at a sensing orifice. An LVDT attached to the manipulator gives an electrical signal that could be used to monitor the movements of the pneumatic servo.

Tool Preloads Screw and Applies Locknut

A special tool attaches tiles with accurately-controlled tensile loading.

Lyndon B. Johnson Space Center, Houston, Texas

The mounting of thermal protection tiles on the skin of the Space Shuttle has led to the development of a special tool for holding and accurately preloading an attachment screw and putting a nut on it. The screwhead is in an auger embedded in the tile (see figure), with a stack of Belleville washers serving as a spring. The body of the screw beyond the threaded portion is reduced in diameter and ends in a flattened region that can fit into a slot.

Many assembly processes involve putting a nut on a screw, without having access to the head of the screw. The head may be on the other side of an extensive bulkhead, for example, or fixed in cement; or the screw may be headless and merely driven into wood. Whatever the details, the protruding screw is put through a hole in another piece of an assembly, and then a nut is fastened on it to hold the two parts together. To fasten the nut securely, the screw must be prevented from turning. Also, if the loading force on the screw is to be controlled, it is necessary to pull on the screw, rather than just twisting the nut to apply the load.

The figure shows that the special tool has three concentric telescoping parts. The middle tube has a threaded end that engages with the screw. The desired preload is applied to the spring washers by pulling on the yoke attached to the top end of the tube.

Inside the spring-preload tube, there is a rod used to hold the screw from turning. It has a cross-pin handle at its upper end and a slot at its lower end to hold the flattened end of the screw.

The lower end of the external sleeve contains a socket wrench for tightening the locknut against the washer. The locknut holds the thermal protection tile firmly against the skin of the Shuttle after the desired preload has been applied.

This work was done by Kenneth E. Wood of Rockwell International Corp. for **Johnson Space Center.** For further information, Circle 61 on the TSP Request Card.

This invention is owned by NASA, and a patent application has been filed. Inquiries concerning nonexclusive or exclusive license for its commercial development should be addressed to the Patent Counsel, Johnson Space Center [see page A5]. Refer to MSC-18791.
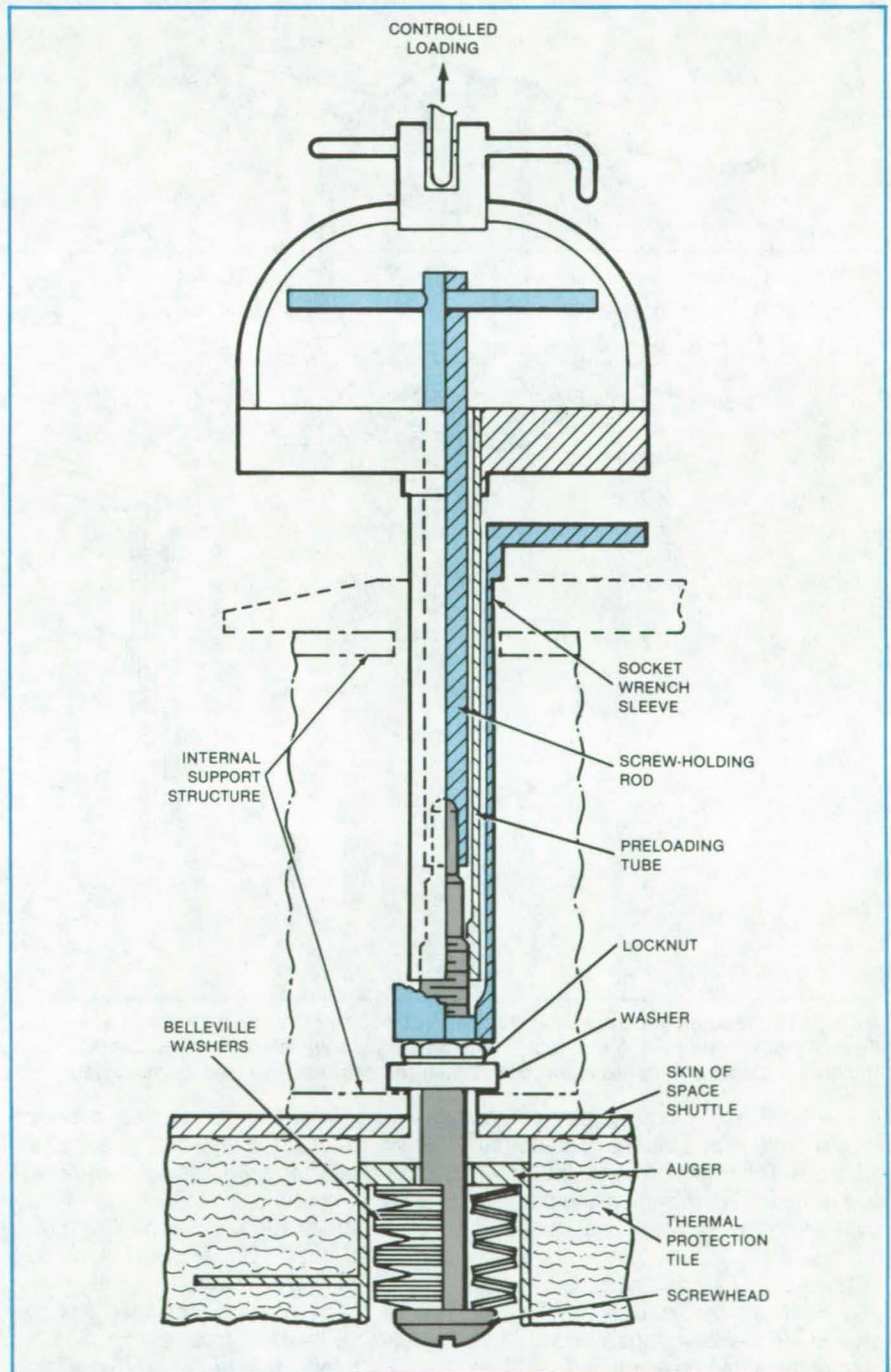
This **Special Tool** reaches through the structural members inside the Space Shuttle to fasten a nut on a preloaded screw that holds a thermal protection tile against the outside skin of the vehicle.

Lock for Gantry Trolley

Safety device secures load while
the gantry is being transported.

Lyndon B. Johnson Space Center, Houston, Texas
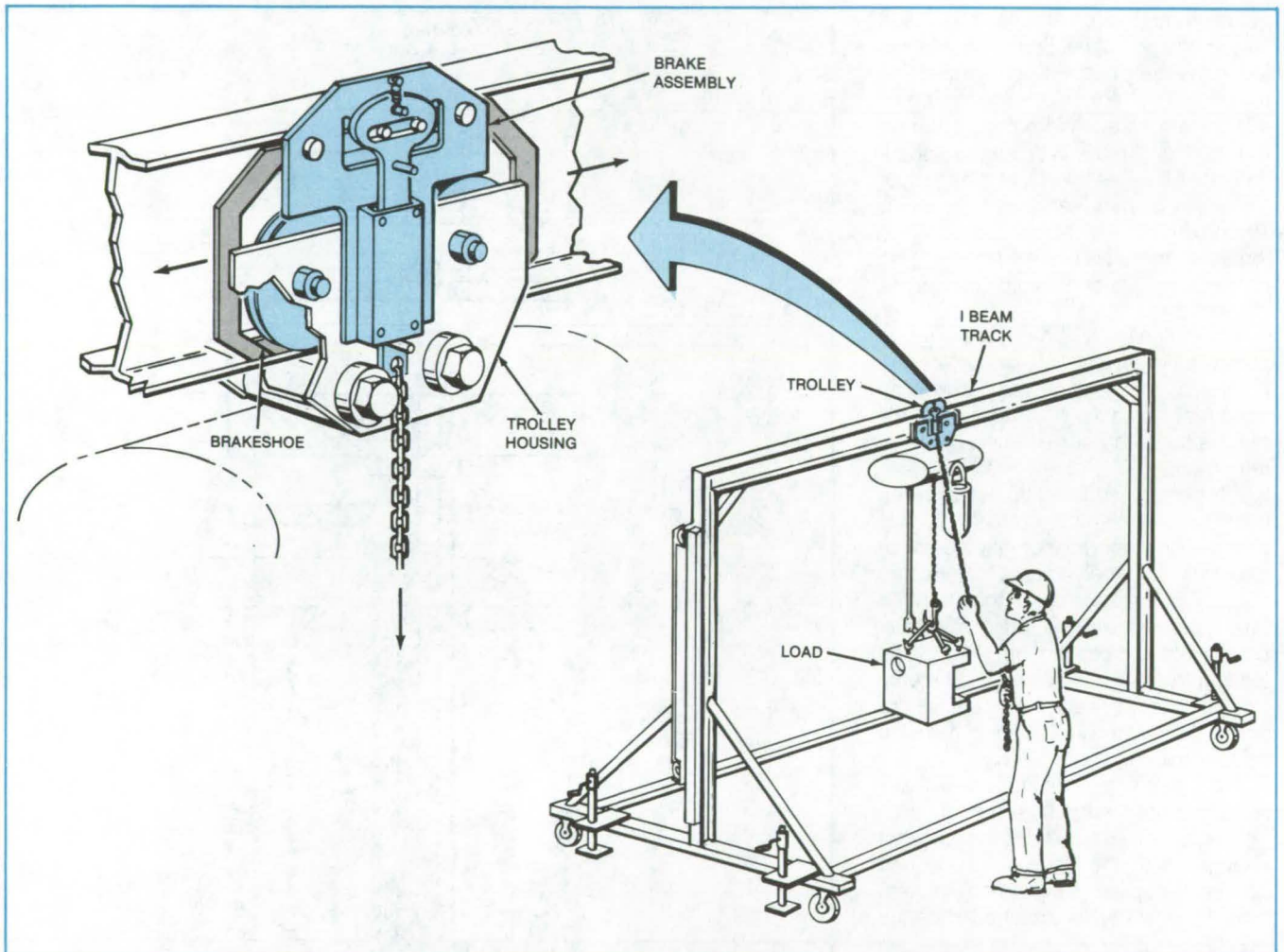
A Single Operator on the ground can control the trolley-locking mechanism on a portable gantry. The mechanism prevents the trolley and its load from moving along the track when the gantry is wheeled from one location to another. A downward pull on the chain withdraws the brakeshoes from the trolley wheels. When the operator releases the chain, the brakeshoes reengage to the wheels.

The hoist trolley on a gantry can be locked in place by a simple hand-operated brake. The brake prevents the trolley and its load from moving along the gantry I-beam track when the gantry is moved.

The trolley can be unlocked, moved, and relocked by an operator on the ground. No ladders are needed. The I-beam track can be as much as 20 feet (6 meters) above the ground.

To unlock the trolley, the operator pulls its chain downward (see figure). The chain forces a sliding cam downward so that it applies leverage to pins on a pair of retractor arms. The arms pivot so that the brakeshoes at their tips move outward, away from the trolley rollers. The operator can then tow the trolley by its chain to a new position.

To relock the trolley, the operator releases the chain, allowing a locking spring to pull up the sliding cam. The cam moves the pins on the retractor arms upward. The arms pivot, wedging the brakeshoes between the wheels and the track so that the trolley is securely locked in place.

Tool Blunts Cotter Pin Legs for Safety

Installation tool eliminates
jagged edges on bent pin legs.

Lyndon B. Johnson Space Center, Houston, Texas
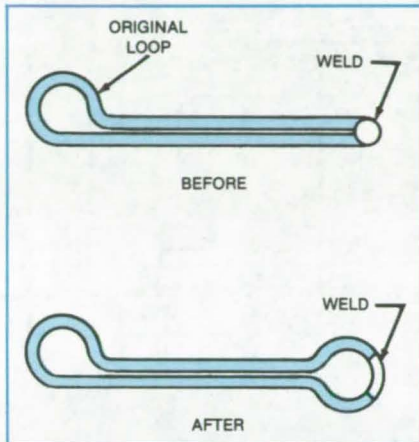
Figure 1. A **Cotter Pin** before insertion consists of a loop and a straight shaft composed of two legs welded together at their tips. After insertion with the tool, the welded legs have been shaped into a loop.

Modified duckbill pliers ensure that sharp edges are eliminated on cotter pins. Developed to protect astronauts' space suits from being punctured when they are working near cotter-pinned bolts in the Space Shuttle cargo bay, the tool can also be used to prevent the bent loose ends of cotter pins from scratching workers' fingers or cutting and entangling wiring.

The tool holds a cotter pin so that the user can insert it in a bolt and bends the inserted end of the pin into a loop. With loops then at both ends, the pin is held securely in place, but presents no hazardous sharp edges (Figure 1).

The jaws of the pliers contain slots to capture the original loop of the cotter pin for insertion of the pin shaft into the bolt. The tip of one jaw contains an upset point. The tip of the other jaw is an anvil with a hole that accepts the upset point (Figure 2).

Having inserted the pin with the tool, the user squeezes the handles so that the upset point penetrates the welded end of the pin shaft. As it enters the hole in the opposite jaw, the upset point presses the end against the anvil, shaping it into the required loop.

*This work was done by John A. Stein and Dean R. Helble of Rockwell International Corp. for **Johnson Space Center.** For further information, Circle 63 on the TSP Request Card.*
MSC-20086
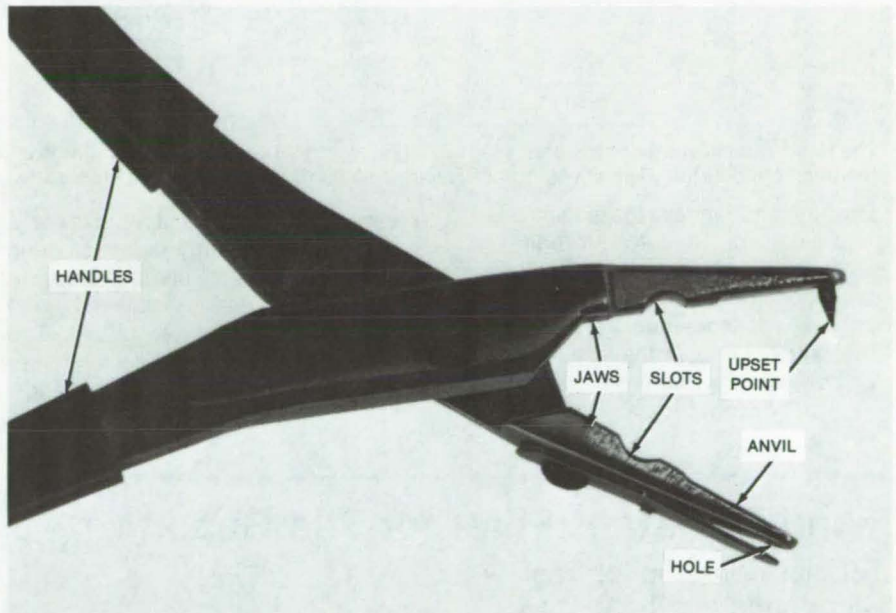
Figure 2. The **Jaws of an Insertion Tool** contain an upset point and an anvil. The point forces the cotter-pin legs into a loop as it engages the anvil.

Overheat Prevention in Solar-Powered Stirling Engines

Power output would be regulated
according to solar-energy input.

NASA's Jet Propulsion Laboratory, Pasadena, California

A proposed controller for a solar-powered Stirling engine would prevent the engine from burning up when the energy added by the Sun exceeds that withdrawn by the load. The controller is suitable for point-focus solar engines, in which reducing the input energy by shuttering the Sunlight or bypassing part of the primary working-fluid flow would reduce the engine efficiency.

In a solar-powered Stirling engine (see figure), concentrated Sunlight evaporates a primary working fluid (liquid sodium). The sodium vapor heats a secondary working fluid (helium) in the cylinder-head heat exchanger. Expanding in the cylinder, the helium drives a piston.

The proposed controller maintains constant cylinder-head temperature regardless of variations in the Sun's intensity; it ensures that all the energy directed to the receiver is used. An electronic circuit senses the head tem-

The **Head-Temperature Controller** uses the existing electrical control unit of a Stirling engine to regulate the power output in response to the head temperature. The power output is varied so as to keep the head temperature fairly constant.

perature and signals the engine electrical control unit to increase or decrease the engine power. For example, when the solar energy increases and the head temperature starts to rise, the controller causes the flow of helium to the engine to increase, thereby increasing the power output. Similarly, when the solar energy decreases and the head temperature starts to drop, the controller reduces the helium flow and consequently the power output. The temperature sensor could be on the receiver rather than on the engine head.

Wind-Resistant Filler for Tile Gaps
Tubular construction resists
wind loads and heat.

Lyndon B. Johnson Space Center, Houston, Texas

A filler developed for the gaps between insulating tiles on the Space Shuttle may also find application in industries that use tiles for thermal or environmental protection. The filler consists of tight-fitting ceramic tubes and fibrous alumina. The combination resists high wind loads while providing the requisite heat protection.

Subject to strong aerodynamic forces as well as to intense heat, the leading edge of the Space Shuttle wing poses special problems for a tile-gap filler. The material used previously was pushed out of place in wind-tunnel tests. Displacement of the filler resulted in loosened tiles.
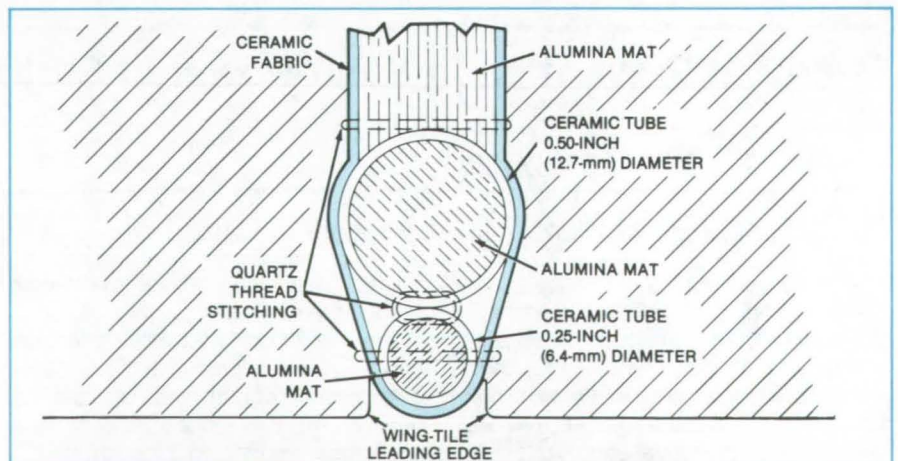
A **Filler Envelope** of ceramic fabric holds alumina-filled ceramic tubes and lower density alumina above the tubes. Quartz-thread stitching holds the envelope together.

The filler contains a 0.25-inch (6.4-mm) ceramic tube at the leading edge of the gap, backed by another ceramic tube 0.5 inch (12.7 mm) in diameter. Both tubes are filled with dense alumina mat. The tubes are encased in a ceramic fabric envelope (see figure), which also holds a lower-density alumina fiber. The assembly is stitched together by quartz thread.

This work was done by John Bellavia, Ian A. Quigley, and Thomas S. Callahan of Rockwell International Corp. for **Johnson Space Center.** *For further information, Circle 65 on the TSP Request Card.*
MSC-18966

Magnetic-Gear Concept for Special Applications

Low-torque, noncontacting gears may
be useful in special environments.

Lyndon B. Johnson Space Center, Houston, Texas

A proposed gear would have magnetic instead of mechanical teeth. As shown in the figure, the conventional stamped, machined, forged, or molded gears are replaced by inexpensive smooth gear blanks of permanent-magnet material. A pattern of alternating poles is magnetized into the material, with pole spacing equal to that of the equivalent mechanical gear teeth. The pole pattern can be helical or straight, as in ordinary gears. The magnetic equivalents of internal, external, or worm gears should all be feasible.

In the case of a worm gear, the requirement for two opposite magnetic poles translates into the need for a double-lead worm: One lead is a north magnetic pole; the other, a south pole. Alternatively, a machined or molded single-lead mechanical worm of magnetically-soft, high-permeability material could be used to form the required flux path between the magnetic poles of the mating gear.

The chief limitation of this concept is that slip torques would be low compared with those of mechanical gears (for which the slip torques are determined by gear breakage or shaft bending). Nevertheless, magnetic gears might be useful in the following applications:

• Where torque requirements are very low;
• Where a detent action is required;
• Where the environment (for example, vacuum or extreme temperatures) is hostile to ordinary gear lubricants;
• In a vacuum, where conventional gears might tend to cold-weld to each other; or
• Where speeds are extremely high.

PERMANENT-MAGNET SOUTH POLE
PERMANENT-MAGNET NORTH POLE
UNMAGNETIZED PORTION
HIGH-PERMEABILITY, MAGNETICALLY-SOFT MATERIAL

STANDARD GEAR

INTERNAL GEAR

DOUBLE-LEAD MAGNETIC POLES

HIGH-PERMEABILITY MATERIAL SINGLE-LEAD WORM

WORM GEAR
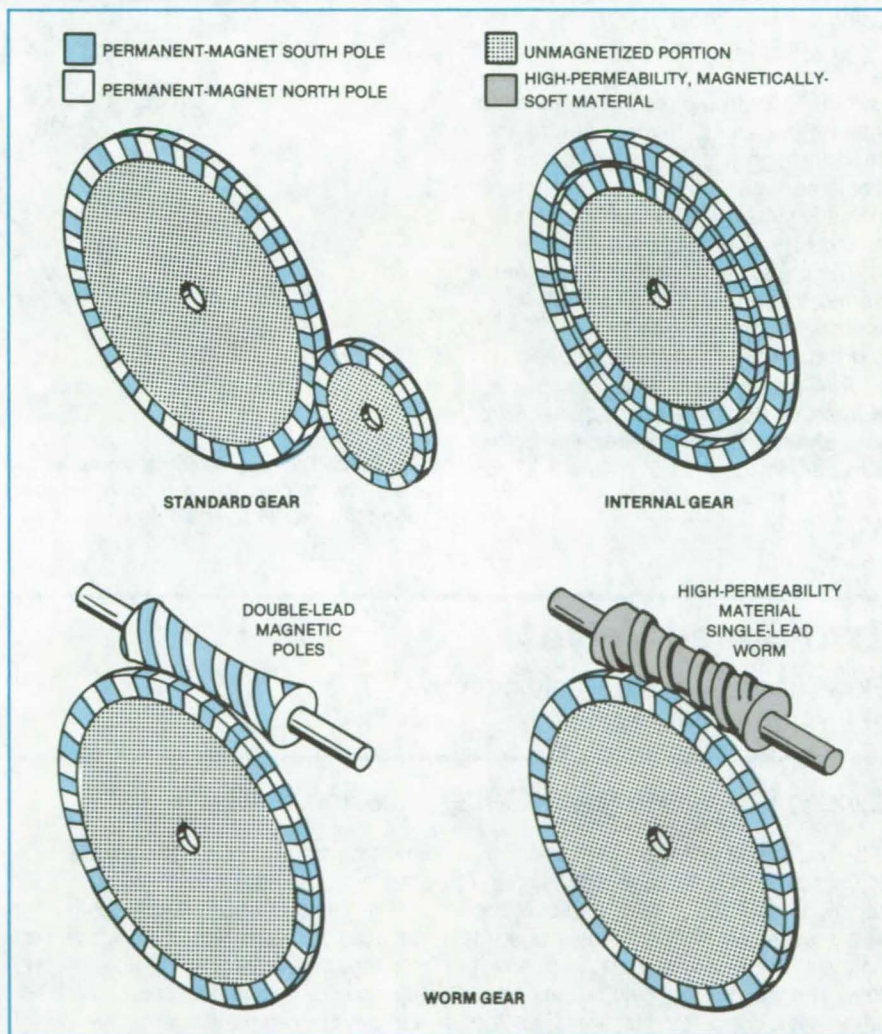
Magnetic Gears would consist of permanent magnets resembling mechanical gears but with smooth faces and alternating magnetic poles in place of mechanical teeth.

This work was done by Joseph A. Chandler of **Johnson Space Center.** *No further documentation is available.*
Inquiries concerning rights for the commercial use of this invention should be addressed to the Patent Counsel, Johnson Space Center *[see page A5].* Refer to MSC-20132.

Cable-Twisting Machine

A small cable twister is ideal
for short production runs.

Lyndon B. Johnson Space Center, Houston, Texas

Uniformly twisted cable composed of up to 26 wires is made by a new machine that is ideal for short production runs. Using it, one operator produces finished cable in about one-fourth the time it previously took three people working by hand. Faster operation than typical industrial cable-twisting machines is made possible by using smaller spools of wire.

As shown in the figure, the spools are mounted on a large revolving wheel. The wires pass through tension rollers and an idler wheel before they feed through a gathering ring into the final configuration. The completed cable is stored on the takeup reel seen in the foreground.

The speed of rotation of the wheel is varied to generate different twists. A meter registers the cable length as it passes through the tension rollers.

This work was done by Stanley Kurnett of Rockwell International Corp. for **Johnson Space Center.** *For further information, Circle 66 on the TSP Request Card.*
MSC-18874
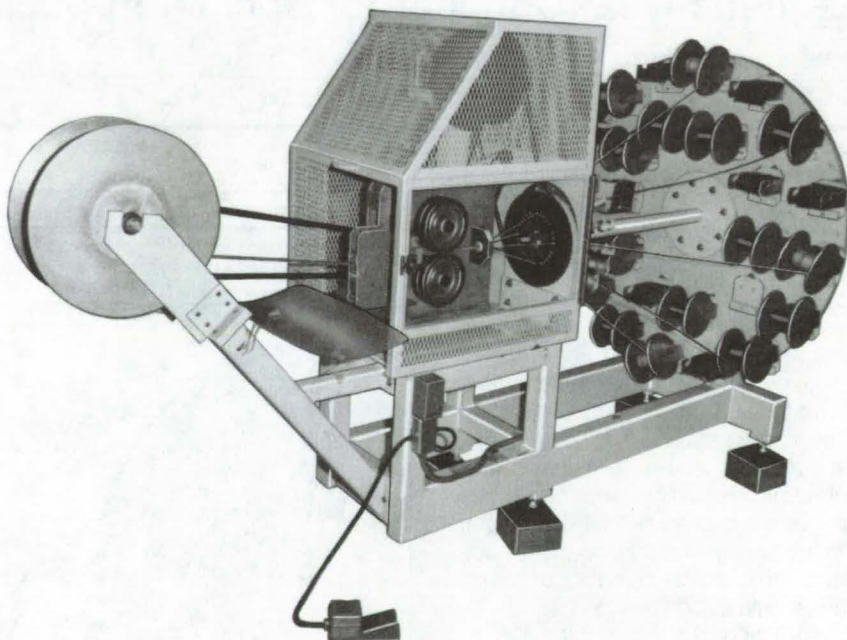
The **Cable-Twisting Machine** is smaller and faster than many production units. It is useful mainly in the production of short-run special cables. An already-twisted cable can be fed along the axis of the machine.

Two-Speed Valve

Flow increases extremely slowly
at first, then very rapidly.

Lyndon B. Johnson Space Center, Houston, Texas

A two-speed valve permits fine control of flow as it is first opened yet opens rapidly as it approaches full flow. The first several turns of the valve open it only slightly, and the last turn opens it fully. The valve is similarly two speeded when it is closed: It is fast acting for the first turn and slow acting for the last several turns.

The valve was designed for the control of oxygen flow on the Space Shuttle. It permits oxygen pressure to be applied gradually when it is first turned on, then rapidly built up to full pressure. It is expected to be useful for similar flow control of gases and liquids in such equipment as home appliances and laboratory instruments.

The valve contains a differential nut on a screw (see figure). For the first (slow) part of valve opening, the differential nut is turned on the screw, which advances the valve stem at a rate determined by the difference between the 36-thread-per-inch (TPI), (approximately 1.42 threads per mm) thread pitch on the inside of the nut and the 34-TPI (approximately 1.34 threads per mm) pitch on the outside. The pitch difference corresponds to a valve opening rate of 0.0016 inch/turn (0.042 mm/turn). For the final (fast) part of valve opening, the differential nut contacts the valve shaft and drives it directly at a rate determined by the nut external pitch, corresponding to 0.0294 inch/turn.

To open the valve, the user rotates the valve handle counterclockwise. The handle drives the differential nut, which in turn drives the differential screw. An antirotation pin prevents the differential screw from turning, and it therefore drives the valve shaft. The shaft, which is spring loaded, moves toward the valve-sealing ball.

When the user has rotated the handle through one turn, the shaft contacts the ball and forces it against its preload spring away from its seat. Gas or liquid then begins to flow through the valve.

Once the handle has been rotated 4½ turns, the differential nut butts against the shaft, driving it directly. The differential screw separates from the stem. Further rotation of the handle opens the valve at the fast rate until the handle strikes a stop in the housing.

For valve closing, the sequence is reversed. The user turns the handle clockwise, retracting the differential nut. The shaft is forced by its preload spring to follow the nut. The valve closes at its fast rate until the user has rotated the handle one turn. At that point, the stem engages the differential screw. Further rotation closes the valve at the slow rate until 4½ turns have been completed and the ball is fully seated. A series of stops prevents the nut and screw threads from being overtorqued and damaged as the valve approaches the fully open (or fully closed) position. The valve handle engages successively five radial stops, the last of which is on the valve housing.

This work was done by Donald F. Drapeau of United Technologies Corp.
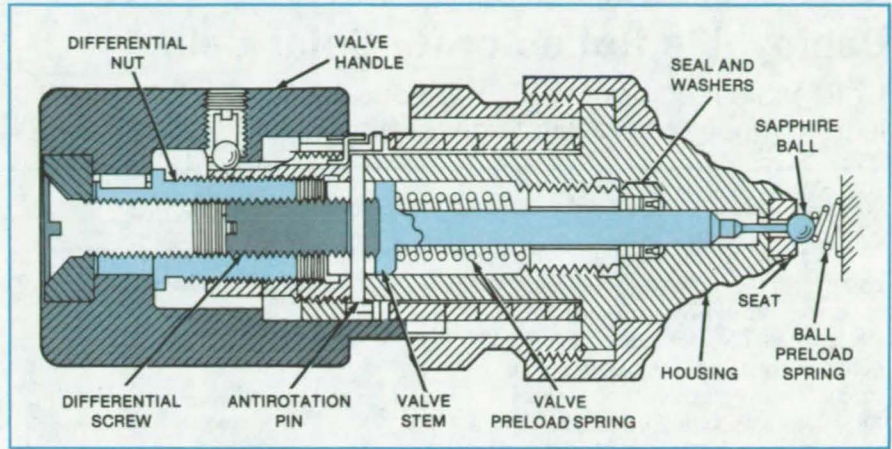
An **Operating Torque Adjustment** on a two-speed valve is provided by a preload spring and nut. The torque can be adjusted so that the user finds the valve easy to turn but does not turn it too quickly during the fast-moving portion of the valve stem travel. A drive pin transmits torque to the differential nut.

Tiedown Bracket

Bracket is easily installed and removed without damage to concrete slab.

John F. Kennedy Space Center, Florida
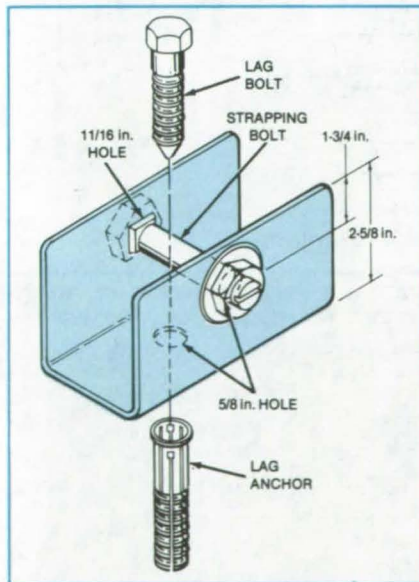
A **Tiedown Bracket** is secured to a concrete slab with a lag anchor and lag bolt. A trailer or other heavy equipment can then be anchored by tethering it to the strapping bolt. When the bracket is no longer needed, it can be removed, leaving behind only the lag anchor.

A lag bolt and an anchor, normally used for permanently anchoring a structure to concrete, can be used as part of a temporary anchor for trailers and heavy equipment. The bolt and anchor secure a tiedown bracket. When not needed, the bolt and bracket are removed, the anchor remains, and the concrete is left relatively undamaged.

As shown in the figure, the tiedown assembly consists of a 1/2-in. (1.3-cm) lag bolt, a lag anchor, and a 4- by 2- by 2-5/8-in. (10.2- by 5.1- by 6.7-cm) bracket, with a strapping bolt spanning the bracket channel. The bracket is made of 1/8-in. (3.2-mm) steel plate.

To secure the tiedown bracket, the lag anchor is installed in a hole drilled in the concrete slab. Inserting the lag bolt through a hole centered at the bottom of the bracket channel and into the lag anchor secures the bracket. The strapping bolt, to which the trailer or other equipment will be tethered, is then inserted and bolted across the channel. To remove the bracket, the steps in the installation procedure are reversed.

One method previously used for anchoring heavy equipment to concrete slabs was to cut the strapping portion off a standard anchor, to weld it to a 3- by 5-in. (7.6- by 12.7-cm) plate, and then to drill anchor holes. In another method, individual angles were fabricated back to back, and anchor holes and two strapping holes were drilled in the angles to accommodate the strapping bolt.

*This work was done by Deyo Mashburn, James E. Wald, and F. K. Helmsin of Boeing Services International, Inc., for **Kennedy Space Center.** No further documentation is available. KSC-11200*

Deployable Reflector for Solar Cells

Unfoldable-membrane-reflector concept could
lead to mobile photovoltaic generators.

NASA's Jet Propulsion Laboratory, Pasadena, California

A compactly folded reflector can be deployed easily to form corner reflectors for a solar array. The reflector concept, developed for a solar/electric-propulsion space vehicle, is applicable also to mobile solar/electric generators on Earth. As envisioned, a flat box can be deployed as a reflector comprising two panels. The panels direct Sunlight into arrays of solar cells that are deployed with the panels.

The box holds two hinged flat containers that rotate to deployment-ready position and a counterbalance beam that rotates into position after the containers (see figure). Each container holds a thin-membrane reflector, folded like a fire-hose. A mast is gradually extended from the box and unfolds the reflector membranes from the two containers. The mast moves the counterbalance beam, which is connected to the supporting structure by a cable, as it is extended.

When the corner reflector is fully deployed, the membrane is stretched out flat, as is the formerly-folded solar-cell array. The assembly is braced by the counterbalance beam and its guy cable.

This work was done by K. L. Johnson of Lockheed Missiles & Space Co., Inc., for **NASA's Jet Propulsion Laboratory.** *For further information, Circle 68 on the TSP Request Card.*
NPO-15027

LENGTHWISE VIEW DURING INITIAL UNFOLDING

SIDE VIEW DURING DEPLOYMENT
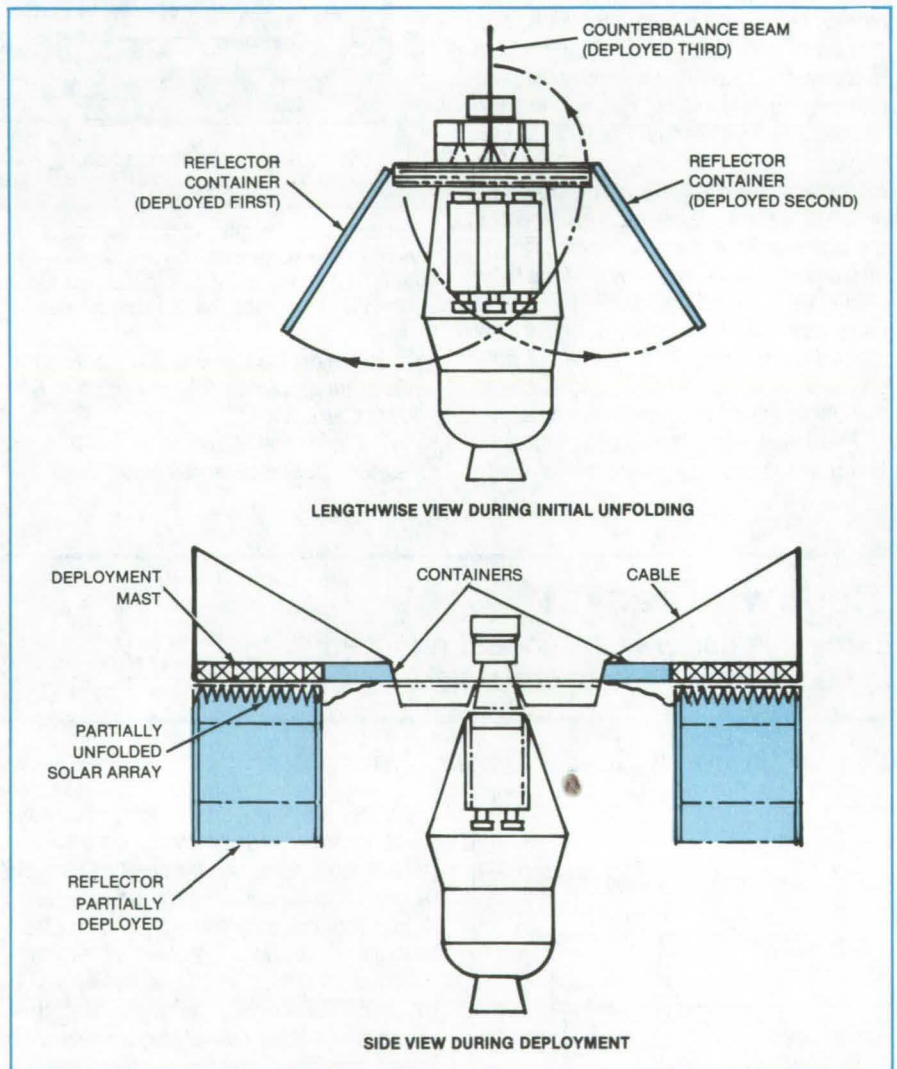
Hinged Containers Swing Open for Deployment, and a counterbalance beam swings into position (top). Folded reflector membranes are unfolded as a deployment mast is extended, until they are stretched out flat.

Fabrication Technology

Hardware, Techniques, and Processes

Gas-Jet Levitation Furnace

Versatile system enables containerless processing
of such small objects as glass microballoons.

Marshall Space Flight Center, Alabama

A gas jet levitates solid and viscous
liquid spheroids at high temperatures in
a new contactless processing system.
The system can be used to observe high-
temperature transformations (for exam-
ple, crystallization without contact with
another solid surface) or in contain-
erless studies to eliminate contamina-
tion by the crucible.

A levitator head with an array of col-
limated holes is shown in Figure 1. The
array can be constructed by drilling
holes in a disk of refractory material (for
example, tungsten) or by close-packing
a bundle of tubes. The array forms the
top of a plenum that is pressurized with
the desired gas.

The plenum may be a simple cham-
ber, or it may incorporate features to
control the sample spin rate or other
process variables. Configurations for
more than one gas supply are also
shown in Figure 1.

Each gas supply is controlled by a
regulator, flowmeter, and metering
valve as shown in Figure 2. Flow control
may be manual or automatic. A heating
coil around the refractory tube heats the
gas as it flows into the plenum.

The sample may be heated by electro-
magnetic radiation, as shown in Figure
2, or by enclosing the levitator in a fur-
nace. If control of the external pressure
is necessary, the levitator may be housed
in a hermetic chamber.

Samples are observed by looking
through a hole in the side of the furnace
and/or chamber with a low-power micro-
scope. An adapter on the eyepiece per-
mits a motion-picture or television cam-
era to be attached. Digital readouts of
the gas temperature can be superim-
posed on the motion picture.

The apparatus has been used to
monitor the evolution of glass micro-
balloons from precursor frit materials, in
the temperature range of 200° to
600° C. Hollow glass microballoons for
fusion experiments require smooth, con-
centric spherical surfaces and uniform
wall thicknesses. Levitated imperfect
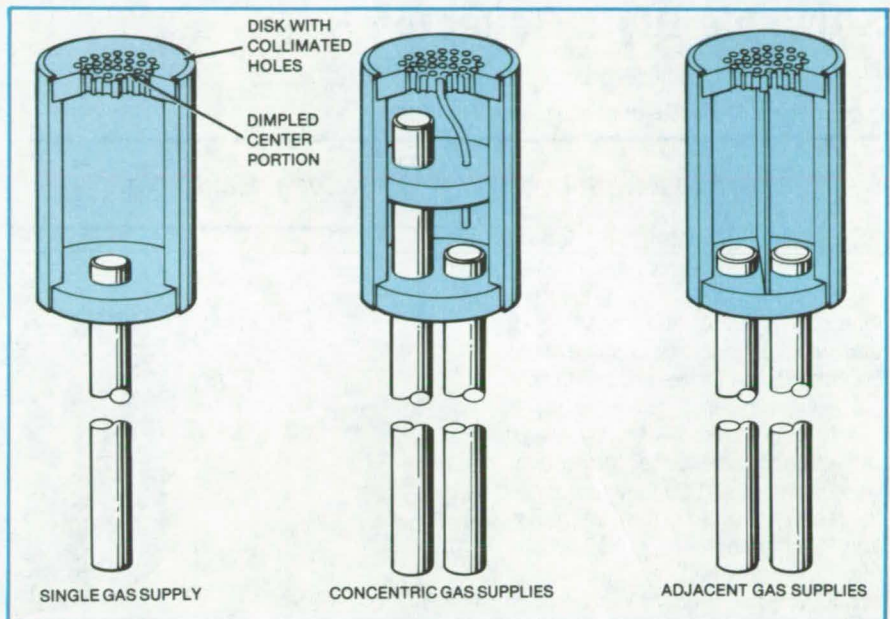
Figure 1. A **Collimated-Hole Gas-Jet Levitator Head** can have various configurations,
such as the ones shown here. In all versions, the levitating flow field is formed by gas
flowing out of the plenum through an array of collimated holes.
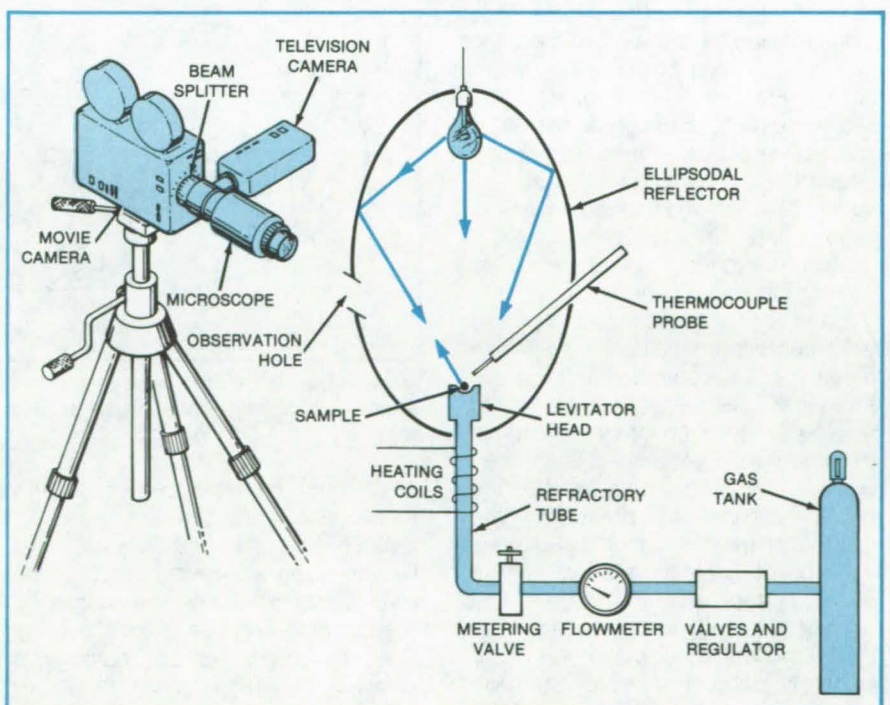
Figure 2. A **Gas-Jet Levitation Apparatus** includes a levitator head like the one shown in
Figure 1, plus ancillary gas-control, heating, and observation equipment.

microballoons can be melted and manipulated under observation in experiments on improving their structure. The system could also be used for coating the small spheres or filling them with fuel gas for fusion.

Stowable Rigid Reflector

Panels are unfolded by hinge mechanisms
to form a parabolic dish.

NASA's Jet Propulsion Laboratory, Pasadena, California

A parabolic reflector 80 feet (24.4 meters) in diameter can be stowed in a space of only 36.5 feet (11.1 meters) long and 14.5 feet (4.4 meters) in diameter with a new folding scheme. Upon command, the stowed reflector is automatically deployed to its full size.

The new method will allow parabolic reflectors for solar collectors and microwave antennas to be fully assembled at the factory, stowed in the compact package for shipment, and automatically deployed onsite. It eliminates time-consuming and costly assembly procedures at the site. In fact, the labor-cost saving could outweigh the added expense of the deployment mechanism.

The reflector is composed of rigid panels. The number of panels depends on the reflector size when deployed and upon the required package size when stowed: For the 80-foot reflector, 54 panels are used. Some of the panels — called drive panels — are hinged to a central fixed section (see figure). The panels between the drive panels are hinged to them and also to each other. In addition, an outer ring of panels is hinged to the inner panels.

In the stowed condition, the panels are folded into a small package. When the deployment command is given, the drive panels are opened in synchronism by springs at their inboard ends. Springs are also used between panels, when required. Hydraulic dampers control the rate of deployment, preventing the panels from becoming fouled or damaging each other. (Alternatively, electric motors can replace the springs and dampers.) When the panels reach their final positions, they could easily be latched in place, if necessary, to mini-
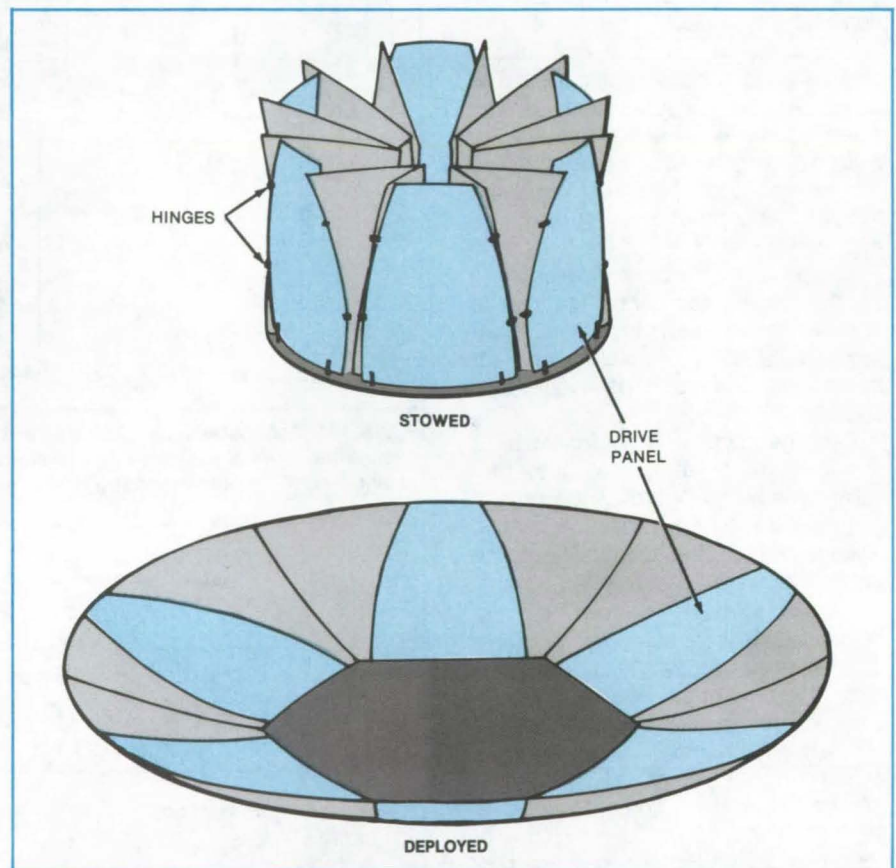
Petallike Panels Unfold from a central fixed section to create an inner reflector dish. This reflector uses only one ring of panels. For clarity, the transmitter/receiver tripod assembly is not shown.

mize distortion due to temperature gradients.

When the number of drive panels is the same in the inner and outer rings, the drive panels on the outer ring can be hinged directly to those on the inner ring. When there are half as many drive panels in the inner ring as in the outer

ring, panels are added behind those in the inner ring to support the drive panels in the outer ring.

Fabricating Thin-Film High-Temperature Thermoset Resins

Cross-linking polymer is cast between
two thin-film substrates.

Langley Research Center, Hampton, Virginia

A two-substrate fabrication technique casts thin films of thermoset polymers to less than 1.0 mil (0.025 mm). Other methods for casting thin polymer films include doctor blades, extrusion, high-pressure casting, injection molding, and ambient-pressure casting in rubber molds. However, these methods are more suitable for thermoplastic polymers. The new technique is for the fabrication of thin films of thermoset polymers.

To prepare an epoxy thin film, the quantity of uncured epoxy to be cast is placed in a vacuum oven and heated to its melting temperature. A vacuum of about 30 mm Hg is applied to deaerate the epoxy charge. The vessel containing the epoxy must be sufficiently large to allow for expansion of the epoxy during deaeration (about 10 to 1 ratio). The pressure is cycled with each foaming until all air and excess volatiles are removed.

While still in the liquid state, the deaerated epoxy is transferred to the casting facility shown in the figure. The facility consists of two steel caul plates, the flat surfaces of which must be $\overset{8}{\bigvee}$ or better smoothness. The plates are separated by two 0.013-mm-thick flexible releasing substrates, each of which is stretched and fastened over a hollow center frame.

One substrate is placed over the bottom caul plate, which has been heated to a temperature that is 25° C below the final cure temperature. The liquid epoxy is poured onto the substrate. The second substrate is then placed over the liquid epoxy, and the second preheated caul plate is placed on top of the second substrate. The film thickness is controlled by placing additional weight on top of the second caul plate. Temperature is maintained for approximately 2.5 hours and then raised to the final cure temperature for an additional 1.5 hours. The substrate/epoxy/substrate sandwich is cut out of the frames after the entire assembly has been cooled to ambient temperature. The substrates are then peeled from the cured epoxy thin film.
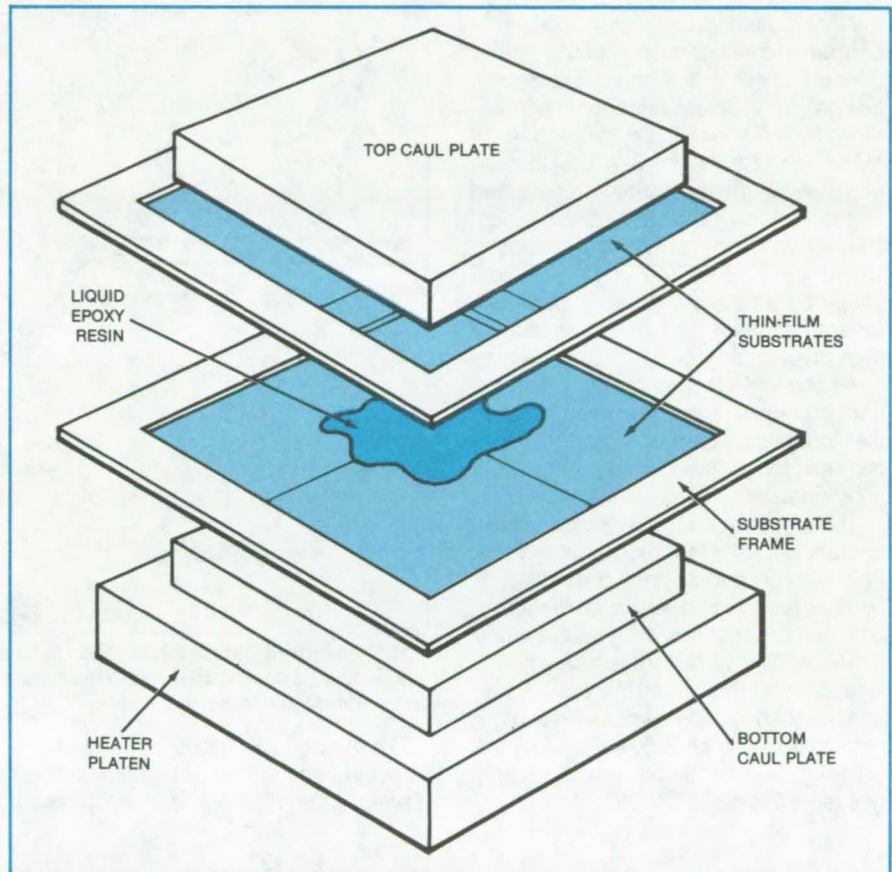
Thermoset (Cross-Linked) Resin Is Cast between thin, flexible, releasing substrate films. Films less than 0.025 mm in thickness are made routinely with this facility.

A major feature of this technique is that the thin-film substrates are removed from the polymer casting instead of the normal procedure of removing the casting from the substrate. This is possible because a flexible substrate that does not adhere to the casting is used. A second major feature is the use of a frame for each thin-film substrate. The frame maintains a constant dimension of casting area and, therefore, prevents such surface imperfections as shrinkage.

This fabrication procedure has been used routinely to make 0.025-mm epoxy films with a variation in thickness less than 5 percent. By changing the cure temperatures and cure times, the procedure can be used to prepare films of other cross-linking polymers. The epoxy films are used in the laboratory to study environmental effects on epoxies using infrared and dielectric spectroscopic techniques. The thin-film epoxies made by this technique have potential commercial applications for polymer membranes in relative-humidity sensors and as interfaces between graphite-based composites and metals to prevent corrosion.

Pressurized Paraboloidal Solar Concentrator

Proposed pressurized reflector
has a rigid substrate.

NASA's Jet Propulsion Laboratory, Pasadena, California

A proposed pressurized solar concentrator would give significantly higher concentration ratios than a previous design. [See "Solar Concentrator is Gas-Filled" (NPO-15416) on page 150 of *NASA Tech Briefs,* Vol. 6, No. 2.] Instead of allowing the pressurized metalized film to assume its natural semispherical shape, as in the previous concept, it would be forced into a paraboloidal shape by a rigid substrate. A parabolic reflector focuses light rays more sharply than does a sphere.

As shown in the figure, the reflecting and protective films are separated by the pressurizing ring manifold. The manifold forms the perimeter of the rigid substrate.

The construction of pressurized reflectors would be less expensive than for rigid concentrators, since the reflective surface, which is a low-cost metalized polymer film, can be quickly and easily replaced. The transparent cover film is significantly smaller and thereby less expensive than full dome enclosures. If the system must be shut down quickly, the reflector can be defocused by simply releasing the gas.
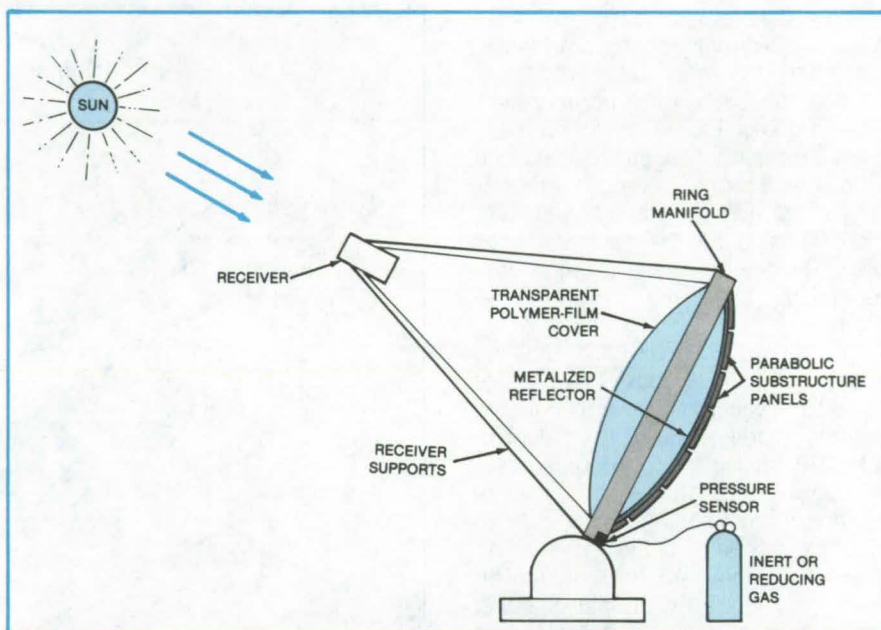
The **Pressurized Paraboloidal Solar Concentrator** would have high concentration ratio and would be easy to maintain. Gas pressure forces the reflecting film into contact with the paraboloidal substrate.

This work was done by Edward L. Cleland and Peter O. Frickland of Caltech for **NASA's Jet Propulsion** **Laboratory.** *For further information, Circle 71 on the TSP Request Card.*
NPO-15427

Pipe-Thread Vacuum Seal

A solder coating on threads
forms a crushable seal.

Lyndon B. Johnson Space Center, Houston, Texas

A lead/tin solder coating on pipe threads can serve as a seal in noncritical vacuum systems. The pipe-thread seal is less expensive than a weld or knife-edge flange. It can also be used in place of sealing tape.

To apply the pipe-thread seal, the male threads are tinned with a heavy coating of solder. As the threads are screwed into the mating part, the solder cold-flows, forming a leakproof seal.

The new seal was used to install thermocouple vacuum gages in 218-cm^3 aluminum bottles. The vacuum-gage connector, a standard 1/8-inch (3.2-mm) nickel-plated stainless-steel pipe thread, was torqued to 250 to 300 lb-in. (28 to 34 N-m). Vacuum was held for more than 6 months below 5 × 10^{-3} torr, indicating a leak rate of less than 1 × 10^{-10} cm^3/s.

Use of the seal should be limited to systems that are not to be outgassed by heating to very high temperatures because of the high lead/tin vapor pressure and low melting point.

This work was done by Joseph A. Chandler of **Johnson Space Center.** *No further documentation is available.*
MSC-20147

Onsite Fabrication of Trusses and Structures

Reinforced-plastic members are fabricated and assembled into trusses for structures at remote or inaccessible locations.

Lyndon B. Johnson Space Center, Houston, Texas

The technology for automatically fabricating structural beams, joining them to one another or to other parts to make rigid structures, and mounting equipment on them has been worked out in detail. Although originally conceived for assembling large structures in space, the proposed techniques could also be applied in remote, cramped, or otherwise-inaccessible terrestrial situations.

The structural beams (see figure) are triangular trusses made from three longitudinal members called caps, held together by crossmembers and braced by diagonal cords. The caps and crossmembers are made of thermoplastic resin reinforced with graphite and glass. They are made onsite to the desired lengths by a beam-builder machine and are assembled by beam-handling, assembly, and ultrasonic-welding machines.

The joints are made by an ultrasonic-welding process that requires no other parts or adhesives. The diagonal cords are glass and lie in the plane of cap/crossmember contact. Thus they do not obstruct objects lying across the surfaces of two caps anywhere between crossmembers and do not obstruct the hollow space inside the triangular beam.

The spacing between crossmembers is larger than the slant height of the beam cross section, so that one beam can be laid across another and welded at the four points of direct contact. The welding tool allows ready access to the insides and/or outsides of the caps.

For fastening beams end-on to other equipment, either in butt joints or hinged joints or at hubs, special triangular plastic fittings have been designed. The fittings slide into the insides of the caps and are ultrasonically welded to the caps to make strong connections.

For fastening equipment to the beams, plastic clips that fit either
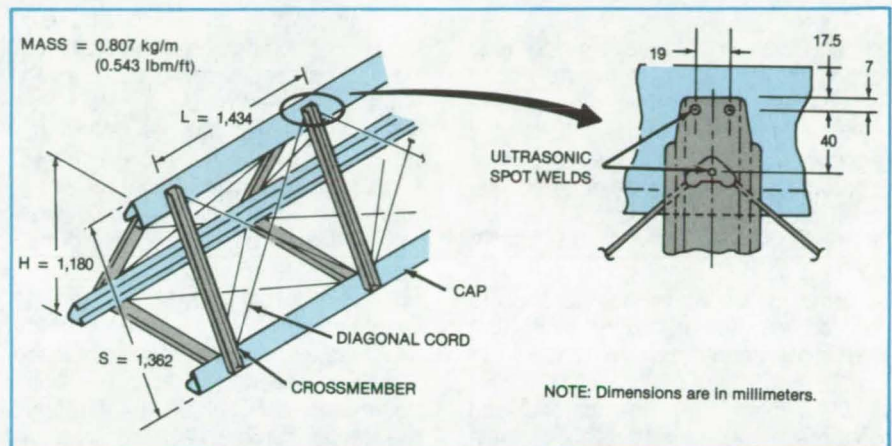
A **Tribeam Truss** that is strong and light can be made at the site where it is to be used. The reinforced plastic members are fabricated by a beam-making machine and are assembled by assembly and welding machines. Although proposed for space-platform assembly, the concept may be useful in terrestrial applications in remote or inaccessible places.

inside or outside the caps can be used. The space within the triangular beam can be used for mounting and moving a variety of instruments and mechanisms conveniently.

The desired degree of straightness or curvature of the beams can be achieved with a control system proposed for use with the beam-builder equipment. The beam control unit would maintain equal travel of the three caps while they are being made, controlling the length of each bay (each longitudinal section between crossmembers is called a bay) within a close tolerance. It would also monitor the error in displacement for each bay length produced and would compute an error correction for the subsequent bay. The overall length error for each cap would be held to within 0.1 mm per meter of cap length. This technique allows precise bending, by making one cap slightly longer (or shorter) than the other two.

To sense cap displacement, a strip of magnetic tape, containing up to 1,180 bits per cm, is applied to the cap strip material and read by the tape head. The readings are fed back to the beam control unit for rate and displacement control.

Dual-Alloy Disks Are Formed by Powder Metallurgy

High-performance disks have widely
varying properties from hub to rim.

Lewis Research Center, Cleveland, Ohio

Operating efficiencies and material conservation impose severe operating conditions on many systems. Advanced turbine disks for example may operate over a range of temperatures and stresses from the hub to the rim. Such a disk would require vastly-differing material properties. For example the hub section operates at 400° to 950° F (200° to 500° C) with high stresses that can induce low-cycle fatigue. The rim section operates at lower stresses, but the temperatures may reach 1,200° to 1,400° F (650° to 750° C).

Disks made from one material and uniformly heat treated are not capable of meeting the property goals required. This difficulty can be overcome by the use of dual-alloy powder-metal process-ing. With this process, alloy components and processing can be tailored to meet the various requirements present in a single component part.

A dual-property disk has been fabricated using two nickel-base alloys, AF-115 for the rim and Rene' 95 for the hub. The higher-temperature-potential powder is first consolidated and formed into the high-temperature rim section by hot isostatic pressing (HIP). Then the lower temperature powder used in the hub is added and hot-isostatic-pressed directly to the rim section. The completed assembly is then heat-treated. The resultant properties of the two-alloy-system disk satisfied the advanced performance requirements.

Dual-alloy fabrication may find applications in automobiles, earth-moving equipment, and energy conversion systems as well as aircraft powerplants. There is also a potential for such applications as shafts, gears, and blades.

*This work was done by F. H. Harf and R. V. Miner of **Lewis Research Center** and C. S. Kortovich and J. M. Marder of TRW, Inc. Further information may be found in NASA CR-165224 [N82-18370/ NSP], "Development of Material and Process Technology for Dual Alloy Disks" [$16.50]. A copy may be purchased [prepayment required] from the National Technical Information Service, Springfield, Virginia 22161.*
LEW-13702

Robot End Effector To Place and Solder Solar Cells

A solar cell is heated by RF induction for reflow soldering
while being carried by a robot end effector.

NASA's Jet Propulsion Laboratory, Pasadena, California

A robot end effector or "hand" has been developed that heats a solar cell to soldering temperature while the robot transports the cell from a preparation station to a solar panel where the cell is simultaneously placed in position and soldered. The use of RF induction heating allows the cell to be heated without requiring direct mechanical and thermal contact of a bonding tool such as a soldering iron. By the time the solar cell arrives at the panel, it is hot enough to reflow the solder paste previously applied to the cell and to solder the cell to the interconnects of the next cell in the string as the robot places it in position.

The robot end effector is used in conjunction with a work station that prepares the cells for soldering. (See the following article.)

At the preparation station the solar cells are unloaded from a storage cassette and are rotated into a standard orientation. (An optical sensor determines when the orientation is correct.)
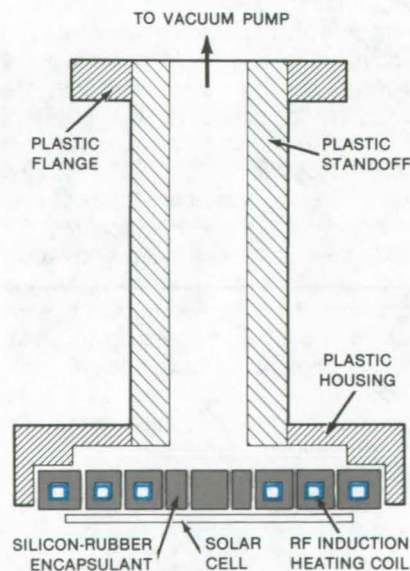
Encapsulated in the **Robot End Effector** is an RF induction-heating coil for heating the solar cell while in transit. Holes in the encapsulant permit the end of the unit to act as a vacuum pickup to grip the solar cell.

Then solder paste and copper interconnect ribbons are applied to the cell.

The robot end effector (see figure) has two functions: to grip the cell and to heat it. The gripping is done by vacuum. Small holes in the end of the effector connect to the hollow interior. Evacuating the interior causes the cell to be gripped on the end of the effector. The end is made larger than the solar cell to support it fully and to minimize handling damage.

A coil embedded in silicone-rubber encapsulant at the end of the effector is used for RF induction heating of the cell. The encapsulant layer between the coil and the solar cell is thin to enhance heating. A thicker layer behind the coil acts as a compliant coupling to compensate for robot positioning tolerances.

Several different coil shapes were tried that were intended to concentrate heating at the interconnect points. However, it turned out that faster heating could be obtained with a simple three-turn flat spiral coil, 4 inches (100 mm) in

diameter, which heats the entire cell. The coil is made from ¼-inch (6.3-mm) thin-wall, square cross-section tubing. (Square tubing provided more efficient heating than did round.)

The long tubular body of the end effector serves to keep the RF induction coil away from metal components of the robot to avoid the loss of RF energy and heating of the robot.

This work was done by John J. Hagerty of MBAssociates for **NASA's Jet Propulsion Laboratory.** *For further information, Circle 72 on the TSP Request Card.*
NPO-15490

System To Prepare Solar Cells for Assembly

To reduce labor, an industrial robot is used for solar-cell positioning and soldering operations.

NASA's Jet Propulsion Laboratory, Pasadena, California

A microprocessor-controlled system comprising a solar-cell preparation station and an industrial robot is used to reduce labor in assembling photovoltaic solar panels. The preparation station (see figure) prepares a cell for soldering; the robot picks up the cell, heats it to soldering temperature, and solders it in place as it positions the cell.

The preparation station accepts standard H-bar cassettes of randomly-oriented solar cells. A commercially-available cassette unloader places a solar cell on a rotatable vacuum chuck. The chuck rotates until an optical sensor signals that the orientation is correct. Then solder paste is applied to the cell by a modified pneumatic dispenser. Finally, interconnect ribbons are formed from roll storage and placed on the solar cell.

This cell, paste, and interconnect-ribbon preparation is picked up by the robot using an end effector or "hand" with a vacuum grip. (See the preceding article.) While carrying the cell to the solar panel, a coil in the end effector heats the cell to soldering temperature by RF induction. The robot then simultaneously positions the cell and solders it in place in the panel.

This work was done by John J. Hagerty of MBAssociates for **NASA's Jet Propulsion Laboratory.** *For further information, Circle 73 on the TSP Request Card.*
NPO-15489
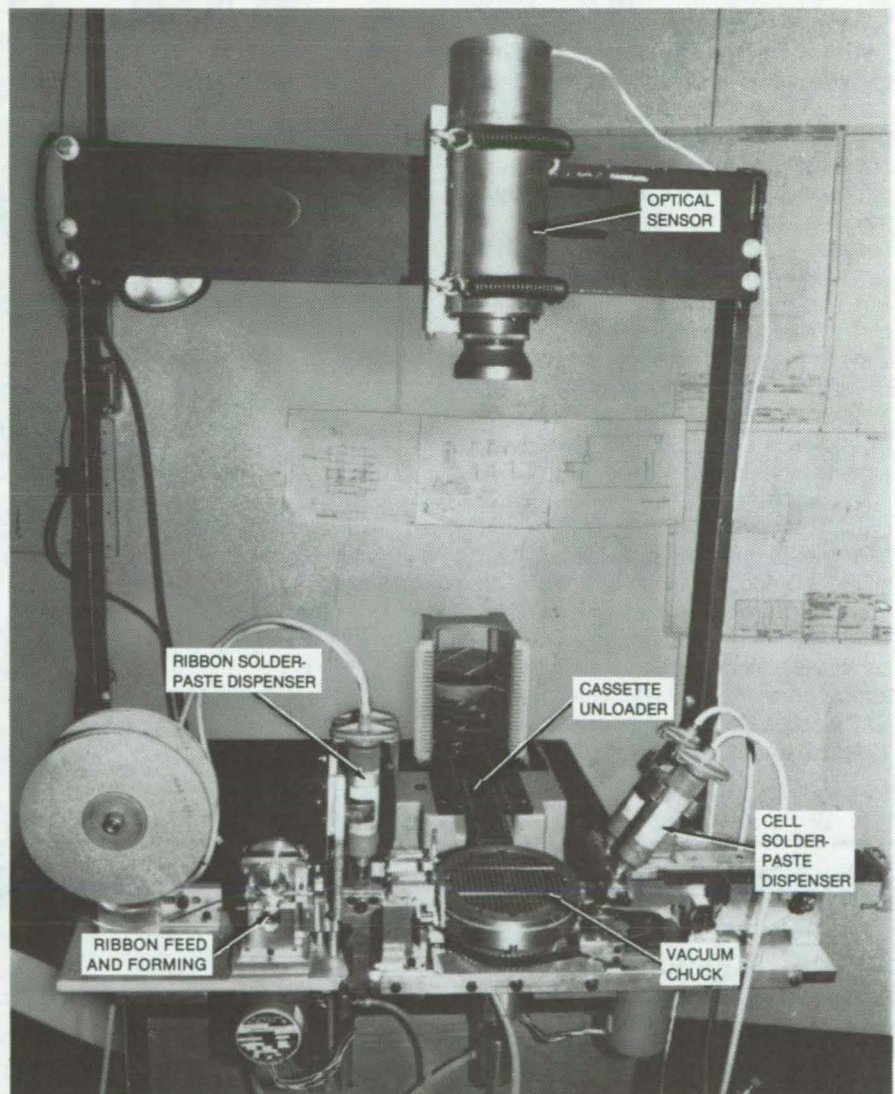
Solar-Cell Preparation is carried out in the work station shown. The cassette unloader feeds a solar cell to the vacuum chuck, which rotates the cell into proper orientation as determined by the optical sensor. Then solder paste and interconnect ribbons are applied to the cell. An industrial robot then picks up the cell, heats it by RF induction, and solders it into position in the solar panel.

Dip-Coating Fabrication of Solar Cells

Jets of gas permit rapid production.

NASA's Jet Propulsion Laboratory, Pasadena, California

Inexpensive silicon solar cells can be made by a simple dip technique — provided that the postdip solidification of the semiconductor material is carefully controlled. A new apparatus provides such control by convective cooling and radiative afterheating.

A ceramic wafer coated on one side with graphite is immersed in molten silicon (see figure). As the wafer is withdrawn, a polycrystalline film of silicon clings to the graphite side but not to the ceramic side. Cooling shoes, cooled by flowing water, direct jets of helium or argon at both sides of the wafer as it leaves the melt. The jets remove heat from the silicon film so that it solidifies rapidly. Two graphite resistance heaters — one on each side of the wafer — retard the cooling of the solid silicon film so that it does not fracture from thermal stress. The combination of cooling and heating allows the filmed substrate to be withdrawn at a relatively high rate — up to 0.2 cm/s. Coatings with smooth regions of thickness up to 300 μm have been grown at this speed.

The substrate is dipped in a quartz crucible supported by a graphite holder in a graphite resistance heater. A heat shield composed of two concentric graphite cylinders spaced with graphite wool surrounds the heater. The ensemble is maintained under an inert-gas atmosphere. In a typical coating operation, a substrate is lowered to just above the melt surface and held there 2 min-
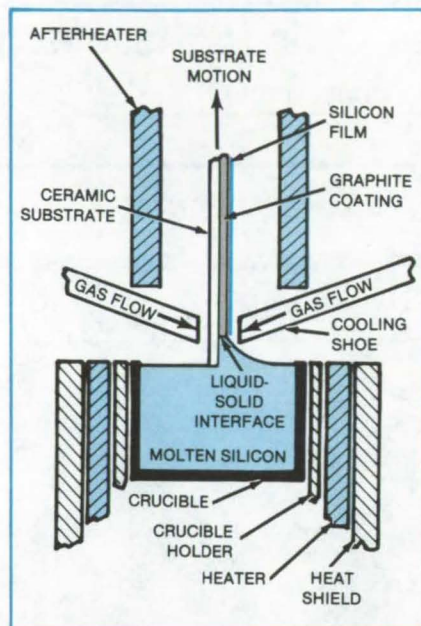
Cooling Shoes Direct a Flow of Helium on a graphite-coated ceramic substrate to solidify a film of liquid silicon on the graphite surface as the substrate is withdrawn from the molten silicon. Afteheaters control the cooling of film and substrate to prevent cracking. The gas jets exit at points about 10 mm from the substrate surfaces and 6 to 10 mm above the melt surface.

utes while it heats through. It is then inserted in the melt, held for 30 seconds, and withdrawn.

The cooling shoes are machined from nickel and contain passages for water and gas flow. The gas exits through holes in the ends of the shoes: Future versions will employ a more carefully designed manifold at the exit to distribute the gas more uniformly over the silicon surface and avoid vertical striations in the newly solidified material.

The shoes are inclined at an angle of 20° to the melt surface. In the shoe facing the uncoated side of the wafer, the gas flow is parallel to the axis of the shoe; while in the shoe facing the coating, the gas exits in a direction perpendicular to the plane of the coating. This arrangement allows the back side of the substrate to be cooled slightly below the liquid/solid interface, while the front side is cooled above the interface. The gas flow rate on the back side is four times that on the front side. Helium is the preferred gas because of its high thermal conductivity (approximately eight times that of argon); it allows thicker coating at a given wafer withdrawal rate.

This work was done by Barry Koepke and Don Sauve of Honeywell Inc. for **NASA's Jet Propulsion Laboratory.** *For further information, Circle 74 on the TSP Request Card.*
NPO-15312

High-Efficiency Solar Cells on Low-Cost Substrates

Epitaxial layers are grown on substrates of commercial-grade silicon.

NASA's Jet Propulsion Laboratory, Pasadena, California

High-efficiency solar cells are made in thin epitaxial films grown on low-cost commercial silicon substrates. The cost of the cells is much less than if high-quality single-crystal silicon were used for the substrates, and the performance of the cells is almost as good.

Epitaxy is generally used to grow layers with specified dopant distributions and thicknesses on high-quality single-crystal silicon substrates. The new technology is based on the growth of thin epitaxial layers on low-cost forms of silicon that are impure and contain a

high density of crystallographic defects. The epitaxial layers are grown rapidly (more than 5 microns per minute) to minimize diffusion of impurities from the substrate; an unexpected benefit is that the defect density in the epitaxial layer is far lower than in the substrate.

A typical structure includes a buffer layer between the substrate and the solar-cell layer. The buffer is grown with an exponential doping gradient to form a built-in electric field that moves photogenerated carriers away from the substrate and toward the collection junction. The junction is formed by growing an n-type layer, either epitaxilly or by diffusion from a gaseous source in a separate furnace. The performances of solar cells fabricated on two representative materials are given in the table. For comparison, the performance of a typical cell made in epitaxial layers

Silicon Substrate	Layer Thickness (μm)	Current Density (mA/cm^2)	Open-Circuit Voltage (mV)	Efficiency (%)
High-Quality Single Crystal	14	28.2	578	13.2
Commercial Single Crystal	15	26.1	605	12.7
Commercial Polycrystal	14	25.0	556	10.6

Solar-Cell Parameters for epitaxial cells on various silicon substrates

grown on a high-quality single-crystal silicon substrate is also shown.

This work was done by Robert V. D'Aiello and Paul H. Robinson of RCA

Corp. for **NASA's Jet Propulsion Laboratory.** For further information, Circle 75 on the TSP Request Card. NPO-15039

Plating To Reinforce Welded Joints

Electrodeposition of nickel is used to reinforce or strengthen weld joints.

Marshall Space Flight Center, Alabama

Electrodeposition is used to strengthen welded joints that have been gouged, nicked, or suffered other mechanical damage. The joint is prepared by grinding or sanding until it is smooth and flush with the adjacent material. As shown in the figure, an acrylic plating cell is assembled to fit around the area to be plated and is sealed to prevent leakage. A weir dam maintains the proper electrolyte level in the cell. Stainless-steel strip electrodes are connected to the negative terminal of a low-voltage dc power supply, and the part is connected to the positive terminal. The cell is filled with Turco 4104 eletrolyte (or equivalent), and etching is carried out at 2 volts and 5.5 to 7.0 amperes for about 5 minutes.

Next, the cell is drained, rinsed, and filled with deionized water. The stainless-steel electrodes are then replaced with platinized titanium electrodes, and the electric polarity is reversed. The cell is again drained and rinsed and is filled with sulfuric acid electrolyte. It is reactivated at 2 volts and 5.5 to 7.0 amperes for 1½ to 2 minutes.

The electrolyte flow nozzle is then attached with the part connected to the negative terminal. The cell is filled with nickel strike electrolyte, and plating is carried out at 2 volts and 4 to 5 amperes for about 5 minutes. The platinized
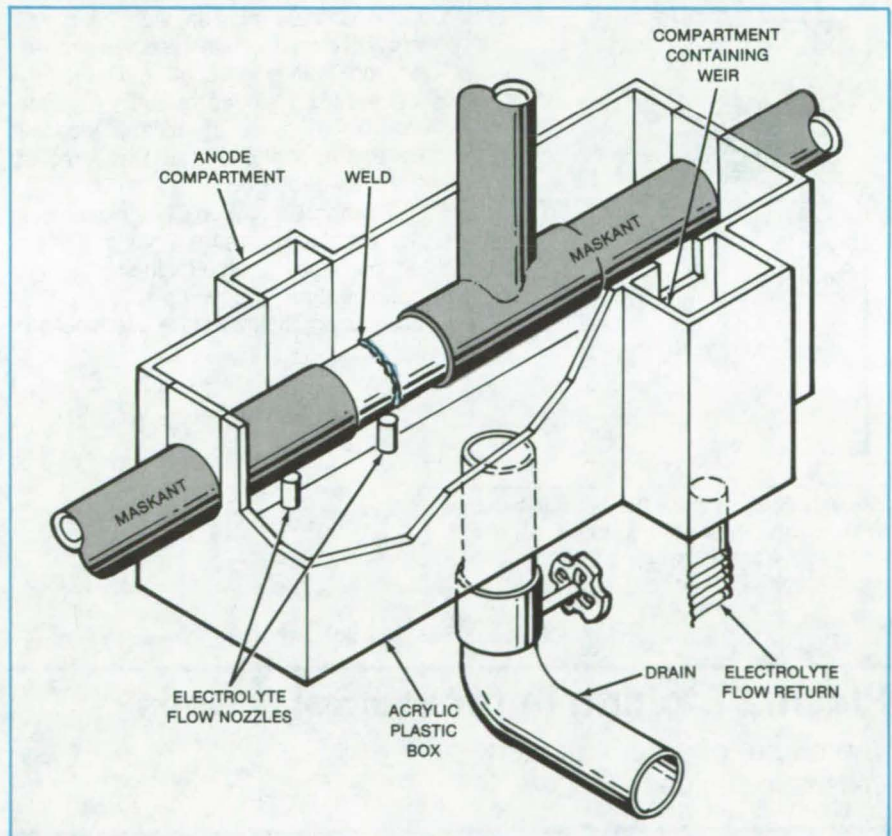
A **Plating Cell,** typically of an acrylic plastic such as poly(methylmethacrylate), is assembled around the part to be plated. Areas not to be plated are masked with plater's tape. The weld area is plated in a standard nickel-plating process.

titanium electrodes are replaced with "s" nickel anode strips.

Finally, the cell is drained, rinsed, and filled with nickel sulfamate electrolyte. Electrolyte is pumped from the reservoir tank through a filter to the cell where it impinges on the part and is then returned to the reservoir tank by gravity after overflowing the weir dam. This procedure removes contaminants from the solution.

This method has been used to reinforce defective weld joints of coolant supply lines of flight nozzle assemblies. It can be used in other situations in which in-place reinforcement of weld joints would result in cost reduction or in a saving of time.

This work was done by J. E. O'Tousa of Rockwell International Corp. for **Marshall Space Flight Center.** *For further information, Circle 76 on the TSP Request Card.*

Inquiries concerning rights for the commercial use of this invention should be addressed to the Patent Counsel, Marshall Space Flight Center [see page A5]. Refer to MFS-19576.

Material Protection During Electron-Beam Welding

Alumina pellets guard material behind the weld area
from weldthrough and burnthrough spatter.

Marshall Space Flight Center, Alabama
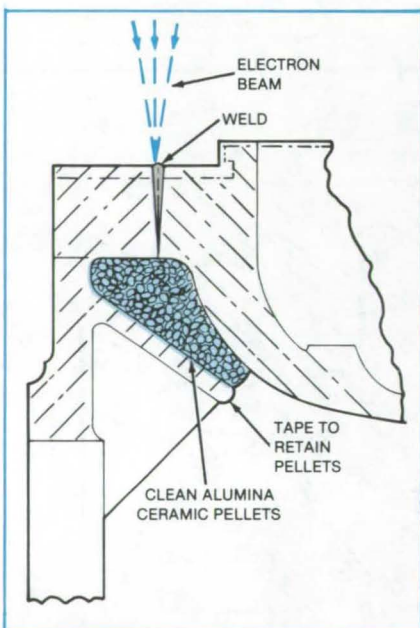
Alumina Pellets behind the electron-beam weld joint protect other parts of this assembly from the beam and from spattered material.

In the electron-beam welding process, areas behind the weld region can be protected by packing the back side of the weld joint with clean alumina pellets and holding them in place with tape or backing material. The alumina pellets prevent damage from the electron beam or from liquid-melt spatter. The joint is welded from the face side by the electron beam as required, and then the pellets and spatter material are removed from the back side.

The figure shows this technique being used in electron-beam welding of a joint on the Space Shuttle main-engine high-pressure-fuel turbopump housing. This application illustrates the usefulness of the protective pellets in blind or partially enclosed areas where other methods of shielding are inconvenient.

The alumina pellets may be cleaned and reused. They are easily applied and removed in regions that are narrow or have complex shapes.

*This work was done by Robert L. Tomlinson and Frank J. Kiluk of Rockwell International Corp. for **Marshall Space Flight Center.** No further documentation is available.*

Inquiries concerning rights for the commercial use of this invention should be addressed to the Patent Counsel, Marshall Space Flight Center [see page A5]. Refer to MFS-19666.

Plasma Etching Improves Solar Cells

The output of screen-printed
cells is increased.

NASA's Jet Propulsion Laboratory, Pasadena, California

Etching the front surfaces of screen-printed silicon photovoltaic cells with a sulfur hexafluoride plasma has been found to increase cell performance while maintaining the integrity of the screen-printed silver contacts. Although the physical mechanism of the improvement is not fully understood, thinning of the junction appears to be a major contributor to cell improvement.

The replacement of evaporated-metal contacts with screen-printed metal contacts has been proposed as one of the ways to reduce the cost of solar cells for terrestrial applications. The evaporated-metal technology allows the use of relatively shallow (0.1-μm-thickness) junctions, which optimizes spectral re-

sponse. With screen printing, a thicker (>0.3-μm) junction must be used to suppress leakage currents. The leakage currents are due to the diffusion of silver and other impurities into the silicon during processing. The thicker junction degrades the cell spectral response.

The proposed solution was to reduce the junction depth by etching after the sensitive cell-processing steps and before applying the antireflection coating. Wet chemical etching of the contacted surface was found to be unsuitable because the etch was nonuniform and the etchant damaged the metal con-

tacts. Plasma etching proved more successful.

Glow-discharge plasmas are usually created at pressures of 0.1 to 1.0 torr (13 to 130 N/m^2) by the action of an electric field on the contained gas molecules. The molecules dissociate into a variety of reactive species that are useful for etching, cleaning, and other processes.

A plasma etch in a mixture of Freon-14 and oxygen resulted in a 15-percent increase in output but with undesirable surface pitting and reactions between the metal contacts and the plasma. Furthermore, most of the in-

creased output was attributed to light trapping in the etch pits. Sulfur hexafluoride was found to be a nonpitting plasma etchant that does not react with the contact metal. A 12-percent increase in cell output was observed after the removal of 1,000 Å from the junction layer.

This work was done by Steven M. Bunyan of Spectrolab, Inc., for NASA's Jet Propulsion Laboratory. For further information, Circle 77 on the TSP Request Card.
NPO-15205

"Sandwich" Stiffener for Composite Structural Panels

Titanium honeycomb core is brazed to
cap material and panel skin.

Langley Research Center, Hampton, Virginia

The sandwich beam stringer is a lightweight, structurally-efficient, low-cost stiffener for metal-matrix composite structural panels. Previous methods of stiffening metal-matrix structural panels incorporate hat or blade stiffeners, which require hot forming during fabrication.

The new concept uses commercial titanium honeycomb core brazed to the cap material and the panel skin (see figure). In the fabrication of the stringers, large sheets of cap material are brazed to pieces of honeycomb core of the desired height. After brazing, individual stringers are cut by electrical-discharge machining, and the stringers are subsequently brazed to the skin.

The new panel design is based on a preliminary analysis using the titanium-clad Borsic® /aluminum panel concept shown in the illustration. Although the concept uses metal-matrix composite material, the same configuration may be fabricated from conventional structural materials using brazing or adhesive bonding. Advantages of this stiffener over previous configurations are that it requires no forming operations and provides high shear, bending, and torsional stiffness to the panel, while adding little mass.

This work was done by Robert R. McWithey, Dick M. Royster, and Thomas T. Bales of Langley Research Center. For further information, Cir-
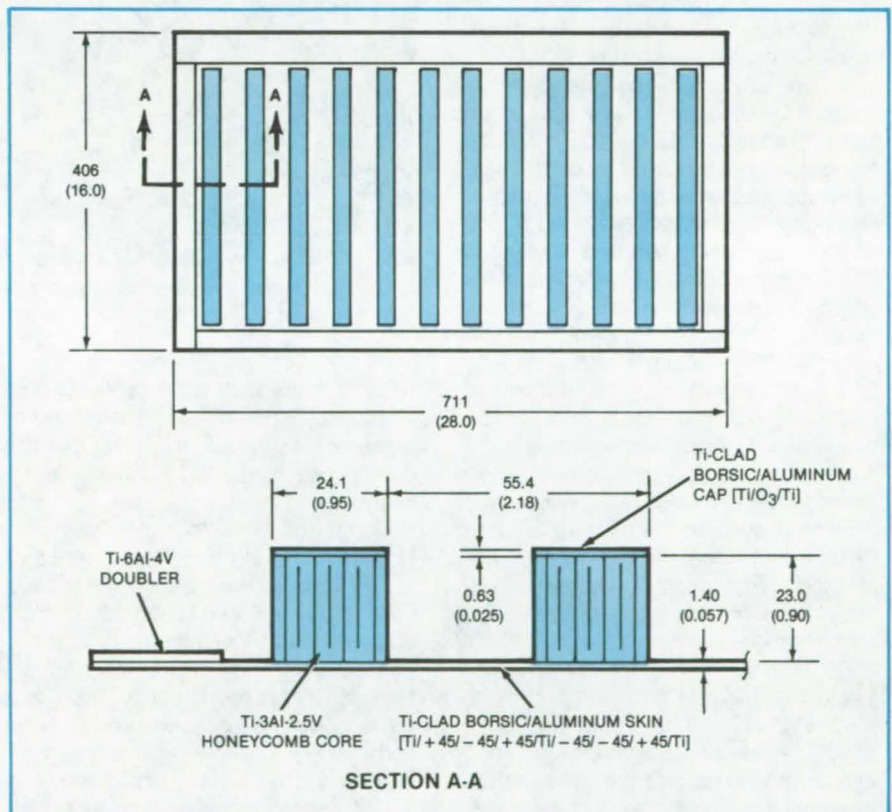
Titanium-Clad Borsic/Aluminum Skin-Stringer Panel is assembled by brazing caps to honeycomb core. Dimensions are given in millimeters (inches).

cle 78 on the TSP Request Card.

This invention is owned by NASA, and a patent application has been filed. Inquiries concerning nonexclusive or ex-

clusive license for its commercial development should be addressed to the Patent Counsel, Langley Research Center [see page A5]. Refer to LAR-12807.

Precipitating Chromium Impurities in Silicon Wafers

Wafers are treated by laser damage and annealing.

NASA's Jet Propulsion Laboratory, Pasadena, California

Two new treatments for silicon wafers can improve solar-cell conversion efficiency by precipitating electrically-active chromium impurities. One method is a simple heat treatment. The other involves laser-induced damage followed by a similar heat treatment.

Chromium is one of the impurities of concern in metallurgical-grade silicon for solar cells. In the new treatments, the chromium active centers are made electrically inactive by precipitating chromium from the solid solution. This enables the use of lower grade, lower cost silicon in cell manufacture. The high solid solubility and diffusivity of chromium in silicon facilitate the precipitation process, making successful heat treatments possible at the relatively low temperature of 200° C.

If the precipitate particle size increases too much, as through aging, then cell degradation may occur. To reduce aging effects, controlled laser damage can be applied to the back surface before annealing. Dislocations produced during the laser damaging serve as nucleation sites for impurities, so that the impurities precipitate toward the back surface, away from the junction depletion region.

Experiments were performed on 1- by 2- by 0.025-cm silicon wafers with a boron doping of 10^{16} atom-cm^{-3} and a deliberate chromium doping of 1×10^{15} cm^{-3}. The junction diffusion was performed at 920° C using phosphine as the phosphorus source. Thin films of Ti/Pd/Ag metalization were evaporated onto the diffused wafers to form the contacts, and tantalum pentoxide was applied as an antireflection coating.

Some wafers were not precipitation-treated. Some were annealed in nitrogen at 200° C for 1 hour, then quenched rapidly. Others were scanned along a pattern of evenly-spaced parallel lines on their back surfaces by a Q-switched Nd:YAG laser operating at 1.06 μm, with the beam focused to a 40-μm spot, then annealed in nitrogen at 200° C for 50 minutes. The important laser-exposure parameters are the damage depth and scan-line spacing. By experimentation, the optimum line spacing was found to be
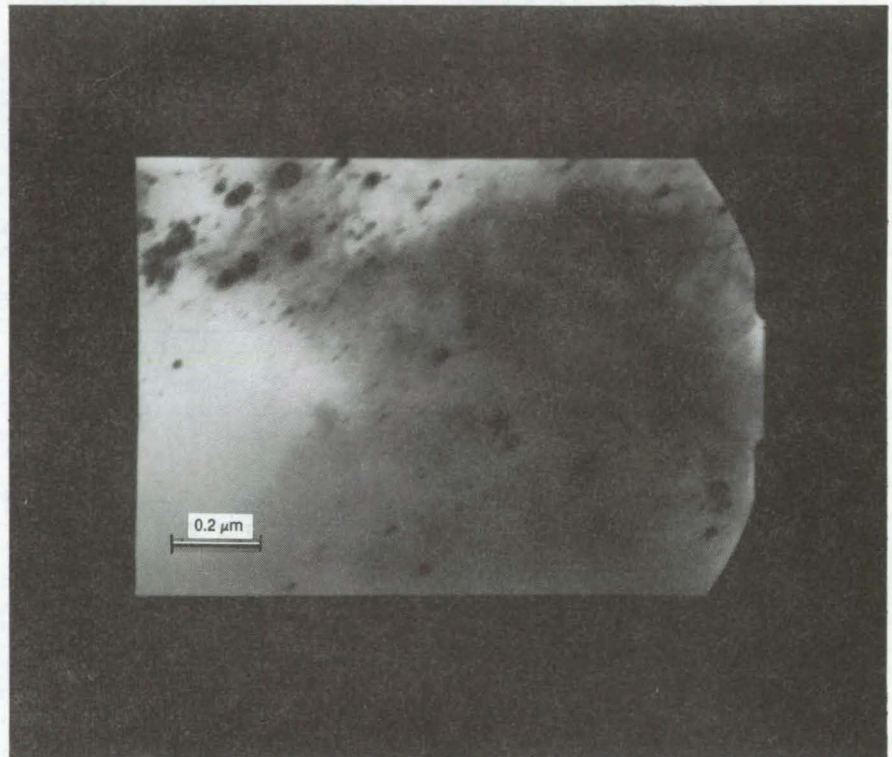
A **Transmission Electron Micrograph** shows chromium particles that were precipitated from the solid solution in silicon.

0.5 mm, and the damage depths were 9 to 12 μm, respectively. The laser energy densities required to produce this damage were 16 and 28 J/cm^3, respectively.

Some of the treated wafers were fabricated into solar cells. Others were subjected to deep-level transient spectroscopy, transmission electron microscopy, and Hall-effect measurements to determine carrier-trapping-center concentration, precipitation-particle size, and majority-carrier concentration. Solar cells were exposed to light and current-vs.-voltage measurements made.

Untreated specimens showed no precipitation, while annealed specimens showed fine precipitate particles of 0.04 μm size (see figure). After annealing, electrically active centers were reduced by 50 to 60 percent from their previous concentration. Majority-carrier concentrations were increased from (3.44 to

3.5) $\times 10^{15}$ cm^{-3} to (4.0 to 4.1) $\times 10^{15}$ cm^{-3} by precipitation annealing.

The conversion efficiency of the annealed cells was about 8.14 percent, representing an increase of 26 percent over the efficiency of 6.45 percent for untreated cells. The laser-damaged and annealed cells achieved a conversion efficiency of 8.55 percent, which is 33 percent above that of the untreated cells.

This invention is owned by NASA, and a patent application has been filed. Inquiries concerning nonexclusive or exclusive license for its commercial development should be addressed to the Patent Counsel, NASA Resident Office-JPL [see page A5]. Refer to NPO-15179.

Split Coil Forms for Rotary Transformers

Both the rotor and the stator bobbins
are installed on split cores.

NASA's Jet Propulsion Laboratory, Pasadena, California
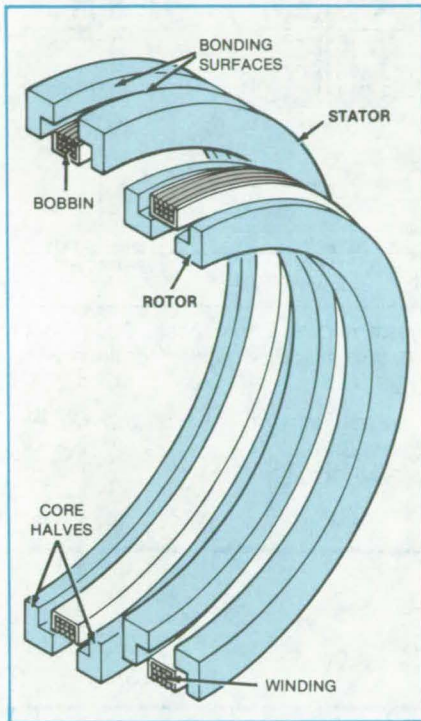
The **Split Cores** for the rotor and stator
windings of a rotary transformer are
mounted around their respective coils
(which are in bobbins) and are cemented
together. This arrangement particularly
simplifies winding of the stator coil, which
has to go in a slot in the inner diameter of
the stator core.

The fabrication of transformers for transmitting power and data across a rotating interface is simplified by a split-core technique. The transformer core is made in two pieces that are cemented together around the bobbins that hold the coils.

A rotary transformer is essentially the same as a conventional transformer except that the primary and secondary windings can be rotated with respect to each other. The rotor coil goes in a slot on the periphery of its core and therefore can easily be wound right in place. The stator coil, however, must go into a slot on the inner diameter of its core (see figure) and therefore cannot be wound directly in place. To resolve this difficulty, the stator can be wound in a bobbin and then the two-piece core mounted around it as shown.

In practice, it is convenient to split both the stator core and the rotor core, to wind both coils on bobbins, and then to bond the core halves together around their respective bobbins. In this way it is possible to wind the coils (on the bobbins) by machine without being concerned about fitting them into place on the cores.

The use of the bobbin protects the windings from the bare core, thus improving the reliability of the rotary transformers. One practical application of rotary transformers fabricated according to this technique is for centrifuges, in which conventional sliprings are of uncertain reliability.

This work was done by Colonel W. T. McLyman of Caltech for **NASA's Jet Propulsion Laboratory.** *For further information, Circle 80 on the TSP Request Card.*
NPO-15457

Recrystallizing Short Lengths of Silicon Ribbon

Techniques are proposed for the efficient
use of short substrates.

NASA's Jet Propulsion Laboratory, Pasadena, California

A short ribbon of polycrystalline silicon can be restructured to large single-crystal grains by moving it through a heating zone where a narrow transverse section is melted. As that section of ribbon moves out of the melting region, the atoms of refreezing silicon build a regular crystal pattern.

In the past, long ribbons have been used in the regrowth process, but the technique can be applied advantageously to short lengths as well. The arrangement for regrowth is shown in the figure. The ribbon moves (on rollers) through a preheating furnace, then past laser beams that produce the narrow

molten zone, and finally through a postheating furnace. The use of very long ribbons in this process has been considered necessary to minimize the time that is lost in setting up and alining each ribbon or substrate, to minimize the amount of material that is lost to regrowth because each segment must

be held at both ends, and because some initial regrowth length is required for grain size to become usefully large.

Experience has shown, however, that grains reach useful size in the first half centimeter of regrowth length. Moreover, startup time and waste material could be almost totally eliminated simply by using rigid-edge growth instead of utilizing a full-width melt. A ribbon guide and other transport rollers would be necessary; but by growing vertically and using the strength of the rigid edges, transport and support could be achieved from only one end at a time. Samples could be merely as long as the distance between input and output rollers — about 8 inches (20 cm) — and could be inserted one after another without any appreciable gap.

The use of a rigid edge also means that no special atmosphere is required; consequently, electron-beam heating could be used (in an evacuated chamber) instead of laser-beam heating.
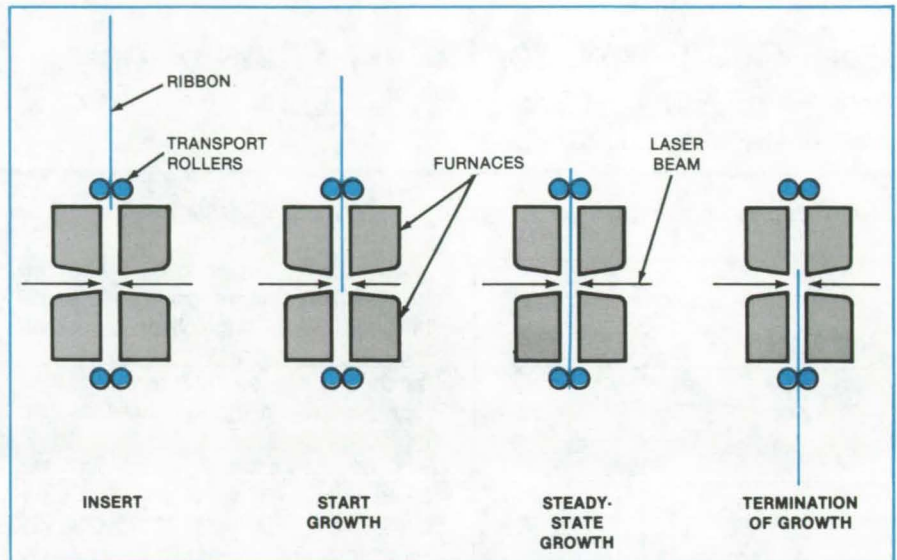
Silicon Recrystallization by laser-beam heating of ribbons is proposed. One or both vertical edges of the ribbon would not be melted, providing rigid support for the moving ribbon.

This work was done by Richard W. Gurtler of Motorola, Inc., for **NASA's Jet Propulsion Laboratory.** *For further* information, Circle 81 on the TSP Request Card.
NPO-14916

Nonslip Wristlet

Simple garment protects a vulnerable area.

Marshall Space Flight Center, Alabama

A wristlet is constructed to stay in place on the wearer's wrist even during strenuous activity. Often when the arms are extended, the wrists are exposed even though gloves and sleeves are worn. The new wristlet ensures that the gap is covered and the wrist is protected from flames, heat, corrosive or caustic substances, and sharp objects. It is especially suitable for people in forge and foundry work and firefighting.

Worn under a glove, the wristlet provides an additional layer of protective material over the palm and back of the hand and over the web of the thumb. Unlike a gauntlet, the new wristlet does not have a flared end to encumber the wearer and entrap water and foreign objects.

The wristlet is essentially a tube with openings for the arm, thumb, and fingers
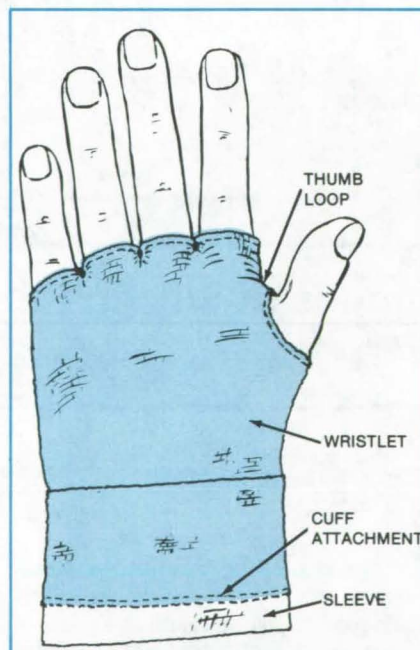
A **Mittenlike Wristlet** is restrained by the thumb loop and the cuff attachment. There can be either a single finger opening or separate openings for each digit.

(see figure). It can be knit or woven of tough, heat-resistant materials, such as Nomex or Kevlar, and can be treated with waterproofing and fireproofing substances. Inserts and reinforcements can be added.

The thumb and finger openings are reinforced by hems. The arm opening may be permanently attached to a coat sleeve by stitches, or it may be temporarily attached by snaps or a zipper. The combination of the loop of material between thumb and forefinger and the cuff attachment holds the wristlet securely in place.

This work was done by V. Himel of Grumman Aerospace Corp. for **Marshall Space Flight Center.** *For further* information, Circle 82 on the TSP Request Card.
MFS-25085

Solar Cells From Metallurgical-Grade Silicon

Less-pure material yields acceptable
properties with an epitaxial process.

NASA's Jet Propulsion Laboratory, Pasadena, California

Epitaxial deposition produces acceptable solar cells from metallurgical-grade silicon. Instead of diffusing dopants into the silicon to form a pn junction, the junction is formed by growing an epitaxial layer — one having a crystal structure continuous with that of the substrate — on metallurgical-grade silicon.

Less-pure forms of silicon, such as metallurgical-grade, are less expensive than semiconductor-grade material and would help to lower the cost of solar cells. However, typical metallurgical-grade silicon contains titanium in concentrations of 10^{14} or more atoms per cubic centimeter, which seriously degrades solar-cell performance.

Cells composed of 15- to 50-μm-thick epitaxial layers on metallurgical-grade silicon substrates had efficiencies as high as 11.7 percent, whereas cells composed of diffused junctions in the same metallurgical-grade material had a top efficiency of 8 percent. The average short-circuit current density was also better: 87.7 percent of the value for control cells made of diffused semiconductor-grade silicon in the case of the epitaxial cells but only 64.5 percent of that for the control cells in the case of the diffused metallurgical-grade devices.

The tolerance of the epitaxial cells to titanium may be a result of its thinness. Current carriers travel a shorter distance in the epitaxial layer than they do in the relatively-thick diffused layer.

This work was done by Robert V. D'Aiello and Paul H. Robinson of RCA Corp. for **NASA's Jet Propulsion Laboratory.** *For further information, Circle 83 on the TSP Request Card.*
NPO-15042

Oxide Control for Silicon Crystal Growth

Jets of gas prevent oxide buildup.

NASA's Jet Propulsion Laboratory, Pasadena, California

Silicon oxide is prevented from depositing on molten silicon and heat shields during crystal growth by a reversed flow of gas. Generated by aspirators, the reversed flow is used in the web dendrite process, which produces sheets of single-crystal silicon for low-cost solar cells.

Clean argon gas is forced down feed tubes above the melt dish and its heat shield (see figure). The gas travels horizontally through passages in the shield and emerges into chimneys as vertical jets through nozzles 1/16 inch (1.6 mm) in diameter. As an argon jet transfers its momentum to the gas already in the chimney, it creates a slight negative pressure in the chimney and the dish. As a result, clean fresh gas is drawn through the central hole of the lid and into the chimneys. The flow carries off silicon oxide gas before it can condense.

Silicon oxide gas is normally generated at the interface between the melt and the quartz dish. In the usual web dendrite growth container, the silicon oxide can escape only through the hole in the shield and tends to condense on it
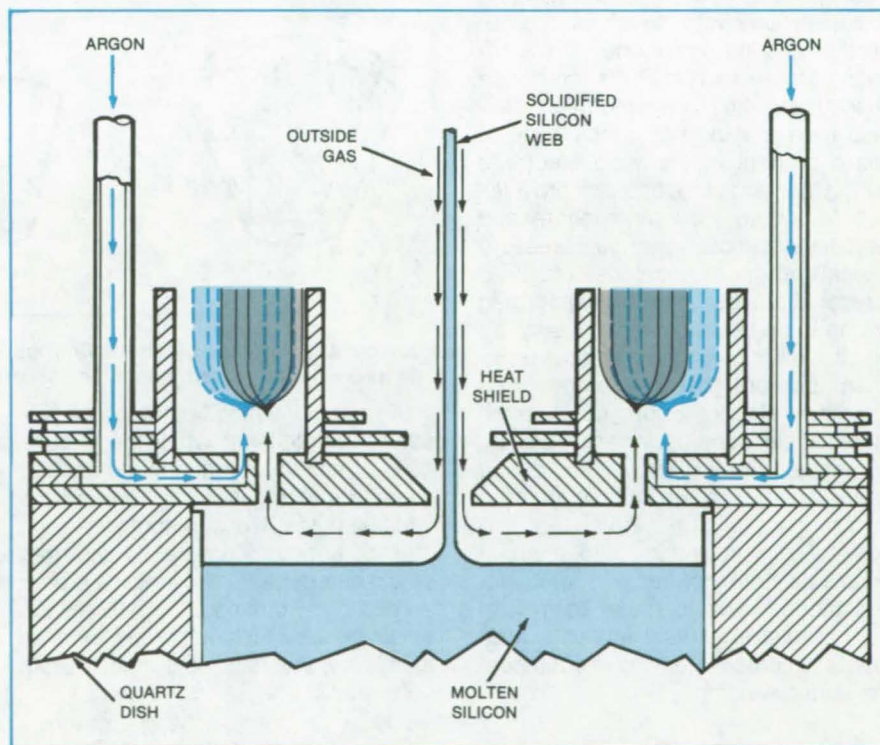
Web Dendrite Growth Process pulls a sheet of newly crystallized silicon from molten silicon. The jets of argon pull outside gas into the melt cavity, preventing silicon oxide from passing through the heat-shield hole and depositing on it.

as a brown-yellow powder as it leaves the hotter growth cavity. As the powder collects, it gradually closes the hole, and the silicon web pulled through it therefore grows thinner and narrower. Often the powder falls into the melt and stops web growth within a few minutes.

Now, however, with the gas flow reversed by the aspirators, the silicon oxide does not come near the shield hole. With an argon flow of 2 ft^3/h (0.057 m^3/h), oxide collects lightly on the lid; but with argon flowing at 4 ft^3/h (0.11 m^3/h), no oxide collects.

Annular Electrode Improves Solar-Cell Welds

A more-uniform field pattern improves the quality of solar-cell interconnections.

Lewis Research Center, Cleveland, Ohio

Previously, weld electrodes utilizing a parallel gap between electrodes have been used to weld solar-cell interconnections. The resulting weld nuggets are rectangular or square shapes with sharp corners and are subject to stress failures. In addition, the use of parallel gap electrodes does not provide a channel for an inert atmosphere or a pressure check prior to welding.

An improved method of electrical-resistance welding of solar-cell interconnections has been developed by using an annular welding-electrode shape (see figure). The improved weld electrode consists of two coaxial cylinders, the outer one with an annular cross section and the inner one with a circular cross section. This electrode shape results in more-uniform electric-field lines that do not concentrate at sharp corners of the weld electrode during the weld pulse and also provides a path for an inert atmosphere and weld-head/sample interface pressure check through the annulus. The weld nugget (i.e., fused materials) formed during the welding pulse from such an electrode will be uniform and devoid of sharp corners that concentrate mechanical stress. Such mechanical stress arises during solar-array assembly and temperature cycling and during operation and is a known contributor to interconnect failures. Thus, the purpose of this invention is to improve solar-cell interconnection electric-resistance welds to make them less subject to stress failure and to provide greater in-process environmental control during welding.
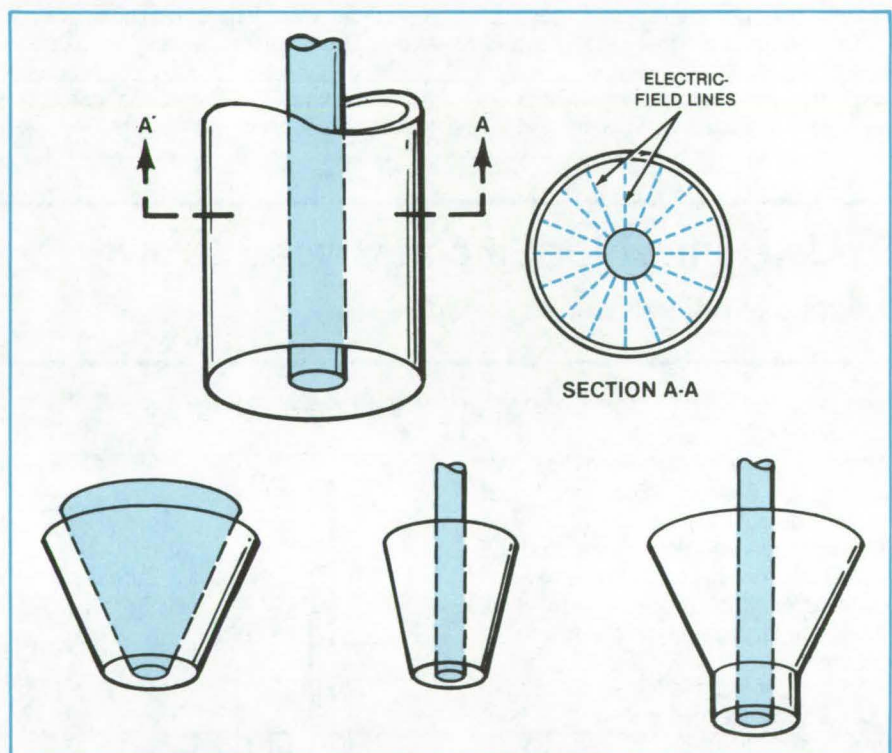
Possible **Annular Weld-Electrode Configurations** are shown here. They result in better quality welds for interconnecting solar-array elements.

An additional modification to the present state-of-the-art would be to combine ultrasonic vibration of the annular welding electrodes while applying the welding pulse. The ultrasonic vibration should remove surface oxides that would otherwise tend to inhibit a proper weld from forming. This technique would be applicable to metals, such as aluminum, that develop surface oxides very easily.

Bridging Gaps Between Refractory Tiles

Gap-filling technique provides
smooth-surfaced insulation.

Lyndon B. Johnson Space Center, Houston, Texas

Excessively large gaps — wider than 0.045 inch (1.14 mm) — between tiles on the Space Shuttle can now be eliminated without the time-consuming and costly procedure of removing and replacing tiles. Instead, a ceramic tile sliver is bonded in a gap, as shown in the figure. The bonded sliver not only prevents the airframe under the gap from getting too hot during reentry but also presents an aerodynamically-smooth exterior surface.

The bonding procedure is carried out when a returned Shuttle shows excessively large gaps between its reusable surface-insulation tiles. The repair must be reinspected after each subsequent mission.

The gap is measured, and a sliver is cut from a ceramic plate to conform to the gap dimensions. The sliver should rise above the adjacent tiles by at least ½ inch (1.27 cm). Later it will be trimmed so that it is flush with the adjacent tiles.

The sliver is prepared for installation by applications of a densifier, an emissivity coating, and waterproofing. The densifier — activated ethyl silicate — is brushed on all faces of the sliver. It penetrates the pores of the ceramic, filling them with dense silicon dioxide near the surface. The densified sliver is dried at
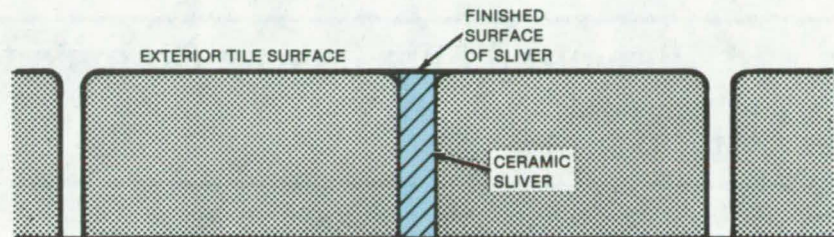
Too Large a Gap between Space Shuttle tiles might allow excessive heating of the airframe. Filling the gap with a ceramic sliver provides insulation and reduces aerodynamic disturbances caused by the gap.

300° F (149° C) for about 15 minutes.

The emissivity coating is prepared from a solution of boron silicide in colloidal silica. It is brushed on one surface of the sliver. The sliver is then baked for half an hour at 300° F.

The sliver is waterproofed by either of two methods. In one method, three coats of a waterproofing compound are brushed on the emissivity-coated surface. Alternatively, the entire sliver is exposed to vapor-phase silane.

The sliver should be bonded to the lower of the two tiles that form the gap sides. The bonding surface of the tile is wiped with a cloth dampened in isopropyl alcohol. A coating of room-temperature-vulcanized elastomer is applied to

the bonding surface of the sliver. The sliver is inserted in the gap, and polyester-film shims are inserted between the uncoated sliver edge and the adjacent tile so that they apply pressure to the bond joint. Excess RTV is wiped away, and the bond is allowed to cure. The portion of the sliver projecting above the surrounding tiles is cut away. An emissivity coating is reapplied to the cut edge and to the available side of the sliver.

This work was done by Joseph W. Haney, Jr., of Rockwell International Corp. for **Johnson Space Center.** *For further information, Circle 85 on the TSP Request Card.*
MSC-20060

Programable Plasma-Spray System

Optics and microprocessor control combine
in a versatile plasma-spray apparatus.

Lewis Research Center, Cleveland, Ohio

A wide variety of metal coating systems has been in commercial use for a number of years. Specific coatings and application processes can impart a wide range of beneficial characteristics to metal surfaces. These coatings can protect surfaces from wear, oxidation, erosion, corrosion, impact damage, and the like. One of the more versatile of the coating systems uses either metallic or high-temperature nonmetallic powders.

These powders are applied with a high-temperature plasma arc system that melts the powder and propels the resultant droplets onto the substrate surface where they fuse and bond, forming an integral structure with the base material.

Two major problems in the plasma-spray operation are that it is labor-intensive and that it is difficult to reproduce coating thickness and contours exactly. It is also difficult for the

operator to vary coating chemistries and densities in a controlled and reproducible manner.

NASA-funded research has led to the development of an automated plasma-spray system that is both programable and reproducible. This system utilizes standard plasma-spray equipment along with a noncoherent light-measuring system and a microprocessor. This

system monitors and controls surface contours and coating thickness. Other advantages of this system are consistent coating reproducibility [±0.015 in. (±0.38 mm)], exact blending and feathering operations, ability to handle the most complex shapes, and the ease of changing spray parameters. The use of this type of automated plasma-spray system results in increased versatility, productivity, reduced material costs, and overall quality improvements.

This work was done by C. W. Fetheroff, T. Derkacs, I. M. Matay, and I. Toth of TRW, Inc., for **Lewis Research Center.** *Further information may be found in NASA CR-165418 [N81-31193/NSP], "Automated Plasma Spray (APS) Process Feasibility Study" [$13.50]. A copy may be purchased [prepayment required] from the National Technical Information Service, Springfield, Virginia 22161.*
LEW-12986

Coated Aluminized Film Resists Corrosion

An organic coating allows aluminum
to be substituted for gold.

Lyndon B. Johnson Space Center, Houston, Texas

A commercially available corrosion-protection coating allows less costly metals — aluminum in particular — to be used in heat-reflecting films for thermal barriers. Heretofore, such films have had to incorporate gold as the reflective layer if they were to withstand humidity, moisture, and salt spray without corroding. This is the first protective coating that prevents the corrosion of metalized films during environmental exposure and still remains flexible, thermally stable, and clear.

The corrosion-protective coating is a plastic material, modified by the addition of antioxidation agents. It is applied to polyimide sheets on which a thin film of aluminum has been deposited. The film thickness is either 0.0003 or 0.002 inch (7.6 or 50.8 μm) thick and may be metalized on one or both sides. The film may be perforated with small, regularly spaced holes, or it may be unperforated. It may be reinforced with a fabric or unreinforced.

Detailed specifications have been prepared for the aluminized, coated film. The specifications include quality assurance tests for heat resistance, thermal emittance, coating adhesion, hardness, and other properties. The emittance of 0.03 maximum must not degrade after exposure to 100 cycles of heating to 400° F (204° C), ten 24-hour high-humidity cycles, and 48-hour exposure to 5 percent salt spray as outlined in military standards. The film was developed for the Space Shuttle orbiter, which uses about 55,000 ft^2 (5,100 m^2) of the material per vehicle.

This work was done by Harley J. Rockoff of Rockwell International Corp. for **Johnson Space Center.** *For further information, Circle 58 on the TSP Request Card.*
MSC-20118

Mathematics and Information Sciences

Computer Programs

Computer Programs

Operations Program Executive

System simplifies job control, data management, and recordkeeping for interacting programs.

The Ground Resource Operations Program Executive (GROPE) is a control program for binding a system of programs into a single, easily operated entity. It relieves the user from the complexities arising from the decomposition of a large application into a number of interacting program units.

Many large-scale computer applications, such as the analysis of ground and resource operations for space programs, are too large to be encompassed by a single computer program. Hence, systems of programs are developed to break the large application into smaller, more manageable units. These program units interact by passing data through storage mediums such as magnetic tape or disk, and collectively they supply the desired output. Unfortunately, while decomposition of the original application simplifies the program units, it increases the complexity of job control, data management, and recordkeeping for the entire system.

GROPE is an interactive executive program that communicates with the user through a set of menus and simple prompter questions. The GROPE system is designed around a model of a large-scale application that includes analysis programs, their associated data elements, input-data files, scratch files, output-data files, and print files, and the manner in which the analysis programs interact. A programer describes each system of programs to

GROPE in terms of this model. Once this has been accomplished, engineers and other users who are not programers can easily set up, execute, and save the results of complex series of interacting analysis programs. GROPE permits multiple simultaneous users; each user can maintain several case studies on the computer at one time.

GROPE is written in FORTRAN IV for interactive execution and has been implemented on a UNIVAC 1100-series computer with a central memory requirement of approximately 20K of 36-bit words. The program can be run from a Tektronix 4014-1 graphics terminal. GROPE was developed in 1981.

This program was written by Michael A. Fague of Computer Sciences Corp. for **Marshall Space Flight Center.** *For further information, Circle H on the COSMIC Request Card.*
MFS-25628

Displaying Geographically-Based Domestic Statistics

Interactive system transforms tables of statistics into color-coded maps.

The Decision Information Display System (DIDS) is a rapid-response information-retrieval and color-graphics display system developed at NASA's Goddard Space Flight Center in conjunction with the Bureau of the Census and other Federal agencies. DIDS transforms tables of geographically-based domestic statistics (such as population or unemployment by county, energy usage by county, or air-quality figures) into high-resolution, color-coded maps on a television display screen.

The response time for map generation by DIDS is typically on the order of a few seconds, allowing the user freedom to experiment with many different data mappings during the course of a brief session. For example, the user can interactively manipulate the data-classification intervals by changing the interval

ranges, changing color codes, increasing or decreasing the number of intervals, and highlighting intervals of special interest on the display map.

DIDS offers the user a wide variety of information-display options. Available interactive functions include the generation of intercomparative (bivariate) maps that display spatial relationships of two data variables, generation of computed variable maps by arithmetic operations on existing data variables, magnifying subregions of a map to increase the resolution of areas of interest, the time-lapse display of chronological data series, and the generation of histograms and scatter plots for graphical display of statistical relationships.

The currently operational version of DIDS accesses geographic and statistical data provided by various Federal agencies. This data base is maintained only for the use of these agencies through DIDS and is not available for transfer to other systems. Software is included in DIDS to preprocess statistical data in a simple ASCII or EBCDIC tape format into the DIDS menus and internal disk file structure.

The DIDS software package includes the following sample geographical map data bases:
- The United States by county,
- The State of California by county,
- The Denver Standard Metropolitan Statistical Area (SMSA) by census tract, and
- The world by country.

A sample data file is included for each geographical base for test purposes.

The DIDS package includes a host system version and a remote system version. A DIDS installation generally consists of a host computer system or a host computer system together with remote terminal systems. The remote terminal systems are not designed for totally independent operation. They depend on the host computer for both map and statistical data file input. All DIDS sites, whether host or remote, have the same basic DIDS mapping and display capabilities.

As currently configured, each DIDS site requires an image-display terminal system designed specifically for DIDS; however, the software can be modified to operate with some other image displays. Both the host and remote versions

consist of several independent program modules that interact during run time, initiating each other as required and transferring data among themselves.

Anyone wishing to implement the DIDS software should be familiar with the concepts of intertask and interprocess communications under the DEC RSX-11M and VMS operating systems, shared global common areas, global and local event flags, task building and installation, VAX quotas and privileges, and other system concepts pertinent to DEC operating systems.

The DIDS host version is written in FORTRAN IV-PLUS and Assembler for interactive execution on a DEC VAX 11/780 computer running the VMS Version 2.0 operating system. The remote version is written in FORTRAN IV and Assembler for interactive execution on the DEC LSI-11/23 computer running the RSX-11M Version 3.2 operating system. The DIDS host-to-remote communications link is via standard DEC asynchronous line interfaces, DZ-11 ports on the VAX and DLV11-E ports on the LSI. Interactive graphics is achieved via the DeAnza ID5512 display terminal that was designed specifically for DIDS. DIDS was completed in 1980.

This program was written by J. Quann, J. Dalton, M. Banks, D. Helfer, M. Szczur, and G. Winkert of **Goddard Space Flight Center;** *J. Billingsley of the Executive Office of the President; R. Borgstede of the Bureau of the Census; J. Chen, L. Chen, and J. Fuh of General Software Corp; and E. Cyprych of Computer Sciences Corp. For further information, Circle J on the COSMIC Request Card.*
GSC-12747

Atmospheric Correction for Remote Sensor Data

Model includes the effects of scattering by gas and aerosols and absorption by ozone.

In the remote sensing of surface features using multispectral sensors, Earth's atmosphere can have adverse effects on the classification of various surface objects. It is therefore desirable to remove the effects of the atmosphere from the multispectral data prior to the implementation of classification processing techniques. A computer model of those atmospheric effects has been developed for that purpose.

The mathematical model is based on radiative transfer theory as applied to a plane parallel, horizontally spatially homogeneous, isotropic atmosphere. The model includes the effects of multiple scattering by gases and aerosols and the effects of absorption by ozone in the near ultraviolet and visible parts of the spectrum. Polarization and absorption by other gaseous constituents are not included in the model. With these limitations, the model is applicable to haze levels ranging from near fog conditions to the clearest possible atmosphere and to the wavelength range from $0.4~\mu m$ to $2.20~\mu m$.

Measured inputs to the model include date, time, barometric pressure, site latitude/longitude, sensor altitude, and atmospheric optical thickness. Estimated inputs include the aerosol phase function, ozone absorption, and standard aerosol optical depths above 5 km. Given the above input data, the model calculates the atmospheric path radiance and transmittance as a function of altitude and look angle, the total downwelling irradiance, and the direct solar irradiance. All output data are spectral quantities.

This program is written in FORTRAN V language for use on a UNIVAC 1100 computer.

This program was written by Robert E. Turner of the Environmental Research Institute of Michigan for **Lewis Research Center.** *For further information, Circle K on the COSMIC Request Card.*
LEW-13344

Project Planning and Reporting

Projects with up to 10,000 activities can be planned, scheduled, and monitored.

The Project Planning Analysis and Reporting System (PPARS) is an automated aid in the monitoring and scheduling of activities within a project. The PPARS system consists of the PPARS Batch Program, five preprocessor programs, and two postprocessor programs. The PPARS Batch Program is a full CPM (Critical Path Method) scheduling program with resource capabilities. It can process networks with up to 10,000 activities. The preprocessor programs prepare input for the PPARS Batch Program. The postprocessor programs generate user-specified displays of output from the PPARS Batch Program. Altogether, PPARS provides a complete, modularized scheduling system.

The PPARS Network Generation Program (NETGEN) is a batch program that generates a CPM logic network based on input of work tasks (in task list or WBS format) and the relationships among the work tasks. NETGEN scans the work task information, creates a predecessor and successor for each work task, and creates the interface activities needed to tie the network together. All of the activity durations not provided by the user are calculated, and all start and end events are determined. NETGEN prepares a file that can be input to the PPARS Batch Program. This file is a standard CPM logic network that can be saved and later updated by cards or by IAPERT.

The PPARS Interactive PERT Program (IAPERT) runs successive iterations on critical paths and scheduling of network activities. IAPERT provides the user with a way to make network additions, deletions, and alterations to any activity in the network. Paths can then be computed and displayed. For situations involving a moderate number of network modifications, IAPERT provides a way to adjust and "tinker" with the network.

Three other preprocessor programs available to the user are KOMPAR, SORTER, and CHARTER. KOMPAR compares two PERT networks and generates detailed reports on the differences between the two networks based on the valid PERT activity card fields. The SORTER program sorts an unsorted PERT network and checks errors on each activity card. The CHARTER program produces Gantt bar charts (schedule plots) directly from input activity records without having to run the PPARS Batch Program.

The PPARS Batch Program is the heart of the PPARS system. It is a full CPM scheduling program with resource capabilities. Input to the PPARS Batch Program consists of such network data as those produced by NETGEN and PERT control cards directing the program options. The input network data may be generated either by updating a previously created network or by input-

ting an entire network from scratch. The activities are read and linked together into paths. The start events and end events of the paths are found. Then the expected and allowed completion dates, slack time, and time remaining are computed for all uncompleted activities.

Expected completion dates are computed by progressing forward from the start dates, and allowed completion dates are computed by progressing backward from the scheduled completion dates. Slack time is the difference between allowed and expected completion dates. Time remaining is the difference between the report date and the expected date. Such logic errors as looping paths and uncompleted activities followed by completed activities are detected and noted as part of the normal PPARS Batch processing. Output is in the form of printed reports, plots, and an updated activity file.

The PPARS system includes the programs PARSRFP and SPPLOT for postprocessing of the data output by PPARS Batch. The PPARS Report Formatting Program (PARSRFP) generates additional reports from the data generated by the PPARS Batch Program. The user may specify the formatting to be used in generating the reports. The Schedule Performance Program (SPPLOT) takes a project network and produces a graph showing the baseline of completed activities over the duration of the project. The plots are actually produced by EZPERT; SPPLOT functions as an interface between the PPARS Batch Program and EZPERT (EZPERT is a product of Systonetics, Inc., and is not included with the PPARS system). However, bar charts can be obtained from the PPARS Batch Program without EZPERT.

The programs in the PPARS system are written in FORTRAN IV for batch and interactive execution and have been implemented on a CDC CYBER 170-series computer with the largest program having a segmented central-memory requirement of approximately 56K (octal) of 60-bit words. The PPARS system was developed in 1981.

This program was written by the Schedule Analysis and Control Office of **Langley Research Center.** *For further information, Circle L on the COSMIC Request Card.*
LAR-12919

Data-Retrieval System

An interactive system for data retrieval by management

Data retrieval for management has always posed a complex problem. Frequently, the data base involved is large and is constantly updated. Also, management requirements for data may vary greatly from month to month or even from day to day. The traditional approach of displaying data as tables, matrices, and reports often generates large reports that obscure trends and relationships represented by the data. This problem is generally resolved by writing specialized programs that reduce the data and produce specialized charts and graphs. In situations where the data base is constantly altered and requirements vary frequently, this approach of writing specialized programs can critically delay the preparation of data for management decisions.

The NASA Graphics and Display System (NGDS) helps to solve the problem of data retrieval for management. Since NGDS is an interactive online system, the user controls the display content and format and has the capability of always working with the latest version of his data.

The user interface for NGDS is a flexible command/control language that is very versatile in its data-selection and display capabilities. The basic display graphics supported are line plots, bar charts, pie charts, and tables. Optional "keyword" parameters are used to reduce selectively the data accessed for display. NGDS also provides a series of "HELP" and "LIST" commands that allow the user to learn how to use the entire system.

A unique feature of NGDS is that it is data-independent. Each new data base requires that a small data-access program be written to address the new data. This program is dynamically invoked whenever data are to be retrieved. The only functional responsibility of this user-written program is to read the data. As each record is read, the data are moved to an array, and con-

trol is passed to other NGDS software, which extracts all the required data for display generation.

NGDS is written in COBOL and FORTRAN and has a central memory requirement of approximately 300K 8-bit bytes. NGDS was designed and written specifically for operation on large IBM mainframes using Time-Sharing Option (TSO). NGDS supports only Tektronix 4010-series terminals.

This program was written by Philip R. Lawrence of Planning Research Corp. for **NASA Headquarters.** *For further information, Circle M on the COSMIC Request Card.*
HQN-10921

Special Report Writer

A flexible information-management system for performing multiple correlations on files containing several data hierarchies

The Special Report Writer (SRR) accepts input submitted by the user, accesses a sequential data base, and produces a desired special report. The program is a batch-oriented information-retrieval system that performs multiple correlations on files containing several data hierarchies. Report requests are specified in a simple notation, readily learned by people without extensive backgrounds in data processing.

SRR was originally developed to meet the operational requirements of NASA's Office of University Affairs (OUA). It is primarily designed for manipulating a financially-oriented data base. The current data base contains such selectable data elements as contract status, cognizant office, a unique project number, geographical location, accounting installation, institution, contract/grant number, and specific dollar amounts. SRR rapidly answers nonstandard questions in a presentable format. Thus SRR can prepare reports in response to such questions as "What were FY 74 obligations to public schools?" and "List the individual FY 75 contracts for basic

research made by NASA's Langley Research Center in the States of Virginia and Maryland that have a funded value greater than $100,000."

SRR acts as a cross-correlation routine, checking each member of the data base against the requirements the question imposes on certain data elements. For example, the second question above requires a six-way correlation. No limit is imposed on the number of correlations. If no member of the data base meets all of the requirements, then a negative report is generated.

Families of output reports can be easily generated. A family consists of reports for which all but one of the selection requirements are the same. For example, one could alter the second question above to generate a family of three reports: one listing all contracts, one listing contracts funded below $100,000, and one listing contracts funded above $100,000. SRR could be adapted to other data bases that are similarly formatted.

The report generated by SRR contains three sections:
1. A cover page indicating what requirements were stated in the question that generated the report;
2. The body pages that list the data-base members that meet the requirements (some sequencing, alphabetically, is available); and
3. A final page summarizing the data in the body.

Each section is uniquely titled for identification purposes. The report can be single or double spaced and in a format of either 8 by 10-½ in. (20 by 27 cm) or 11 by 15 in. (28 by 38 cm).

Data-select cards, input to SRR, are sorted prior to execution by the IBM Utility "SORT." This sort procedure requires approximately 150K of 8-bit bytes. SRR is a COBOL program that utilizes the input-procedure/output-procedure method of sorting.

SRR has been implemented on an IBM 370/158 OS/VS2 Release 3.7 with JES2 spooling system utilizing an IBM 3330 disk drive and an IBM 3420 tape drive. In this environment SRR requires approximately 392K bytes of real storage with execution time ranging from 4 to 30 minutes, depending on requested options. SRR has previously been implemented on an IBM 360/50

OS/MVT with HASP spooling utilizing an IBM 2314 disk drive and an IBM 2400 tape drive. In this environment SRR requires approximately 180K bytes of real storage with execution time ranging from 80 to 110 minutes, depending on requested options.

This program was written by the Office of University Affairs of **NASA Headquarters.** *For further information, Circle N on the COSMIC Request Card.*
HQN-10889

Out-of-Core Solutions of Complex Sparse Linear Equations

Routines assume no special properties of the coefficient matrix other than nonsingularity.

ETCLIB is a library of subroutines for obtaining the out-of-core solutions of complex sparse linear equations. The routines apply to dense and sparse matrices that are too large to be stored in core. They are therefore useful for solving any set of linear equations, but are particularly useful in cases where the coefficient matrix has no special properties that guarantee convergence with any of the iterative processes. The only assumption made is that the coefficient matrix is not singular.

There are two main subprograms in ETCLIB, both of which use a direct solution method. In the first main subprogram, the basic idea is to reduce the coefficient matrix to an upper triangular system. In the second main subprogram, the basic idea is to reduce the coefficient matrix to the sum of a block-banded matrix and a matrix with only a few active columns and to employ a variant of the Sherman-Morrison updating formula. Both main subprograms include options to control the frequency of pivoting and to take advantage of block sparsity in the coefficient matrix.

The ETCLIB routines are written in FORTRAN IV and Assembler for batch execution and have been implemented on a CDC CYBER 170-series computer

with a central memory requirement of approximately 45K (octal) of 60-bit words. The ETCLIB routines were developed in 1979.

This program was written by Elizabeth L. Yip of The Boeing Co. for **Langley Research Center.** *For further information, Circle P on the COSMIC Request Card.*
LAR-12874

FORTRAN Static Source Code Analyzer

Program determines an overall "figure of complexity" for FORTRAN programs.

The FORTRAN Static Source Code Analyzer program (SAP) automatically gathers and reports statistics on the occurrences of statements and structures within a FORTRAN program. Provisions are made for weighing each statistic, providing the user with an overall figure of complexity. Statistics, as well as figures of complexity, are gathered on a module-by-module basis. Overall summed statistics are also accumulated for the complete input source file.

SAP accepts as input syntactically-correct FORTRAN source code written for the DEC PDP-11/70 FORTRAN IV Plus compiler or the IBM S/360 FORTRAN IV Level H compiler. SAP utilizes two external files in its analysis: A keyword file allows flexibility in classifying statements and in marking a statement as either "executable" or "nonexecutable." A statistical-weight file allows the user to assign weights to all output statistics, thus allowing flexibility in defining the figure of complexity.

SAP is written in FORTRAN IV for batch execution and has been implemented on a DEC PDP-11/70 computer under RSX-11M with a central memory requirement of approximately 26K of 16-bit words. SAP was developed in 1978.

This program was written by Phillip Merwarth of **Goddard Space Flight Center.** *For further information, Circle R on the COSMIC Request Card.*
GSC-12693

SUBJECT INDEX

THIRD-CLASS BULK

NASA

The San Francisco Bay Area Rapid Transit (BART) system has tested a flame-resistant polyimide foam originally developed for spacecraft interiors. The new material promises to improve safety in the BART equipment, as well as in other surface and air vehicles. [See the bottom of page A1.]